Contemporary Endocrinology *Series Editor:* Leonid Poretsky

Leslie S. Eldeiry · Nora M. V. Laver ·
Gregory W. Randolph · Barry Sacks ·
Jeffrey R. Garber *Editors*

Handbook of Thyroid and Neck Ultrasonography

An Illustrated Case Compendium with Clinical and Pathologic Correlation

Springer

Contemporary Endocrinology

Series Editor
Leonid Poretsky, Division of Endocrinology
Lenox Hill Hospital, New York, NY, USA

Contemporary Endocrinology offers an array of titles covering clinical as well as bench research topics of interest to practicing endocrinologists and researchers. Topics include obesity management, androgen excess disorders, stem cells in endocrinology, evidence-based endocrinology, diabetes, genomics and endocrinology, as well as others. Series Editor Leonid Poretsky, MD, is Chief of the Division of Endocrinology and Associate Chairman for Research at Lenox Hill Hospital, and Professor of Medicine at Hofstra North Shore-LIJ School of Medicine.

Leslie S. Eldeiry • Nora M. V. Laver
Gregory W. Randolph
Barry Sacks • Jeffrey R. Garber
Editors

Handbook of Thyroid and Neck Ultrasonography

An Illustrated Case Compendium with Clinical and Pathologic Correlation

Springer

Editors
Leslie S. Eldeiry
Department of Endocrinology
Harvard Vanguard Medical Associates/Atrius Health and Harvard Medical School
Boston, MA, USA

Gregory W. Randolph
Massachusetts Eye and Ear Infirmary
Boston, MA, USA

Massachusetts General Hospital
Boston, MA, USA

Jeffrey R. Garber
Department of Endocrinology
Harvard Vanguard Medical Associates/Atrius Health and Harvard Medical School
Boston, MA, USA

Nora M. V. Laver
Departments of Pathology and Laboratory Medicine and Ophthalmology
Tufts Medicine, Tufts Medical Center
Boston, MA, USA

Barry Sacks
Department of Radiology
Beth Israel Deaconess Medical Center
Boston, MA, USA

ISSN 2523-3785 ISSN 2523-3793 (electronic)
Contemporary Endocrinology
ISBN 978-3-031-18447-5 ISBN 978-3-031-18448-2 (eBook)
https://doi.org/10.1007/978-3-031-18448-2

To my father, Dr. Subhi Eldeiry, a lifelong learner who always inspired and encouraged me to do my best
—Leslie S. Eldeiry

To my mentors, colleagues, and trainees who educated me
To my family: Sheri, Ben, Solly, Sarah, Bram, and Pierce for their support
—Jeffrey R. Garber

To my dad Dr. Orlando Vitale, who embraced and supported my interests in medicine, and to my loving husband Roberto Laver, Esq, a staunch supporter of my career
—Nora M. V. Laver

To our patients
—Gregory W. Randolph

To my wife, Yvonne, who patiently tolerated the hours in front of my computer
—Barry Sacks

Preface

Neck ultrasonography plays a key role in the evaluation of thyroid nodules and parathyroid disease. This handbook arose from regular multidisciplinary clinical-pathological medical education conferences centering on patients with thyroid and parathyroid disease that the editors participated in over a number of years. Our goal was to make it a clinically anchored, case-based, easy to use, concise volume that covers key points that endocrinologists, radiologists, surgeons, and pathologists feel are most important to know about neck ultrasonography.

Chapters cover major types of thyroid nodule ultrasound features: composition, echogenicity, shape, margins, rim calcifications, echogenic foci, and vascularity; parathyroid, lymph node, and non-thyroid neck masses. Characteristic ultrasound images, cytology and histopathology images along with representative cases and key clinical data are presented. Differential diagnoses are reviewed, and suggested references are provided.

Our intended audience is the clinician wishing to become proficient in the evaluation of patients with thyroid and parathyroid disease, who may also be interested in performing thyroid and neck ultrasound exams. We welcome our readers' feedback and suggestions for improving and updating our first edition.

Boston, MA, USA — Leslie S. Eldeiry
Boston, MA, USA — Nora M. V. Laver
Boston, MA, USA — Gregory W. Randolph
Boston, MA, USA — Barry Sacks
Boston, MA, USA — Jeffrey R. Garber

Series Editor Preface

Point of care (or, using the regular English, bedside) ultrasound is rapidly becoming a widely used tool in many medical and surgical specialties. Endocrinologists have been using ultrasonography for assessing thyroid anatomy for several decades, since its introduction in the 1960s. More recently, training in thyroid and neck ultrasound, including its use in the course of fine needle aspiration (FNA) biopsy of thyroid nodules, has become a universal feature in endocrine fellowship training programs. Although ultrasonography used by endocrinologists is primarily directed toward the assessment of thyroid anatomy, other structures in the neck, such as parathyroid glands, lymph nodes, large vessels, and incidentally discovered lesions, can be also observed and assessed.

All of these issues, as well as many other aspects of thyroid and neck ultrasonography, are covered comprehensively yet concisely in the current volume of the *Contemporary Endocrinology* series. A multidisciplinary writing crew is comprised of endocrinologists, surgeons, pathologists, and radiologists with extraordinary depth of expertise (full disclosure: one of the editors, Dr. Jeffrey Garber, was my mentor when I was an endocrine fellow almost 40 years ago).

This guide for students and practitioners in all relevant specialties is highly recommended and, in my opinion, is destined to become a classic.

New York, NY, USA — Leonid Poretsky

Acknowledgments

As editor-in-chief, I would like to express my sincere gratitude to my colleagues for all of their contributions and insights toward this project: Dr. Jeffrey R. Garber, for first proposing the concept of a clinical, case-based handbook for ultrasound education and providing much support throughout all stages of this project; Dr. Barry Sacks, for providing invaluable contributions not only to chapters he authored, but also supplying images and feedback related to all of the images in the Handbook, and for keeping me on my toes; Dr. Nora M. V. Laver, for providing her expertise for all of the pathology images in the Handbook, and for her moral support; and finally, Dr. Gregory W. Randolph, for collaborating with our surgical and radiology colleagues as well as providing razor-sharp feedback to improve our design and final product. It was a pleasure working with each of you.

Leslie S. Eldeiry

Contents

Contributors

Omonigho Aisagbonhi, MD, PhD Department of Pathology, University of California, San Diego, San Diego, CA, USA

Chelsey Baldwin, MD Division of Endocrinology and Metabolism, The George Washington University, Washington, DC, USA

Nora S. Call, BS, RDMS, RT(R) Department of Ultrasound, Beth Israel Deaconess Medical Center and Harvard Medical School, Boston, MA, USA

Mary Beth Cunnane, MD Department of Radiology, Massachusetts Eye and Ear Institute, Boston, MA, USA

Preethika S. Ekanayake, MD Division of Endocrinology, Diabetes and Metabolism, University of California, San Diego, San Diego, CA, USA

Leslie S. Eldeiry, MD Department of Endocrinology, Harvard Vanguard Medical Associates/Atrius Health and Harvard Medical School, Boston, MA, USA

Jeffrey R. Garber, MD Department of Endocrinology, Atrius Health/Harvard Vanguard Medical Associates and Harvard Medical School, Boston, MA, USA

Chia A. Haddad, MD Harvard Vanguard Medical Associates, Massachusetts Eye and Ear, Harvard Medical School, Boston, MA, USA

James V. Hennessey, MD Harvard Medical School, Beth Israel Deaconess Medical Center, Boston, MA, USA

Amy Juliano, MD Department of Radiology, Massachusetts Eye and Ear Infirmary, Boston, MA, USA

Teresa H. Kim, MD Department of Pathology and Laboratory Medicine, David Geffen School of Medicine at UCLA, Los Angeles, CA, USA

Jeffrey F. Krane, MD, PhD Department of Pathology and Laboratory Medicine, David Geffen School of Medicine at UCLA, Los Angeles, CA, USA

Matthew J. Levine, MD Division of Diabetes and Endocrinology, Scripps Clinic, La Jolla, CA, USA

Priyanka Majety, MD Beth Israel Deaconess Medical Center, Boston, MA, USA

Karen C. McCowen, MD Division of Endocrinology, Diabetes and Metabolism, University of California, San Diego, San Diego, CA, USA

Pamela L. Mok, MD Department of Radiology, Atrius Health, Boston, MA, USA

Michael D. Otremba, MD Department of Otolaryngology-Head and Neck Surgery, Massachusetts Eye and Ear, Harvard Medical School, Boston, MA, USA

Rachel Pessah-Pollack, MD Division of Endocrinology, Diabetes and Metabolism, NYU School of Medicine, New York, NY, USA

Gregory W. Randolph, MD, FACS, FACE, FEBS (Endocrine) Massachusetts Eye and Ear Infirmary, Boston, MA, USA

Massachusetts General Hospital, Boston, MA, USA

Department of Otorhinolaryngology, Head and Neck Surgery, Massachusetts Eye and Ear Infirmary, Boston, MA, USA

Navya M. Reddy Division of Diabetes and Endocrinology, Scripps Clinic, La Jolla, CA, USA

Barry Sacks, MD, FSIR, FACR Department of Radiology, Beth Israel Deaconess Medical Center, Boston, MA, USA

Alison M. Savicke, BS, RDMS, RVT Department of Ultrasound, Beth Israel Deaconess Medical Center and Harvard Medical School, Boston, MA, USA

Hien Tierney, MD Atrius Health/Harvard Medical School, Boston, MA, USA

The Basics of Thyroid and Neck Ultrasound

1

Nora S. Call, Alison M. Savicke, and Barry Sacks

Key Points

- Ultrasound is entirely operator-dependent. As a result, it is critical for the operator to be thorough, identify, and document both normal structures and abnormalities while obtaining high quality images.
- Knowledge about the clinical presentation, past exams, and labs will result in a more insightful imaging study.
- Thyroid nodules should be carefully evaluated for suspicious features. This is particularly important for each nodule in a multinodular goiter.

N. S. Call · A. M. Savicke
Department of Ultrasound, Beth Israel Deaconess Medical Center and Harvard Medical School, Boston, MA, USA
e-mail: nasulliv@bidmc.harvard.edu; asavicke@bidmc.harvard.edu

B. Sacks (✉)
Department of Radiology, Beth Israel Deaconess Medical Center, Boston, MA, USA
e-mail: bsacks@bidmc.harvard.edu

L. S. Eldeiry et al. (eds.), *Handbook of Thyroid and Neck Ultrasonography*, Contemporary Endocrinology,
https://doi.org/10.1007/978-3-031-18448-2_1

- If a suspicious nodule is identified, a central and lateral cervical lymph node evaluation should be performed.
- Cine loops, when available, are extremely helpful during exam review and reporting.

Introduction

Ultrasound (US) is often the initial modality of choice in evaluating structures in the neck, including the thyroid, lymph nodes, salivary glands, arteries/veins, and musculature, due to their superficiality and the ability to obtain image clarity. Ultrasound is entirely operator-dependent. As a result, it is critical for the operator to optimize images, understand the patient's clinical presentation, and know what additional information should be sought based on the findings.

Ultrasound is a medical imaging modality utilizing sound waves at a frequency of over 20 KHz (beyond/higher than the audible range), to create high resolution images of anatomical structures.

- US is cost-effective, noninvasive, with no known detrimental bioeffects.
- With the proper equipment, transducers, and settings, the diagnostic capabilities are invaluable.

Basic Ultrasound Physics

Almost all clinical ultrasound is performed using a B-mode (brightness) scanner, producing real time, two-dimensional images.

- Each transducer contains numerous piezoelectric crystals, which emit brief sequential pulses of energy into the underlying tissue.
- A liquid medium, or gel, is necessary to attain contact between the transducer and skin.

- As the sound waves pass through the tissue, the transducer receives portions that are reflected by the traversed structures. Two-dimensional images are created that are constantly updated as the transducer moves.
- It is important to realize that the deeper the sound beam travels, the more the sound beam attenuates, decreasing image resolution.

Ultrasound Artifacts

Usually the word "artifact" has a negative connotation. However, many ultrasound artifacts can actually be helpful.

- *Posterior Acoustic Enhancement:* In fluid-filled structures (anechoic) the speed of the pulse accelerates causing the deeper structures to increase in echogenicity (posterior enhancement).
- *Acoustic Shadowing:* A calcification, bone, or surgical clip will entirely reflect the sound beam, and the result is a "shadow," deep to the structure. Air also disperses the beam, which nearly completely obscures the image.
- *Reverberation Artifact:* Occurs when the sound beam encounters a highly reflective surface and reflects multiple times. This can occur when structures are very close to the transducer, as an example, the trachea during a thyroid study.
- Reverberation is also seen in the setting of a colloid crystal/inspissated colloid within a cyst. The punctate echogenic foci within produce a "ring-down" or "comet-tail" artifact.

Equipment

- There are several high quality, sophisticated ultrasound machines, providing a large selection of transducer options and image optimization functions (Image 1.1).
  - Produced by a number of companies including General Electric, Philips, Samsung, and Siemens.
- They are expensive, require regular servicing, and each has strengths and weaknesses, depending on the specific ultrasound study being performed (small parts, abdomen, obstet-

Image 1.1 Two examples of top-of-the-line ultrasound units

rics, etc.). Selection of equipment should be based on optimizing the quality of images for the majority of exams being performed at the operator's site.

- For offices or departments with limited budgets, refurbished or leasing machines are viable options.
- Point-of-care handheld ultrasound system technology is rapidly evolving (Image 1.2).
  - Advantages: Images display on a smartphone or tablet, providing convenience, transportability, and lower cost.
  - Disadvantages: Small display size, reduced image quality, limited transducer versatility and hardware options.

Image 1.2 Butterfly point-of-care system (left), an image displayed on an iPhone, with examples of transverse (middle panel) and sagittal (right panel) images of the thyroid

Transducer Selection

Transducers used in ultrasound differ in frequency, footprint size, and shape.

- Transducer frequency is directly related to image quality, as it determines image resolution. The higher the frequency, the better the resolution, but at the expense of limited deep penetration.
- For imaging of the neck, high-frequency transducers are optimal, preferably a 12-18 MHz linear array, providing both optimal image quality and adequate penetration. Linear transducers provide a rectangular image, but some have the ability to widen the field of view to a trapezoidal shape, which is helpful in cases of thyromegaly.
- In cases with suboptimal penetration, such as a thick neck or large multinodular goiter, a linear 7–9 MHz transducer can provide acceptable image quality. The lower frequency allows for greater penetration to visualize the deeper tissue.
- Alternatively, a lower frequency 5 MHz curved transducer will provide a larger field by emitting a fan-shaped beam, but at the expense of reduction in resolution.
- It is important to have a variety of transducers available to fully assess each individual's anatomy (Images 1.3,1.4, and 1.5).
- Bottom row: Curved transducers for deeper penetration and larger field of view.

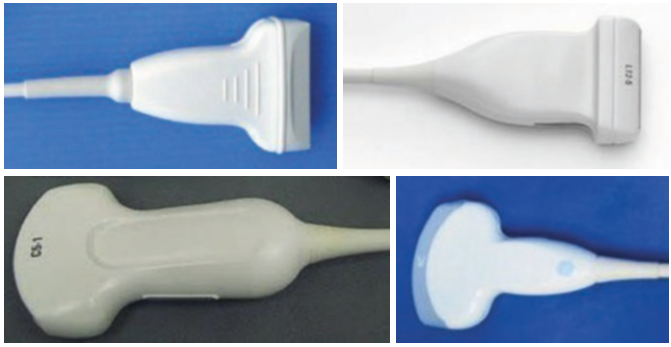

Image 1.3 Top row: Linear array transducers for superficial structures

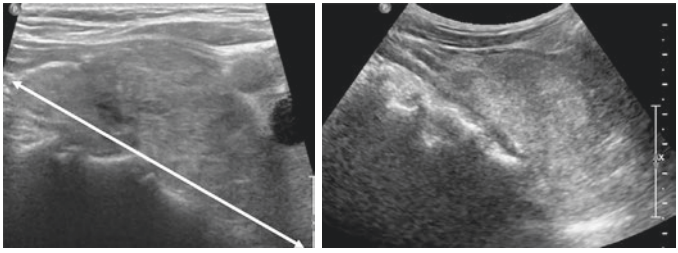

Image 1.4 Enlarged thyroid gland. Left: Linear array transducer utilizing a wide angle beam to increase the field of view; Right: Curved C-5 probe which has a naturally divergent beam was used to produce a wider, complete image

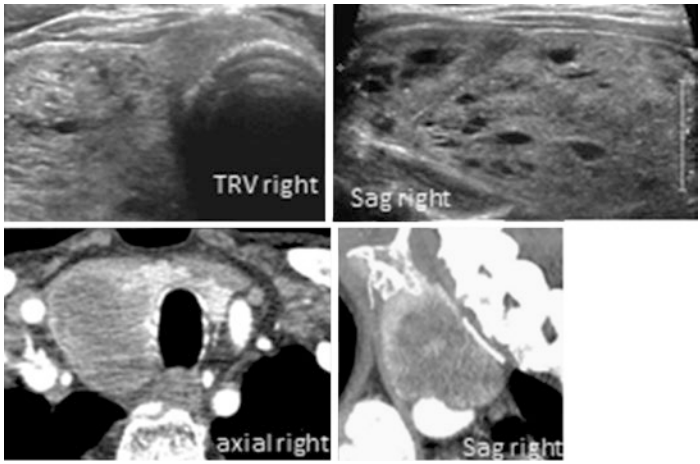

Image 1.5 Top row: Transverse (left) and sagittal (right) ultrasound images of a large gland extending into the thoracic inlet, requiring a C-5 curved transducer to measure the entire sagittal length of the lobe; Bottom row: CT showing axial and sagittal images of the same large, right-sided goiter

Patient Positioning and Scanning Techniques (Image 1.6)

- The patient is placed in a supine position with a towel or pillow behind the shoulders to extend the neck, creating a large imaging window.
- As indicated in the diagram below, transverse scans are initially obtained from superior to inferior bilaterally with the transducer notch facing the patient's right side, first with the head in neutral position, and repeated rotating the head to left for the right lobe and to the right for the left lobe.
- Sagittal scans are obtained bilaterally, medial to lateral, with the transducer notch pointed superiorly.
- Color Doppler images should be documented to determine vascularity of the gland.

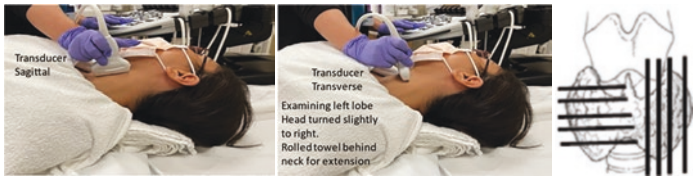

Image 1.6 (Left panel) Neutral position-transducer sagittal for both sides of the neck. (Middle panel) Head rotated right for left side of the neck with the transducer transverse. Neck extended by placing a pillow or towel under the shoulders, with the head tilted back. Right panel showing the required images in both transverse and sagittal projections (on both sides)

- All pathologic lesions should be documented in transverse and sagittal planes and color Doppler included.
- If available, cine loops should be obtained. These are extremely valuable, allowing review of the entire study during reporting.

Two additional techniques can be helpful in adding specificity to the ultrasound assessment of thyroid nodules. These include *elastography and ultrasound contrast enhancement.*

Tissue or nodule firmness has always been considered a biomarker of tissue pathology. Thyroid elastography is a method that evaluates the stiffness of the tissue, a capability available on most new US machines. Since all firm thyroid nodules on palpation are suspicious for malignancy, the ability to assess whether a nodule is firm on US adds diagnostic value in determining that malignancy potential. Having this capability provides an additional technique to evaluate thyroid nodules, particularly those deep within the thyroid substance, not easily palpable. During the standard US exam, after documenting the normal ultrasound and color Doppler images, the elastography is activated and provides color images of the nodule. Depending on the color profile, the degree of softness or firmness of the nodule can be determined. This technology has also been referred to as "electronic palpation." There are two types, strain elastography (SE) and shear wave elastography (SWE), essentially two different mechanisms to evalu-

ate tissue stiffness. A more detailed discussion is beyond the scope of this chapter.

Contrast-enhanced ultrasound (CEUS) is a new noninvasive modality for the diagnosis of thyroid nodules. It involves an intravenous injection of an ultrasound contrast agent during real time continuous ultrasound imaging of the lesion of interest.

In the last decade, the applicability of CEUS to thyroid-related disease greatly improved due to the development of more advanced US equipment and the introduction of second-generation contrast agents (SonoVue, Bracco Imaging, Milan, Italy). SonoVue consists of sulfur hexafluoride microbubbles (2–10 μm) which is injected intravenously as a small bolus. The microbubbles stay in circulation for a limited period. Immediately following the injection continuous real time scanning is performed over the lesion of interest. The microbubbles in the blood flow reach the lesion, reflecting unique prominent echoes very different to the surrounding tissue. There is a pattern of increased echogenicity into a contrast-enhanced image of the region of interest (ROI) that represents the bubbles in the microvasculature. The microbubbles last only 5–10 min in circulation because they are taken up either by immune system cells, liver, or spleen. Previous studies have shown enhancement patterns that were different in benign and malignant lesions. Ring enhancement was predictive of benign lesions, whereas heterogeneous enhancement was helpful in suggesting the possibility of malignant lesions.

Although both of these technical advancements have provided additional ways of improving nodule assessment, they have thus far not caught on for routine use in the day-to-day evaluation of thyroid or neck lesions.

Potential Scanning Pitfalls

- Air and bone attenuate the ultrasound waves; as a result, a variety of maneuvers may be necessary to obtain adequate diagnostic images. These include angling the transducer from an unusual direction or opposite side, rotating the patient's head

in various degrees, or having the patient swallow (which causes the thyroid to move cephalad).

- The esophagus has a ring-like appearance and is usually seen posterior and medial to the left thyroid. This should not be mistaken for an abnormality (nodule, enlarged parathyroid, or lymph node).

The following sections represent recommendations or tips for the operator performing a variety of neck exams. The intention is to stress identification and documentation of the critical findings for those exams, to provide the referring clinician all the necessary information to make therapeutic decisions or determine the need for additional studies. For in-depth discussions of the specific findings, please refer to the chapters dedicated to each subject.

Thyroid Anatomy (Image 1.7)

A normal thyroid gland has a homogenous texture and is typically more echogenic than surrounding musculature. It is important to recognize that images from various manufacturers will have slight

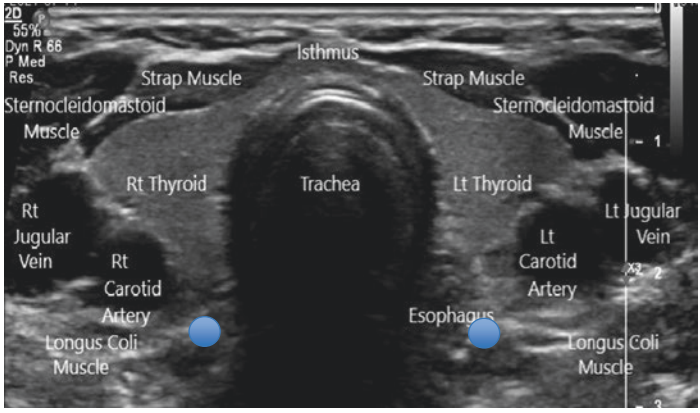

Image 1.7 Important anatomic structures (see diagram below)

differences in appearance on the display. Each operator should become familiar with the normal appearance on their equipment, enabling detection of subtle textural changes.

- The sternohyoid and omohyoid (or strap muscles) are thin muscular hypoechoic bands located anterior to the thyroid gland. The longus coli muscles are located posterior to both lobes.
- The esophagus is usually posterior and medial on the left, but often switches to the right side when the head is rotated to the left.
- The recurrent laryngeal nerves are extremely important structures, not identifiable on ultrasound, but their approximate location is labeled with the blue circles.
- The carotid arteries and internal jugular veins are lateral to the thyroid bilaterally.

Normal Thyroid Texture (Image 1.8)

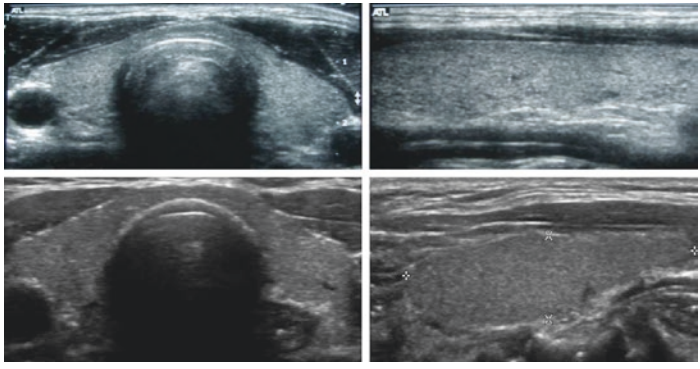

Image 1.8 Different presentations of a normal thyroid appearance—slightly different settings, contrast levels, and image presentation. Left images are transverse; right images are sagittal views. Note the difference in contrast between the thyroid gland and muscles above it between the top and bottom images

Textural Changes (Images 1.9, 1.10, and 1.11)

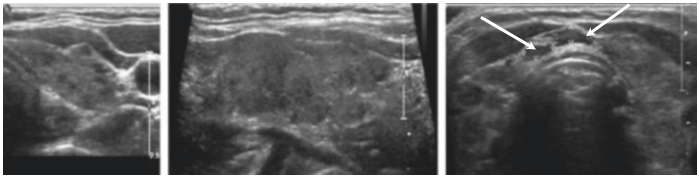

Image 1.9 Three examples of slight textural changes in the early stages of Hashimoto's Thyroiditis. Right panel: Delphian lymph nodes above the isthmus (arrows), common in Hashimoto's

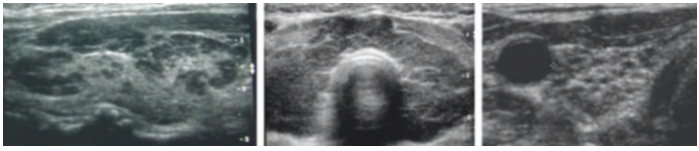

Image 1.10 Later stages of Hashimoto's. Patchy heterogeneity of the gland. Middle panel: More severe and diffusely enlarged gland; Right panel: A fibrotic, atrophic gland, often representing the end stage

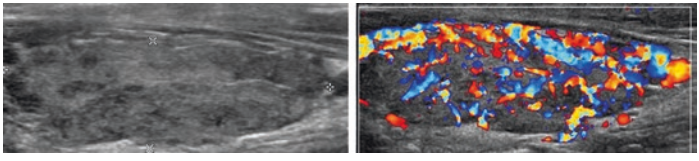

Image 1.11 Color Doppler is useful in evaluating the thyroid parenchyma. Increased vascularity is usually indicative of a diffuse process, such as Hashimoto's thyroiditis or Graves' disease, or drug effect, particularly lithium therapy

Anatomic Variants (Images 1.12 and 1.13)

Pyramidal lobe is an extension of thyroid tissue in the isthmus and is a normal variant.

- It is prone to the same thyroid diseases as the rest of the gland and is important to note, especially when a thyroidectomy is needed, so the remnant is not left behind at surgery.

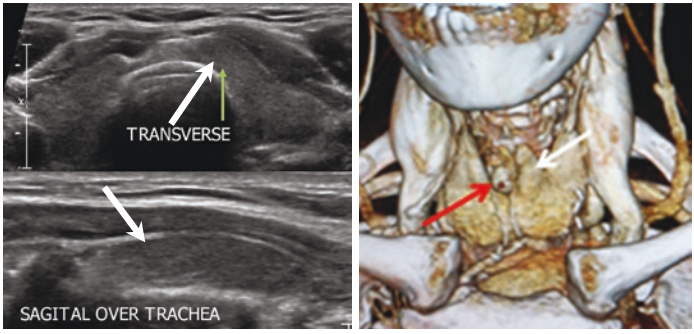

Image 1.12 Left: US showing a transverse (top) and sagittal (bottom) view of a left pyramidal lobe. Right: 3D reconstruction of CT in a patient with a parathyroid adenoma (red arrow). The patient has an incidental left pyramidal lobe (white arrow)

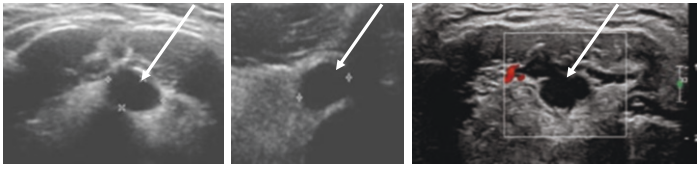

Image 1.13 Classic thyroglossal duct cysts. Left and middle panels: Transverse and sagittal views of the lesion located at the midline superior to the thyroid; it is anechoic and avascular (arrows); Right: Color Doppler of a separate thyroglossal duct cyst with a septation (arrow)

Thyroglossal Duct Cyst

A usually benign, fluid-filled cyst.

- Typically found in the midline region of the neck, anywhere from the base of the tongue to the gland itself (most commonly, just inferior to the hyoid bone).
- Important to document the size, presence of solid elements, extension into the hyoid bone, and other possible thyroid remnants.

Thyroid Nodules

Thyroid nodules vary in composition, from simple cysts, to spongiform, complex solid/cystic, and solid lesions.

Simple Cysts (Image 1.14)

- Thin-walled, fluid filled, avascular, and completely anechoic.
- Low level internal echoes may be due to debris or old hemorrhage.

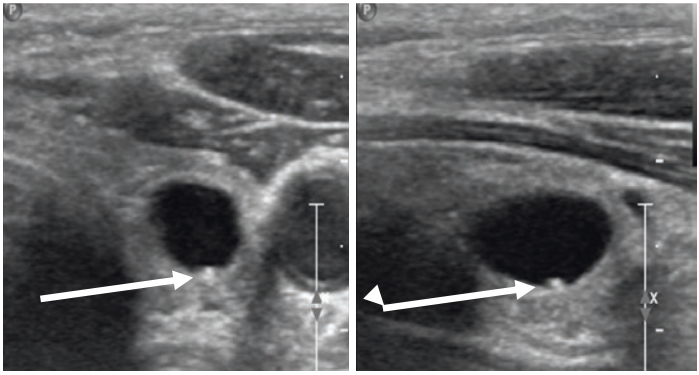

Image 1.14 Simple thyroid cyst with a dependent colloid crystal/inspissated colloid (left panel transverse, right panel sagittal). Also note acoustic enhancement posterior to the cyst (arrows)

- Often contain high reflective echoes, described as colloid crystals or inspissated colloid. This finding suggests a benign lesion.
- Posterior enhancement behind the cyst.

Spongiform Nodules (Uniformly Microcystic throughout) (Image 1.15)

- Typically demonstrate aggregates of microcystic areas, giving the appearance of the cross section of a sponge (but the spaces are fluid filled).
- Highly reflective echoes are commonly found within the cysts, often in the dependent portions.
- Demonstration of a comet-tail artifact projecting behind the echo differentiates colloid from microcalcification.

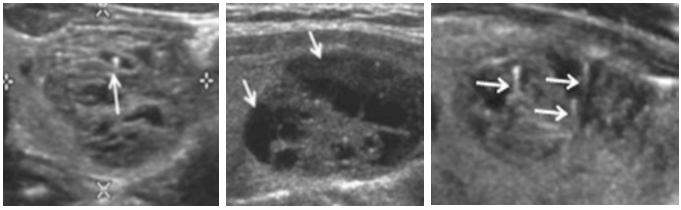

Image 1.15 Spongiform nodules with microcysts (left); middle panel demonstrates macro-cysts; right panel shows dependent colloid crystals with a "comet tail" (arrows)

Solid Nodules (Images 1.16, 1.17, 1.18, 1.19, and 1.20)

When a solid nodule is identified, it is important to document the following characteristics:

- Size, presence of a halo, shape, echotexture, vascularity, the presence of colloid crystals or calcification, margins, and whether there is extrathyroidal extension.

Any concerning features warrant a lymph node evaluation and biopsy.

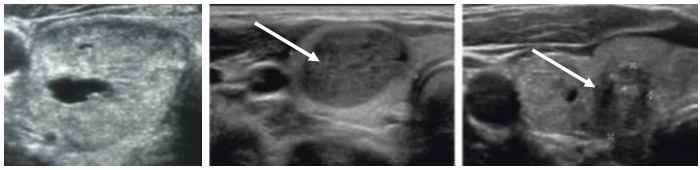

Image 1.16 Examples of predominantly solid nodules. Left panel: Isoechoic, benign nodule with small cystic component; Middle panel: Hypoechoic nodule for which FNA is warranted; Right panel: Small, hypoechoic nodule, taller than wide with calcification—FNA is warranted to rule out papillary thyroid cancer (PTC)

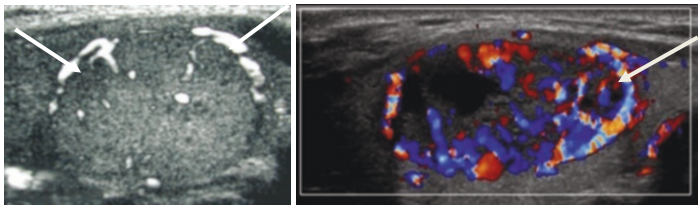

Image 1.17 Vascularity. Left*:* Isoechoic nodule with minimal vascularity, mostly peripheral; Right*:* Hypoechoic nodule with hypervascularity. Both require FNA

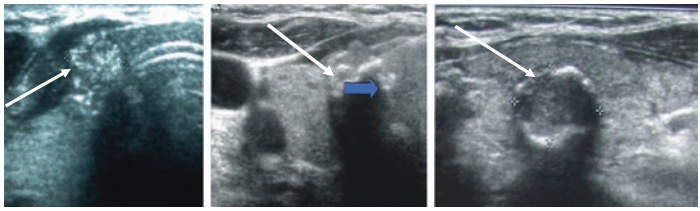

Image 1.18 Calcification. Multiple examples of malignant calcification (arrows). These vary from fine, high reflective echoes to irregular macrocalcifications and discontinuous rim calcifications

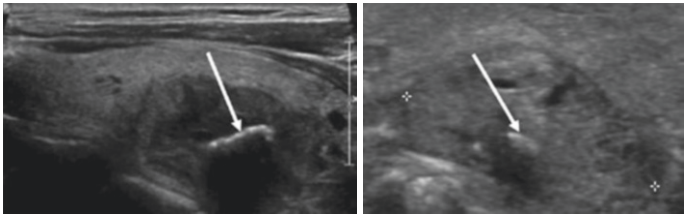

Image 1.19 Two images of the same nodule. Well-defined hypoechoic nodule with dense calcification (usually dystrophic—secondary to either necrosis or old hemorrhage), which showed benign cytology

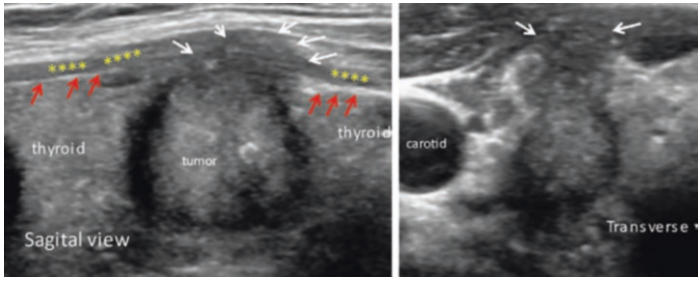

Image 1.20 Focal thyroid nodule with anterior extrathyroidal extension (white arrows) into the strap muscles (yellow stars). Red arrows indicate thyroid capsule, which is disrupted at site of extrathyroidal extension

Lymph Node Assessment

- In cases of thyroid nodules with suspicious features, or in the setting of a known or prior thyroid cancer, a careful central and lateral compartment nodal evaluation should be performed. Accurate documentation of lymph node levels is critical (Image 1.21).
- Recurrent carcinoma most commonly presents in the thyroid bed or the central and lateral compartments ipsilateral to the primary lesion. Nevertheless, a full, bilateral nodal assessment should always be performed.

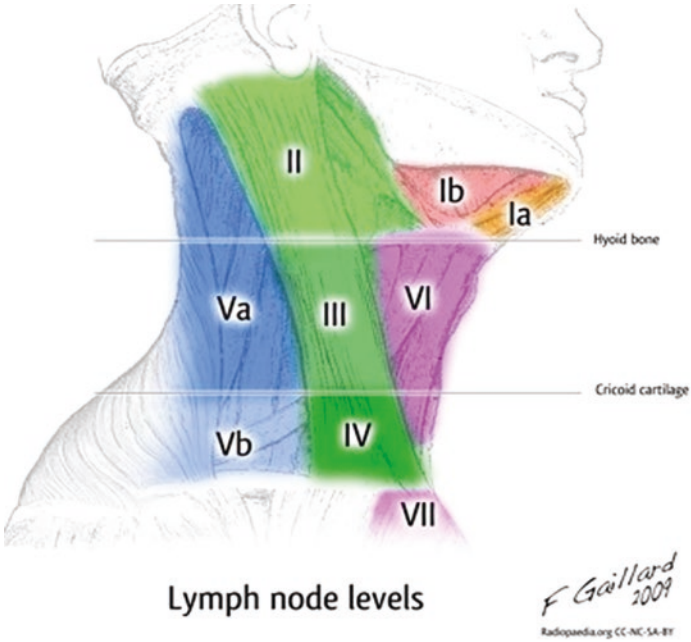

Image 1.21 Diagrammatic demonstration of the cervical lymph node levels

Ultrasound Appearance of Lymph Nodes

Normal lymph nodes (Image 1.22) demonstrate a hypoechoic cortex and an echogenic fatty line or hilum.

- The normal shapes are small and round on transverse, oblong longitudinal.

Abnormal lymph nodes (Images 1.23 and 1.24) have a variable appearance. They may appear enlarged, with an atypical texture, lack the echogenic hilum, demonstrate cystic changes, or contain calcification (usually multiple microcalcifications). Hyperemia (increased vascularity) may also be an important indicator of underlying pathology (but is not specific—can also be inflammatory).

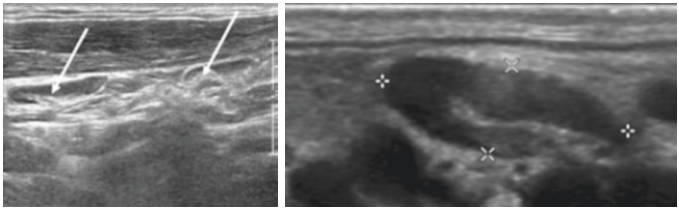

Image 1.22 Normal lymph nodes. Left, longitudinal, long and thin lymph nodes with echogenic hila (arrows). Right, larger node but morphologically normal with well-defined hilar line

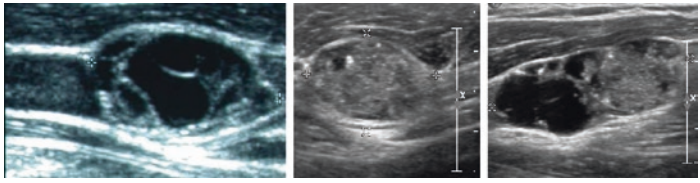

Image 1.23 Abnormal lymph nodes: Variable appearance in metastatic papillary thyroid carcinoma. Left panel: Cystic lymph node; Middle panel: Mostly solid lymph node with microcalcifications; Right panel: Solid and cystic with microcalcifications

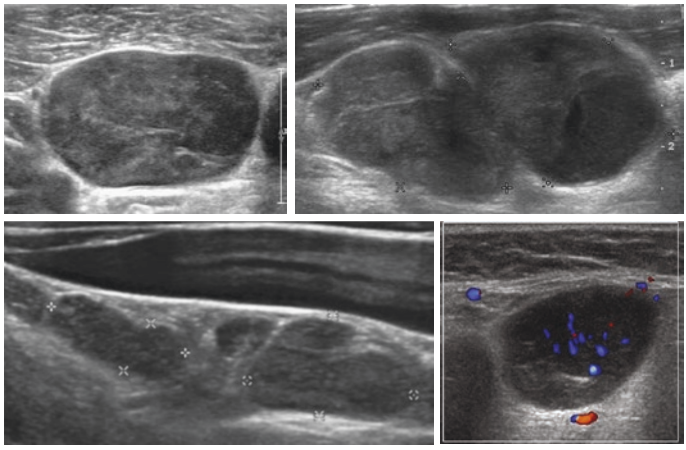

Image 1.24 Pathologic lymph nodes. Above left*:* Metastatic lymph node; Above right*:* Metastatic medullary thyroid carcinoma node; Lower left*:* Multiple lymphoma nodes. Lower right*:* Lymphoma with intralesional vascularity

Other Neck Masses

Ultrasound is usually the initial imaging study of choice for other neck masses, including parathyroid glands, salivary glands, branchial cleft cysts, carotid body tumors, and a variety of soft tissue tumors.

Parathyroid Glands

Normal parathyroid glands are not typically visualized on ultrasound, due to their small size. When they are identified, this usually implies enlargement, either due to hyperplasia or parathyroid adenoma.

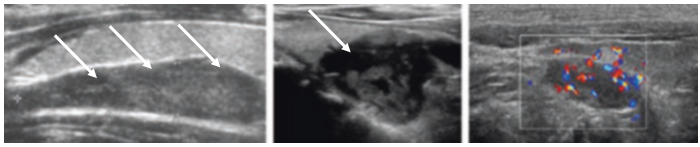

Image 1.25 Left panel*:* Large parathyroid adenoma; Middle panel*:* Complex solid/cystic parathyroid adenoma; Right*:* Hypervascular parathyroid adenoma

- Parathyroid adenomas vary in size and shape (Image 1.25), but are almost always hypoechoic and hypervascular on color Doppler imaging.

Please see the dedicated Parathyroid chapter for detailed information and ultrasound localization techniques.

Salivary Glands (Image 1.26)

- The parotid and submandibular glands are commonly seen on ultrasound and may contain intra-glandular lymph nodes, calculi, or masses, such as cystic or solid tumors.
- On ultrasound, the glands should appear homogeneous, minimally vascular, and symmetric in size. Side to side comparison is essential. Heterogeneity, hyperemia, and/or asymmetrical enlargement may indicate signs of an inflammatory process.

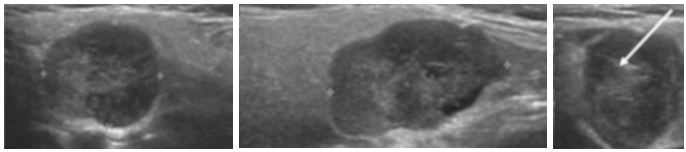

Image 1.26 Left panel: Transverse view of a pleomorphic adenoma of the parotid; Middle panel: Sagittal view of the same lesion; Right panel: FNA showing biopsy needle in the lesion (arrow)

Branchial Cleft Cyst

Congenital cysts arising from the head and neck.

- Second branch cleft cysts are most common, accounting for 90-95% of branchial cleft cysts, and are found between the angle of the mandible and the carotid bifurcation.

Carotid Body Tumor

A carotid body tumor (also called a chemodectoma or paraganglioma, Image 1.27) is usually benign, unilateral, and lying in the carotid artery bifurcation separating the internal and external carotid arteries.

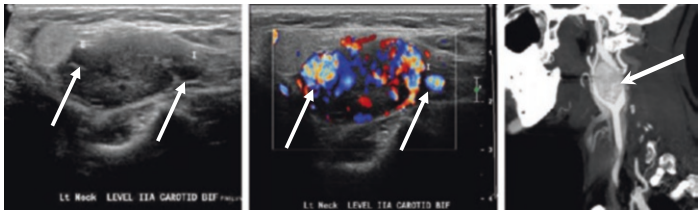

Image 1.27 Left panel: Heterogeneous mass dividing the left external (E) and internal (I) carotid arteries (arrows); Middle panel: Same mass, hypervascular on color Doppler. Note the internal and external carotid arteries (arrows) contrasting with the scattered hyperemia within the mass; Right panel: Corresponding computed tomography angiography (CTA) imaging, confirming the enhancing carotid body tumor within the carotid bifurcation (arrow)

Further Reading

AIUM practice guideline for the performance of ultrasound examinations of the head and neck. J Ultrasound Med. 2014;33(2):366–82.

Baskin HJ, Duick DS, Levine RA. Thyroid ultrasound and ultrasound-guided FNA. New York, NY: Springer; 2013.

Jiang H, Tan Q, He F, Yang W, Liu J, Zhou F, Zhang M. Ultrasound in patients with treated head and neck carcinomas: a retrospective analysis for effectiveness of follow-up care. Medicine. 2021;100(16):e25496.

Kotecha S, Bhatia P, Rout PG. Diagnostic ultrasound in the head and neck region. Dent Update. 2008;35(8):529–30, 533–4. https://doi.org/10.12968/denu.2008.35.8.529. PMID: 19055089.

Rumack CM, Levine D. Diagnostic ultrasound. Elsevier; 2018.

2 Ultrasound Scoring Systems, Clinical Risk Calculators, and Emerging Tools

Priyanka Majety and Jeffrey R. Garber

Key Points

- Currently available tools to risk stratify thyroid nodules include clinical practice guidelines, scoring systems (qualitative or quantitative), web-based calculators, and an interactive algorithm.
- Web-based tools provide an easy-to-use and easily modifiable approach in evaluating risk of malignancy for thyroid nodules.
- Many web-based tools generally do not include clinical considerations.
- TNAPP is a novel attempt to convert a comprehensive clinical practice guideline to a web-based tool that employs clinical and radiologic characteristics.
- The application of AI to evaluate thyroid nodules holds promise for the future.

P. Majety (✉)
Beth Israel Deaconess Medical Center, Boston, MA, USA

J. R. Garber
Department of Endocrinology, Atrius Health/Harvard Vanguard Medical Associates and Harvard Medical School, Boston, MA, USA
e-mail: jgarber@bidmc.harvard.edu

L. S. Eldeiry et al. (eds.), *Handbook of Thyroid and Neck Ultrasonography*, Contemporary Endocrinology,
https://doi.org/10.1007/978-3-031-18448-2_2

Introduction

Thyroid nodules are common. These are three-dimensional lesions within the thyroid gland that are radiologically distinct from the surrounding thyroid parenchyma. In the USA, over 500,000 fine-needle aspirations (FNAs) are performed annually, with as many as 200,000 of them being unnecessary. The vast majority of these nodules are benign, while most thyroid malignancies are low-risk neoplasms that do not have an impact on survival.

The evaluation of patients with a suspected or known thyroid nodule should include a careful medical history, physical examination, TSH level, followed generally by ultrasound (US) evaluation. Sonographic characteristics of thyroid nodules have been used to better assess the risk of malignancy (RoM). Currently, the principal tools available to clinicians are: (1) clinical practice guidelines (CPG) from professional societies, (2) scoring systems (qualitative or quantitative), (3) web-based calculators, and (4) an interactive algorithm. Guidelines are large documents with extensive information. The latter tools are easier to use, interactive, trackable, can be integrated into electronic health records, establish the sequence of clinical steps, and generate patient-specific recommendations. To date these tools have been retrospectively, but not prospectively, studied. Artificial intelligence (AI) is emerging as a promising approach to evaluating thyroid ultrasound, but is beyond the scope of this chapter.

Case Presentation

A 51-year-old woman with a past medical history of breast cancer in remission (after treatment with chemotherapy, surgery, and XRT), on anastrozole, was referred for osteopenia management. Her physical exam was notable for an approximately 1 cm right mid-pole thyroid nodule with no lymph nodes of significance. Her TSH was 2.27 mIU/L.

Her mother was diagnosed with papillary thyroid cancer at age 30 and died of complications of advanced disease. Thyroid ultrasound showed a 0.9 × 0.7 × 0.9 cm hypoechoic, posterior right

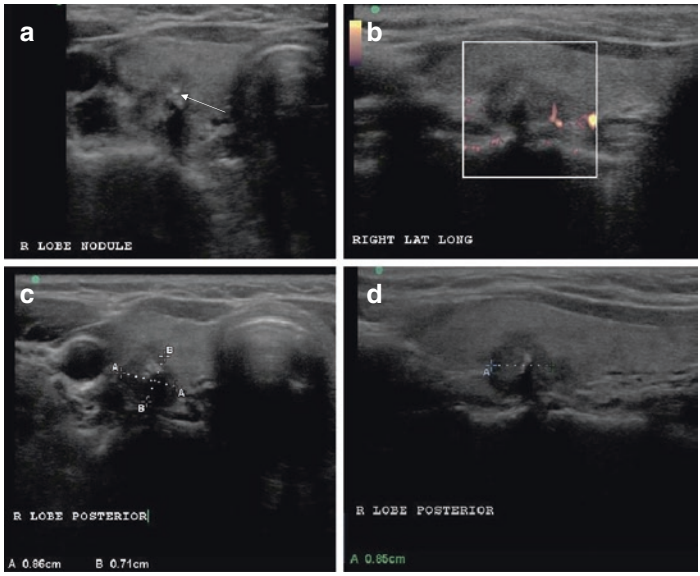

Fig. 2.1 (**a**–**d**) US demonstrated a 0.9 × 0.7 × 0.9 cm hypoechoic, posterior right mid-pole nodule with a coarse calcification (arrow in panel **a**) and irregular borders (all panels)

mid-pole nodule with irregular margins and a coarse calcification (Fig. 2.1, below). Inferior and adjacent to this, there was a patchy hypoechoic region that was well defined. No abnormal cervical lymph nodes were identified.

Given her history of breast cancer and family history of lethal thyroid cancer, she requested a fine-needle aspiration (FNA) of the nodule.

Risk Calculators Versus Clinical Practice Guidelines

CPGs are important evidence-based, narrative tools that aid clinicians in managing various medical conditions and are used as a basis for medical decision-making in both clinical and adminis-

trative settings. They require widespread dissemination and internalization by the clinicians making medical decisions. Despite their widespread clinical use, however, there are limitations. Their length makes them hard to navigate, read, absorb, retain, and ultimately follow the guidelines. Vetting mechanisms to gauge use and effectiveness in various clinical situations and populations do not exist currently. Providing timely updates of narrative, multi-authored, and highly validated documents is an ongoing challenge.

Conversely, calculators and computer-interpretable guidelines (CIG) offer a novel approach to some of these challenges and bring guidelines to "point of care." Unambiguous, sequential recommendations are made. They are easier to use, interactive, not very time-consuming and can be used as a tool to engage patients and track data about use and outcomes by being integrated into electronic health records. Unlike CPGs, these are not static documents that take substantial effort and time to update. They facilitate testing and validating recommendations prospectively and retrospectively. Expert users' feedback can continually guide revisions that can be readily and rapidly implemented.

Calculators can be used in a variety of clinical settings, e.g., in solo-practice, large multi-specialty delivery systems, regional and national databases, or research consortiums. There are limitations, however. Features that are key to clinical decision-making (for example, patient anxiety, cosmetic concerns, etc.) are usually omitted from these tools. They are typically introduced in a companion publication, e.g., an American College of Radiology "white paper" for TI-RADS. They are not as comprehensive and therefore not as instructive as CPGs.

CIGs have been shown to be effective in additional clinical domains, such as chronic diseases, diabetes, stroke, and hypertension. Examples of some of the widely used risk calculators include the fracture risk assessment tool, FRAX (https://www.sheffield.ac.uk/FRAX/), and the ASCVD (atherosclerotic cardiovascular disease) risk estimator (https://tools.acc.org/ascvd-risk-estimator-plus/#!/calculate/estimate/). Since the latter employs standardized data, it serves as a prototype calculator to automatically generate cardiovascular risk in electronic health record systems.

Ultrasound Scoring Systems

The widely used US risk stratification systems are based on the presence of one or more discrete features. One notable exception is the ATA system which uses discrete features and patterns comprised of a combination of these features.

AACE/ACE/AME

The 2016 American Association of Clinical Endocrinologists/American College of Endocrinology/Associazione Medici Endocrinologi (AACE/ACE/AME) guidelines were updated in 2021 as a novel interactive electronic algorithmic tool entitled, The Thyroid Nodule App (termed TNAPP). This tool classifies thyroid nodules into 3 categories based on US features: US 1 (low-risk), US 2 (intermediate-risk), and US 3 (high-risk). Tables 2.1, 2.2, and 2.3 and Figs. 2.2, 2.3, and 2.4 outline the features of these categories and FNA recommendations.

Table 2.1 2021 AACE/ACE-AME risk stratification based on clinical features

Clinical 1	Clinical 2
One or more of the following clinical factors are against performing FNA:	One or more of the following clinical factors favor FNA:
• Low thyrotropin and not on thyroid hormone • Autonomous nodule on imaging • Prior benign FNA of the same nodule Other medical conditions that take precedence at the time • History of prior lobectomy with vocal cord paralysis • Significant comorbidity making thyroid surgery high risk at the time • Limited life expectancy (<1 year)	• Head and neck radiation in the past • Compressive symptoms: dysphonia, dysphagia, or dyspnea without another cause • Nodule position either posterior or adjacent to thyroid capsule or trachea • History of documented growth • History of progressive growth, i.e., ≥50% increase in volume in <1 year, especially of the solid component, or 20% increase in 1 dimension • History of sudden enlargement • Planned thyroid or parathyroid surgery • Cosmetic concerns • Patient preference or anxiety • Protocol requiring documentation of cancer

Table 2.2 2021 AACE/ACE-AME risk stratification. Adapted from 2021 American Association of Clinical Endocrinology and Associazione Medici Endocrinologi thyroid nodule algorithmic tool by Garber et al.

2021AACE/ACE-AME risk stratification		
Ultrasound risk category	**Corresponding ultrasound feature(s)**	**Numerical score**
US 1 (low)	Benign or low risk ultrasound features	
One or more of the corresponding low-risk features is present and none of the intermediate or high-risk features is present	Spongiformcomposition(uniformly micro-cystic throughout)	0
	Margin is either smooth, ill-defined or the margin cannot be determined	0
	Shape is oval or round	0
	Cystic **and** anechoic	0
	Either solid or mixed **and** marked hyperechoic nodule-described as "white knight", is often seen in a gland with clear features of Hashimotos thyroiditis	0
	Comet tail echogenic foci and its variants are present on ultrasound	0
	Either solid or mixed **and** hyperechoic	1
	Either solid or mixed **and** isoechoic nodule **and** size < 20 mm **and** none of the US 2/3 features such as microcalcifications, intranodular macrocalcifications, peripheral rim calcifications, echogenic foci difficult to characterize, spiculated or irregular margin, extra-thyroidal extension	2
	Mixed solid cystic nodule thathas reverberating artifacts, which is a low-riskfeature compared with eccentric mural component (excluded from scoring)	No score
	Peripheral vascularity (excluded from scoring)	No score
	Mixed solid cystic nodule has a solid concentric/spongiform like component (excluded from scoring)	No score
US 2 (intermediate)	Intermediate risk ultrasound features	
One or more of the corresponding intermediate-risk features is present and none of the high-risk features is present	Margin on ultrasound is irregular with protrusion into adjacent thyroid tissue	1
	Echogenic foci include either intra-nodular macrocalcifications or foci that are difficult to characterize or peripheral rim calcifications include either interrupted rim calcification or uninterrupted rim calcifications	1
	Composition is either solid or mixed **and** the echogenicity of solid part is either slightly hypoechoic or hypoechoic	3
	Either solid or mixed nodule **and** isoechoic **and** either size >= 20 mm or at least one more US 2 feature such as irregular margin or intranodular macrocalcifications or foci that are difficult to characterize or peripheral rim calcifications **and** none of US 3	3

Table 2.2 (continued)

	characteristics such as microcalcifications, extrathyroidal extension, spiculated margins	
	Mixed solid cystic nodule that has a solid eccentric mural component (excluded from scoring)	No score
	Solid or mixed–with solid part showing intranodular vascularity (excluded from scoring)	No score
	Mixed solid cystic nodule that has indeterminate hyperechoic spots, which increases the risk of malignancy (excluded from scoring)	No score
US 3 (High)	High-risk ultrasound features	
One or more of the corresponding high-risk features present	Margin is spiculated or sharp angles	5
	Echogenicity is profoundly hypoechoic	5
	Microcalcifications within the nodule	5
	Shape is taller than wide	5
	Solid **and** hypoechoic **and** either intranodularmacrocalcifications or nonspecific echogenic foci or peripheral rim calcifications present (excluded from scoring)	No score
	Extrathyroidal extension is noted (excluded from scoring)	No score

Table 2.3 2021 AACE/ACE-AME (TNAPP) guidelines regarding FNA. Adapted from 2021 American Association of Clinical Endocrinologists and Associazione Medici Endocrinologi thyroid nodule algorithmic tool by Garber et al.

Nodule size	Clinical 1	Clinical 2
< 5 mm		
Ultrasound 1	No follow up	No follow up
Ultrasound 2	No follow up	No follow up
Ultrasound 3	Monitor at 18-24 months then stop	Monitor at 18-24 months then stop
5 – 10 mm		
Ultrasound 1	No follow up	No follow up
Ultrasound 2	Monitor at 18-24 months	Either ▪ Consider FNA ▪ If no FNA then Monitor at 12-24 months
Ultrasound 3	Either ▪ Consider FNA ▪ If no FNA then Monitor at 18-24 months	Either ▪ Consider FNA ▪ If no FNA then Monitor at 12-24 months
>10 – 20 mm		
Ultrasound 1	Monitor at 12-24 months	Monitor at 12 months
Ultrasound 2	Either ▪ Consider FNA ▪ If no FNA then Monitor at 12 months	Recommend FNA
Ultrasound 3	Recommend FNA	Recommend FNA
>20 – 40 mm		
Ultrasound 1	Either ▪ Consider FNA ▪ If no FNA then Monitor at 12 months	Either ▪ Consider FNA If no FNA then Monitor at 12 months
Ultrasound 2	Recommend FNA	Recommend FNA
Ultrasound 3	Recommend FNA	Recommend FNA
> 40 mm		
Ultrasound 1	Recommend FNA	Recommend FNA
Ultrasound 2	Recommend FNA	Recommend FNA
Ultrasound 3	Recommend FNA	Recommend FNA

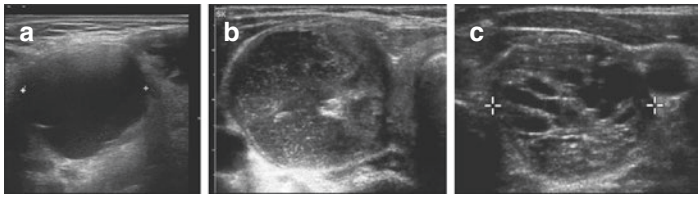

Fig. 2.2 2016 and 2021 AACE/ACE-AME risk stratification with images. Adapted from 2016 AACE/ACE-AME guidelines for clinical practice for diagnosis and management of thyroid nodules—2016 update by Gharib et al. US 1 (low-risk) features: Thyroid cyst (**a**), mostly cystic nodule with reverberating artifacts (**b**), isoechoic spongiform nodule (**c**)

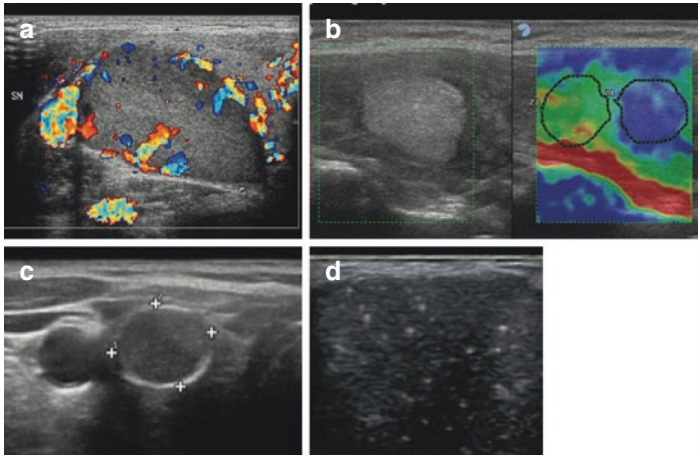

Fig. 2.3 US 2 (Intermediate-risk) features: Isoechoic nodules with: central vascularity* (**a**), elevated stiffness on elastography (**b**), macrocalcifications (**c**), and indeterminate hyperechoic spots (**d**). *Not assigned a score

TNAPP provides guidance in the initial evaluation of ambulatory patients with thyroid nodules that are not extremely likely to be malignant. Thus, nodules in those who presented with elevated calcitonin levels, multiple endocrine neoplasia type 2 syndromes, previously documented thyroid cancer, and suspicious lymphadenopathy were excluded.

Clinical factors (Table 2.1) were comprised of features in favor of performing FNA, termed Clinical 2, and those with

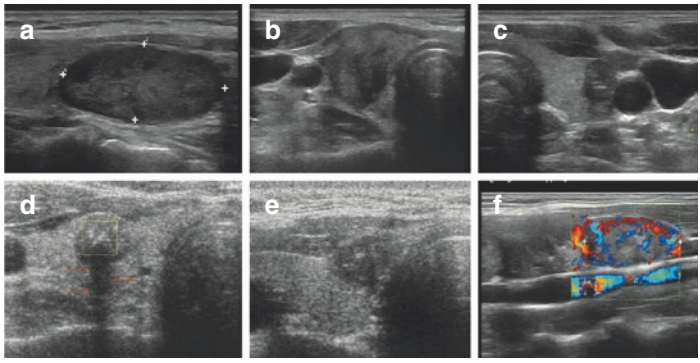

Fig. 2.4 US 3 (High-risk) features: Marked hypoechogenicity (**a**), irregular (spiculated) margins (**b**), extracapsular growth (**c**), microcalcifications (**d**), taller than wide shape (**e**), and a suspicious regional lymph node (**f**).

features against performing FNA, termed Clinical 1. When factors for and against doing an FNA are present, clinical judgment becomes the default decision-making factor (e.g., consideration of other medical conditions that take precedence at the time).

Management recommendations are informed by nodule size, US, and clinical characteristics (Table 2.3). Thus, according to these guidelines, nodules with a major diameter <5 mm should only be monitored with US if they have high-risk ultrasound features (US 3). Nodules with a major diameter 5–10 mm with intermediate- or high-risk ultrasound features (US 2/US 3) can either be monitored or aspirated. All nodules with a major diameter >10 mm require monitoring or FNA regardless of ultrasound characterization (US 1/US 2/US 3).

American Thyroid Association (ATA)

The 2015 ATA guidelines (update is in progress) categorize nodules based on ultrasound features into 5 categories: benign, very low, low, intermediate, or high suspicion (Table 2.4). Recommendations are informed by nodule size and ultrasound characteristics.

Table 2.4 Sonographic patterns, estimated risk of malignancy, and fine-needle aspiration guidance for thyroid nodules, ATA. Based on 2015 ATA management guidelines for adult patients with thyroid nodules and differentiated thyroid cancer by Haugen et al.

2015 ATA		
US pattern with features	Estimated risk of malignancy (%)	Nodule size threshold for FNA (largest dimension)
Benign Purely cystic nodules with no solid component	<1	No biopsy
Very low suspicion Spongiform or partially cystic nodules *without* any of the sonographic features described in low, intermediate, or high suspicion patterns	<3	Consider FNA at ≥2 cm. Observation without FNA is also a reasonable option
Low suspicion Isoechoic or hyperechoic solid nodule, or partially cystic nodule with eccentric solid areas, *without*: • Microcalcification • Irregular margin • Extrathyroidal extension (ETE) • Taller than wide shape	5–10	Recommend FNA at ≥1.5 cm
Intermediate suspicion Hypoechoic solid nodule with smooth margins *without:* • Microcalcifications • Extrathyroidal extension (ETE) • Taller than wide shape	10–20	Recommend FNA at ≥1 cm
High suspicion Solid hypoechoic nodule or solid hypoechoic component of a partially cystic nodule *with 1 or more* of the following features: • Irregular margins (infiltrative, microlobulated). • Microcalcifications. • Taller than wide shape. • Rim calcifications with small extrusive soft tissue component. • Evidence of extrathyroidal extension (ETE).	>70–90	Recommend FNA at ≥1 cm

ACR TI-RADS and AI TI-RADS

American College of Radiology Thyroid Imaging Reporting and Data System (ACR TI-RADS) is based on the US features defined in the ACR's previously published lexicon. With this system, nodules are classified into TI-RADS categories, as follows: TR1 = benign (RoM ≤2%), TR2 = not suspicious for malignancy (RoM ≤2%), TR3 = mildly suspicious (RoM 2.1–5%), TR4 = moderately suspicious (RoM 5.1–20%), and TR5 = highly suspicious (RoM ≥20%). A follow-up study by Middelton et al. which evaluated a total of 3422 nodules concluded that the aggregate risk levels for TR1, TR2, TR3, TR4, and TR5 nodules were 0.3%, 1.5%, 4.8%, 9.1%, and 35.0%, respectively.

Assessing a nodule with TI-RADS involves evaluation of its composition, echogenicity, shape, margin, and echogenic foci. Points are assigned to each US feature, with higher values indicating greater degrees of suspicion (Fig. 2.5). Recommendations for FNA or ultrasound follow-up are based on a nodule's ACR TI-RADS level and its maximum diameter.

Overall, TI-RADS has a higher size threshold for recommending biopsy compared with other systems. In a study of 2847 patients with biopsy results proven by pathology data, ACR TI-RADS classification had a specificity of 98.8% for diagnosing benign nodules at the cost of missing a small number of papillary cancers in TR2 and TR3 nodules that were smaller than 2.5 cm (i.e., lower sensitivity for nodules <2.5 cm).

More recently, artificial intelligence (AI) has been used to update ACR TI-RADS, though its use is not yet as widespread as ACR-TIRADS. AI TI-RADS assigned new point values for eight ACR TI-RADS features (Fig. 2.6). The five imaging characteristic categories were maintained with the following changes in each:

- *Composition—only solid nodules receive points*
  - Mixed cystic/solid nodules receive 0 points instead of 1 point
  - Solid or near-completely solid nodules receive 3 points instead of 2 points
  - Nodules that cannot be classified receive 0 points instead of 2 points

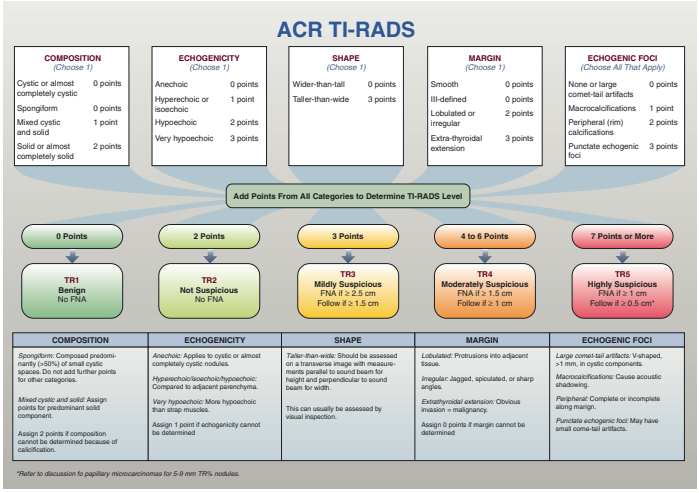

Fig. 2.5 Scoring systems: ACR Thyroid Imaging, Reporting and Data System (TI-RADS) lexicon, TR levels, and criteria for fine-needle aspiration or follow-up ultrasound and Artificial Intelligence-optimized Thyroid Imaging, Reporting and Data System (AI TIRADS). Adapted from ACR: TI-RADS: White paper of the ACR TI-RADS committee by Franklin N Tessler et al., 2017

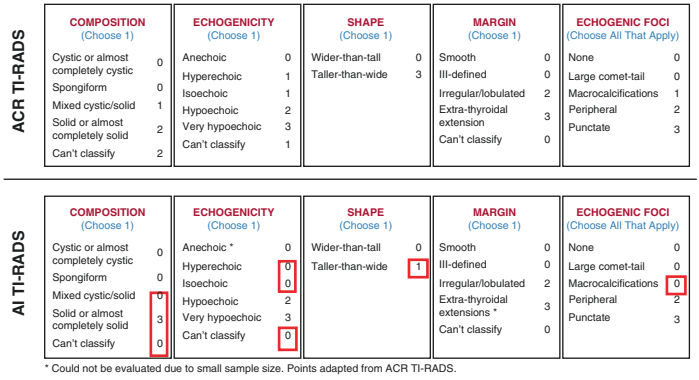

Fig. 2.6 Comparison of ACR TI-RADS and AI TI-RADS

- *Echogenicity—only hypoechoic nodules receive points*
  - Iso/hyperechoic and nodules that cannot be classified receive 0 points instead of 1 point
- *Shape*
  - Taller than wide nodules receive only 1 point instead of 3 points
- *Margins*
  - No change
- *Echogenic foci*
  - Macrocalcifications receive 0 points instead of 1 point

EU-TIRADS

The European Thyroid Association (ETA), namely EU-TIRADS, categorizes nodules into five classes from TR1 (no nodules) to TR5, which is the highest risk level (Table 2.5). It is an ultrasound risk stratification system that considers tumor composition, echogenicity, and suspicious US features with recommendations for FNA informed by size cut-offs.

Table 2.5 EU-TIRADS. Based on 2017 European Thyroid Association guidelines for ultrasound malignancy risk stratification of thyroid nodules in adults: the EU-TIRADS by Russ et al.

EU-TIRADS stratification with risk of malignancy				
Category	US features	Definition	Nodule size threshold for FNA	Malignancy risk %
TR1	No nodules	Normal	–	None
TR2	Pure cyst Entirely spongiform	Benign	Not indicated (unless compressive)	~0
TR3	Ovoid, smooth, iso/hyperechoic No features of high suspicion	Low-risk	>2.0 cm	2–4
TR4	Ovoid, smooth, mildly hypoechoic No features of high suspicion	Intermediate-risk	>1.5 cm	6–17
TR5	At least 1 of the following features of high suspicion: • Irregular shape • Irregular margins • Microcalcifications • Marked hypoechogenicity (and solid)	High-risk	>1.0 cm	26–87

K-TIRADS

The Korean Thyroid Imaging Reporting and Data System (K-TIRADS) is an ultrasound-based risk stratification system for thyroid nodules that was endorsed by the Korean Society of Thyroid Radiology (KSThR) and Korean Thyroid Association (KTA) in 2016. Risk stratification is based on tumor composition, echogenicity, and suspicious US features with FNA informed by size cut-offs (Table 2.6).

Table 2.6 K-TIRADS. Based on ultrasonography diagnosis and imaging-based management of thyroid nodules: revised Korean society of thyroid radiology consensus statement and recommendations by Shin et al.

K-TIRADS stratification with risk of malignancy			
Category	US features	Nodule size threshold for FNA	Malignancy risk %
Benign (K-TIRADS 2)	(1) Spongiform (2) Partially cystic nodule with intracystic echogenic foci with comet tail artifact (3) Pure cyst	Not indicated[a]	<3
Low suspicion (K-TIRADS 3)	Partially cystic or iso/hyperechoic nodule without any of three suspicious US features	≥1.5 cm	3–15
Intermediate suspicion (K-TIRADS 4)	(1) Solid hypoechoic nodule without any of three suspicious US features (*microcalcification, nonparallel orientation, spiculated/microlobulated margin*) or (2) partially cystic or isohyperechoic nodule with any of three suspicious US features	≥1.0 cm	15–50
High suspicion (K-TIRADS 5)	Solid hypoechoic nodule with any of three suspicious US features	≥1.0 cm	>60

[a]Not routinely indicated, but may be selectively considered for a spongiform nodule when the nodule size is ≥2 cm and indicated for the therapeutic drainage of the cystic content as well as for diagnosis prior to ablation therapy

C-TIRADS

The Chinese Thyroid Imaging Reporting and Data System (C-TIRADS) is an ultrasound-based risk stratification system for thyroid nodules that was developed by the Superficial Organ and Vascular Ultrasound Group of the Society of Ultrasound in Medi-

cine of the Chinese Medical Association in 2020. Risk stratification is based on US features that are categorized as positive features (orientation, composition, echogenicity, microcalcifications and margins/extrathyroidal extension) and negative features (comet tail artifact). Positive features receive +1 point and comet-tail artifact was considered as a sign of benignity and receives -1 point.

Comparison of Risk Stratification Tools

Multiple studies have been done to compare various risk stratification tools, with no one system being demonstrated consistently superior to the others, which may be due to different inclusion criteria, patient populations, and analytic methods.

In a study that looked at a total of 2000 consecutive thyroid nodules (≥1 cm) in 1802 patients, comparing seven society guidelines, ACR TI-RADS recommended the fewest "unnecessary" (benign) thyroid nodule FNAs at 25.3%, followed by the 2016 AACE/ACE/AME guidelines (32.5%), ATA (51.7%), and K-TIRADS (56.9%). K-TIRADS (94.5%) and ATA (89.6%) guidelines were more sensitive than those of the AACE/ACE/AME (80.4%) and ACR (74.7%), while the latter guidelines were more specific (ACR 67.3%, AACE/ACE/AME 58%, and ATA 33.2%). Table 2.7 summarizes 2 meta-analyses comparing various risk stratification systems (RSS).

An important question that remains is: What is an acceptable rate of missing or postponing the diagnosis of relatively small thyroid cancers between 10 and 15 mm in size? ACR TI-RADS does not recommend FNA for TR4 nodules between 10 and 15 mm. For example, in one study, 17% of nodules with histology proven cancer of size >10 mm, FNA was not recommended by ACR TI-RADS.

Table 2.7 Two meta-analyses comparing various RSS

Summary of meta-analyses comparing various ultrasound RSS			
12 studies; 28,750 nodules (15.2% malignant) Castellana, M., et al., *Performance of five ultrasound risk stratification systems in selecting thyroid nodules for FNA*. The Journal of Clinical Endocrinology & Metabolism, 2019. 105(5): p. 1659–1669			
RSS	Positive predictive value (%) (95% CI)	Negative predictive value (%) (95% CI)	DOR (diagnostic odds ratio)
ACR TI-RADS	43% (25–61)	84% (77–93)	4.9
ATA	27% (17–36)	88% (83–93)	3.1
AACE/ACE-AME	17% (4–30)	93% (87–98)	3.1
EU TI-RADS	29% (7–52)	81% (60–100)	2.2
K TI-RADS	25% (12–39)	87% (75–99)	2.5
Comments: 5 head-to-head studies: ACR TI-RADS had higher relative diagnostic odds ratio (DOR) than ATA To avoid the bias that arises from the different methodologies of the published reports in a meta-analysis, summary operating measures assumed to be independent of the disease prevalence were used such as DOR, which is the odds of a positive test in those with disease relative to the odds of a positive test in those without disease			

29 studies; 33,748 nodules with pathological or imaging follow-up Kim PH., et al., *Diagnostic performance of four ultrasound risk stratification systems: a systematic review and meta-analysis*. Thyroid. 2020 Aug;30(8):1159–1168		
RSS	Median unnecessary FNA (%)	AUC (area under the curve)
ACR TI-RADS	25	88
ATA	52	78
EU TI-RADS	39	90
K TI-RADS	59	85
Comments: When high-risk categories (categories 4–5) were evaluated, no difference was found between RSS. Unnecessary FNA was defined as biopsy-proven benign nodules		

Risk Calculators

ACR TI-RADS and AI TI-RADS

An online calculator was developed for TI-RADS (Fig. 2.5) based on the ACR white paper in 2017, to facilitate the application of TI-RADS in clinical practice (https://tiradscalculator.com/). To serve as an educational and clinical tool, images demonstrating each of the ultrasound features are included in the online calculator. Once the US features are entered, it provides a score and TI-RADS category along with recommendations for FNA.

The Artificial Intelligence-optimized Thyroid Imaging Reporting and Data System (AI TI-RADS) was developed in 2019 (https://deckard.duhs.duke.edu/~ai-ti-rads/index.html) using a data set of 1425 thyroid nodules. This revised AI TI-RADS assigned new point values for eight features, including a simplified scheme for some categories (Fig. 2.6). AI TI-RADS resulted in slightly higher specificity for identifying malignant nodules and recommending fine-needle aspiration (mean increase of 7.6% across eight radiologist readers; $P < 0.001$).

Malignancy Risk Estimation of Lesions with AUS/ FLUS

A web-based malignancy risk stratification system using a combination of ultrasound characteristics and subcategorized biopsy results for Bethesda III, atypia of undetermined significance/follicular lesion of undetermined significance (AUS/FLUS) thyroid nodules was developed in 2018 (http://www.gap.kr/thyroidnodule_b3.php). This was based on patients enrolled in the Korean Thyroid Study Group multicenter retrospective study and on the cytology reporting system developed by the Korean Endocrine Pathology Thyroid Core Needle Biopsy Study Group. US images from 672 thyroid nodules and biopsy results according to nuclear atypia and architectural atypia were analyzed and a 13-point risk scoring system was developed.

The Brigham and Women's Hospital (BWH) Thyroid Nodule Risk Estimator

A calculator using clinical and sonographic variables obtained during thyroid nodule assessment was developed in 2019 to assess the risk of thyroid malignancy (https://thyroidcancerrisk.brighamandwomens.org/). This was based on a mixed-effect logistic regression analysis of consecutive adult patients evaluated between 1995 and 2017 with ultrasound-guided fine-needle aspiration for thyroid nodules ≥1 cm. Significant odds ratios for malignancy were demonstrated for patient age <52 years, male sex, nodule size, cystic content (lower odds ratio with higher cystic content), and the presence of additional nodules ≥1 cm. The tool is easy-to-use and reproducible; however, the only US characteristics it employs are size and composition. Thus, it is best for assigning risk to patient populations rather than individuals.

Thyroid Nodule Malignancy Risk Calculator: Spain

A predictive model for the individual risk of malignancy of thyroid nodules was developed and validated using clinical, analytical, and ultrasound variables in 2020 (https://obgynreference.shinyapps.io/calccdt/). A retrospective case-control study was carried out in 542 patients with thyroid nodules that underwent thyroidectomy and a predictive model for thyroid cancer risk was devised. In the final model, the independent predictors of risk of malignancy were: male gender, very young or old age, a family history of thyroid cancer, TSH level >4.7 mcU/L, presence of autoimmune thyroiditis, solid composition, hypoechogenicity, irregular or microlobed borders, taller than wide shape, microcalcifications, and suspicious adenopathy. This tool requires extensive data input and employs features such as anti-thyroid antibodies which are not always available nor required when evaluating nodules.

Risk of Malignant Thyroid Nodules Based on Clinical, Biochemical, Ultrasound Characteristics, with or without Cytologic Features: Cleveland Clinic

A nomogram that can quantify the risk of malignancy in a thyroid nodule based on biochemical, ultrasonographic, and cytologic features was developed in 2010 (https://riskcalc.org/ThyroidCancer/). This was one of the early calculators available.

Clinical records of all patients with thyroid nodules who underwent ultrasound-guided FNA and operative resection at Cleveland Clinic during 2007–2008 were analyzed. The eight variables with the greatest predictive value were biochemical (thyroid-stimulating hormone), ultrasonographic (shape, echotexture, and vascularity), and cytologic (nuclear grooves, pseudoinclusions, cellularity, and presence of colloid). The tool employs vascularity as one of its inputs which is no longer generally used for nodule risk stratification.

The Thyroid Nodule App: TNAPP

TNAPP was developed in 2021 and is an update of the 2016 AACE/AME guidelines (https://aace-thyroid.deontics.com/dwe/int/public/welcome.jsp). It is a novel interactive web-based tool based on a comprehensive narrative clinical practice guideline that uses clinical, imaging, cytologic, and molecular marker data to guide *sequential clinical decision-making* to evaluate and manage thyroid nodules. Simultaneously, it calculates malignancy probability ranges based on published data, as well as ACR TI-RADS risk category, when sufficient data is provided.

The sequence is as follows:

- Checks for the eligibility for using TNAPP (yes/no)
- If eligible, the tool:
  - Calculates the AACE US category (US1/U2/U3)
  - Queries clinical factors for and against performing an FNA (clinical 1/clinical 2)
- Provides guidance about whether to perform an FNA and advice about follow-up
- Uses results of FNA when available to serve as the basis for:
  - Recommending surgery
  - Considering the use of molecular markers
  - Repeating FNA
  - Duration of follow-up, if any

The inputs used in this tool are: clinical features (a total of 26 clinical features, optional); US features (a total of 36 features). Size, composition, and echogenicity are the only data that must be provided for TNAPP to categorize the US as US 1 [low-risk], US 2 [intermediate-risk], or US 3 [high risk]); cytology features (a combined total of 45 options from which to select). These are comprised of required Bethesda categories (I-VI) (6), optional subcategories (33), or a combination of a main category and a subcategory (6) and molecular marker data can be used.

Table 2.8 summarizes the features of the risk calculators discussed above, along with delineating their strengths and weaknesses. Apart from the BWH thyroid nodule risk estimator, which does not utilize cytology data, other calculators are subject to the variability in interpretation of US or cytologic features.

Table 2.8 Thyroid nodule risk calculators

Inputs	Outputs	Link	Comments
ACR TI-RADS and AI TI-RADS: • Composition • Echogenicity • Shape • Margin • Echogenic foci	• Total points • TI-RADS score • Recommendation for FNA	https://tiradscalculator.com/ https://deckard.duhs.duke.edu/~ai-ti-rads/index.html	Most widely used US risk calculator, particularly among radiologists Is restricted to thyroid US features and size (does not consider clinical factors)
Malignancy risk estimation of lesions with AUS/FLUS: • Biopsy results (nuclear vs architectural atypia) • Diameter • Internal content • Shape • Margin • Echogenicity • Calcification	• Total score • Estimated malignancy risk in %	http://www.gap.kr/thyroidnodule_b3.php	It is restricted to nodules with AUS/FLUS It provides statistics about the risk of malignancy but not guidance about whether to perform FNA

(continued)

Table 2.8 (continued)

Inputs	Outputs	Link	Comments
The BWH thyroid nodule risk estimator: • Age at time of diagnosis • Sex • Largest diameter • Cystic content • Additional nodules (≥1 cm)	Risk of malignancy in %	https://thyroidcancerrisk.brighamandwomens.org/	Strengths: Simple, reproducible (due to relatively objective data used as inputs), and best suited for populations Weaknesses: By only employing a limited amount of reproducible data, it is best suited for evaluating risk of malignancy in populations rather than individual patients It provides statistics about the risk of malignancy but not guidance about whether to perform FNA

The thyroid nodule malignancy risk calculator—Spain		• Risk of malignancy in % • FNA recommendations	https://obgynreference.shinyapps.io/calccdt/	Requires data such as anti-thyroid antibodies which are not routinely performed in the evaluation of thyroid nodules
Patient characteristics: • Age • Sex • Family history of thyroid cancer (first degree relatives) • TSH • Autoimmune thyroiditis (positive antibodies)	*Nodule characteristics*: • Maximum diameter • Content • Echogenicity • Margins • Calcifications • Shape • Suspicious lymph node			

(continued)

Table 2.8 (continued)

Inputs		Outputs	Link	Comments
Cleveland Clinic calculator:		Probability of thyroid cancer (%)	https://riskcalc.org/ThyroidCancer/	Employs vascularity, which is no longer recognized as a key determinant of thyroid malignancy
(a) FNA—No: • Shape • Vascularity • TSH • Echo texture • Age • Margin • Tumor size • Calcification	b) FNA—Yes: • Shape • Vascularity • TSH • Echo texture • Calcification • Grooves • Pseudo-inclusions • Cellularity • Colloid (scant or abundant)			

TNAPP: (a) Clinical features (b) US features (c) Cytology features	• Eligibility for using TNAPP • AACE US category • AACE clinical category • FNA recommendations • ACR TI-RADS risk category • ACR TI-RADS biopsy advice • Probability of cancer (%) • If FNA available, recommendations on molecular testing, surgery, follow-up	https://aace-thyroid.deontics.com/dwe/int/public/welcome.jsp	Strengths: Interactive, comprehensive, paralleling CPG guidance Integrates clinical, sonographic, and cytologic variables together to assess risk Limited data required for each recommendation Guides the clinician at various stages: Eligibility to use the application, FNA and follow-up advice, post-FNA advice Modifies recommendations as more information is provided Weaknesses: Requires familiarity with the user interface Creation of an account login is necessary but is easy to do

Table 2.9 Recommendations based on various guidelines

Guideline	Score/risk category	FNA recommendation
2021 AACE/ ACE-AME (TNAPP)	Clinical 2; intermediate-risk/ US2	Consider FNA or monitor with repeat US at 18–24 months
2015 ATA	High suspicion	No FNA (as it is ≤1 cm)
ACR TI-RADS	Score 7 (2 for composition + 2 for echogenicity + 2 for borders +1 for macrocalcification); highly suspicious	No FNA (as it is ≤1 cm) or consider FNA after shared decision-making; if no FNA, follow annually for 5 years (as it is ≥0.5 cm)
AI TI-RADS	Score 7 (3 for composition + 2 for echogenicity + 2 for borders); highly suspicious	No FNA (as it is ≤1.5 cm) or consider FNA after shared decision-making; if no FNA, follow annually for 5 years (as it is ≥0.5 cm)
EU TI-RADS	TR 5; high risk	Consider FNA or active surveillance
K TI-RADS	K TI-RADS 5; high suspicion	No FNA (as it is ≤1 cm)

Case Conclusion:

FNA of the patient's 0.9 × 0.7 × 0.9 cm posterior right mid-pole nodule was performed, and cytology was consistent with papillary thyroid carcinoma (Bethesda category VI). She then underwent right hemithyroidectomy and pathology showed a 1.2 cm, unifocal, conventional papillary thyroid carcinoma with focal lymphovascular invasion and positive BRAF-V600E mutation.

This case highlights the discrepancy between recommendations, based on inclusion or exclusion of clinical features and variability in US size cut-offs informing guidance regarding FNA (Table 2.9).

Further Reading

Garber JR, et al. AACE thyroid nodule algorithmic tool. Endocr Pract. 2021;27(7):649–60.

Ha EJ, et al. US fine-needle aspiration biopsy for thyroid malignancy: diagnostic performance of seven society guidelines applied to 2000 thyroid nodules. Radiology. 2018;287(3):893–900.

Haugen BR, et al. 2015 American Thyroid Association management guidelines for adult patients with thyroid nodules and differentiated thyroid cancer: the American Thyroid Association guidelines task force on thyroid nodules and differentiated thyroid cancer. Thyroid. 2016;26(1):1–133.

Wildman-Tobriner B, Buda M, Hoang JK, Middleton WD, Thayer D, Short RG, Tessler FN, Mazurowski MA. Using artificial intelligence to revise ACR TI-RADS risk stratification of thyroid nodules: diagnostic accuracy and utility. Radiology. 2019;292(1):112–9. PMID: 31112088.

3 Thyroid Fine Needle Aspiration and Biopsy Techniques for Lesions in the Neck

Barry Sacks

Key Points

- Biopsy of neck masses is safe, can be done on an outpatient basis, and provides valuable diagnostic information.
- Thyroid FNA is best performed with 25G or 27G needles using capillary action, rather than active aspiration. Aspiration is only necessary when limited specimens are obtained with the capillary technique.
- In a heterogeneous thyroid nodule, aspirates should be obtained from different regions. In particular, hypoechoic areas should be specifically targeted.
- Core biopsies may be necessary for indeterminate lymph nodes, or unusual head, neck, and salivary gland masses.

B. Sacks (✉)
Department of Radiology, Beth Israel Deaconess Medical Center, Boston, MA, USA
e-mail: bsacks@bidmc.harvard.edu

L. S. Eldeiry et al. (eds.), *Handbook of Thyroid and Neck Ultrasonography*, Contemporary Endocrinology,
https://doi.org/10.1007/978-3-031-18448-2_3

- Specimens from conditions that involve either multiple or bilateral neck lymph nodes (in the absence of a known primary tumor) should be submitted for cytology and flow cytometry from a representative lymph node FNA. Depending on the initial cytology result, core biopsy may be necessary to establish a definitive diagnosis.

Introduction

This chapter discusses the practical aspects of fine needle aspiration (FNA) and core biopsies of a spectrum of neck lesions, including thyroid nodules, technical suggestions to obtain optimal samples, and several miscellaneous tips. A successful FNA alone will frequently establish the diagnosis in the majority of cervical lesions, is simple and safe to perform. For some lesions, performing both FNA and core biopsy at the initial procedure provides the most expeditious diagnosis and management.

Recommendations in the following sections dealing with specific organs or disease processes will include:

- When to pursue FNA alone versus when core biopsies are warranted.
- The number and type of specimens to be collected based on the potential diagnoses.
- The various media or fluids in which specimens should be submitted.
- Biopsy pitfalls and complications.

Case Presentation

A 52-year-old woman underwent total thyroidectomy for multifocal, bilateral papillary thyroid carcinoma (PTC), and parathyroid exploration for primary hyperparathyroidism. Four glands were

felt to have been identified at surgery, but the hyperparathyroidism persisted immediately postoperatively. Follow-up 4DCT (four-dimensional computed tomography, Fig. 3.1) demonstrated 2 areas of marked increased activity (enhancement), one in the left thyroid bed, just medial to the carotid artery, and the other in the right thyroid bed. This was confirmed on the follow-up ultrasound (Fig. 3.2).

Aspiration from the right thyroid bed lesion (Fig. 3.3) showed a parathyroid hormone (PTH) level of 8.5 pg/mL (6–65 pg/mL) and thyroglobulin of >30,000 ng/mL (<3 ng/mL). Cytology showed normal thyroid tissue. The PTH level was 4270 pg/mL from the left thyroid bed lesion. This confirmed a diagnosis of right thyroid remnant and a left-sided parathyroid adenoma. She

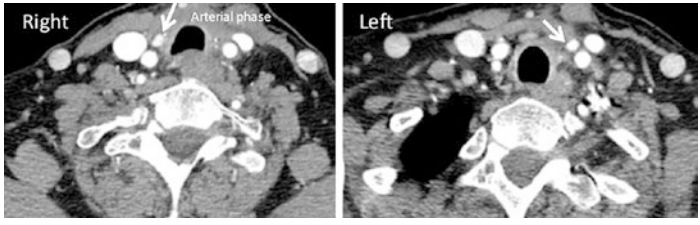

Fig. 3.1 4DCT demonstrating 2 enhancing lesions, one on each side (arrows), possibly representing 2 parathyroid adenomas

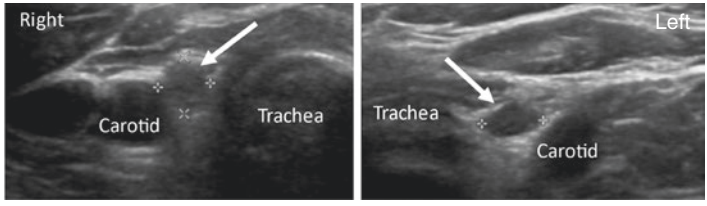

Fig. 3.2 Ultrasound confirmed the lesions: The left-sided lesion was well-defined, hypoechoic and vascular, consistent with a parathyroid adenoma (right panel, arrow). The right-sided lesion was less well-defined and had low-level internal echoes (left panel, arrow), but also vascular, consistent with either a parathyroid adenoma or thyroid remnant. The differential diagnosis of these lesions is indicated in Table 3.1. FNA of both lesions was performed

Table 3.1 Differential diagnosis

1. Right thyroid gland remnant
2. Persistent thyroid carcinoma/thyroid bed recurrence
3. Bilateral parathyroid adenomas

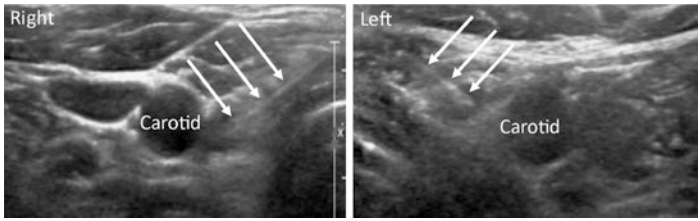

Fig. 3.3 Arrows indicating needle shaft in the right-sided lesion (right panel) and left-sided lesion (right panel)

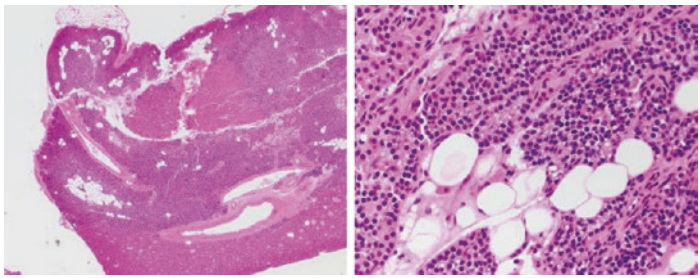

Fig. 3.4 Left panel: Parathyroid adenoma. There is a well-circumscribed lesion comprised predominantly of chief cells and oxyphilic cells with reduced stromal adipocytes (H&E, 4×). Right panel: Higher magnification of chief cells and scattered adipocytes at one of the edges of the adenoma (H&E, 10×)

underwent a unilateral neck exploration and successful left parathyroidectomy (Fig. 3.4), which cured the hyperparathyroidism. She continues routine ultrasound (US) follow-up for the papillary thyroid cancer.

Equipment: Needles and Core Biopsy Devices

For FNA, standard 25 gauge (G) or 27G needles are adequate (in some instances, a 21G). We prefer the technique of attaching the 25G needle to a syringe with the plunger removed. On entering the lesion, a back-and-forth motion draws the cellular specimen into the needle by capillary action, limiting the amount of blood. The specimen is then expressed onto a slide or into Cytolyt (Fig. 3.12). The needle can also be attached to a 5 or 10 cc Syringe for aspiration if the initial sample is minimal. Devices are available that allow single handed aspiration (Fig. 3.5).

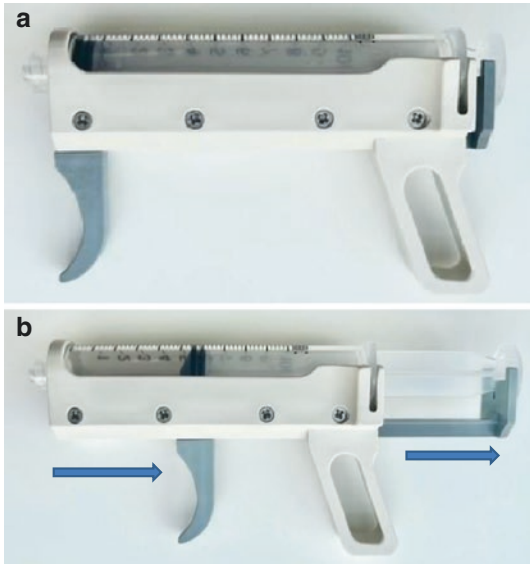

Fig. 3.5 Example of an aspiration device used single handed. (**a**) Syringe placed in device, in neutral position. Needle attached and introduced into lesion. (**b**) By pulling on the trigger, the plunger is withdrawn, creating suction. Device/syringe removed and specimen expressed into Cytolyt or a smear made

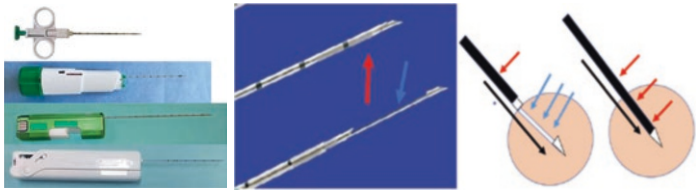

Fig. 3.6 Below left: Examples of available core biopsy needles. Middle: Demonstrates the inner core containing the notch (blue arrow) and the outer spring-loaded metallic sheath (red arrow). Right: The inner core, advanced into the lesion. Tissue collects in the notch (blue arrows). The spring-loaded outer metallic sheath is fired, slicing off the specimen (red arrows). The needles vary in caliber (13G–21G) and the notch varies from 11 to 22 mm in length. As expected, the larger the needle and the longer the notch, the larger the specimen

Multiple companies supply core biopsy devices with needle gauges from 11G to 21G. For neck lesions, 18G-21G needles are adequate. Most core biopsy devices have 2 important components: a sharp inner core containing a notch and a spring-loaded outer sleeve. The inner core is initially advanced into the lesion (manually or automatically). The tissue specimen prolapses into the notch. The outer core is then fired, slicing off the specimen. The notch size varies in depth and length. There are several designs (Fig. 3.6).

Solutions and Media

The FNA and core biopsy specimens are submitted in different solutions and media for optimal specimen preservation (Fig. 3.7).

Formalin	Cytolyte	RPMI	Saline	Afirma and ThyroSeq
Pathology	All Cytology	Flow Cytometry Cytogenetics	PTH Thyro-globulin	Thyroid Molecular Markers

Fig. 3.7 Standard solutions for FNA and core biopsy specimens

Thyroid Nodule Biopsy

- FNA specimens are submitted in Cytolyt solution (methanol-based solution, Cytyc Corporation). If separate smears are made, the slides are placed in 95% alcohol for PAP stain or are air-dried for Wright-Giemsa stain. When molecular markers are needed, the specimen is submitted in a special medium provided by the company (ThyroSeq, Afirma, etc.). Core biopsies are infrequently indicated.

Lymph Node

- Specimens required will depend on lymph node location and suspected pathology.
- For thyroid cancer: Cytology is collected in CytoLyt solution, and needle washings in 1 cc (mL) of normal saline (N/S) are sent for Thyroglobulin measurement.
- For head and neck tumor: Cytology is collected in CytoLyt solution; core biopsy specimen in 10% buffered formalin may be necessary.

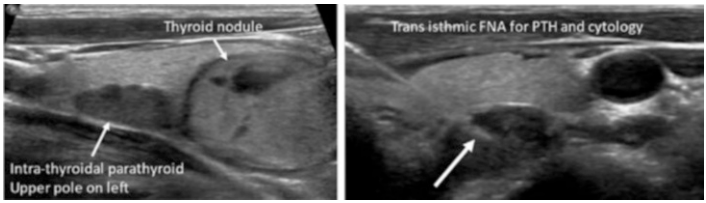

Fig. 3.8 Left panel: Sagittal view of left thyroid lobe with suspected intrathyroidal parathyroid adenoma superior to a thyroid nodule (arrows); Right panel: FNA of the lesion was performed for cytology and PTH washout (arrow shows needle tip in the nodule)

- Suspected lymphoma: Cytology is collected in CytoLyt solution and flow cytometry in RPMI medium (Roswell Park Memorial Institute).
- If core biopsies are obtained (18G or larger), specimens are collected in 10% buffered formalin for pathology and additional samples in RPMI for cytogenetics.
- For suspected parathyroid adenoma: PTH sample is collected in ½ to 1 cc N/S. If the lesion is intrathyroidal, add cytology in Cytolyt solution (in case the PTH is negative, cytology will establish the nature of the intrathyroidal nodule) (Fig. 3.8).

Biopsy Techniques

Preparation

Protocols vary from institution to institution and between inpatient and outpatient sites. Teaching institutions usually require gown, mask, gloves, and the transducer in a sterile sheath. However, for outpatient sites, simple protocols may be more practical. After standard skin preparation with a sterile solution, the ultrasound probe is wiped with absolute alcohol to prevent infection. This measure has been proven safe and effective.

Anesthesia

The approach to anesthesia also varies tremendously. Some clinicians use no local anesthesia, or a topical/skin spray for thyroid FNA, such as ethyl chloride. Our preference is to use adequate lidocaine 1% anesthesia, injected from the skin down to the thyroid capsule. Using this technique, the lidocaine volume is 3–4 cc, which typically results in a painless procedure (and a happier patient). This also allows the operator to make as many passes as necessary to obtain a diagnostic sample. For other neck lesions, particularly core biopsies, standard local anesthesia is generously used.

US Guidance Techniques (Fig. 3.9)

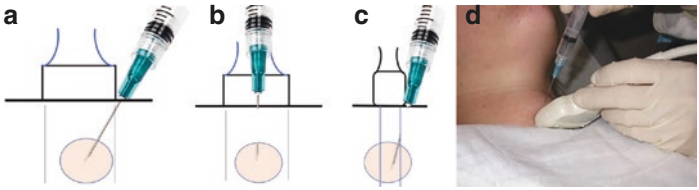

Fig. 3.9 The diagrams above demonstrate two optional approaches to ultrasound-guided FNA. (**a**) Demonstrates the needle approach from the side of the transducer, allowing continuous visualization of the needle from skin, through the subcutaneous tissue, and into the nodule (US field between the two thin vertical lines). This also allows accurate targeting of specific areas within the nodule. (**b**) Demonstrates the puncture from a site in the middle of the transducer. (**c**) Is a view from the narrow side, also demonstrated in image (**d**) With this approach, the needle cannot be seen until the tip enters the ultrasound beam path within the target, usually as a single high reflective echo. Many clinicians prefer this approach but its main value is in ultrasound-guided vascular access

Thyroid Nodules

The indications and criteria for thyroid nodule biopsy are dealt with extensively in other chapters of this handbook.

- Although thyroid nodule biopsy can be performed from either side, optimal access is contralateral to the lesion, using a trans-isthmic approach. The thyroid arterial supply enters the lobes laterally. The medial to lateral approach (Figs. 3.10, 3.11, 3.12, 3.13, and 3.14), therefore, reduces potential bleeding and bruising.
- Sometimes the lateral approach is necessary, particularly when the target nodule is in the posterior and medial aspect of the lobe, limiting adequate access from the opposite side.

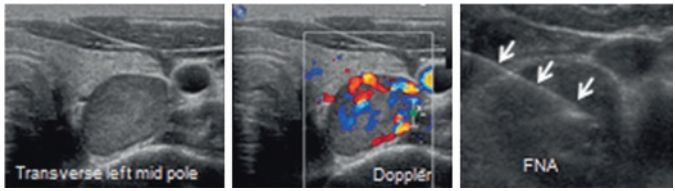

Fig. 3.10 Left, middle panels: Large, hypoechoic and hypervascular left thyroid nodule. Right: Trans-isthmic FNA performed, with the entire length of the needle visible (arrows)

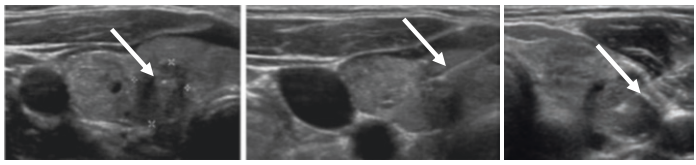

Fig. 3.11 Left and middle panels: Suspicious lesion in the right thyroid lobe, taller than wide (arrow, left), with microcalcifications. Trans-isthmic FNA was performed. Right panel: Posterior lesion on the left thyroid. FNA access is better from a lateral approach

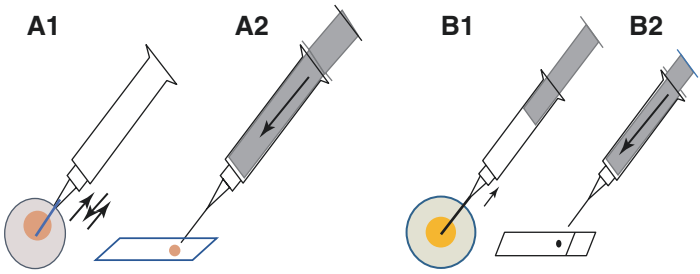

Fig. 3.12 Capillary action. A1: The plunger of the syringe is removed, the barrel/needle is advanced into the lesion. After forward and back motions, the plunger is reintroduced (A2) and the specimen is ejected onto a slide or into CytoLyt solution. Standard aspiration technique. B1: The needle, attached to a syringe, is advanced into the lesion, suction is applied during a forward and back movement. B2: The specimen is then ejected onto a slide or irrigated into CytoLyt solution

Fig. 3.13 Left, middle panels: Patient with hyperparathyroidism and a suspicious intrathyroidal nodule that may represent either thyroid vs parathyroid. Right panel: FNA (arrow) done with specimens sent for cytology and PTH. The PTH was >5000 pg/mL (measurement of thyroglobulin is not helpful in this case because the needle has to pass through thyroid tissue to access the lesion)

- It is advisable to obtain 3–4 separate samples for thyroid FNA using new 25G needles for each pass and to target different regions within the same nodule. Sampling the most heterogeneous and/or hypoechoic area is advised, as it is likely to be the most de-differentiated.
- Capillary action vs active aspiration: For the capillary technique, the syringe plunger is removed and a 25G needle is attached only to the syringe barrel. On entering the nodule, the

Fig. 3.14 Patient with persistent hyperparathyroidism after surgery that included a left lobectomy. Left 2 panels: Sestamibi scan shows activity in the right neck and a small focus on the left (arrows). The differential diagnosis includes thyroid remnant vs parathyroid adenoma. Third panel: US confirms the lesion on the left, lying on a tortuous right brachiocephalic artery (arrow). Right panel: FNA of the lesion (arrow) with PTH measurement demonstrated marked PTH elevation, confirming a parathyroid adenoma

needle/syringe barrel combination is moved back and forth a few times, then removed. The plunger is reinserted and the specimen is either smeared on a slide or irrigated into ThinPrep CytoLyt solution. In active aspiration compared to capillary action, the likelihood of a moderately bloody specimen is increased, diluting the cellular component. Aspiration is necessary when the initial passes yield limited material.

FNA Specimens

- Some institutions have the benefit of having a cytologist on hand to immediately prepare and review the adequacy of the specimen. At most non-academic sites, this service is not available and samples need to be transported to the laboratory. As a result, excellent technique and specimen handling are imperative to getting a diagnostic specimen.

Molecular Markers

- When the cytology is indeterminate, repeat FNA for molecular markers may be performed (see indications in the chapter dedicated to this topic).

- For clinicians with substantial experience in thyroid nodule evaluation, particularly if the US appearance of the nodule is concerning, the 2-step protocol can be modified. At the initial FNA procedure, an extra specimen for molecular markers can be collected and stored in a freezer, pending the cytology result. If the cytology is benign, the specimen is discarded; if indeterminate, the sample is submitted for genetic testing. The advantage of this approach is twofold. First, a repeat biopsy is avoided and second, the diagnostic process is significantly sped up. Additionally, there is a lower likelihood that a second FNA will miss the targeted area.

Thyroid Cyst Aspiration and Sclerosis

- Patients with large thyroid cysts may require aspiration to relieve pressure symptoms or treat a prominent visible nodule. The cysts may be simple or complex (solid and cystic). The cystic component often originates from spontaneous (often painless) hemorrhage into a spongiform nodule, with the fluid containing low-level echoes on US or dependent echogenic material (usually due to debris, proteinaceous or blood). The reason for spongiform lesions spontaneously bleeding is still unclear.
- The presence of a solid component requires FNA for cytologic evaluation before contemplating sclerosis of the cyst.
- Recurrence rates after cyst aspiration alone are about 70%.
- Lastly, if acute or subacute hemorrhage is detected, aspiration/sclerosis should be delayed for 6–12 weeks to allow the original bleeding site to heal. Premature aspiration often results in re-bleeding and re-accumulation into the cyst.

Procedure

Aspiration: The initial setup is identical to thyroid nodule FNA. Following administration of local anesthesia, a 21G needle is advanced into the cyst and aspiration is performed. If the fluid is too viscous, a larger (18G) needle may be required. If the fluid is still too viscous, gentle repeated irrigation with small volumes

of saline and aspiration will dilute the contents and allow the cyst to ultimately be completely collapsed.

Sclerosis: Once the cyst has been aspirated completely, a tiny bubble of gas is injected to confirm the needle tip is still in the cyst lumen, then either absolute alcohol or doxycycline is introduced into the cyst cavity. Doxycycline (100 mg ampule reconstituted with 1 cc of Lidocaine) is preferred, as it is safe and very effective (absolute alcohol can be painful if a small leak into the surrounding tissues occurs). The needle is then withdrawn. Follow-up US at 3 months is recommended. In larger cysts, there is a possibility that a repeat procedure may be required.

Lymph Node Aspiration

- FNA/biopsy technique for lymph nodes is strongly influenced by the patient's clinical presentation. If there is a known history of or current thyroid malignancy, nodal FNA is done to exclude metastatic disease, or during pre-operative assessment, to guide the surgical approach.
- Confirmed pathologic lateral neck lymph nodes warrant a lateral neck dissection, in addition to total thyroidectomy. Elevated thyroglobulin post-thyroidectomy demands a careful search for nodal metastases.
- Lymph node biopsy involves 25–27G US-guided active FNA (1–2 passes), with samples submitted for cytology and thyroglobulin washout (needle irrigated into 1–2 cc saline and submitted in a red top tube).
- Suspicious nodes in the absence of a thyroid cancer history are submitted for cytology (to exclude thyroid or other neck malignancy), thyroglobulin, and flow cytometry (in RPMI solution), to exclude lymphoma.

FNA vs Core Biopsy

- In general, in most neck lesions, FNA alone is performed as the first step, with the decision to perform core biopsy depending on cytology results.

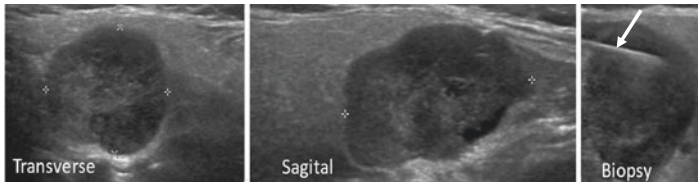

Fig. 3.15 Left, middle panels: Two images of an indeterminate right parotid gland mass. Right panel: Biopsy of the lesion (arrow). Usually with these lesions, both FNA and core biopsies yield the best results

- If lymphoma is suspected based on initial cytology and flow cytometry results, core biopsies will be needed for pathology and cytogenetics, to more accurately characterize the lesion for treatment purposes.
- Surgical excision may occasionally be required to obtain adequate tissue for more sophisticated molecular studies.
- For salivary gland masses, both FNA and core biopsies can be performed at the initial biopsy procedure. An acceptable alternative would be to perform the FNA for cytology and follow-up core only if indicated based on the cytology result (Fig. 3.15).

Parathyroid Adenomas

- The combination of ultrasound and 4DCT can diagnose and localize a single parathyroid adenoma or multi-gland disease in the vast majority of patients with hyperparathyroidism, whether the glands are in an orthotopic (eutopic) or ectopic location. As a result, the need for parathyroid FNA for parathyroid hormone (PTH) is limited to complex cases, including postoperative recurrent or persistent disease that remains unresolved after performing the usual imaging techniques. Additional examples include intrathyroidal parathyroid (Fig. 3.8), or patients with hyperparathyroidism and Hashimoto's thyroiditis, in whom the presence of reactive lymph nodes near the thyroid gland makes it difficult to differentiate lymph nodes from parathyroid.

- The FNA technique is identical to the one for nodal aspiration. However, usually only a single needle pass is required. The specimen is actively aspirated and submitted in a red top tube containing 0.5–1 cc of saline. PTH assay is ordered and a significant elevation (usually in the thousands) definitively confirms the diagnosis of a parathyroid adenoma.

Salivary Gland and Other Miscellaneous Neck Masses

- The biopsy approach to these lesions will vary depending on the specific circumstances. In some situations, FNA may adequately establish the diagnosis, while in others it may be necessary to obtain a larger core biopsy specimen for pathology (or consider core biopsy if the initial cytology is indeterminate or warrants a larger specimen for diagnosis).

Further Reading

Chen C-N, Yang T-L. Review Article: Application of ultrasound-guided core-biop head and neck. J Med Ultras. 2014;22(3):133–9.

Haugen BR, et al. The American Thyroid Association guidelines task force on thyroid nodules and differentiated thyroid cancer. Thyroid. 2016;26(1):1–133.

Learned KO, Lev-Toaff AS, Brake BJ, Wu RI, Langer JE, Loevner LA. US-guided biopsy of neck lesions: the head and neck neuroradiologist's perspective. Radiographics. 2016;36(1):226–43.

Pynnonen MA, Gillespie MB, Roman B, Rosenfeld RM, Tunkel DE, Bontempo L, et al. Clinical practice guideline: evaluation of the neck mass in adults executive summary. Otolaryngol Head Neck Surg. 2017;157(3):355–71.

Singh Nanda KD, Mehta A, Nanda J. Fine-needle aspiration cytology: a reliable tool in the diagnosis of salivary gland lesions. J Oral Pathol Med. 2012;41(1):106–12.

Tessler FN, et al. ACR thyroid imaging, reporting and data system (TI-RADS): white paper of the ACR TIRADS committee. J Am Coll Radiol. 2017;14(5):587–95.

Overview of the Bethesda System for Reporting Thyroid Cytopathology

4

Teresa H. Kim and Jeffrey F. Krane

Key Points

- Fine needle aspiration (FNA) is the most valuable screening and diagnostic test for thyroid nodules and plays a crucial role in managing patients with thyroid cancer.
- The Bethesda System for Reporting Thyroid Cytopathology classifies aspirates of thyroid nodules into six diagnostic categories.
- Each diagnostic category is associated with an evidence-based cancer risk and clinical management guidelines, which are endorsed by the American Thyroid Association.
- Incorporating the clinical and radiologic findings, thyroid FNA allows for a standardized, team-based approach to managing patients with thyroid nodules.

T. H. Kim · J. F. Krane (✉)
Department of Pathology and Laboratory Medicine, David Geffen School of Medicine at UCLA, Los Angeles, CA, USA
e-mail: TeresaKim@mednet.ucla.edu; jkrane@mednet.ucla.edu

L. S. Eldeiry et al. (eds.), *Handbook of Thyroid and Neck Ultrasonography*, Contemporary Endocrinology,
https://doi.org/10.1007/978-3-031-18448-2_4

Introduction

Thyroid nodules are very common, found in up to 70% of adults by imaging.

Although the majority are benign, it is important to identify the small percentage of nodules that are malignant and require surgical management. The recommended workup includes a dedicated ultrasound examination, which risk stratifies the nodule based on size and ultrasonographic features. If the criteria for biopsy are met, a fine needle aspiration (FNA) is performed. Since its introduction, FNA has become the most valuable screening and diagnostic test for thyroid nodules. Many are now performed under ultrasound guidance, with optional rapid on-site evaluation to ensure proper placement of the needle, which improves accuracy and decreases the number of nondiagnostic specimens. The results are then reported using The Bethesda System for Reporting Thyroid Cytopathology (TBSRTC).

TBSRTC is the most widely used standardized system for reporting thyroid fine needle aspiration biopsy results. TBSRTC is a six-tiered scheme with evidence-based anticipated risk of malignancy (ROM) and standard treatment approaches associated with each diagnostic category.

Since its introduction, TBSRTC has been widely adopted worldwide and endorsed by the American Thyroid Association. It outlines six distinct diagnostic categories and provides a standardized, well-defined approach to reporting thyroid cytopathology. Each category is associated with an anticipated risk of malignancy (ROM) and linked to evidence-based clinical management guidelines (Table 4.1). As a result, TBSRTC not only allows for improved communication within a healthcare team, but also provides guidance for appropriate clinical management. A brief discussion of each diagnostic category within TBSRTC follows.

Table 4.1 The 2017 Bethesda system for reporting thyroid cytopathology

Diagnostic category	Risk of malignancy if NIFTP is not considered malignant (%)	Risk of malignancy if NIFTP is considered malignant (%)	Usual management
Nondiagnostic or unsatisfactory	5–10	5–10	Repeat FNA with ultrasound guidance
Benign	<3	<3	Clinical and sonographic follow-up
Atypia of undetermined significance or follicular lesion of undetermined significance	6–18	~10–30	Repeat FNA, molecular testing, or lobectomy
Follicular neoplasm or suspicious for a follicular neoplasm	10–40	25–40	Molecular testing or lobectomy
Suspicious for malignancy	45–60	50–75	Near-total thyroidectomy or lobectomy
Malignant	94–96	97–99	Near-total thyroidectomy or lobectomy

NIFTP noninvasive follicular thyroid neoplasm with papillary-like nuclear features

Table adapted from: Cibas ES, Ali SZ. The 2017 Bethesda System for Reporting Thyroid Cytopathology. Thyroid. 2017;27(11):1341–1346. doi:10.1089/thy.2017.0500

Discussion

Nondiagnostic

This category includes specimens that are unsatisfactory for interpretation due to scant cellularity or are compromised by obscuring blood, air-drying artifact, or overly thick smears (Fig. 4.1a).

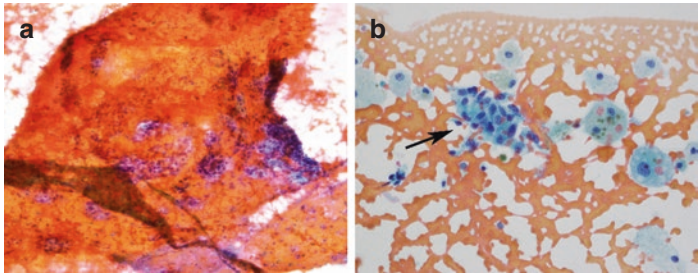

Fig. 4.1 Nondiagnostic. (**a**) Extensive blood and clotting artifact obscures the follicular cells and distorts architecture, precluding evaluation. (**b**) Nodules with cystic degeneration often contain abundant hemosiderin-laden macrophages and cyst lining cells (arrow). If insufficient follicular cells are present, cystic aspirates are classified as nondiagnostic

Normal thyroid aspirates consist of follicular cells and colloid. A thyroid FNA requires six or more groups of well-visualized follicular cells, with at least ten cells in each group, to be considered adequate for evaluation. Specimens that fail to meet the criteria for adequacy, including cystic lesions (Fig. 4.1b), are considered nondiagnostic.

The three exceptions to this rule include cases with any atypia, abundant colloid indicative of a benign colloid nodule, or specific diagnostic conditions such as chronic lymphocytic (Hashimoto) thyroiditis. The precise ROM for nondiagnostic nodules varies but is estimated as 5–10%. Nondiagnostic nodules are generally managed with a repeat FNA under ultrasound guidance with rapid on-site evaluation. In up to 60% of cases, a subsequent FNA results in a diagnostic interpretation, with a majority proving to be benign. However, FNAs that are repeatedly nondiagnostic may require surgery depending on other clinical and radiologic factors.

Benign

Since most thyroid nodules are benign, the most common FNA interpretation is a benign result. This category comprises approximately 60–70% of all cases and may be subclassified further into

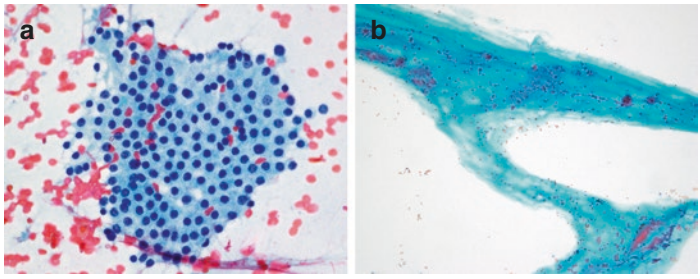

Fig. 4.2 Benign follicular nodule. (**a**) Macrofollicles rupture with FNA and appear as flat, monolayered sheets of evenly spaced follicular cells on cytologic preparations. Benign follicular cells have round to oval nuclei, finely granular chromatin, smooth nuclear contours, inconspicuous nucleoli, and scant amounts of delicate cytoplasm. (**b**) Colloid may have a watery or dense appearance staining pink or green-blue on alcohol-fixed Papanicolaou-stained slides. Abundant colloid favors a benign process and, if sufficiently plentiful, may be called benign even if follicular cells are absent

specific entities. A diagnosis of "benign follicular nodule" on cytology encompasses a group of histologic entities with identical cytologic features, including nodular hyperplasia in multinodular goiter, adenomatoid nodules, and colloid nodules. These are all predominantly composed of macrofollicles that once aspirated rupture to release luminal colloid and appear as flat sheets of unremarkable follicular cells (Fig. 4.2).

Benign follicular cells have small and round nuclei, smooth nuclear contours, uniformly granular chromatin, and scant to moderate amounts of delicate cytoplasm. Mild nuclear size variation and oncocytic (Hürthle cell) or cystic degenerative changes with hemosiderin-laden macrophages are acceptable. A colloid nodule may be sparsely cellular, but is considered benign as it also consists of macrofollicles with abundant colloid.

Hashimoto thyroiditis aspirates are characterized by numerous lymphoid cells admixed with normal follicular cells and occasional Hürthle cells (Fig. 4.3). Although generally straight forward on cytology, the diagnosis should be confirmed clinically by serologic tests. Examples of other less common benign conditions

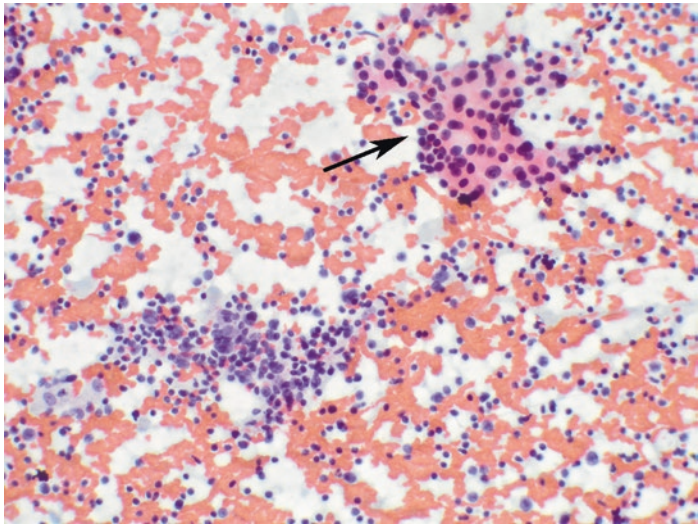

Fig. 4.3 Chronic lymphocytic (Hashimoto) thyroiditis. A group of Hürthle cells (arrow) with abundant granular cytoplasm is present in a background of abundant polymorphous lymphocytes

encountered in FNA specimens include subacute (de Quervain) thyroiditis, amyloid goiter, and black or pigmented thyroid.

A benign interpretation is associated with a very low ROM (<3%). These patients are managed conservatively, and follow-up intervals are determined by risk stratification algorithms based on ultrasound patterns.

Atypia of Undetermined Significance (AUS)/ Follicular Lesion of Undetermined Significance (FLUS)

This category encompasses a heterogeneous group of aspirates demonstrating a degree of atypia that is greater than normally attributable to benign, reactive changes, but insufficient for a malignant or suspicious diagnosis. Since "AUS" and "FLUS" are synonymous, one term should be selected for use by a laboratory

and further subclassified using descriptive language. Subclassification is encouraged to enhance communication between pathologists and clinicians and is particularly important for distinguishing the presence of cytologic/nuclear atypia, which has demonstrated a greater ROM than AUS with architectural atypia or a prominent Hürthle cell component.

TBSRTC defines six common patterns of AUS/FLUS and the preferred language used to describe the degree and nature of atypia. One pattern demonstrates focal or extensive, but mild **cytologic atypia**, raising the possibility of a papillary thyroid carcinoma (PTC) (Fig. 4.4a). In contrast, **AUS with architectural atypia** may be appropriate when the possibility of a follicular neoplasm cannot be ruled out, due to the diffuse presence of microfollicles (defined as 6 to 15 follicular cells arranged in a circular pattern around a central portion of colloid) in a scantly cellular specimen (Fig. 4.4b).

A combination of both **cytologic and architectural atypia** can be observed in the same specimen as these patterns are not mutually exclusive. Scantly cellular specimens may contain a pure population of Hürthle cells (**AUS, Hürthle cell type**), making it impossible to rule out the chance of a Hürthle cell neoplasm. Hürthle cells refer to oncocytic cells with enlarged, often eccentri-

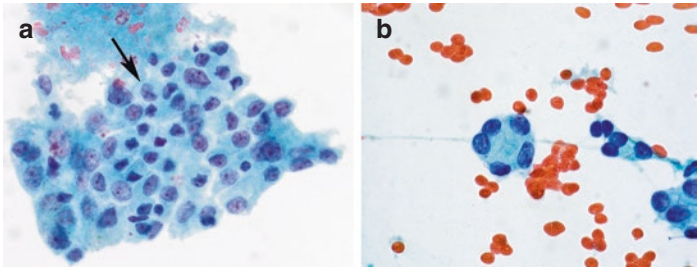

Fig. 4.4 AUS/FLUS. (**a**) Follicular cells show mild cytologic atypia associated with Hürthle cell change. Nuclear enlargement, pallor, pinpoint nucleoli, and occasional nuclear grooves (arrow) are seen. Intranuclear pseudoinclusions are absent. (**b**) High power image of a microfollicle. When predominant in a modestly cellular specimen, a diagnosis of AUS/FLUS with architectural atypia is warranted

cally located nuclei, prominent nucleoli, and abundant finely granular cytoplasm. **AUS, Hürthle cell type**, may also apply to cellular samples composed of bland Hürthle cells in a clinical setting that suggests benignity, such as Hashimoto thyroiditis or multinodular goiter.

This category is intended to be used as a last resort, and it is recommended to make up no more than 10% of all thyroid FNAs. The implied ROM ranges from 10% to 30%. Several options for managing AUS/FLUS nodules are available, including repeat FNA, molecular testing, or diagnostic lobectomy.

Molecular testing helps triage patients with AUS/FLUS or FN/SFN results and is recognized by TBSRTC and the ATA as a valid approach to further inform clinical management. Most classic and tall cell variants of PTC harbor a *BRAF* V600E mutation, while many follicular variants of PTC and follicular neoplasms have *RAS* or *RAS*-like mutations. Enhanced understanding of the genetic alterations underlying thyroid tumorigenesis has created a potential role for the routine use of commercially available molecular tests, such as the Afirma Genomic Sequencing Classifier and ThyroSeq v.3. The high negative predictive values of the most recent iterations of these tests make it appropriate to triage patients with negative results to conservative management.

Follicular Neoplasm (FN)/Suspicious for a Follicular Neoplasm (SFN) (Specify if Oncocytic/Hürthle Cell Type)

The FN/SFN category identifies nodules with significant architectural abnormalities that raise the possibility of a follicular carcinoma. On histologic evaluation, follicular carcinoma is distinguished from an adenoma by the presence of capsular and/or vascular invasion. However, these criteria cannot be reliably assessed on cytology. Therefore, FNA of follicular neoplasms is considered a screening, rather than a diagnostic test.

In contrast to benign follicular nodules that are comprised of predominantly macrofollicles with abundant colloid, FN/SFN lesions demonstrate follicular cells arranged in crowded, overlap-

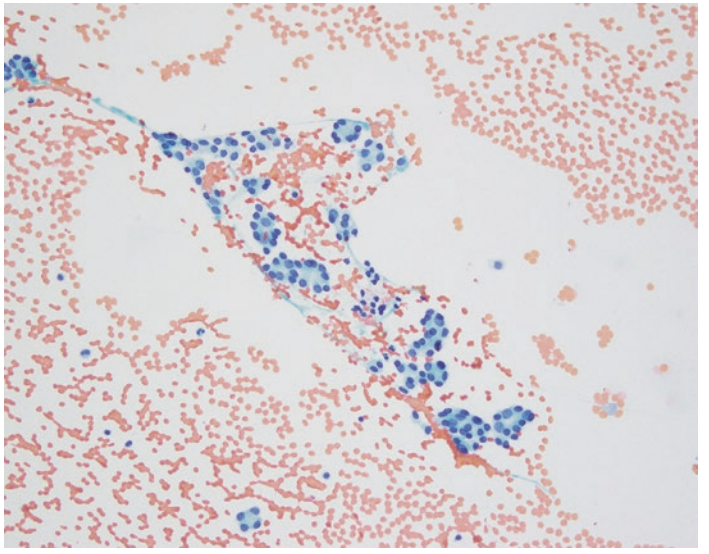

Fig. 4.5 FN/SFN. This cellular aspirate shows crowded, uniform follicular cells predominantly in microfollicular arrangements

ping groups, microfollicles, or trabeculae, with scant to absent colloid (Fig. 4.5).

Most cases diagnosed as FN/SFN are ultimately benign, but 25–40% of cases prove to be malignant. As a result, the differential diagnosis includes benign follicular nodules, a subset of which can have prominent microfollicles without clinical significance, as well as other follicular-patterned lesions, such as noninvasive follicular thyroid neoplasm with papillary-like nuclear features (NIFTP). Strict histologic criteria preclude a definitive diagnosis of NIFTP on FNA, but cytologic preparations often show a predominance of microfollicles in addition to mild nuclear changes that are abnormal enough to fall within the indeterminate categories (Fig. 4.6).

These lesions are classified as FN/SFN when nuclear changes are mild and intranuclear pseudoinclusions, papillae, or psammoma bodies are absent. When nuclear changes are more pronounced and these suspicious features are present, a diagnosis of at least suspi-

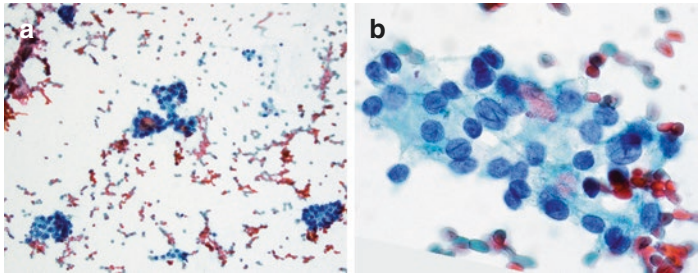

Fig. 4.6 NIFTP. (**a**) Aspirates show microfollicles with nuclear crowding and enlargement. (**b**) At high power, powdery chromatin and nuclear grooves are seen. The diagnosis of NIFTP requires histologic examination, but FNA specimens are usually classified as AUS/FLUS, FN/SFN, or suspicious for PTC. An explanatory note suggesting the possibility of NIFTP is recommended when the diagnosis is suspected

cious for malignancy is warranted. If NIFTP is suspected on FNA, TBSRTC suggests adding an explanatory note to encourage limited surgical management (typically diagnostic lobectomy).

The interpretation "suspicious for a follicular neoplasm/ follicular neoplasm, Hürthle cell type (FNHCT/SFNHCT)" refers to a subset of aspirates within the FN/SFN category that consists (almost) exclusively of Hürthle cells and raises the possibility of a Hürthle cell carcinoma (Fig. 4.7).

As with its conventional follicular counterpart, it is impossible to identify the presence of invasion to confirm malignancy on cytology. However, the mere presence of Hürthle cells is not diagnostic of FNHCT/SFNHCT. For example, Hashimoto thyroiditis often shows Hürthle cells admixed with numerous lymphoid cells. Similarly, Hürthle cell change is a common focal finding in benign follicular nodules. In addition to extensive Hürthle cell change, the most concerning lesions in the FNHCT/SFNHCT category also show the following worrisome cytologic or architectural features: small cell or large cell dysplasia, dyscohesion (loosened inter-cellular connections), or crowding. The background contains little to no colloid and transgressing blood vessels may also be seen.

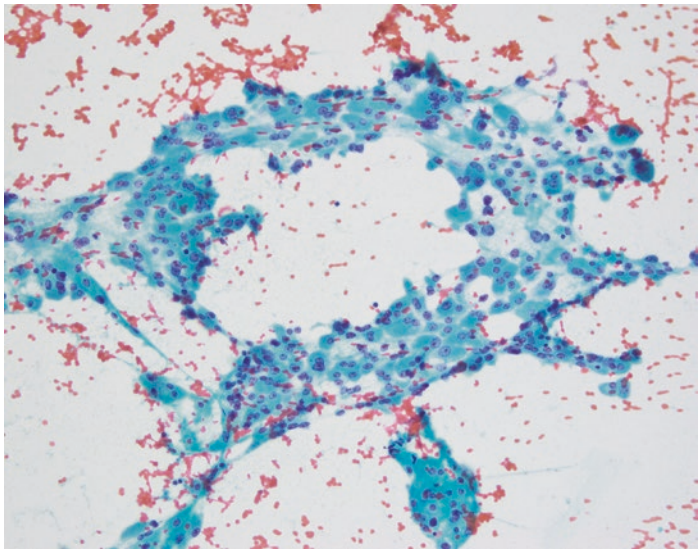

Fig. 4.7 FNHCT/SFNHCT. Cellular smears show a pure population of Hürthle cells arranged in loosely cohesive groups. Colloid and lymphocytes are absent from the background

As a minority of FN/SFN cases are malignant, they are typically managed conservatively with diagnostic lobectomy or molecular testing with the potential to avoid surgery.

Suspicious for Malignancy (SFM)

"Suspicious for malignancy" (SFM) is the last indeterminate category in TBSRTC and is indicated for cases with cytomorphologic features that are strongly suspicious for malignancy but are quantitatively and/or qualitatively insufficient for a conclusive diagnosis. SFM includes a variety of potential malignancies, although most cases are suspicious for PTC (Fig. 4.8).

As with AUS/FLUS, this interpretation should be used judiciously to ensure that patients are managed appropriately. Often the sample may lack cellularity or the characteristic features are

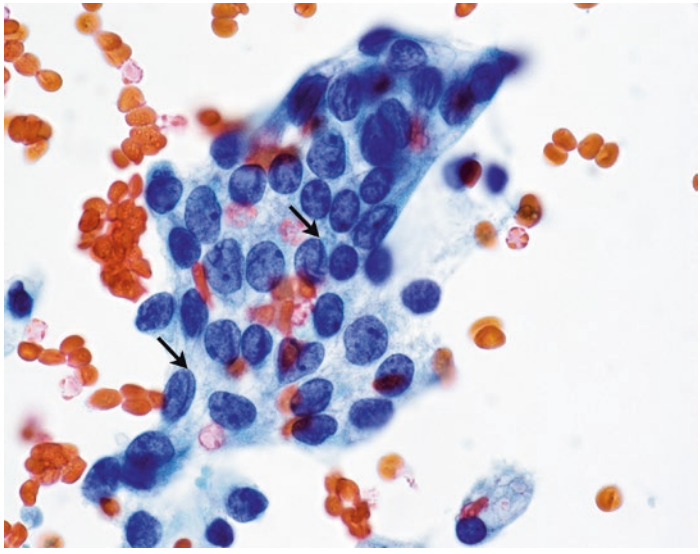

Fig. 4.8 Suspicious for papillary thyroid carcinoma. Sheets of follicular cells demonstrate nuclear enlargement, crowding, powdery chromatin, and nuclear grooves (arrows). Intranuclear pseudoinclusions, psammoma bodies, and papillary architecture are absent

patchy and incomplete. A SFM interpretation still conveys a degree of uncertainty but suggests that malignancy is considered more likely than not. Given the relatively high ROM (50–75%), ancillary molecular studies are not utilized for risk stratification. Instead, these cases are managed surgically, and the clinical and radiologic findings are crucial for determining the extent of surgery.

Malignant

PTC is the most common cancer of the thyroid, accounting for approximately 85% of malignancies. Its characteristic nuclear features are readily identified on cytology, making FNA biopsy an ideal diagnostic test for PTC (Fig. 4.9). Common features are

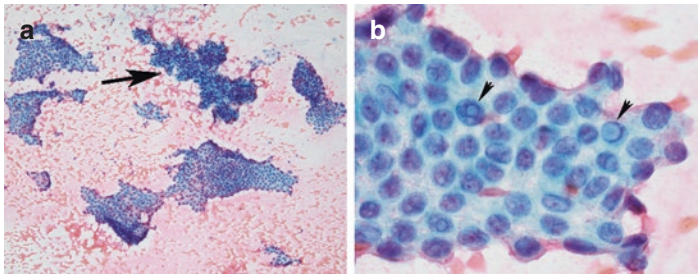

Fig. 4.9 Papillary thyroid carcinoma. (**a**) Hypercellular smears show sheets of malignant cells with a syncytial-like appearance. At low power, nuclear enlargement, pallor, and crowding are appreciated. A papillary structure with a fibrovascular core is present (arrow). (**b**) At high power, the nuclear features of papillary thyroid carcinoma, including nuclear membrane irregularities, grooves, and numerous pseudoinclusions (highlighted with arrows), are readily identified

nuclear grooves and pseudoinclusions, membrane irregularities, chromatin pallor, crowding, or overlapping. Classical PTC is the most common type and has papillary architecture, which is appreciable on FNA as fibrovascular cores lined by malignant cells. Other helpful features include psammomatous calcifications and multinucleated giant cells. In most cases, it is difficult and unnecessary to identify the specific subtype of PTC. However, some variants can demonstrate more focal or subtle nuclear changes. Patients with low-risk PTC up to 4 cm in size may be treated with lobectomy, according to current ATA guidelines, otherwise with near-total thyroidectomy, and prognosis is excellent overall.

Poorly differentiated (insular) thyroid carcinoma has an intermediate degree of cytomorphologic atypia and clinical behavior between a well-differentiated and an undifferentiated thyroid carcinoma. The diagnosis is difficult to make on FNA and rests on histologic evaluation. However, cytologic preparations are usually hypercellular and demonstrate nuclear overlapping, with nested, trabecular, or solid architectural patterns (Fig. 4.10). Tumor cells are typically uniform, but more pronounced atypia may also be appreciated. The presence of increased mitotic activ-

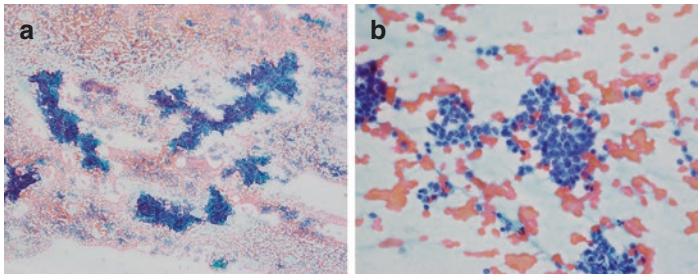

Fig. 4.10 Poorly differentiated thyroid carcinoma. (**a**) Low magnification image shows abundant groups of monotonous follicular cells arranged in crowded insulae. (**b**) Tumor cells show mild nuclear atypia with granular chromatin and overlapping nuclei. Scattered isolated tumor cells are present in the background

ity, apoptosis, and necrosis further suggests the diagnosis. Poorly differentiated thyroid carcinoma can resemble other entities, such as follicular neoplasms, medullary thyroid carcinoma, or anaplastic carcinoma. Immunohistochemical stains may help with the distinction on FNA, but surgical pathology evaluation is often necessary for definitive classification.

Undifferentiated (anaplastic) thyroid carcinoma is even more unfavorable than poorly differentiated thyroid carcinoma. This disease behaves aggressively and clinically presents as a rapidly enlarging mass, which has often already spread to adjacent structures or distant sites. The cytologic appearance is variable, comprised of large, markedly pleomorphic tumor cells that can demonstrate epithelioid, spindled, rhabdoid, or giant-cell morphology (Fig. 4.11). The nuclear features are undoubtedly malignant, and necrosis and abundant mitoses are also present. A proportion of cases focally demonstrate features of a well-differentiated precursor lesion, either PTC or follicular carcinoma. Prognosis is extremely poor, and the diagnosis relies on clinical and radiologic correlation.

In contrast to the previously described thyroid neoplasms which are derived from follicular cells, medullary thyroid carcinoma (MTC) arises from the parafollicular (C) cells of the thyroid. MTC is rare, accounting for 1–2% of all thyroid carcinomas.

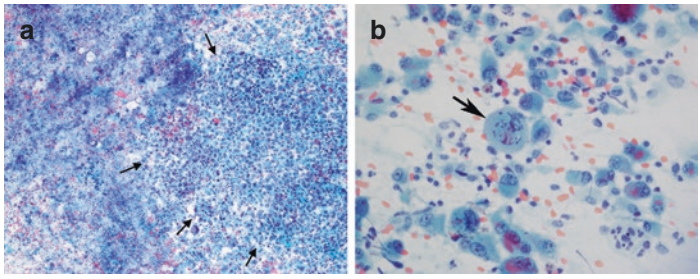

Fig. 4.11 Anaplastic thyroid carcinoma. (**a**) Hypercellular smear shows abundant tumor necrosis (left portion of image) with well-preserved, malignant cells (highlighted with arrows in right portion of image). (**b**) Significant pleomorphism is seen with enlarged, eccentrically located nuclei, irregular nuclear contours, coarse chromatin, prominent nucleoli, and abundant dense cytoplasm. Increased mitotic activity is present (arrow)

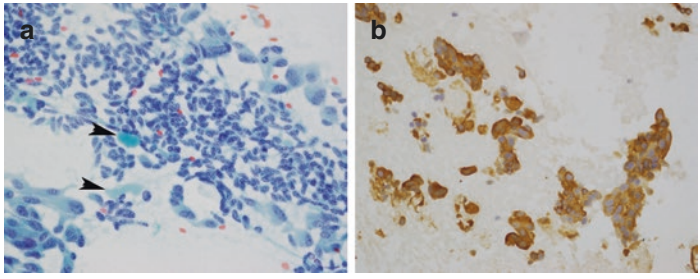

Fig. 4.12 Medullary thyroid carcinoma. (**a**) Hypercellular preparations are composed of abundant, loosely cohesive, and variably shaped (epithelioid, plasmacytoid, and spindled) cells. The background contains scattered amorphous material, consistent with amyloid (arrows). The malignant cells show stippled "salt and pepper" chromatin, anisonucleosis, small nucleoli, and scant to abundant amounts of delicate to granular cytoplasm. (**b**) Cell block preparations show tumor cells that are immunoreactive for calcitonin (brown cytoplasmic staining)

They are often sporadic in adults but may be associated with germline *RET* mutations and multiple endocrine neoplasia (MEN) syndromes. Aspirates show loose aggregates or singly dispersed cells with coarsely granular, "salt and pepper" chromatin, typical of neuroendocrine tumors (Fig. 4.12a). The cells are plasmacytoid

to spindled, with eccentrically located nuclei and occasional binucleation. They have moderate to abundant amounts of finely granular cytoplasm, which may appear metachromatic to reddish-brown, depending on the stain used, and require distinction from Hürthle cells. As some MTCs have large, pleomorphic cells or intranuclear pseudoinclusions, the differential diagnosis often includes poorly differentiated, anaplastic, or papillary thyroid carcinomas. Positive calcitonin, CEA, and chromogranin stains are confirmatory in virtually all cases (Fig. 4.12b). Amyloid can be highlighted by a Congo red stain. Elevated serum calcitonin level is diagnostic of MTC and measurement of this marker generally plays a first line role in confirmation of the diagnosis, particularly when immunohistochemical stains, which are not universally available, cannot be performed. MTC is usually treated with total thyroidectomy and regional lymphadenectomy.

Primary thyroid lymphomas are rare, comprising 1–5% of all thyroid malignancies, with up to 5% reported at some referral centers. These tumors usually occur in older-aged females with a longstanding history of Hashimoto thyroiditis. Patients present with an enlarging thyroid mass, often accompanied by compressive symptoms and involvement of cervical lymph nodes. Aspirates are highly cellular and consist of isolated lymphoid cells (Fig. 4.13). A majority are B-cell lymphomas, most commonly extranodal marginal zone B-cell lymphoma of mucosa-

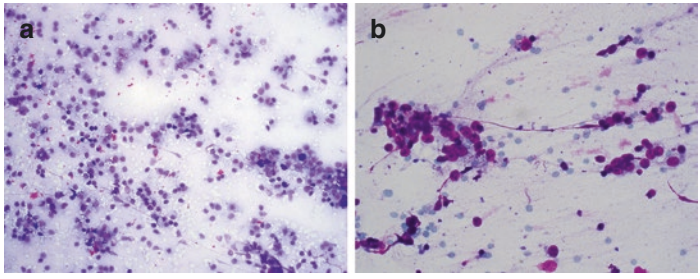

Fig. 4.13 Lymphoma. (**a**) MALT lymphoma of the thyroid showing a monotonous population of intermediate-sized lymphoid cells. (**b**) Diffuse large B-cell lymphoma (DLBCL) of the thyroid with large, atypical lymphoid cells with nuclear enlargement and prominent nucleoli

associated lymphoid tissue (MALT lymphoma) and diffuse large B-cell lymphoma (DLBCL). If the clinical presentation and/or cytomorphology suggests a lymphoma, ancillary studies such as immunohistochemistry, flow cytometry, and molecular genetics are useful for accurate diagnosis and further classification.

Lastly, metastatic disease to the thyroid can rarely occur and is usually recognized by the patient's clinical history or cytomorphologic dissimilarity to primary thyroid neoplasms. Immunohistochemistry is helpful in determining the origin.

Further Reading

Ali SZ, Cibas ES, editors. The Bethesda system for reporting thyroid cytopathology. Definitions, criteria, and explanatory notes. 2nd ed. New York: Wiley; 2017.

Haugen BR, Alexander EK, Bible KC, et al. 2015 American Thyroid Association Management guidelines for adult patients with thyroid nodules and differentiated thyroid cancer: the American Thyroid Association guidelines task force on thyroid nodules and differentiated thyroid cancer. Thyroid. 2016;26:1–133.

Krane JF, Alexander EK, Cibas ES, Barletta JA. Coming to terms with NIFTP: a provisional approach for cytologists. Cancer Cytopathol. 2016;124:767–72.

Patel KN, Angell TE, Babiarz J, et al. Performance of a genomic sequencing classifier for the preoperative diagnosis of cytologically indeterminate thyroid nodules. JAMA Surg. 2018;153(9):817–24.

Steward DL, Carty SE, Sippel RS, et al. Performance of a multigene genomic classifier in thyroid nodules with indeterminate cytology: a prospective blinded multicenter study [published correction appears in JAMA Oncol. 2019 Feb 1;5(2):271]. JAMA Oncol. 2019;5(2):204–12.

Fine Needle Aspiration: Role of Molecular Testing

5

James V. Hennessey

Key Points

- The malignant potential of thyroid nodules is determined through consideration of clinical risk, clinical findings, ultrasonographic features, and cytopathologic results, as classified by the Bethesda System of Reporting Thyroid Cytopathology.
- Cytologically indeterminate lesions yield a wide range of malignant outcomes on histopathology, which can be more precisely predicted using molecular information obtained by FNA.
- Clinically available methods of assessing the genetic profile of indeterminate thyroid nodules have been developed and include immunochemical staining for markers of thyroid cancer, identification of specific molecular

J. V. Hennessey (✉)
Harvard Medical School, Beth Israel Deaconess Medical Center, Boston, MA, USA
e-mail: jhenness@bidmc.harvard.edu

L. S. Eldeiry et al. (eds.), *Handbook of Thyroid and Neck Ultrasonography*, Contemporary Endocrinology,
https://doi.org/10.1007/978-3-031-18448-2_5

mutations and microRNAs (markers) of thyroid malignancy, as well as a system which primarly was designed to identify molecular markers of benign lesions.
- Genetic mutation panels currently perform well at identifying indeterminate nodules that are most likely malignant, indicating the need for surgical intervention. As the number of molecular markers is so comprehensive, the absence of these markers is a good negative predictor of malignancy.
- The identification of benign pathology among BSRTC indeterminate nodules is accomplished through a system which provides a high level of accuracy to rule out malignancy, avoiding the need for surgery, while the ability to predict the presence of malignancy is more modest.

Introduction

Fine needle aspiration (FNA) findings are interpreted considering the pretest probability of malignancy. The Bethesda System of Reporting Thyroid Cytopathology (BSRTC [Bethesda will be referred to as B in this chapter]) was introduced to standardize reporting of results and associate an evidence-based risk of malignancy (ROM) for each category. Clinical action is taken based on ROM projections in 70–80% of BSRTC results. Surgical intervention is indicated for B VI lesions and follow-up is generally suggested for B II nodules; however, management is less certain for the 20–30% of cases that are B III (atypia of unknown significance [AUS] or follicular lesion of unknown significance [FLUS], with an estimated ROM 5–47%) and B IV lesions (follicular/Hürthle cell neoplasm [FN] or suspicious for follicular/Hürthle cell neoplasm [SFN], with an estimated ROM of 15–40%). Surgery has usually been carried out in B V lesions (suspicious for malignancy), due to the high ROM (60–75%). When originally

published, repeat FNA was recommended for B III lesions and hemithyroidectomy for B IV nodules. However, up to 70 + % of surgical procedures on B III and IV nodules result in benign pathology, and whereas surgery was previously deemed necessary to detect cancers that could not otherwise be diagnosed, concerns regarding "unnecessary surgery" have arisen, particularly in view of the risk of post-operative complications.

Investigation of the Indeterminate Thyroid Nodule

The pretest probably of malignancy is established by considering individual clinical risk factors, ultrasound and cytology findings (which may lead to adjustment of pretest malignancy risk rates from those originally reported in the BSRTC). To better define the ROM posed by a cytologically indeterminate thyroid nodule, a good test should be accurate, accessible, affordable, and have impact on patient management to "rule out" or "rule in" the presence of thyroid malignancy. A useful additional investigation would then predict the ROM to below 5% or well above the 30 + % range represented by the B III or B IV finding when risk factors are otherwise reassuring. In this context, a "rule-in" test would provide a positive predictive value (PPV) similar to a B VI diagnosis (≅ 96%) and an ideal "rule-out" test would generate a negative predictive value (NPV) of about 3–5%. The American Thyroid Association (ATA) recommends that patients be counseled regarding the potential benefits and limitations of molecular marker testing (no test will be 100%). Current ATA guidelines also recommend that these tests be performed in established, CLIA-certified molecular laboratories for the most consistent clinical reliability.

Several approaches have been investigated to further define the ROM of indeterminate nodules. One technique has used immunochemistry staining of prepared cytopathology specimens using markers of thyroid malignancy ("rule-in" tests with high PPV) such as galectin-3, cytokeratin-19, Hector Battifora mesothelial-1(HBME1), and trophoblast cell surface antigen 2 (TROP2).

Alternatively, one can seek specific molecular markers of thyroid malignancy such as genetic mutations and rearrangements, for example, those that result in activation of the MAPK or PI3K/AKT pathways of malignancy. These include mutations of B-type RAF kinase (BRAF) and retrovirus-associated DNA sequences (RAS), as well as rearrangements of the RET proto-oncogene (a marker of medullary thyroid cancer) with regions of unrelated genes (e.g. RET/PTC), and fusion of the promoter and 5′-coding portion of the thyroid transcription factor PAX8 gene with the gene of the peroxisome proliferator-activated receptor γ (PAX8/PPARγ).

An alternative approach uses molecular techniques designed to identify benign thyroid tissue and provides a high NPV. Such a technique analyzes the mRNA expression of 167 genes in a gene expression classifier (GEC) and its current form, the gene sequencing classifier (GSC).

Immunohistochemical Staining

Immunohistochemical stains for galectin-3 and HBME-1 done on cell block specimens from material obtained by FNA using various methodologies have been reported. Using reverse transcriptase-PCR (RT-PCR), a small study of FNA samples classified as indeterminate was analyzed for the expression of galectin-3 and/or CD44v6 and resulted in a 100% sensitivity and 60% specificity for thyroid cancer. While potentially representing a good "rule-out test," the low specificity, technical difficulty in performing these tests, lack of widespread availability, and small series represent limitations of the clinical utility of this type of testing. Cytokeratin-19 and HBME1 (usually negative in normal thyroid cells) were assessed in a series of 150 FNAs from indeterminate nodules and were reported to be 100% sensitive and 85% specific for the presence of thyroid cancer. Overall, the accuracy of immunohistochemical staining has been limited in follicular cell lesions, particularly for distinguishing benign follicular adenomas from follicular thyroid cancer (FTC) and the follicular variant of papillary thyroid cancer (FVPTC).

Genetic Mutations in Thyroid Nodule Diagnosis

The discovery of molecular pathways driving carcinogenesis of thyroid follicular cell tumors has provided an opportunity to identify thyroid cancer at the molecular level, in order to differentiate benign from malignant B III and B IV nodules. Specific single mutations such as the BRAFV600E mutation have an estimated specificity of about 99% (high PPV) for papillary thyroid cancer (PTC) and the prevalence of this mutation is generally greater than 50% in PTC, though this estimate is population-dependent. In the past, BRAF positivity was viewed as an indication to perform a total thyroidectomy, as it confirms the presence of PTC. This mutation is not or is infrequently found in FTC, FVPTC, and Hürthle cell carcinoma (HCC). The prevalence of this mutation in cytologically indeterminate cases ranges from 0 to 48% (lower rates in Western countries). The MAPK pathway drives several human cancers and is strongly activated by the B-type RAF kinase (BRAF). The sensitivity of the BRAFV600E point mutation is too low, however, to reliably exclude the presence of thyroid malignancy in the assessment of indeterminate thyroid nodules.

Retrovirus-associated DNA sequences (RAS) point mutations constitute the second most frequently encountered (0–36%) finding in thyroid malignancy discovered among indeterminate BSRTC results. The 3 RAS subtypes are associated with follicular-patterned histology such as follicular adenoma (FA), FTC, FVPTC, and non-invasive follicular thyroid neoplasm with papillary-like nuclear features (NIFTP). Gene mutations identified in the oncogenic Harvey rat sarcoma (HRAS) predict the presence of malignancy in 56% of cases, while mutations of the Kirsten murine sarcoma virus (KRAS) and neuroblastoma cells (NRAS) have been reported to be 100% and 74% predictive, respectively. Each encodes for RAS proteins that are involved in signaling in the MAPK/ERK pathway. Mutations in the RAS genes result in overactive RAS signaling, inducing malignant growth. In general, the presence of RAS mutations predicts thyroid cancer in more than 80% of cases, though generally with favorable clinical features, such as encapsulation and a paucity of lymph node metastases, for which hemithyroidectomy may be

considered as a therapeutic intervention. The remaining 16 + % represent benign lesions such as FA (which has been considered pre-malignant by some). Conversely, poor cell differentiation may be present in some, more aggressive cancers. Because the RAS mutations are not exclusive to thyroid malignancy, RAS positivity (unlike BRAFV600E) does not predict malignancy with high accuracy. Approximately 1/3 of malignancies in subjects with indeterminate cytopathology findings (FVPTC, FTC) are RAS-mutated.

Genetic Translocations

Genetic translocation products, such as the Ret proto-oncogene rearrangements (RET/PTC), activate the MAPK and PI3K/AKT pathways through BRAF signaling, resulting in malignant transformation. Of the 12+ fusion variants identified, RET/PTC1 and RET/PTC3 are the most common. RET/PTC3 occurs in PTC in children and those exposed to irradiation and is associated with lymph node metastases. Benign adenomas that are positive for RET/PTC and occur after irradiation are considered pre-cancerous. RET/PTC rearrangements are seldom reported in most series of indeterminate nodules; however, one Italian series reported a 36% incidence in this setting. As such RET/PTC has low utility as a stand-alone test, but is most useful when included in a panel of molecular tests.

Rearrangements of the PAX8 and PPARγ (PAX8/PPARγ) genetic material have been detected in up to 45% of FTC, 33% of FA's, and up to 38% of FVPTC, but have not been routinely observed in Hürthle cell lesions. Some have reported that the presence of this fusion is associated with malignancy. In general, the PAX8/PPARγ fusion predicts encapsulated, indolent lesions and does not activate the MAPK pathway. PAX8/PPARγ does not occur frequently in cytologically indeterminate nodules. Approximately 2/3 of PAX8/PPARγ-positive nodules are malignant (FVPTC, FTC). Benign lesions known to be PAX8/PPARγ positive are also considered pre-malignant.

Other Genetic Anomalies of Interest

Special attention should be paid to another genetic alteration that has the potential to enhance prognostication of thyroid nodules. Telomerase enzymatically maintains healthy chromosomal telomeres. Telomerase reverse transcriptase (hTERT) is inactive in normal cells, but when hTERT promoter mutations are present, reactivation results in malignant behavior of thyroid cells. TERT promoter mutations have been described in PTC, FTC, and HCC. TERT promoter mutations are seen with higher positivity in more aggressive variants of thyroid cancer, such as poorly differentiated and anaplastic (70%) cancers. The presence of the TERT promoter mutation is highly correlated with mortality in differentiated thyroid cancer, especially when present in conjunction with BRAFV600E. TERT is potentially useful in the preoperative identification of differentiated thyroid cancer (DTC), with reported sensitivity and specificity rates of 57–88% and 75–85%, respectively.

Other genetic alterations observed in thyroid cancers include the eukaryotic translation initiation factor 1A, X chromosomal (EIF1AX), found in low percentages of PTC and FTC. The presence of this mutation in poorly differentiated thyroid cancers, however, is associated with poorer clinical outcomes. A gene normally encoding endoribonucleases (DICER1) has been found to be mutated in germline and somatic pediatric thyroid cancers (FTC and PTC). This mutation is usually reported in the context of a hereditary pediatric cancer predisposition syndrome, which includes pleuro-pulmonary blastoma, ovarian sex cord-stromal tumors, lung cysts, cystic nephroma, renal sarcoma and Wilms' tumor, and other lesions. In adults, the presence of a germline DICER1 mutation seems to be a risk factor for renal sarcoma, Wilms tumor, and other lesions and is associated with having had a thyroidectomy for reasons other than thyroid cancer or goiter.

Alterations in a gene encoding adenylate cyclase-stimulating G α-protein at codon 201 (GNAS) may result in activation of the cyclic AMP process affecting cell proliferation and function. GNAS alterations are more frequently found in hyperfunctioning adenomas of the thyroid, but may also be present in FTC. Long

known mutations in RET (RET proto-oncogene) may be detected by FNA specimens in medullary thyroid cancer.

Genetic Mutation Panels

A functional strategy toward the search for molecular markers to include multiple mutations/translocations including BRAFV600E, BRAFK601E, NRAS codon 61, HRAS codon 61, KRAS codon 12–13 point mutations, along with RET/PTC1, RET/PTC3, and PAX/PPARγ gene rearrangements, is designed to assess the malignant potential of indeterminate nodules more comprehensively (including newly described pre-malignant lesions such as NIFTP [see below]). This approach enhances the power of detection, given that these mutations are generally mutually exclusive. Usually, the presence of one characteristic mutation among those in the panel is a significant indicator of malignancy. In B III cases that are positive for BRAF, RET/PTC, or PAX8/PPARγ, a malignancy has been reported in all cases, while some RAS mutations may point to cancer in 84% of cases in this same series. In studies of B IV lesions, where a 15–30% risk of malignancy is assumed to exist, this seven-gene mutational panel was demonstrated to have a 57–75% sensitivity for malignancy, a specificity of 97–100%, PPV of 87–100% (highlighting its usefulness as a "rule-in" test), and a NPV of 79–86%. However, nodules lacking all 7 of these markers still harbored a significant risk of malignancy, limiting its utility as a "rule-out" test. In one study of these panels, only 1 of 18 nodules with Hürthle cell cytology tested positive, likely providing early evidence that the genetic basis of Hürthle cell lesions differs from that of other types of DTC. Additionally, the PPV of these panels is unlikely to ever exceed 90%, as RAS mutations trigger positive results and the prevalence of malignancy of populations studied has been 15–40%. A limitation to the accuracy of PPV and NPV calculations is the fact that histology data is not available for all nodules characterized as "not malignant" in these panels, rendering a precise calculation of false negatives impossible. Extending a 7-gene panel to include additional markers observed in thyroid cancer

and processed through next-generation sequencing (NGS) allows targeted testing of large panels with multiple mutations.

ThyroSeq®, now in version 3 (v3), analyzes 112 genes for point mutations, insertions, deletions, copy number alterations, fusions, and gene expression alterations, accounting for about 95% of genetic alterations known to occur in PTC, as well as including TERT promoter variants (See Table 5.1). Evaluation of B IV lesions yields predictably higher sensitivity (90%), but lower specificity (83%) and PPV (83%) while reportedly increasing the power to rule out the presence of cancer (NPV 96%). ThyroSeq v3 was assessed in a multi-institutional study of 286 indeterminate nodules: 72% were classified as benign, and a total of 28% (including NIFTP: 14% of the total, which likely impacted clinical management and calculation of PPV) were classified as malignant. A sensitivity of 94%, specificity of 82%, and NPV of 97% were observed, while the PPV for malignancy was 66%. ROM of positive tests ranged from 50 to 100% depending on the pattern of genetic abnormalities identified. An independent assessment of ThyroSeq v3 performance in 415 B III and B IV qualifying nodules resulted in a total of 121 positive (29%) and 294 negative (71%) results. Of ThyroSeq v3-positive cases with histopatho-

Table 5.1 Methods employed in molecular testing of indeterminate thyroid nodules

Method	Diagnostic utility	Markers of malignancy
Immunocytochemistry	"Rule-in" tests with high PPV	Proteins detected—Galectin-3, CytoKeratin, HBME1, TROP2
Molecular marker (mutation panel) testing	"Rule-in" tests with high PPV and in the absence of markers, good NPV	Mutations—BRAF, EIF1AX, DICER1, GNAS, RAS, RET proto-oncogene, hTERT Rearrangements—RET/PTC, PAX8/PPARγ
GEC (no longer available), GSC	Identification of benign thyroid tissue	Additional gene mutation/rearrangment expression available

See text for detail. *NPV* negative predictive value, *PPV* positive predictive value, *GEC* gene expression classifier, *GSC* gene sequencing classifier

logic confirmation, 32% were benign and 51% were malignant (NIFTP: 17% of malignant nodules). Assuming that those with negative ThyroSeq v3 results were indeed true-negatives (a common assumption among studies of this type), an overall sensitivity of 92.9% and specificity of 90.3% were observed. The NPV was 98.3% and PPV 67.7%, validating the "rule-out test" characteristics necessary to reassure patients. The performance of ThyroSeq has recently been assessed in practice in cases for which surgical pathology results were available and was found to perform better in larger thyroid nodules (<2 cm: PPV 25%; NPV 79% versus >4 cm: PPV 50%; NPV 89%).

MicroRNA (miRNA) Analysis

MicroRNA (miRNA) markers have been evaluated in nodules with indeterminate cytology. MicroRNAs are small, endogenous non-coding RNAs about 22 nucleotides in length that play a role in the regulation of posttranscriptional protein synthesis. Human cancers are associated with dysregulation of miRNA expression and these miRNAs appear as a pre-malignant event before deregulating tumor suppressor and oncogenes. These miRNAs are more stable than mRNA, may be detected in the circulation, and maintain their expression in formalin-fixed tissue and FNA samples, making retrieval from cytopathology slides possible. Studies have found that different miRNAs and levels of expression are of clinical utility in the identification of malignancy. For example, in PTC, there is a reported up-regulation of miR-146b, miR-221, miR-222, and miR-187 and a down-regulation of miR-1 and miR-138. Additionally, FTC, poorly differentiated, and anaplastic thyroid cancers are also associated with up-regulation of miR-221, miR-222, and miR-187. The degree of overexpression may also be of utility, as FVPTC appears to have twice the expression of miR-221 and miR-222 than PTC and FTC. Based on these and further characteristic variances in expression, diagnostic panels of miRNAs have been combined to evaluate the malignant potential of thyroid nodules with variable degrees of success. A commercial product evaluating 24 up- and down-regulated miRNAs

(RosettaGX Reveal®) using routinely stained cytology slide samples was reported to have a 90% PPV but only a 39% NPV, limiting its clinical utility.

Mutation and miRNA (Multiplatform) Analysis Combined

Combined sequential analysis of a gene mutational panel with an miRNA classifier if no mutations are identified has demonstrated promising results for both "rule in" and "rule out" purposes. A commercial product combining the sequencing of 8 genes (ThyGenX®) and 10 miRNAs (ThyraMIR®) reported a sensitivity of 94%, specificity of 85%, PPV of 68%, and a NPV of 97% in B III lesions. The most recent configuration includes an expanded gene panel (ThyGeNEXT®) with the ThyraMIR panel and has been reported to have a PPV of 75% and NPV of 97%.

Identification of Benign Nodule Characteristics

When first introduced, the 167 Afirma® gene expression classifier (GEC [a historical term, as this version is no longer in clinical use]) used quantification of messenger RNA (mRNA) run through a proprietary algorithm to differentiate benign from potentially malignant ("suspicious") thyroid nodules. The GEC was processed on material obtained by 2 additional FNA passes and was introduced as a "rule-out" test based on an initial reported 92% sensitivity and NPV of 93%. In one study, this resulted in a reduction of malignancy risk from 24% in AUS/FLUS lesions to 5%. In cases where surgical pathology was available, the relatively low specificity for predicting the presence of malignancy in indeterminate nodules (48–53%), however, was acknowledged to be a limitation to use as a "rule-in" test. The reporting protocol indicated that the results were either "likely benign," as reflected by the high NPV or designated as "suspicious." Some misinterpreted these reports to equate to the 7-gene mutation panel reporting nomenclature, which was reported as "positive" (for malignancy), an indication for total

thyroidectomy, or "negative," where a hemithyroidectomy was suggested as initial management due to the low NPV of the limited mutation panel. Performance of the GEC in those with B IV lesions in general showed a higher NPV (94%) but much more modest PPV (37%). Studies subsequently documented a limitation of the GEC in Hürthle cell lesions, where a "suspicious" result was often associated with benign final histopathology, although the NPV of the GEC was retained. Since 2018 the Afirma® system has been based upon next-generation sequencing (NGS), analyzing nuclear and mitochondrial RNA transcriptome gene expression, RNA sequencing, and genomic copy number analysis. This version is designated as the gene sequencing classifier (GSC) and incorporates BRAFV600E, RET/PTC fusion, parathyroid tissue, and medullary thyroid cancer (MCT) markers. The GSC was validated on a subset of the original pivotal GEC data set and demonstrated a sensitivity of 91% and specificity of 68% in a population with a 24% cancer prevalence. The NPV was 96% and PPV was 47%. Independent, real world evaluation from several institutions comparing the GSC performance with that of the original GEC configuration has led to a decrease in suspicious results by 21–54%, classification of more Hürthle cell lesions as benign, and a higher PPV of 57.1–61.5% (with a higher PPV in B IV vs. B III). Currently, the Afirma® system also offers optional testing for a limited number of specific driver mutations (as included in the mutation panels described above) when overall results are designated as suspicious. Use of this optional marker panel has enhanced preoperative PPV and surgical planning when specific markers are present. Meta-analysis of 4 independent studies evaluating the clinical performance of the GSC indicates an overall sensitivity of 95%, specificity of 51%, PPV of 60%, and NPV of 91%.

Genetic Testing and NIFTP Lesions

The performance of genetic testing in the identification of lesions diagnosed as NIFTP, an entity considered to have low malignant potential, is limited. Although the initial series of 109 cases of NIFTP reported no adverse clinical outcomes, subsequent studies have

reported lymph node (5%) and lung metastases (1%) in the follow-up of patients who had histologically classified NIFTP. Cytopathology findings are typically indeterminate or suggestive of PTC. As the definition of these lesions is based on presence or absence of invasion, only surgical histology is currently sufficient to establish this diagnosis. The BSRTC acknowledges that B III, IV, and V categories may all be seen in cases diagnosed as NIFTP. In the calculation of PPV, NIFTP lesions are considered by some as "malignant" in preoperative testing. As such, the PPV of malignancy in various systems is enhanced when NIFTP is present. Some consider such a designation a false positive. Although surgical removal of NIFTP lesions is appropriate due to NIFTP's potential pre-malignant nature, some have (retrospectively) opined that surgery may be overly aggressive for this final diagnosis. In the past, a total rather than limited (hemi) thyroidectomy was recommended for confirmed malignancy. Currently, as aggressive surgery or I-131 therapy is not indicated for NIFTP, excessive surgical intervention is generally to be avoided, though given the limitations of preoperative diagnosis and some challenges in making this pathology diagnosis, for example, in the distinction from FVPTC, an individualized management approach is needed, particularly in the case of larger nodules (>4 cm).

Genetic alterations detected in the evaluation of the indeterminate thyroid nodule differ depending on the approach taken. The presence of BRAF or RET/PTC would not generally support the diagnosis of NIFTP preoperatively (in fact the presence of BRAFV600E mutation is an exclusion criterion for the diagnosis of NIFTP). Other "positive" indicators of cancer, such as RAS mutations, occur more frequently in NIFTP. In addition, PAX8-PPARγ, THADA fusions and EIF1AX mutations may be found in NIFTP. In a similar way, a proportion of indeterminate nodules labeled as "suspicious" in the Afirma® GEC as well as GSC system have been found to be NIFTP.

Given these findings, repeat FNA of cytologically indeterminate nodules prior to molecular testing and following a conservative pathway to initial surgical intervention or, alternatively, clinical observation, seems prudent.

Table 5.2 summarizes the currently available commercial panels, their performance and method of collection.

Table 5.2 Comparison of commercial panels, their performance and the method of collection

Commercial panel	Sensitivity	Specificity	PPV	NPV	Reference	Collection
ThyroSeq v3™ (genomic classifier)	94%	82%	66%	97%	[1]	Rinsing residual FNA
NGS, 112 genes, point mutations	93%	90%	68%	98%	[2][a]	1 dedicated pass
Gene fusions, copy # alterations	99%	64%	78%	96%	[3][b]	
Gene expression alterations						
ThyGenX/ThyraMIR®	57%	92%	74%	94%	[4, 5]	Fixed, stained slides
NGS, 7 gene mutations	Due to limited data no meta-analysis estimation				[3][b]	
3 Gene fusions and 10 miRNAs						
Afirma GSC™	91%	68%	47%	96%	[6]	2 separate passes
NGS, RNA transcriptome	94%	61%	33%	98%	[7][a]	
Expression, specific gene	100%	73.7	62%	NR	[8][a]	
Mutations available	95%	51%	60%	91%	[3][b]	

[1] Steward DL, Carty SE, Sippel RS, Yang SP, Sosa JA, Sipos JA, et al. Performance of a multigene genomic classifier in thyroid nodules with indeterminate cytology: a prospective blinded multicenter study. JAMA Oncol. 2019;5(2):204–12.
[2] Desai D, Lepe M, Baloch ZW, Mandel SJ. ThyroSeq v3 for Bethesda III and IV: an institutional experience. Cancer Cytopathol. 2021;129(2):164–70.

[3] Silaghi CA, Lozovanu V, Silaghi H, Georgescu RD, Pop C, Dobrean A, et al. The Prognostic value of microRNAs in thyroid cancers—a systematic review and meta-analysis. Cancers (Basel). 2020;12(9).
[4] Ullmann TM, Gray KD, Moore MD, Zarnegar R, Fahey TJ 3rd. Current controversies and future directions in the diagnosis and management of differentiated thyroid cancers. Gland Surg. 2018;7(5):473–86.
[5] de Koster EJ, de Geus-Oei LF, Dekkers OM, van Engen-van Grunsven I, Hamming J, Corssmit EPM, et al. Diagnostic utility of molecular and imaging biomarkers in cytological indeterminate thyroid nodules. Endocr Rev 2018;39(2):154–191.
[6] Patel KN, Angell TE, Babiarz J, Barth NM, Blevins T, Duh QY, et al. Performance of a genomic sequencing classifier for the preoperative diagnosis of cytologically indeterminate thyroid nodules. JAMA Surg. 2018;153(9):817–24.
[7] Endo M, Nabhan F, Porter K, Roll K, Shirley LA, Azaryan I, et al. Afirma gene sequencing classifier compared with gene expression classifier in indeterminate thyroid nodules. Thyroid. 2019;29(8):1115–24.
[8] Gortakowski M, Feghali K, Osakwe IN. Single institution experience with Afirma and Thyroseq testing in indeterminate thyroid nodules. Thyroid. 2021;31:1376.
[a]Real world confirmation
[b]Meta-analysis
NGS next generation sequencing, *GSC* gene sequencing classifier

Initial Intervention Based on Molecular Results

The high PPV of mutation panels with a positive test result has been used to identify thyroid nodules with a high risk of malignancy. At the time of the original BSRTC report, total thyroidectomy was recommended by the ATA for all thyroid malignancies greater than 1 cm. As such, positive results were used to plan total thyroidectomy for >1 cm nodules that were identified as malignant. More recent guidelines and current practice, however, recommend hemithyroidectomy for unifocal lesions that are less than 4 cm with no clinical or ultrasound evidence of local invasion or metastases that are suspected of being malignant. This is based on the observation that specific tumor types (including minimally invasive FTC, FVPTC, and NIFTP, which may be molecularly identified as positive by these methods) have an observed clinical course that does not justify aggressive surgery and post-operative 131-I ablation, given a less favorable risk-benefit profile for total thyroidectomy. Any decision to recommend surgery, including hemithyroidectomy, however, is not without long-term consequences, as up to 43% of patients may develop hypothyroidism post-operatively. Ongoing investigation into how molecular information may guide preoperative planning and modify the subsequent clinical course of DTC is expected to further enhance the management of patients with indeterminate thyroid nodules (with the potential exception of finding a clinically unexpected medullary thyroid cancer). Figure 5.1 shows a suggested management approach for the incorporation of molecular testing in the evaluation of indeterminate thyroid nodules.

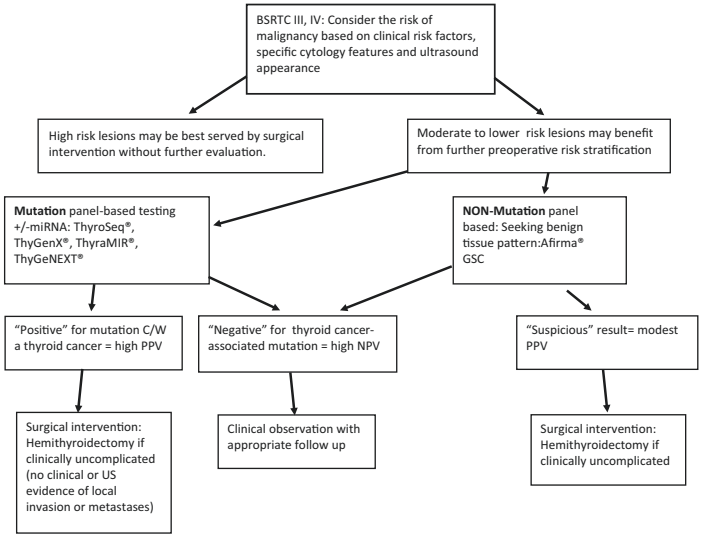

Fig. 5.1 Molecular testing of the indeterminate thyroid nodule

Further Reading

de Koster EJ, de Geus-Oei LF, Dekkers OM, van Grunsven IVE, Hamming J, Corssmit EPM, et al. Diagnostic utility of molecular and imaging biomarkers in cytological indeterminate thyroid nodules. Endocr Rev. 2018;39(2):154–91.

Desai D, Lepe M, Baloch ZW, Mandel SJ. ThyroSeq v3 for Bethesda III and IV: an institutional experience. Cancer Cytopathol. 2021;129(2):164–70.

Endo M, Nabhan F, Porter K, Roll K, Shirley LA, Azaryan I, et al. Afirma gene sequencing classifier compared with gene expression classifier in indeterminate thyroid nodules. Thyroid. 2019;29(8):1115–24.

Gortakowski M, Feghali K, Osakwe IN. Single institution experience with Afirma and Thyroseq testing in indeterminate thyroid nodules. Thyroid. 2021;31:1376.

Grani G, Sponziello M, Pecce V, Ramundo V, Durante C. Contemporary thyroid nodule evaluation and management. J Clin Endocrinol Metab. 2020;105(9):2869.

Kumar N, Gupta R, Gupta S. Molecular testing in diagnosis of indeterminate thyroid cytology: trends and drivers. Diagn Cytopathol. 2020;48(11):1144–51.

Patel KN, Angell TE, Babiarz J, Barth NM, Blevins T, Duh QY, et al. Performance of a genomic sequencing classifier for the preoperative diagnosis of Cytologically indeterminate thyroid nodules. JAMA Surg. 2018;153(9):817–24.

Sliaghi CA, Lozovanu V, Georgescu CE, Geogescu RD, Susman S, Nasui BA, et al. Thyroseq v3, Afirma GSC and microRNA panels versus previous molecular tests in the preoperative diagnosis of indeterminate thyroid nodules: a systematic review and meta-analysis. Front Endocrinol. 2021;12(649522):19.

Steward DL, Carty SE, Sippel RS, Yang SP, Sosa JA, Sipos JA, et al. Performance of a multigene genomic classifier in thyroid nodules with indeterminate cytology: a prospective blinded multicenter study. JAMA Oncol. 2019;5(2):204–12.

Ullmann TM, Gray KD, Moore MD, Zarnegar R, Fahey TJ 3rd. Current controversies and future directions in the diagnosis and management of differentiated thyroid cancers. Gland Surg. 2018;7(5):473–86.

6 Thyroid Gland Ultrasonography: Hashimoto's, Graves', Thyroiditis, Toxic Multinodular Goiter

Preethika S. Ekanayake, Omonigho Aisagbonhi, and Karen C. McCowen

Key Points

- Hashimotos' and Graves' disease glands exhibit hypoechogenicity on ultrasound (US).
- "Thyroid inferno" has a high positive predictive value (PPV) for diagnosing and monitoring relapse of Graves' disease.
- Hashimoto's glands are characterized by hypoechogenicity, micronodules, "white knight" and "giraffe pat-

P. S. Ekanayake (✉) · K. C. McCowen
Division of Endocrinology, Diabetes and Metabolism, University of California, San Diego, San Diego, CA, USA
e-mail: pekanayake@health.ucsd.edu; kmccowen@ucsd.edu

O. Aisagbonhi
Department of Pathology, University of California, San Diego, San Diego, CA, USA
e-mail: oaisagbonhi@health.ucsd.edu

L. S. Eldeiry et al. (eds.), *Handbook of Thyroid and Neck Ultrasonography*, Contemporary Endocrinology,
https://doi.org/10.1007/978-3-031-18448-2_6

terns." Vascularity can be high (but less than Graves') in the initial part of the disease course.
- Destructive thyroiditis is characterized by very low parenchymal vascularity on US color flow Doppler and very low I-123 uptake.
- "Hot" nodules in a TMNG may appear hyperechoic on ultrasound.

Introduction

Apart from history, physical examination, and laboratory work-up, ultrasound (US) characteristics may be useful in distinguishing between various diffuse thyroid conditions such as Hashimoto's thyroiditis, Graves' disease, acute/subacute thyroiditis, and toxic multinodular goiter (TMNG). For example, the gland usually appears heterogeneous, enlarged, and hypervascular in Graves' disease, whereas a heterogeneous, hypoechoic thyroid with pseudonodules is suggestive of Hashimoto's. Thyroiditis can be characterized by early reduced vascularity followed by a hypervascular phase as the thyroid recovers. The diagnosis of TMNG often requires additional imaging such as a radioactive iodine uptake and scan.

Case Presentation 1
A 29-year-old woman was referred for abnormal lab tests and a several month history of severe fatigue, worsening depression, menorrhagia, and weight gain of 30 lbs. There was a strong family history of hypothyroidism. Physical exam was pertinent for an enlarged thyroid without any palpable nodules. Neck ultrasound was performed (see Image 6.1). Table 6.1 shows the potential differential diagnosis for this ultrasound image.

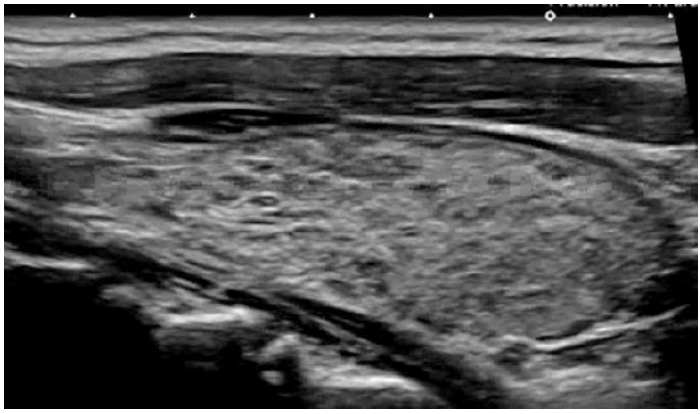

Image 6.1 Sagittal view of the left lobe. Thyroid parenchyma is hypoechoic with a heterogeneous echotexture. There are micronodules with internal colloid and irregular "puff pastry" or "honeycomb" appearance, with thin surrounding echogenic walls. The gland is also enlarged

Table 6.1 Differential diagnosis of ultrasound

1. Hashimoto's thyroiditis
2. Subacute thyroiditis
3. Graves' disease

Laboratory tests showed significantly elevated TSH of 296 uIU/L (ref 0.49–4.67), undetectable free T4 < 0.25 ng/dL (ref 0.7–1.9), and total T3 < 20 ng/dL (60–181). Thyroid peroxidase (TPO) antibody titer was elevated at 420 U/mL (ref <60), confirming the diagnosis of Hashimoto's thyroiditis with severe hypothyroidism. While the ultrasound was consistent with this diagnosis, it is worth noting that appearance on sonography is variable and in no way predicts the severity of thyroid dysfunction. The gland may vary from greatly enlarged to atrophic. She was treated with thyroid hormone replacement and subsequently had shrinkage of the goiter, although ultrasound was not repeated. Additional imaging as well as pathology examples of Hashimoto's thyroiditis are seen on Images 6.2, 6.3, 6.4, 6.5, 6.6, 6.7, 6.8 and 6.9.

Additional Imaging Examples of Hashimoto's Thyroiditis

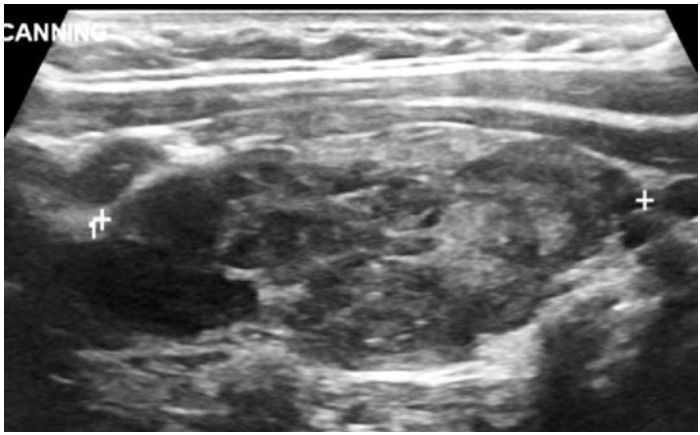

Image 6.2 Sagittal view of the left lobe shows a hypoechoic, very heterogeneous thyroid lobe. Borders of the gland have a lobular and irregular contour.

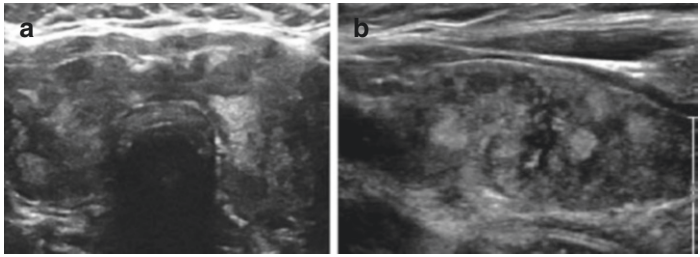

Image 6.3 Transverse (**a**) and sagittal (**b**) views showing a "giraffe hide" pattern of Hashimoto's, which is characterized by globular hyperechogenic (bright) areas surrounded by linear, thin hypoechoic (dark) areas similar to the two-color patterns seen on a giraffe. Margins of the Hashimoto's gland are also lobulated

Case Presentation 2

A 26-year-old female with a history of refractory acute lymphocytic leukemia and allogenic stem cell transplant was referred to endocrinology for weight loss, palpitations, proximal muscle weakness, tremors, and dry eyes. Physical exam was notable for sinus tachycardia, proptosis, and a firm, diffusely enlarged thyroid without palpable nodules.

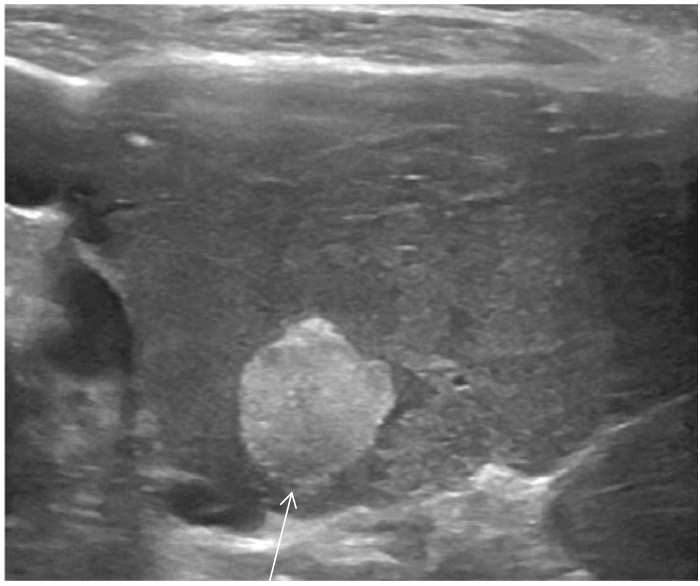

Image 6.4 The classic "white knight" (arrow), which is a well-demarcated, hyperechoic nodule with a dark/hypoechoic halo. This is sometimes referred to as "nodular Hashimoto's." These lesions are composed of hyperplastic islands surrounded by hypoechoic tissue. Some patients with long-standing Hashimoto's have sonographic findings of a "hypoechoic triangle" (HET) sign, which is a 10 mm triangular hypoechoic region between the lateral wall of the atrophic thyroid lobe and the medial wall of the carotid (not shown)

Her mother had hypothyroidism. Images 6.10 and 6.11 show her initial ultrasonography. Table 6.2 shows the correct differential diagnosis based on this ultrasonography pattern.

Bloodwork revealed a suppressed TSH of <0.01 uIU/mL (ref <0.3 uIU/mL), elevated free T4 of 4.15 ng/dL (ref 0.9-2.3 ng/dL) and total T3 of 3.5 ng/mL (ref 0.8-2 ng/mL). Thyroid stimulating immunoglobulins (TSI) were elevated at 5.49 IU/L (ref <0.54) and TSH receptor antibodies (TRAB) were 8.61 IU/L (ref <1.75). She was diagnosed with Graves' disease and started on methimazole 10 mg twice a day. After two doses, she had a severe anaphylactic reaction requiring epinephrine. Given the severity of the thyrotoxicosis and inability to tolerate thionamides, she under-

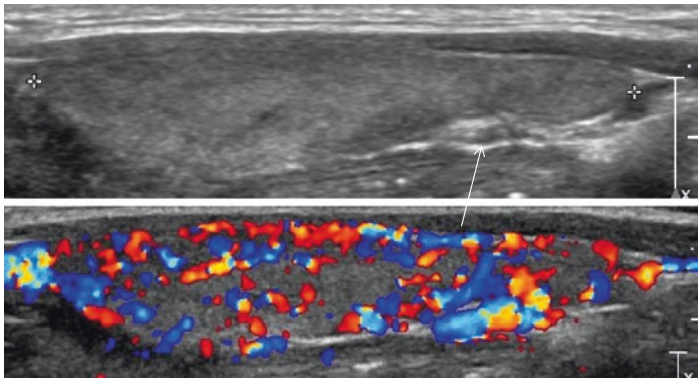

Image 6.5 The thyroid parenchyma can have increased vascularity in the early stages of Hashimoto's (sagittal image above shows slight textural patchiness; color Doppler below). In later, atrophic stages, thyroid vascularity can be decreased, due to extensive fibrosis. The hypervascularity of Hashimoto's is not as impressive as that in Graves' disease

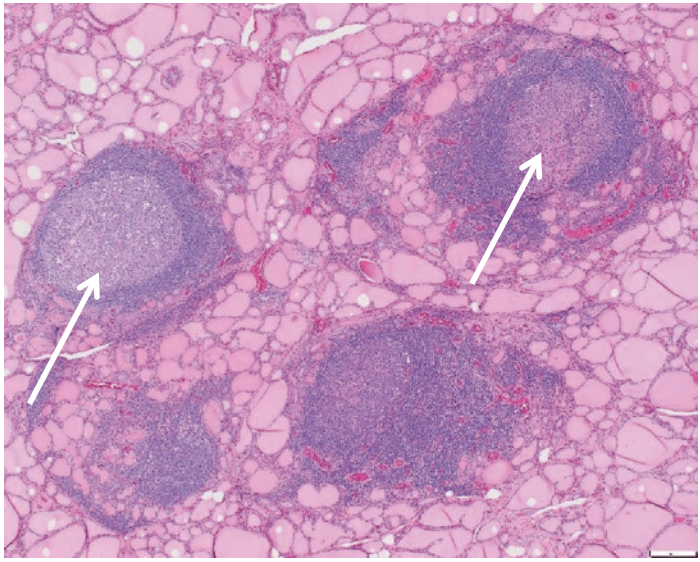

Image 6.6 Chronic lymphocytic thyroiditis (Hashimoto's) classically shows diffuse involvement of the thyroid gland by a prominent lymphoid infiltrate with associated germinal centers (arrows) (×4 H&E)

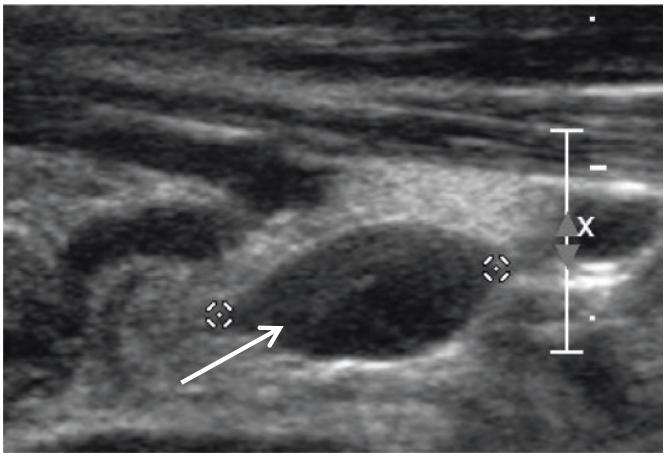

Image 6.7 Hashimoto's may be associated with reactive adenopathy (arrow) that is especially common around the inferior thyroid lobes

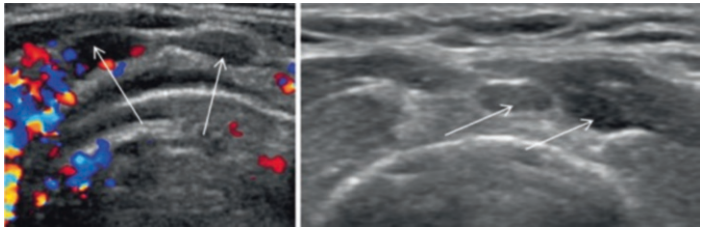

Image 6.8 Occasionally noted in cases of Hashimoto's are Delphian lymph nodes, located superior to the isthmus, giving the appearance of one or two "eyes" (arrows)

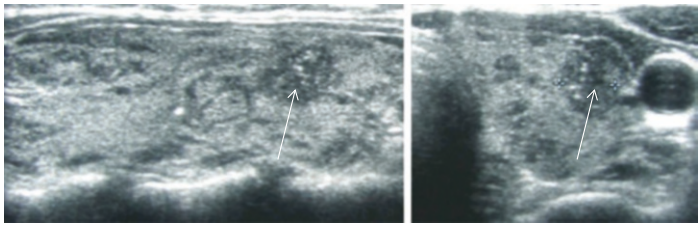

Image 6.9 Since the echotexture can be so heterogeneous, identification of papillary thyroid carcinoma (arrow) in a Hashimoto's gland may be difficult and delayed. In this case, a nodule with irregular margins and microcalcifications can be seen in sagittal (left panel) and transverse views (right panel)

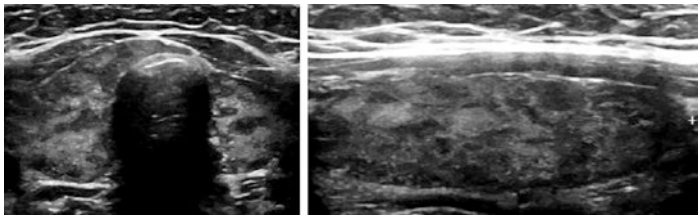

Image 6.10 Transverse (left) image showing a heterogeneous, hypoechoic thyroid parenchyma with a coarse echotexture. The margins are smooth like the normal thyroid gland, but anteroposterior diameter is increased. Longitudinal view (right) shows smooth borders (in contrast to the lobulated contours of Hashimoto's) and a hypoechogenic, coarse parenchyma

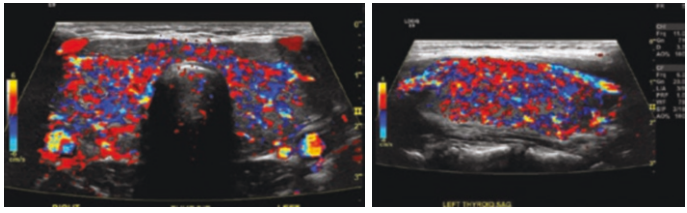

Image 6.11 The thyroid parenchyma is markedly hypervascular on color flow Doppler

Table 6.2 Differential diagnosis of the Ultrasound Image 6.10

1. Graves' disease
2. Hashimoto's thyroiditis
3. Silent thyroiditis

went total thyroidectomy. Image 6.12a, b shows the pathology of the resected thyroid. Images 6.13 and 6.14 show additional radiological images for Graves' disease.

Additional Imaging Examples of Graves' Disease:

In qualitative color flow Doppler (CFD), pattern 0 is blood flow limited to the peripheral thyroid arteries, while parenchymal flow is absent (i.e., normal thyroid); pattern I is mildly increased parenchymal flow; pattern II is clearly increased flow with a diffuse distribution; and pattern III is markedly increased color flow with a homogenous distribution. The cutoff for the quantitative

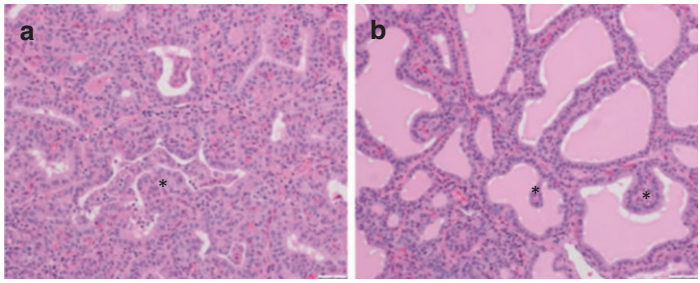

Image 6.12 (**a**, **b**) The thyroid gland in Graves' disease shows diffuse hyperplasia with reduced colloid and follicles that exhibit non-branching papillary projections (asterisk*) into the lumen (**a**; ×20 H&E). Treated Graves may exhibit some colloid; thyroid follicles have papillary projections (asterisks*) that are often associated with prominent colloid scalloping (**b**; ×20 H&E)

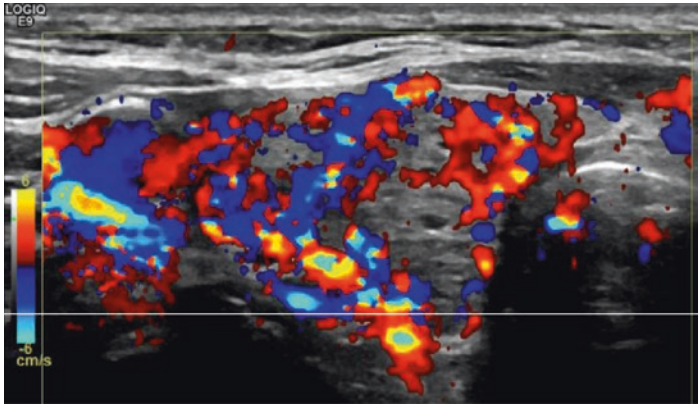

Image 6.13 A different example of "thyroid inferno" sign, which is a marked increase in parenchymal thyroid blood flow, pathognomonic of untreated and/or uncontrolled Graves' disease. The thyroid blood flow can be measured qualitatively by color flow Doppler (CFD) (as above), or quantitatively by peak systolic velocity (PSV) at the inferior thyroid artery (not shown). Graves' disease patients who become euthyroid have low or normal CFD and PSV compared to uncontrolled Graves' patients. Therefore, an increase in CFD can be an early marker for identifying a euthyroid patient that is progressing to hyperthyroidism during a thionamide hiatus

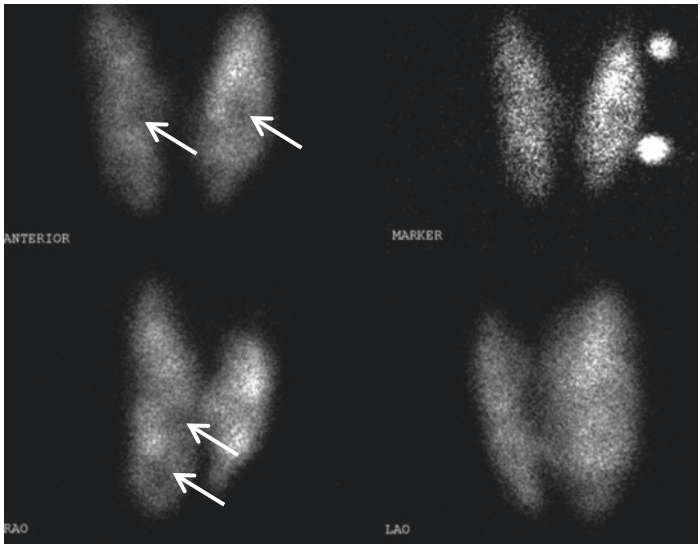

Image 6.14 The patient in Image 6.13 had an I-123 radioiodine uptake and scan. Uptake at 6 h was 46.1% (normal, 5–15%) and at 24 h was 67.6% (normal, 15–35%). There are also multiple, bilateral small cold nodules (arrows demonstrate darker areas within the thyroid). The cold nodules were biopsied and showed benign (Bethesda II) cytology

measurement, the PSV, differentiating Graves' disease from thyroiditis is ~40 to 50 cm/s. Image 6.13 shows pattern III CFD.

Case Presentation 3

A 59-year-old woman with a history of atrial fibrillation presented with worsening palpitations, dyspnea on exertion, peripheral edema, and tremor. She was treated with amiodarone for many years. She denied neck pain, but reported new anterior neck fullness. On physical examination, she was in no apparent distress, but had signs of congestive heart failure, including tachycardia, peripheral edema, and jugular venous distension. Thyroid gland had an irregular texture and was marginally enlarged. Laboratory values showed a suppressed TSH of <0.01 uIU/mL (ref <0.3 uIU/mL), high free T4 of >7.77 ng/dL (ref 0.9-2.3 ng/dL), and total T3 of 3.1 ng/mL (0.8-2 ng/mL). Images 6.15 and 6.16 show her initial ultrasound. Table 6.3 shows the differential diagnosis based on image findings.

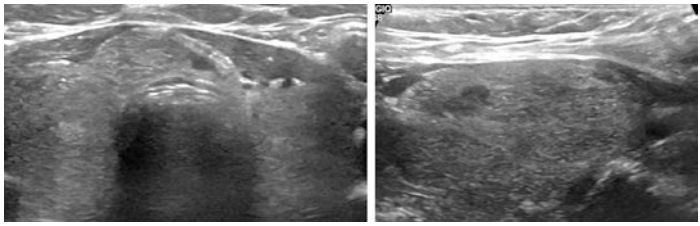

Image 6.15 Thyroid parenchyma is mildly hypoechogenic with coarse echotexture. Both bright and darker areas are seen in transverse view (left) and sagittal view (right). Both lobes are enlarged (~ 5.3 × 3.0 × 1.6 cm) and there are no nodules

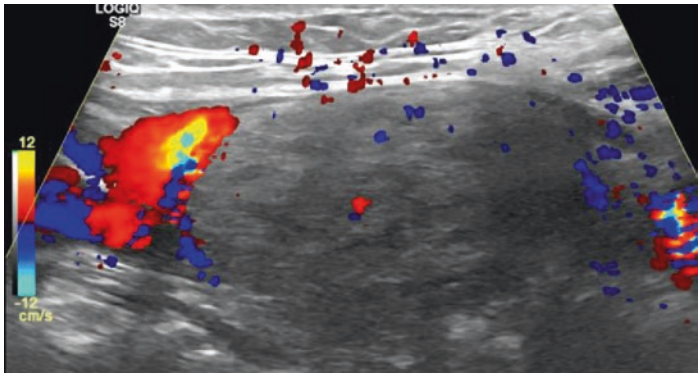

Image 6.16 Sagittal view of the right lobe shows very low parenchymal vascularity

Table 6.3 Differential diagnosis of the ultrasound

1. Hashimoto's thyroiditis
2. Subacute thyroiditis
3. Graves' disease

The patient's TSI and TRAB antibodies were negative, making autoimmune thyrotoxicosis less likely. Inflammatory markers (CRP, ESR, IL-6) were all elevated. Given the delayed presentation of thyrotoxicosis following years of amiodarone use, in an otherwise previously normal appearing thyroid (no nodules and no history of Graves' disease), amiodarone-induced thyrotoxicosis type II (AIT II) was diagnosed. In this condition, destruction of the gland leads to thyroid hormone release. Ultrasound features resemble subacute and post-partum thyroiditis. In the acute phase, vascularity may be reduced.

Destructive thyroiditis may respond well to glucocorticoids. This patient was started on high doses of prednisone, but due to worsening heart failure and inability to effectively control the thyrotoxicosis, she required thyroidectomy. The resected thyroid appeared edematous and enlarged, due to acute inflammation. Image 6.17 shows a pathology slide of the patient's resected thy-

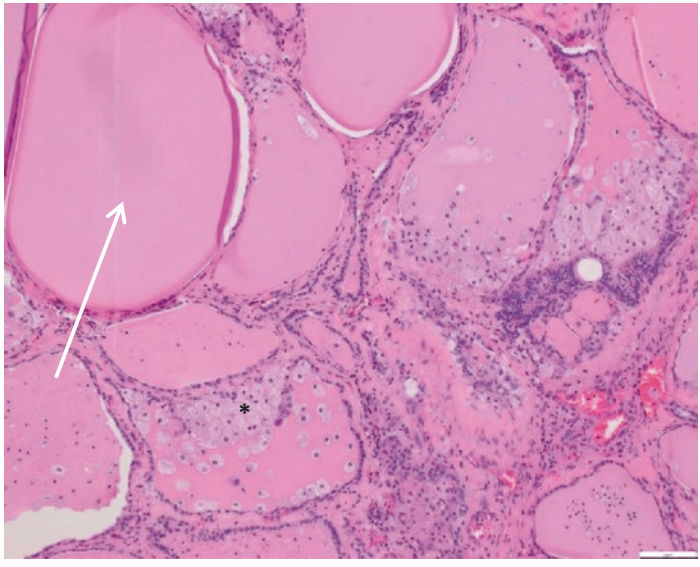

Image 6.17 Light microscopy of the above patient's resected thyroid with thyroiditis. The thyroid has colloid-rich, denuded thyroid follicles, and vacuolated cytoplasm (white arrow) with surrounding areas infiltrated by foamy histiocytes (black asterisk). (×10 H&E)

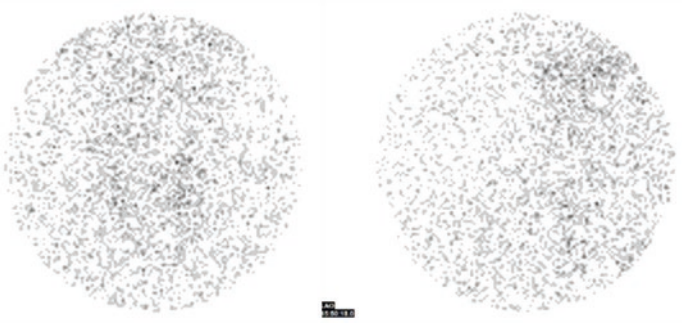

Image 6.18 I-123 uptake and scan of another patient with destructive thyroiditis. Uptake at 6 h is 0.8% and at 24 h is 0.4%, which is very low

roid. Image 6.18 shows I-123 uptake and scan of a different patient with destructive thyroiditis.

Additional Imaging Examples of Non-Autoimmune, Destructive Thyroiditis:

Case Presentation 4

A 70-year-old female smoker with atrial fibrillation, osteoporosis, and a goiter presented with long-standing fatigue, weight loss, proximal muscle weakness, palpitations, and tremors. She denied a family history of thyroid disease. Exam was notable for a visible goiter with bilateral thyroid nodules, an irregularly irregular heart rhythm, and fine hand tremor. Lab work demonstrated a suppressed TSH of <0.16 uIU/mL (ref <0.3 uIU/mL) and normal free T4 of 1.4 ng/dL (ref 0.9-2.3 ng/dL). Images 6.19 and 6.20 show her initial ultrasound. Table 6.4 shows the differential diagnosis in this case based on the image findings.

Thyroid autoantibodies were negative. Given the patient's age and comorbidities, methimazole was prescribed for subclinical hyperthyroidism. Subsequent I-123 uptake and scan showed both "hot" and "cold" nodules. Diagnosis of TMNG was made, based on the presence of palpable and sonographically localized thyroid nodules, increased radioiodine uptake in the nodules with a low uptake in surrounding thyroid tissue, and excess thyroid hormone

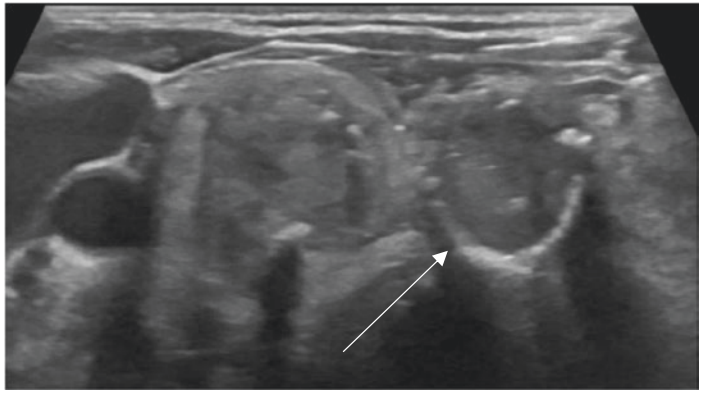

Image 6.19 Multiple nodules were demonstrated bilaterally. The nodule in the right inferior lobe is solid and hypoechoic, with peripheral rim calcifications (arrow)

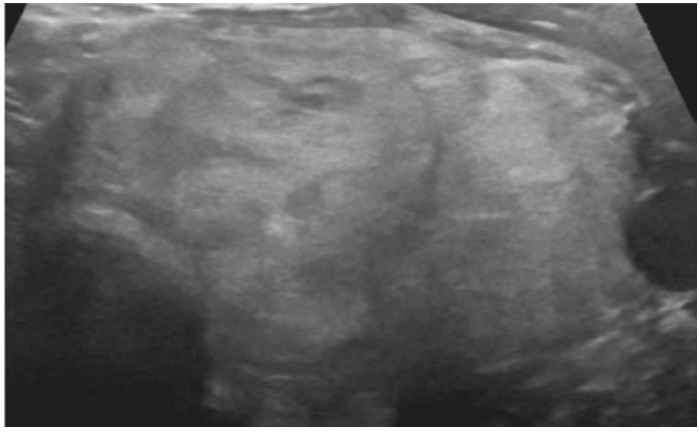

Image 6.20 In contrast to the inferior lobe nodules, the superior lobe nodules are solid and hyperechoic. Glands with multiple overlapping or confluent nodules/lobules should be distinguished from those with distinct nodules, as often in the former case, biopsy is not required and observation is sufficient

Table 6.4 Differential diagnosis of the ultrasound

1. Euthyroid nodular goiter
2. Toxic multinodular goiter

Image 6.21 I-123 uptake scan of a different patient with TMNG. "Hot" nodules with high radioiodine uptake in the superior right lobe (left panel: bright areas, top two arrows). "Cold" nodules with low radioiodine uptake (darker areas) are in the right inferior lobe (left panel, bottom arrow)

production leading to TSH suppression. TMNG results from autonomously functioning thyrocytes.

On ultrasound, "hot" (autonomous) nodules may appear hyperechoic compared to "cold" nodules. But a hyperechoic nodule on US does not exclude the presence of thyroid cancer since follicular thyroid cancer may present this way. I-123 scan with increased iodine uptake corresponding to the hyperechoic nodules generally excludes thyroid cancer within these nodules. "Cold" nodules (with reduced iodine uptake) meeting fine needle aspiration (FNA) size criteria should be biopsied. This patient had FNAs of the cold nodules, which showed benign cytology. Images 6.21 and 6.22 show two different patients with toxic multinodular goiter with hot and cold nodules. Image 6.23 is the pathology slide of the resected thyroid of the patient on image 6.22 with a large, compressive multinodular goiter.

Other Imaging Examples of Diffuse Thyroid Disease:
Subacute Thyroiditis Sonography of subacute (also known as painful or granulomatous) thyroiditis can be misleading when nodular areas are evident. In this condition, thyroid parenchyma can be patchy, with hypoechoic, focal areas. Vascularity is generally decreased. Over time, these abnormalities resolve, thus care-

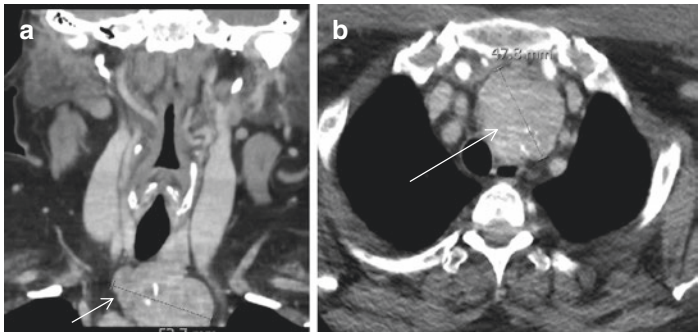

Image 6.22 A severe case of TMNG with a suppressed TSH of 0.015, negative thyroid autoantibodies, and symptoms of compression. Contrast-enhanced coronal (**a**) and axial (**b**) CT images of the neck show a large, exophytic mass (arrows) projecting along the inferior aspect of the left thyroid gland, measuring approximately 5 × 4.4 × 4.6 cm, compressing the esophagus, and deviating the trachea. Note: iodinated contrast commonly used in radiologic examinations and interventional procedures results in a huge iodide exposure to the thyroid, which, in individucals with pre-existing thyroid disease, can result in thyrotoxicosis

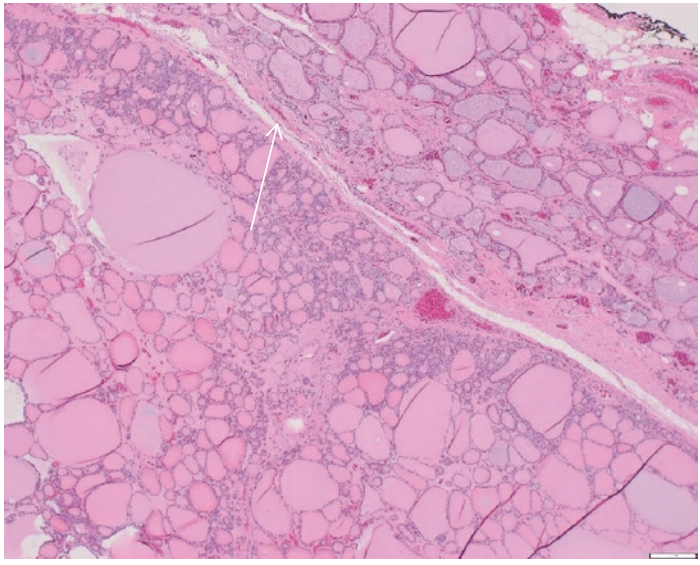

Image 6.23 The above patient with TMNG had a thyroidectomy for mechanical compression symptoms. Histologic sections show adenomatoid nodules that are circumscribed, unencapsulated nodules (arrow) comprised of benign thyroid follicles benign thyroid follicles (×4 H&E)

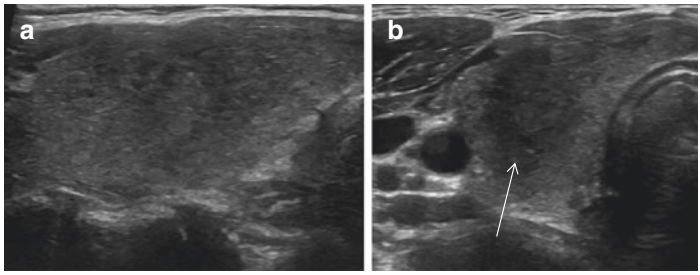

Image 6.24 Sagittal (**a**) and transverse (**b**) views of the thyroid in a patient with subacute thyroiditis. Irregular echotexture is common and hypoechoic areas can sometimes resemble nodules (arrow)

ful consideration should be given before pursuing fine needle aspiration**.** Image 6.24 shows this additional example.

Discussion

In general, ultrasonography is not a major component of the diagnosis of autoimmune thyroid disease (AITD), which is primarily driven by clinical and biochemical findings. However, due to the finding of thyromegaly on physical exam, ultrasound is often performed to rule out the presence of nodules that may require biopsy.

Hashimoto's and Graves' disease, as well as non-immune thyroid diseases (such as destructive thyroiditis and TMNG) have some defining characteristics on US. Reduced thyroid echogenicity is a strong predictor of AITD. This finding can occur early in the disease course, even before the onset of thyroid dysfunction. Although the sensitivity of this finding is high, hypoechogenicity is not specific to AITD, as thyroiditis can also present with this feature. However, micronodularity has a positive predictive value (PPV) of 95% for Hashimoto's thyroiditis. Large pseudonodules (which often appear as nodular regions surrounded by white, fibrous bands) are relatively common in Hashimoto's and a less experienced operator may not recognize that such

lesions do not require biopsy. Pseudonodules may be distinguished from true nodules by imaging in a second plane, whereby it becomes evident that the mass is not three-dimensional.

Differences in thyroid vascularity may be useful in distinguishing Graves' disease, and AIT type I (associated with hypervascularity) from the very low vascularity seen in destructive thyroiditis (e.g., in AIT type II). This is often important in critically ill patients in whom the distinction between different causes of thyrotoxicosis is necessary, but radioiodine imaging is not possible. "Thyroid inferno" has a high PPV of 95.2% for Graves' disease.

Further Reading

Chung J, et al. Clinical applications of Doppler ultrasonography for thyroid disease: consensus statement by the Korean Society of Thyroid Radiology. Ultrasonography. 2020;39:315–30.

Pedersen OM, et al. The value of ultrasonography in predicting autoimmune thyroid disease. Thyroid. 2000;10(3):251–9.

Scappaticcio L, et al. Diagnostic testing for Graves' or non-Graves' hyperthyroidism: a comparison of two thyrotropin receptor antibody immunoassays with thyroid scintigraphy and ultrasonography. Clin Endocrinol (Oxf). 2020;92(2):169–78.

Solivetti FM, et al. "Hypoechoic triangle": a new sonographic sign or marker of advanced autoimmune thyroiditis. Thyroid. 2011;21(3):285–9.

Vitti P, et al. Thyroid blood flow evaluation by color-flow Doppler sonography distinguishes graves' disease from Hashimoto's thyroiditis. J Endocrinol Invest. 1995;18:857–61.

Thyroid Nodule Composition

7

Leslie S. Eldeiry

Key Points

- Thyroid nodule composition can be described as solid, cystic, or complex, with >50% of the nodule contents determining the overall composition.
- Spongiform nodules contain numerous tiny cysts in >50% of the nodule. The presence of colloid artifact must be distinguished from microcalcifications, as both can appear as tiny echogenic foci.
- Fine needle aspiration (FNA) is recommended for solid nodules >1–1.5 cm, and some smaller nodules, depending on other ultrasound characteristics.
- FNA can be considered for spongiform nodules >2 cm, though these nodules may also be observed clinically.

L. S. Eldeiry (✉)
Department of Endocrinology, Harvard Vanguard Medical Associates/ Atrius Health and Harvard Medical School, Boston, MA, USA
e-mail: Leslie_eldeiry@atriushealth.org

L. S. Eldeiry et al. (eds.), *Handbook of Thyroid and Neck Ultrasonography*, Contemporary Endocrinology,
https://doi.org/10.1007/978-3-031-18448-2_7

- Purely cystic or partially cystic nodules without other suspicious ultrasound features may be observed.
- The cytologic diagnosis of cystic thyroid nodules can be challenging due to hypocellularity and atypical cell features of cyst fluid contents.

- **Composition:** The description of thyroid nodule composition is based on the **ratio of cystic to solid components**: cystic nodules have no solid components, while solid nodules have no cystic components.
- **Complex nodules:** have both solid and cystic components, with predominantly cystic lesions comprised of ≥50% cyst fluid and predominantly solid lesions comprised of ≥50% solid components.
- **Spongiform nodules:** are comprised of numerous tiny micro- and macro-cysts in >50% of the nodule. Examples are presented later in the chapter (Images 7.8 and 7.9).

Case Presentation

A 29-year-old woman with no significant medical history or family history of thyroid disease presented with a large midline neck mass. The mass was painless and non-tender, located in the midline and lower neck, measured 4 × 6 cm on physical exam, elevated with swallowing, and was not associated with cervical adenopathy. Laryngoscopic examination was normal. TSH was 1.43 mIU/L. Neck ultrasound demonstrated a 6.3 × 6.2 × 3.3 cm midline complex neck nodule (Image 7.1). Neck MRI was obtained for further evaluation and showed a 6.7 cm large cystic mass probably arising from the inferior thyroid containing a 2.1 cm enhancing nodule (Images 7.2 and 7.3) and no adenopathy. The differential diagnosis of the neck mass is presented in Table 7.1.

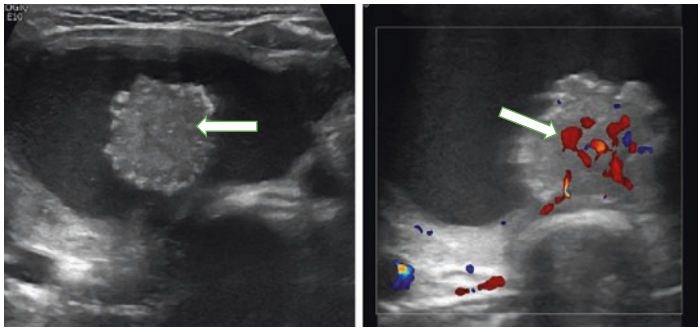

Image 7.1 A complex, predominantly cystic nodule. Left: A cystic isthmic nodule extending into the right lobe of the thyroid. The solid component is pedunculated, irregular, with calcifications around the border and some internal echogenic foci (arrow). Right: Hypervascular solid component on color Doppler

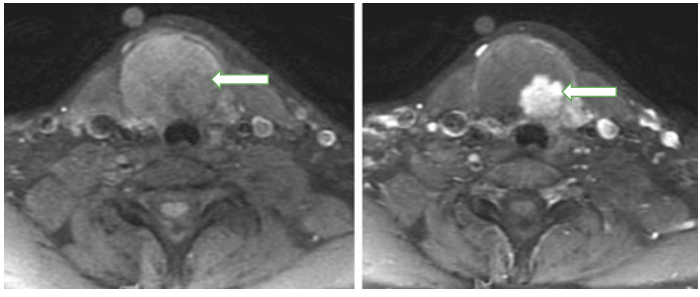

Image 7.2 Axial MRI. Left: Axial T1 fat-saturated precontrast image. Right: Axial T1 fat-saturated postcontrast image. This image shows the nodular enhancement of the solid component of the cystic lesion (arrows)

Ultrasound-guided FNA of the solid portion of the nodule was performed. Several mL's of gelatinous, hemorrhagic fluid was drained from the cystic portion. Cytology evaluation was challenging because of the cystic changes in the lesion. Cytology showed groups of vacuolated plasmacytoid cells with basophilic cytoplasm (Image 7.4a, b). Cellblock preparation demonstrated

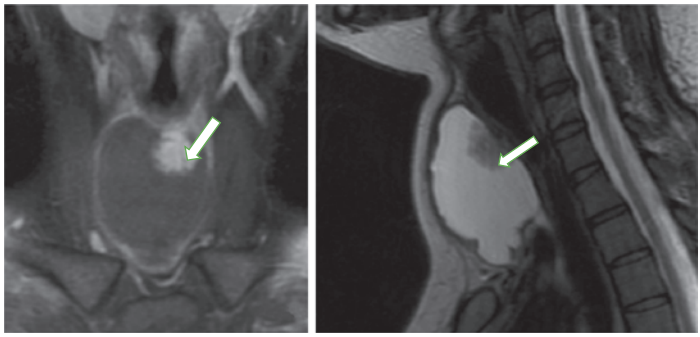

Image 7.3 Sagittal MRI T1 and T2 sequences demonstrate the solid (arrows indicate solid component) and cystic components. Left: Coronal T1 fat-saturated postcontrast image. Right: Sagittal T2 image without contrast

Table 7.1 Differential diagnosis

1. Thyroglossal duct cyst
2. Benign cystic thyroid nodule
3. Cystic papillary thyroid carcinoma
4. Cystic parathyroid adenoma
5. Metastasis from extrathyroidal malignancy

papillary architecture with single detached vacuolated cells, pseudonuclear inclusions, and psammoma bodies. Positive immunohistochemistry for CK7 stain highlighted the papillary fragments (Image 7.5a, b). The overall findings were interpreted as consistent with papillary thyroid carcinoma (PTC).

The patient underwent total thyroidectomy. Histopathology showed a 6.7 cm cystic PTC in the isthmus and inferior right lobe, classical subtype with a 2.0 cm solid portion (Image 7.6); and 2 sub-centimeter metastatic paratracheal lymph nodes. Staining for BRAFV600E mutation was positive. She was subsequently treated with radioactive iodine. Post-therapy whole body imaging and subsequent surveillance testing indicated no distant metastasis or persistent disease.

Thyroid Nodule Composition: Additional Examples

See Images 7.7, 7.8, 7.9, 7.10 and 7.11.

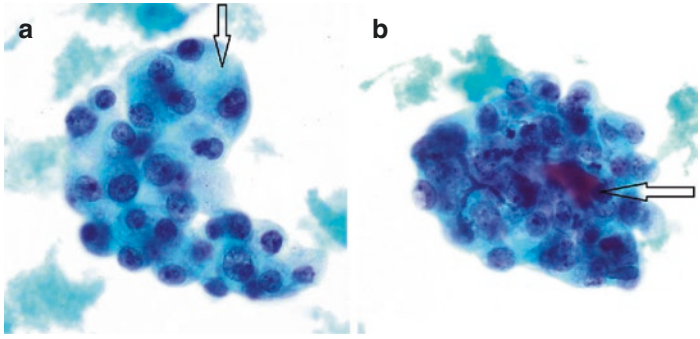

Image 7.4 (**a**) Follicular cells arranged in clusters (arrow) with hyperchromatic, enlarged nuclei and prominent nucleoli (Thin-prep cytology, PAP stain, ×40). (**b**) Cluster of follicular cells with enlarged, hyperchromatic nuclei and thick inspissated colloid (arrow) (Thin-prep cytology, PAP stain, ×40)

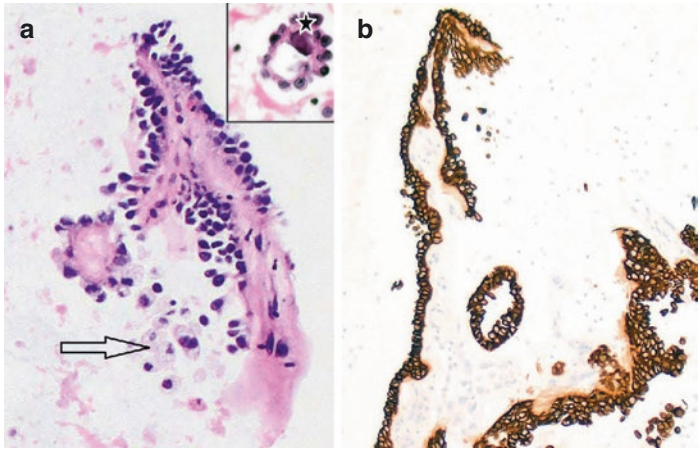

Image 7.5 (**a**) Cellblock preparation demonstrated papillary architecture with single detached vacuolated cells (**a**, arrow, H&E, ×40), pseudonuclear inclusions, and psammoma bodies (**a** insert, asterisk, H&E, ×60). Positive immunohistochemistry for CK7 stain highlighted the papillary fragments (**b**, CK7 immunohistochemical stain, ×20).

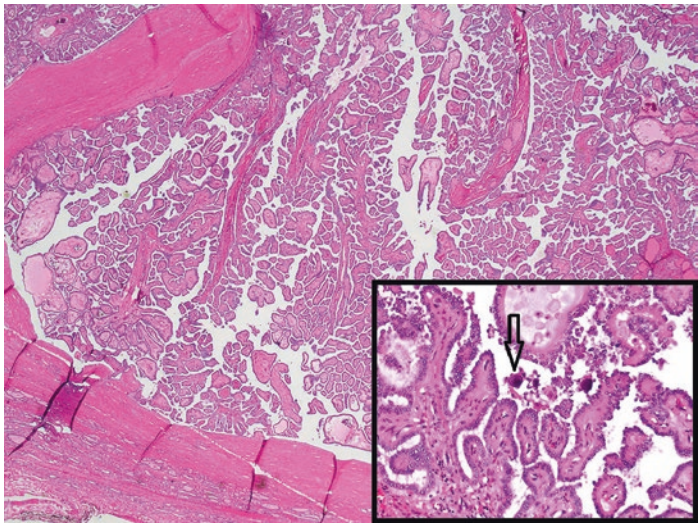

Image 7.6 Papillary thyroid carcinoma (H&E, ×2); insert shows typical psammoma bodies (arrow, H&E ×4)

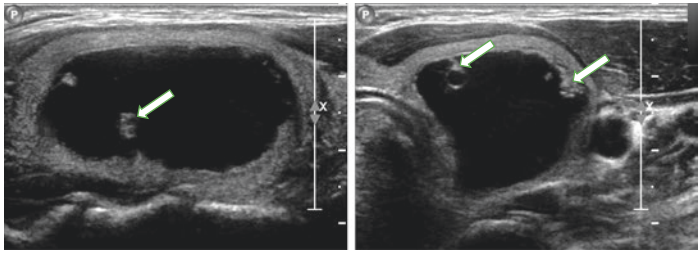

Image 7.7 Left, sagittal and Right, transverse views of the left mid thyroid. **Predominantly cystic** 3.5 cm, benign left lobe nodule with peripheral soft tissue elements (arrows). Cystic lesions of this type are often initially spongiform nodules in which a macro-cystic component predominates. The fluid may contain low reflective echoes, representing either debris or recent or old spontaneous hemorrhage

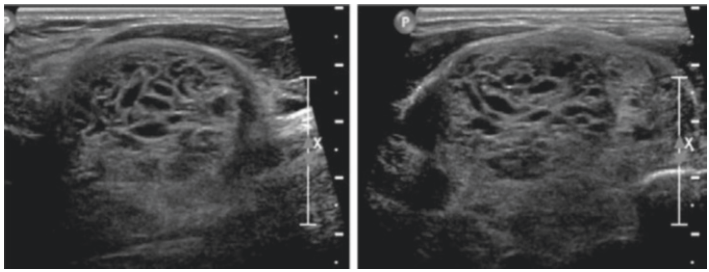

Image 7.8 Left, sagittal and Right, transverse views of a palpable right thyroid nodule. **Classic spongiform nodule** containing scattered tiny echogenic foci in the posterior portion of the cysts that most likely represent colloid. FNA is not recommended but may be considered for larger nodules. Observation and follow-up imaging in 1 year is another aproach

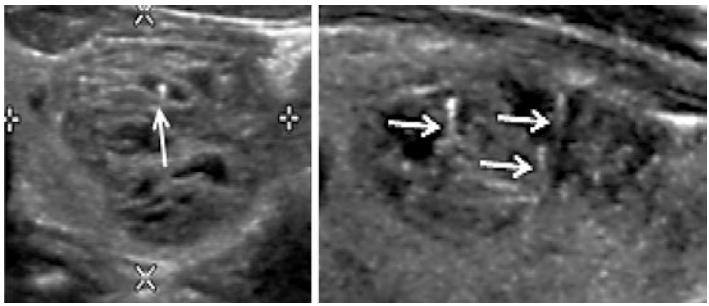

Image 7.9 Microcystic components may contain bright reflective echoes with comet tail artifact. These represent colloid crystals/inspissated colloid rather than microcalcifications. They are often located in the dependent portion of the cysts (arrows)

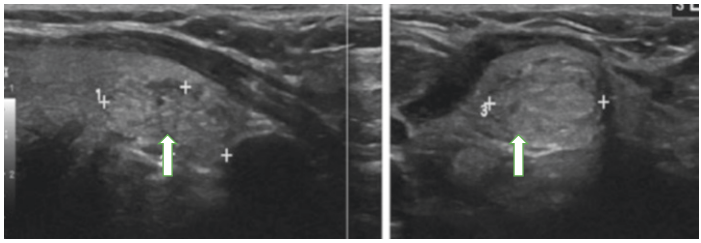

Image 7.10 Left, sagittal and Right, transverse images of the inferior isthmus. A 1.7 cm isoechoic, **predominantly solid**, likely benign, well-circumscribed nodule (arrows). FNA is recommended due to size and solid composition

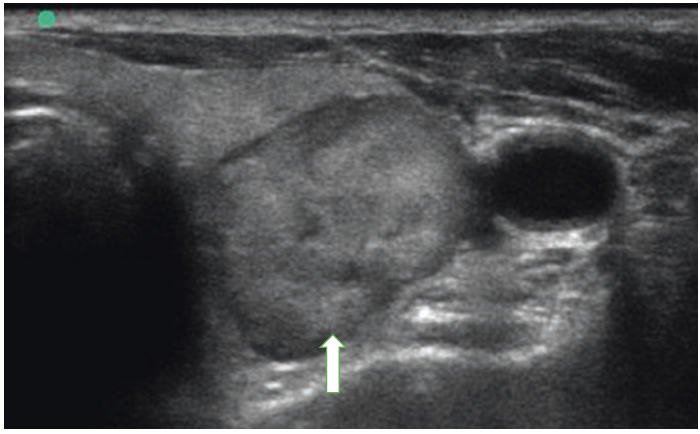

Image 7.11 Transverse image of a 2.5 cm **solid, heterogeneous** left lobe nodule (arrow). FNA is recommended, with targeting of the heterogeneous, hypoechoic components of the nodule

Discussion

A purely cystic nodule is highly unlikely to be malignant. These nodules are either simple colloid cysts or may result from cystic degeneration or hemorrhage into a benign, hyperplastic nodule. The majority of predominantly cystic thyroid nodules are benign.

However, when a solid component is present, that will determine the likelihood of benignity or malignancy, making careful assessment of that component important. Cystic lesions with multiple septations are usually benign. Other ultrasound features favoring benignity include a spongiform composition, oval or round shape, and smooth margins. Isoechoic echotexture and absence of calcifications suggest benignity. Ultrasound features suggesting malignancy in a partially cystic nodule include a polypoid solid component or eccentric location of the solid region. A hypoechoic echotexture, irregular border and the presence of microcalcifications are also worrisome features.

Sometimes the determination of composition of a thyroid nodule on ultrasound can be challenging. For example, in spongiform nodules, which are essentially a cluster of numerous micro- and various sized macro-cysts, there are often high reflective echoes. Differentiating microcalcifications from colloid crystals/inspissated colloid can sometimes be difficult. Colloid is classically identified either by a comet tail projecting posteriorly from the high reflective echo or by the presence of the high reflective echo in the most dependent portion of the micro- or macro-cyst (see Images 7.8 and 7.9). When it is not possible to differentiate colloid artifact from microcalcifications, FNA may be necessary to confirm benign cytology. Spongiform nodules, which are often a feature of colloid nodules or goiter, can be avascular or hypervascular. Doppler evaluation to assess vascularity may therefore not be helpful.

Another difficult distinction in the assessment of nodule composition is distinguishing cysts from pseudocystic nodules. Cysts usually contain homogeneous fluid, are anechoic, have smooth margins, and remain relatively stable or enlarge very slowly. Pseudocystic nodules often contain heterogeneous-appearing fluid with low level reflective echoes, sometimes with dependent debris. These lesions may appear suddenly, most commonly due to spontaneous bleeding in a spongiform nodule. They either slowly resolve on their own or the blood may be slowly resorbed, ultimately resulting in a remnant pure cyst.

Approximately 5–10% of solid thyroid nodules are malignant and depending on the size and ultrasound characteristics, evaluation with FNA for cytology is usually necessary. FNA of the solid

component of a complex cystic nodule can be challenging, specifically to obtain adequate diagnostic cytologic material. For inadequate (non-diagnostic) FNAs, management decisions should be based on ultrasound appearance and clinical factors. Hypocellularity, nuclear debris, and cyst content features may also complicate the ability to distinguish between benign and malignant nodules (e.g. due to the presence of nuclear atypia and prominent nucleoli in benign histiocytes or the presence of squamous cells, which can mimic PTC). Essentially, given the variability of the composition of thyroid nodules and of other features, FNA should be considered to resolve any uncertainties. When cytology is indeterminate, repeat sampling and molecular marker testing may be useful.

Further Reading

Chung R, Kim D. Imaging of thyroid nodules. Appl Radiol. https://www.appliedradiology.com/Communities/Pediatric-Imaging/imaging-of-thyroid-nodules

Haugen BR, et al. Management guidelines for adult patients with thyroid nodules and differentiated thyroid cancer. Thyroid. 2016;26(1):1–133.

Kim JY, Kim E-K, Lee HS, Kwak JY. Conventional papillary thyroid carcinoma: effects of cystic changes visible on ultrasonography on disease prognosis. Ultrasonography. 2014;33(4):291–7.

Mokhtari M, Kumar PV, Hayati K. Fine-needle aspiration study of cystic papillary thyroid carcinoma: rare cytological findings. J Cytol. 2016;33(3):120–4.

Yang GCH, Stern CM, Messina AV. Cystic papillary thyroid carcinoma in fine needle aspiration may represent a subset of the encapsulated variant in WHO classification. Diagn Cytopathol. 2009;38(10):721–6.

Echogenicity of the Thyroid

8

Pamela L. Mok

Key Points

- The echogenicity of the thyroid is an important indicator of underlying thyroid disorders and/or the presence of focal thyroid masses.
- Technical factors can affect the classification of echogenicity and may alter risk assessment. Settings may need to be adjusted carefully during real-time scanning to properly characterize lesions.
- Recognition of certain patterns of echogenicity may prevent unnecessary tissue sampling of common benign conditions.
- Anechoic cysts and classic spongiform nodules are highly likely to be benign.
- Hashimoto's thyroiditis commonly has a diffuse hypoechoic, micronodular echotexture or a variegated pattern of hypoechoic bands and interspersed echogenic areas, similar to a giraffe hide.

P. L. Mok (✉)
Department of Radiology, Atrius Health, Boston, MA, USA
e-mail: Pamela_Mok@AtriusHealth.org

L. S. Eldeiry et al. (eds.), *Handbook of Thyroid and Neck Ultrasonography*, Contemporary Endocrinology,
https://doi.org/10.1007/978-3-031-18448-2_8

- A uniformly hyperechoic nodule within a background of Hashimoto's thyroiditis ("white knight" appearance) is usually benign.
- Hypoechoic masses have a higher risk of malignancy, especially if the mass is markedly hypoechoic (darker than adjacent neck muscles) or if other suspicious features are present.
- The echogenicity of a thyroid nodule plays a valuable role in the risk assessment for thyroid malignancy; however, other features must also be taken into consideration.

Introduction

Echogenicity refers to the grayscale appearance of an organ or structure on ultrasound based on the acoustic impedance of sound waves through the tissue. When sound waves are introduced into the body, they are both transmitted deeper into tissue and reflected back to the transducer to a variable degree, depending on the density of each tissue. Assessment of the echogenicity of the thyroid gland and of thyroid nodules is an important factor in thyroid evaluation.

- **Anechoic:** Anechoic refers to a fluid-filled structure that appears black on ultrasound. Fluid-filled structures allow sound waves to pass through easily, with no sound waves reflected back to the transducer. Examples include the urinary bladder, gallbladder, cysts, or blood vessels.
- **Hypoechoic:** Hypoechoic structures transmit some sound waves and have a relatively dark appearance, but not to the same degree as simple cysts or other fluid-containing structures. Examples of hypoechoic tissue include muscle, kidney, or complicated cysts containing either protein (e.g. colloid) or hemorrhage.

- **Hyperechoic:** Hyperechoic refers to higher density tissue including fatty and fibrous tissue, bone, and calcification, which appears white on imaging, due to significant reflection of sound waves returning to the transducer. Bone and calcification appear the brightest since their high density reflects most of the sound waves and prevents deeper penetration, resulting in a dark shadow posteriorly.
- **Isoechoic:** Refers to echogenicity in which two adjacent structures have exactly the same echotexture.
- **Echogenic:** Similar to hyperechoic, echogenic describes focal bright areas that reflect sound waves. The term "punctate echogenic foci" is often used to describe small areas within nodules that can represent microcalcifications or inspissated colloid (sometimes referred to as colloid crystals).

Case Presentation

A 64-year-old woman with hypertension and atrial fibrillation on anticoagulation presented with a rapidly enlarging left neck mass that was determined to be within the left thyroid lobe. She was asked to stop the anticoagulation pending a biopsy of the lesion and was admitted to the hospital for airway management. Thyroid ultrasound (Image 8.1) showed a diffusely enlarged, hypoechoic, and nodular thyroid gland with a very large 8 cm left thyroid mass. A contrast-enhanced neck CT scan (Image 8.2) showed marked deviation of the trachea to the right of midline by the large left thyroid mass and lateral displacement of the left carotid artery

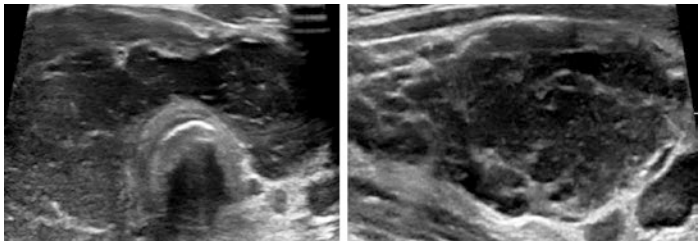

Image 8.1 Transverse (left) and sagittal (right) US images demonstrate diffuse thyroid enlargement with a large lobulated hypoechoic mass

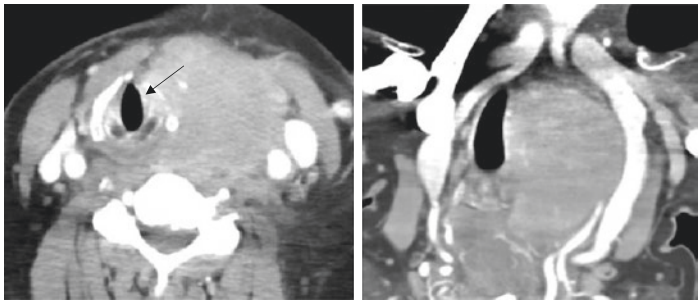

Image 8.2 Axial (left) and coronal (right) contrast-enhanced neck CT scan images show the large thyroid mass markedly displacing the trachea to the right of midline (arrow) and the left carotid artery to the left

Table 8.1 Differential diagnosis

1. Hashimoto's thyroiditis
2. Thyroid malignancy, such as anaplastic carcinoma
3. Thyroid lymphoma
4. Hemorrhage into the thyroid gland related to anticoagulation

to the left. Table 8.1 lists potential differential diagnoses in this case, including possible thyroiditis, thyroid malignancy, and hemorrhage related to anticoagulation.

FNA and core biopsy done under ultrasound guidance revealed a B-cell lymphoma of the germinal cell type (Images 8.3 and 8.4). CD20 immunostain was positive (Image 8.5), supporting the diagnosis of high-grade B-cell lymphoma. Based on additional immunohistochemical and cytogenetic studies, the lymphoma was classified as diffuse large B-cell lymphoma with a germinal center phenotype.

The patient was treated with 3 cycles of combination chemotherapy (R-EPOCH/Filgrastim/Neupogen) and responded well. Positron emission tomography (PET) scan obtained 4 months later revealed a dramatic response of the thyroid mass with return of the thyroid gland back to midline (Image 8.6), but imaging of the mediastinum showed a PET-positive lymph node in the subcarinal region of the chest (Image 8.7). She was there-

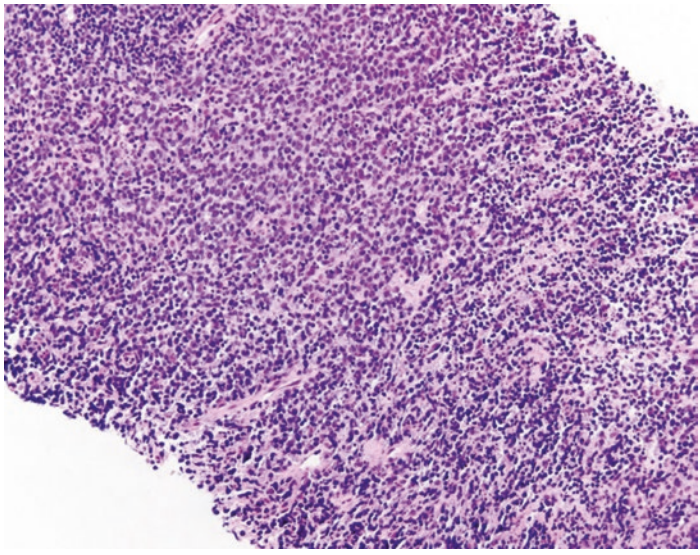

Image 8.3 Low magnification slide from the thyroid core biopsy shows a densely cellular lymphoid infiltrate that effaces the thyroid parenchyma

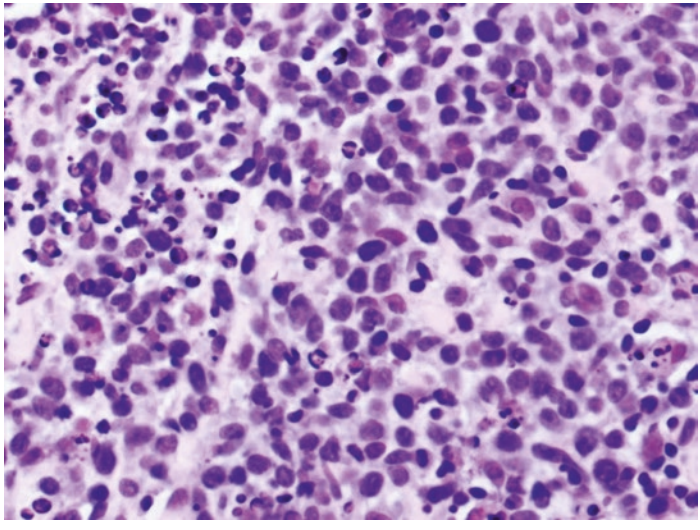

Image 8.4 High magnification pathology slide shows high-grade lymphoma with large, irregular nuclei and numerous apoptotic bodies

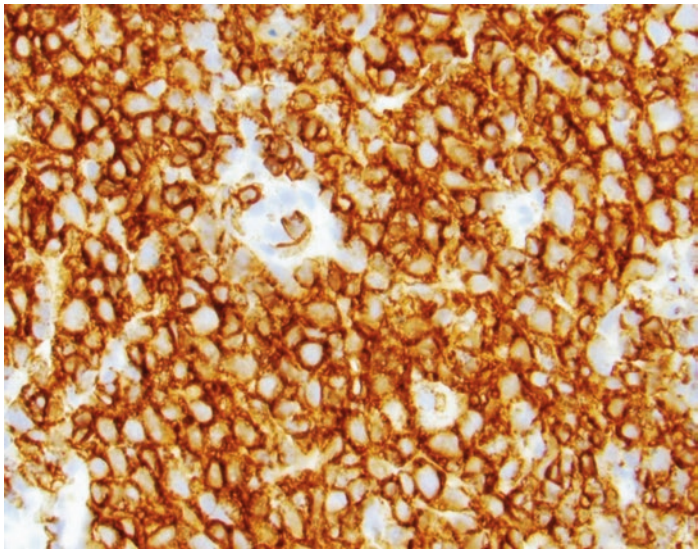

Image 8.5 Positive CD20 immunostain, supporting the diagnosis of high-grade B-cell lymphoma

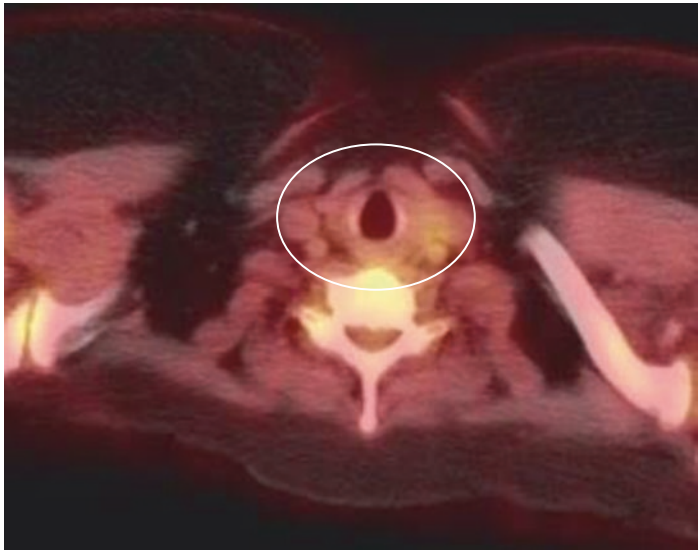

Image 8.6 Axial PET CT scan of the neck after treatment shows marked reduction in size of the thyroid with return of the trachea back to midline

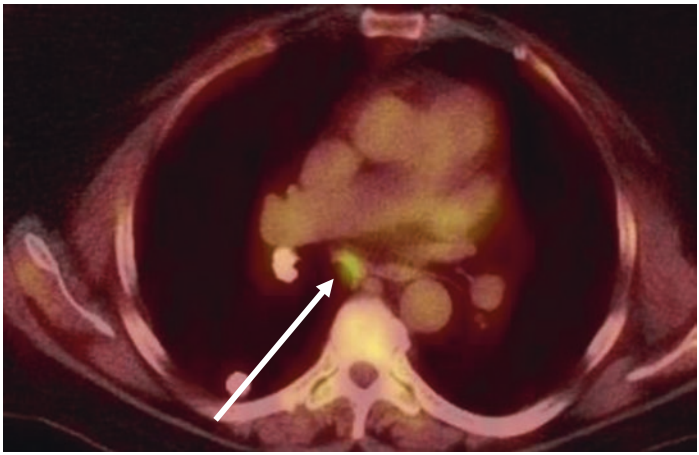

Image 8.7 Axial PET CT scan of the mediastinum shows a positive subcarinal lymph node (arrow)

fore classified as a stage II B-cell lymphoma and was treated with three additional cycles of R-CHOP chemotherapy and Filgrastim/Neupogen and has subsequently been rendered free of disease. A small lung nodule has been followed and has remained stable.

Additional examples of different thyroid echogenicity patterns from a variety of conditions are presented in Images 8.8, 8.9, 8.10, 8.11, 8.12, 8.13, 8.14, 8.15, 8.16, 8.17, 8.18, 8.19, 8.20, 8.21, 8.22, 8.23, 8.24, 8.25 and 8.26.

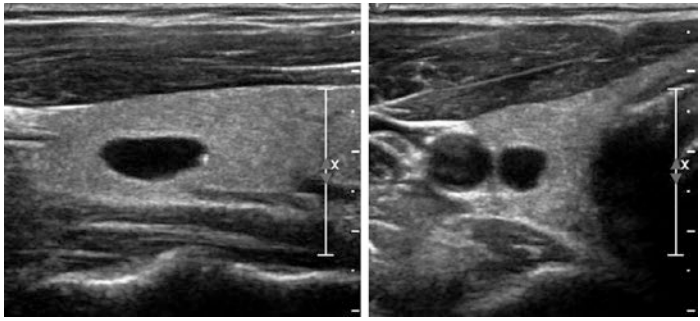

Image 8.8 Sagittal (left) and transverse (right) views of a benign anechoic cyst

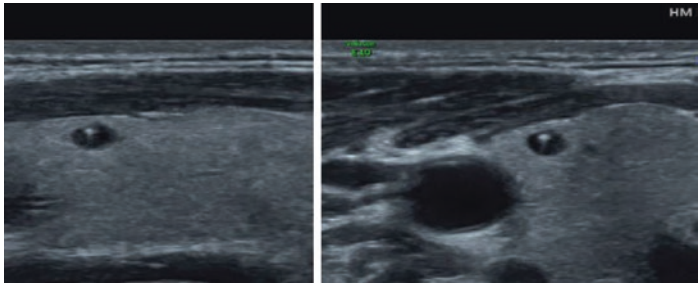

Image 8.9 Sagittal (left) and transverse (right) images show a typical benign anechoic colloid cyst containing a punctate hyperechoic focus which demonstrates characteristic echogenic comet tail artifact. The comet tail artifact is attributed to reverberation of sound waves within inspissated colloid and is recognized by the tapering attenuated V-shaped echoes beyond the echogenic focus

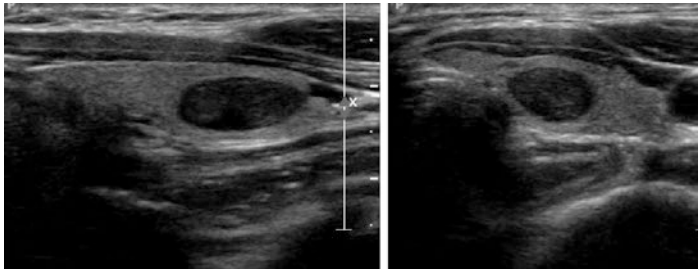

Image 8.10 Sagittal (left) and transverse (right) views of a hypoechoic nodule. Pathology showed a benign follicular adenoma

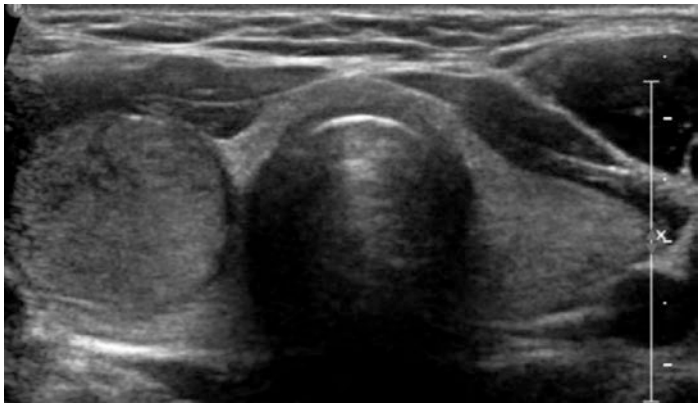

Image 8.11 Transverse view demonstrates a slightly hypoechoic mass. Pathology showed a follicular carcinoma

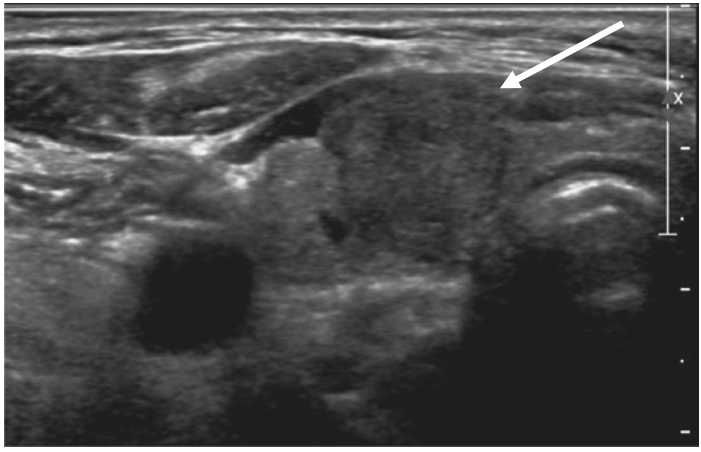

Image 8.12 Transverse view demonstrates a hypoechoic mass that was confirmed to be a papillary carcinoma. Note the anterior extrathyroidal extension of the mass (long white arrow)

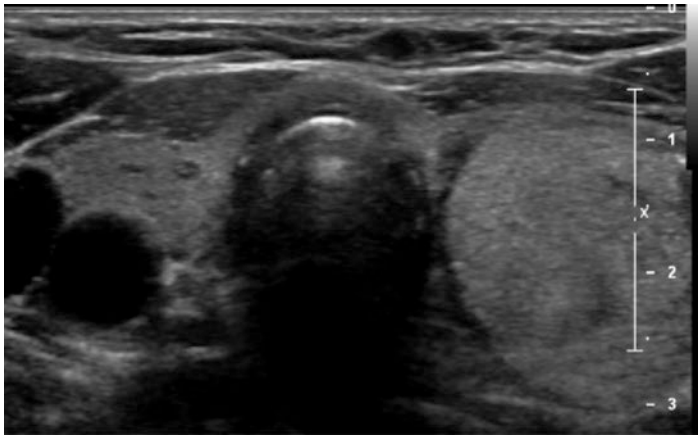

Image 8.13 Transverse view demonstrates a hyperechoic mass in the left lobe. Pathology showed benign follicular cells

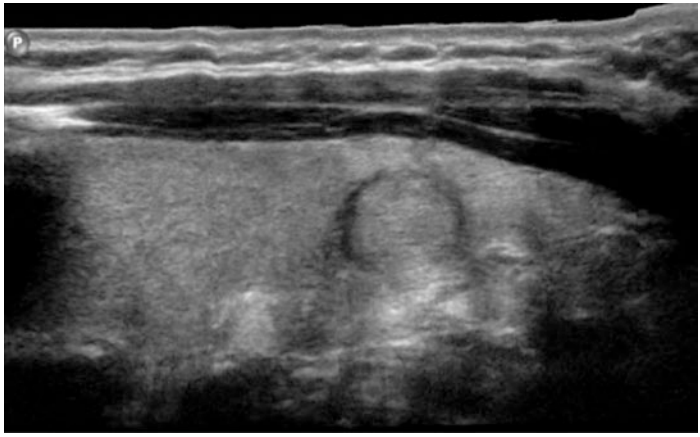

Image 8.14 Sagittal view demonstrating an isoechoic nodule. The nodule is the same echogenicity as the surrounding thyroid gland and is only visible due to the hypoechoic rim

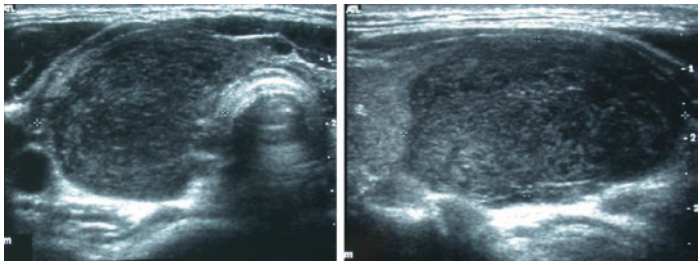

Image 8.15 Transverse (left) and sagittal (right) views show a markedly hypoechoic mass. Pathology showed lymphoma

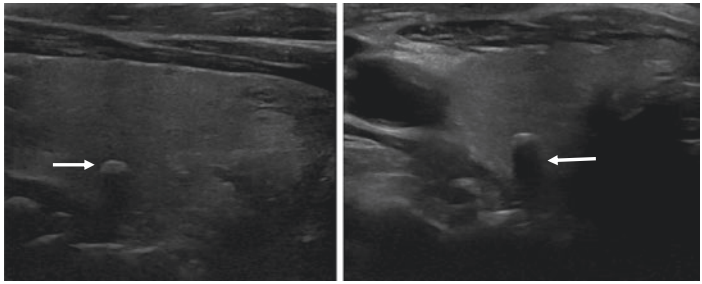

Image 8.16 Sagittal (left) and transverse (right) views of a hyperechoic calcification (arrow, left) demonstrating posterior hypoechoic shadowing (arrow, right)

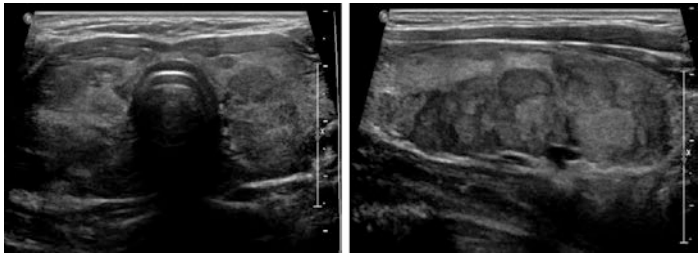

Image 8.17 Transverse (left) and sagittal (right) images showing a multinodular goiter with multiple hypoechoic nodules throughout the gland

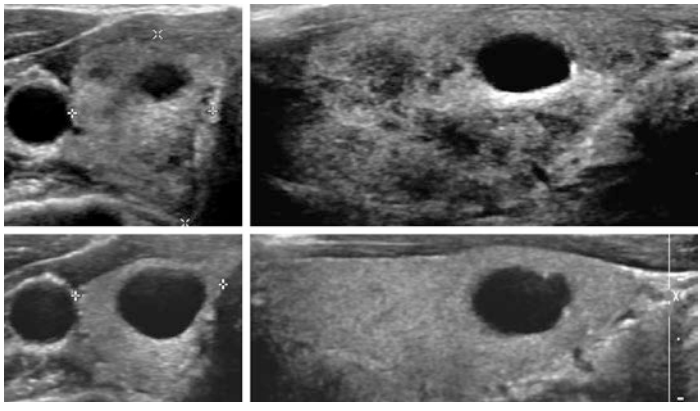

Image 8.18 Thyroiditis. Top: Transverse and sagittal images during an episode of acute thyroiditis show a heterogeneous right lobe with an incidental simple cyst. Bottom, transverse and sagittal images: Exactly 1 year later, after complete resolution of the thyroiditis

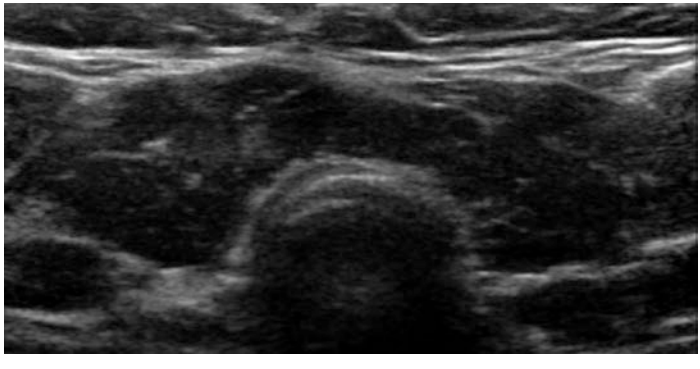

Image 8.19 Transverse view showing chronic thyroiditis. The thyroid is diffusely and markedly hypoechoic, similar to the adjacent muscle. This appearance can be seen in chronic, end-stage Hashimoto's thyroiditis or as a result of radioactive iodine therapy

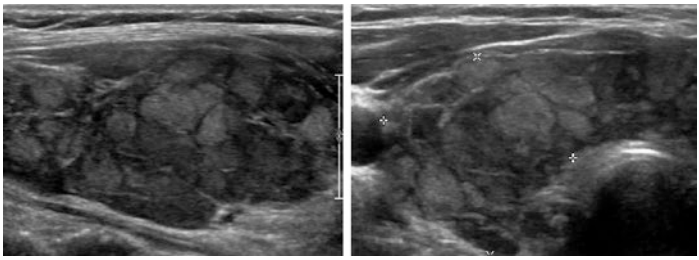

Image 8.20 Another appearance of thyroiditis, particularly Hashimoto's, shows a diffuse variegated echotexture with ill-defined "pseudonodules" resembling a giraffe hide. Sagittal (left) and transverse (right) views show a diffuse, "giraffe hide" appearance of thyroiditis

Image 8.21 Pair of giraffes with distinctive reticulated hide

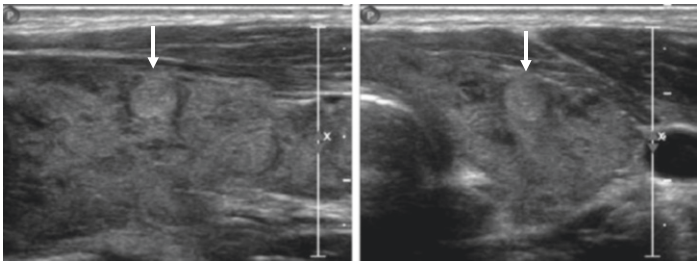

Image 8.22 In other cases of thyroiditis, typically associated with Hashimoto's, focal scattered hyperechoic areas can be detected within an underlying heterogeneous, patchy hypoechoic echotexture. These echogenic areas are termed "white knight" lesions and are essentially benign regenerative nodules superimposed on the background of thyroiditis. Sagittal (left) and transverse (right) views of a "white knight" nodule, representing a regenerative nodule in Hashimoto's thyroiditis

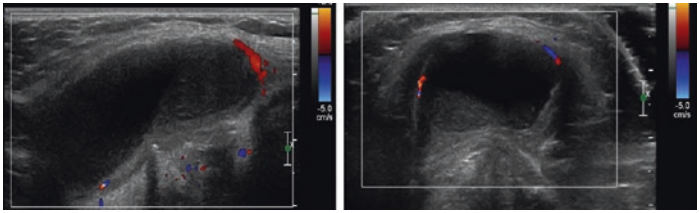

Image 8.23 Sagittal (left) and transverse (right) images of a hypoechoic mass with layering echoes and no central vascularity that was found to be a thyroglossal duct cyst containing proteinaceous debris

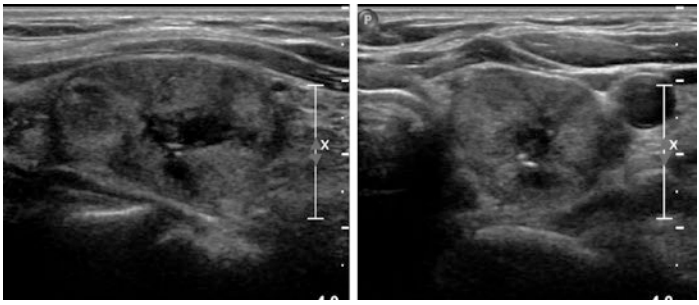

Image 8.24 Sagittal (left) and transverse (right) images show a mixed echogenicity mass with hyperechoic, hypoechoic, and anechoic areas as well as central calcification. Fine needle aspiration showed benign follicular cells, many macrophages, and colloid, consistent with a benign follicular nodule with cystic degeneration

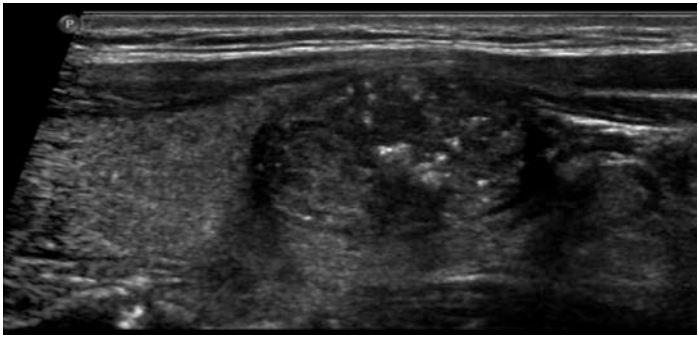

Image 8.25 Sagittal view showing a slightly hypoechoic mass containing small echogenic foci without posterior shadowing consistent with microcalcifications. Pathology showed papillary thyroid carcinoma

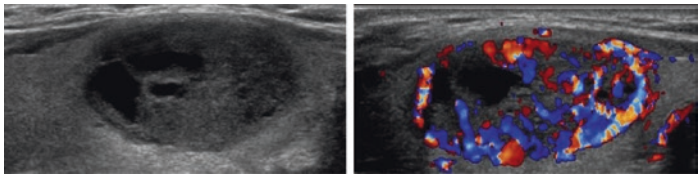

Image 8.26 Sagittal view (left) showing a markedly hypoechoic mass. Color Doppler imaging (right) shows marked peripheral and central vascularity. Pathology showed medullary thyroid carcinoma. Medullary carcinoma can also be partially cystic

Discussion

During thyroid ultrasound, the initial task is to assess the thyroid echogenicity, which is normally homogeneous and hyperechoic. If the texture is heterogeneous, determine whether the process is diffuse, involving the entire gland as in multinodular goiter, or whether normal thyroid tissue is interspersed with patchy areas, such as in Hashimoto's thyroiditis.

Whenever possible, the interpreting clinician should personally scan the patient; however, when this is not feasible, review of cine images in addition to static images is preferable. Scanning in person or viewing cine images in multiple planes has several advantages, including more thorough assessment of the underlying thyroid echogenicity and borders of an entire mass, differentiation of a true mass from a less-defined area of heterogeneity or "pseudonodule," and discrimination of microcalcifications from other types of echogenic foci, including those associated with inspissated colloid (colloid crystals).

Technical details, such as overall gain, frequency, focal zones, tissue harmonics, and spatial compound imaging are important factors to consider when assessing echogenicity and image quality. For example, an overall gain that is too low may make it difficult to distinguish a benign anechoic cyst from a very hypoechoic nodule, which has a higher risk of malignancy. Tissue harmonic imaging and spatial compound imaging help reduce reverberation and artifactual echoes, allowing differentiation of a benign cyst

from a solid hypoechoic mass. Depending on the size of the patient's neck and depth of the lesion, these technical factors may need to be adjusted during real-time scanning to improve tissue characterization.

The echogenicity of a mass, along with other factors, is used in the risk assessment for thyroid malignancy. An anechoic or almost completely anechoic cystic mass has a very high likelihood of benignity. Partially cystic anechoic masses or spongiform nodules with no other suspicious features are also likely benign; however, the amount and echogenicity of any solid tissue are important to assess. Isoechoic and hyperechoic masses are usually benign nodules such as follicular adenomas; however, 5–10% of isoechoic or hyperechoic solid masses are malignant, such as follicular carcinomas. The presence of a well-defined hypoechoic sonographic halo surrounding an isoechoic or hyperechoic nodule increases the likelihood of benignity.

Hypoechoic masses harbor a higher risk of malignancy, especially if the mass is very hypoechoic relative to adjacent neck musculature, or if other suspicious findings are present. A single mass may also have mixed echogenicity with hyperechoic, hypoechoic, and anechoic cystic components, and the dominant echotexture should be considered along with other characteristics such as shape, borders, and presence of calcifications.

Further Reading

Grant EG, et al. Thyroid Ultrasound Reporting Lexicon. White paper of the ACR Thyroid Imaging, Reporting and Data System (TIRADS) Committee. J Am Coll Radiol. 2015;12(12 Pt A):1272.

Haugen BR, et al. 2015 American Thyroid Association Management Guidelines for adult patients with thyroid nodules and differentiated thyroid cancer. Thyroid. 2016;26(1):1–133.

Lee JY, et al. Ultrasound malignancy risk stratification of thyroid nodules based on the degree of hypoechogenicity and echotexture. Eur Radiol. 2020 Mar;30(3):1653–63.

Tessler FN, et al. Thyroid Imaging Reporting and Data System (TI-RADS): a user's guide. Radiology. 2018;287:29.

Xie C, et al. Ultrasonography of thyroid nodules: a pictorial review. Insights Imaging. 2016;7(1):77–86.

Thyroid Nodule Ultrasonography: Margins and Shape

9

Michael D. Otremba, Chia A. Haddad, and Gregory W. Randolph

Key Points

- Thyroid nodule margins are based on the sonographic border between the nodule and surrounding parenchyma and can help distinguish between benign and malignant nodules.

The original version of the chapter has been revised. A correction to this chapter can be found at https://doi.org/10.1007/978-3-031-18448-2_15

M. D. Otremba (✉)
Department of Otolaryngology-Head and Neck Surgery, Massachusetts Eye and Ear, Harvard Medical School, Boston, MA, USA
e-mail: Michael_Otremba@meei.harvard.edu

C. A. Haddad
Harvard Vanguard Medical Associates, Massachusetts Eye and Ear, Harvard Medical School, Boston, MA, USA
e-mail: Chia_Haddad@atriushealth.org

G. W. Randolph
Massachusetts Eye and Ear Infirmary, Boston, MA, USA

Massachusetts General Hospital, Boston, MA, USA
e-mail: Gregory_Randolph@meei.harvard.edu

L. S. Eldeiry et al. (eds.), *Handbook of Thyroid and Neck Ultrasonography*, Contemporary Endocrinology,
https://doi.org/10.1007/978-3-031-18448-2_9

- Infiltrative, irregular, and lobulated margins are associated with malignancy.
- Thyroid nodule shape is determined by the ratio of the antero-posterior (AP) and transverse (T) diameters when measured on transverse view and is described as either wider than tall (T > AP) or taller than wide (AP > T).
- Taller than wide shape has high specificity but low sensitivity for malignancy.
- Poorly defined nodules are not associated with a higher risk of malignancy.
- Extrathyroidal extension suggests advanced or aggressive disease.
- Interobserver variability for nodule margin is common.

Introduction

This chapter deals with two specific ultrasound characteristics of thyroid nodules and their influence in determining whether the nodule is of concern and a biopsy is indicated.

- **Margins:** The description of the margins of a thyroid nodule is based on the sonographic border between the nodule and surrounding thyroid parenchyma. While a given nodule may have a variable margin along its entire circumference, nodule margins can be categorized as:
  - **Smooth:** a clear, continuous, rounded border between nodule and parenchyma (Image 9.4).
  - **Irregular/Infiltrative:** a non-uniform, jagged, or spiculated border between nodule and parenchyma (Image 9.5).
  - **Lobulated:** focal areas of bulging along the border between the nodule and parenchyma (Image 9.1).
  - **Poorly (ill)-defined:** a poorly defined border between the nodule and parenchyma where more than 50% of the border is not clearly demarcated (Image 9.6).
  - **Extrathyroidal Extension:** Describes the border of the nodule extending beyond the thyroid capsule into surround-

ing structures (either the strap muscles anteriorly, the trachea or esophagus medially, or the posterior structures, including the recurrent laryngeal nerve) (Image 9.7).

- **Shape:** The shape of a nodule can be well-defined, oval, round, or irregular. However when irregular, the ratio of the antero-posterior and transverse diameters is an important indicator.
  - **Wider Than Tall:** greater transverse diameter than antero-posterior diameter (Image 9.8).
  - **Taller Than Wide:** greater antero-posterior diameter than transverse diameter; this is usually concerning and may require a biopsy (Image 9.9).

Case Presentation

A 68-year-old man with no significant past medical history was found to have an enlarged right-sided thyroid mass on annual physical exam by his primary care physician and was referred for further evaluation. There was no family history of thyroid disease and he had no swallowing or voice complaints. TSH was 3.75 uIU/mL (0.5–4.5 uIU/mL). On physical exam, there was an approximately 4 cm nontender, firm nodule within the right thyroid lobe that elevated with swallowing. Laryngoscopic examination was normal. Ultrasound demonstrated a $2.3 \times 2.8 \times 4.3$ cm, hypoechoic solid, lobular nodule (Images 9.1a, b) occupying the majority of the right thyroid lobe. No suspicious adenopathy or contralateral nodules were present.

Ultrasound-guided fine needle aspiration (FNA) of the lobulated nodule was performed. Cytology showed sheets and clusters of atypical oncocytic cells (Hurthle cells) with scattered psammoma bodies, favoring a malignant oncocytic neoplasm, including in the differential diagnosis, papillary carcinoma with Hurthle cell differentiation. The patient subsequently underwent a total thyroidectomy. Histopathology showed a 4.3 cm invasive oncocytic thyroid carcinoma (Hurthle cell) with extensive capsular and angioinvasion (Image 9.2).

Postoperatively, serum thyroglobulin level was 38 ng/mL. computed tomography (CT) chest imaging revealed multiple bilateral “small lung nodules, with the largest measuring 8 mm,

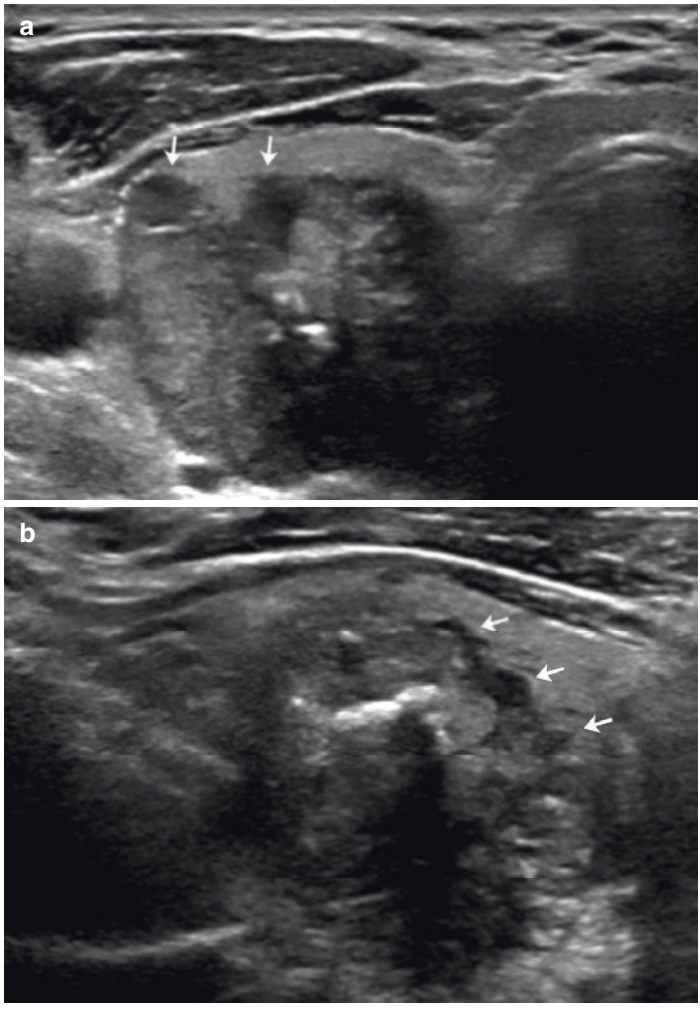

Image 9.1 Lobulated Margins. Transverse (**a**) and sagittal (**b**) view of a hypoechoic solid nodule with lobulated borders (Arrows) within the inferior pole of the right thyroid. The nodule was found to be an aggressive Hürthle cell carcinoma on surgical pathology

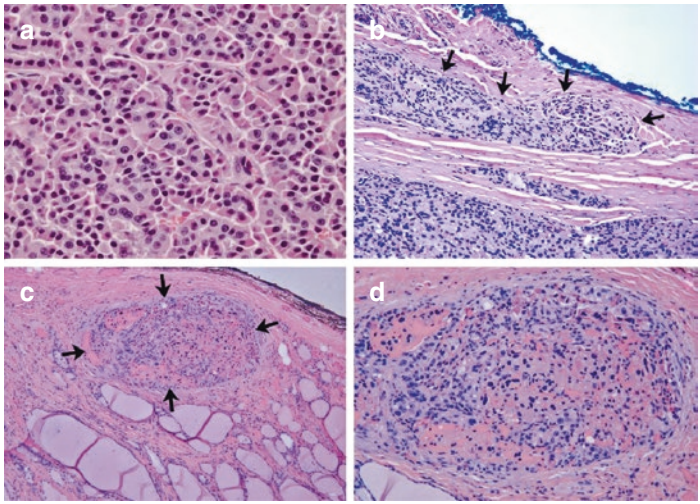

Image 9.2 Histopathology (H&E) showing invasive oncocytic thyroid carcinoma (Hurthle cell) (**a**, 400x) with extensive capsular involvement (**b**, 200x, arrows) and angioinvasion (**c**, 100x, arrows; and **d**, 200x)

concerning for metastatic disease. He was subsequently treated with radioactive iodine. Post-treatment, follow-up imaging with whole body positron emission tomography (PET)/CT scan and surveillance thyroglobulin testing remained suspicious for active pulmonary metastases (Image 9.3a, b). Biopsy of a lung nodule confirmed metastatic Hürthle cell carcinoma. Two years after initial therapy, he remains asymptomatic with slow-growing, low volume pulmonary disease that is being managed with active surveillance.

Thyroid Nodule Margins and Shape: Additional Examples

See Images 9.4, 9.5, 9.6, 9.7, 9.8 and 9.9.

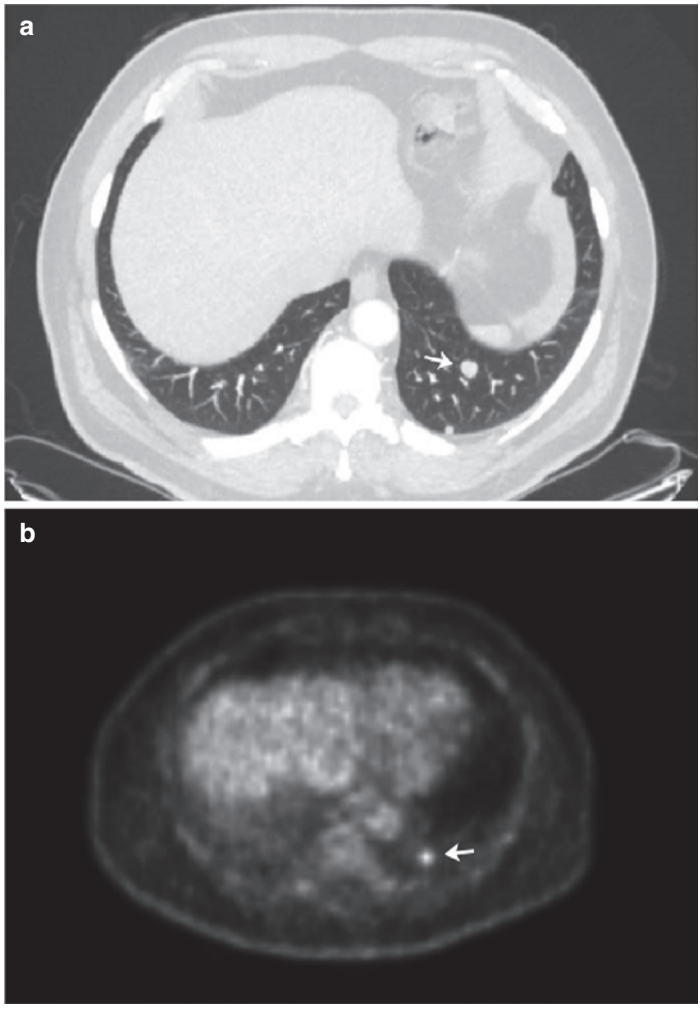

Image 9.3 CT scan of the chest showing a suspicious nodule in the left lower lung lobe (**a**, arrow) that was also FDG-PET-avid (**b**, arrow), and consistent with metastatic Hürthle cell carcinoma on biopsy

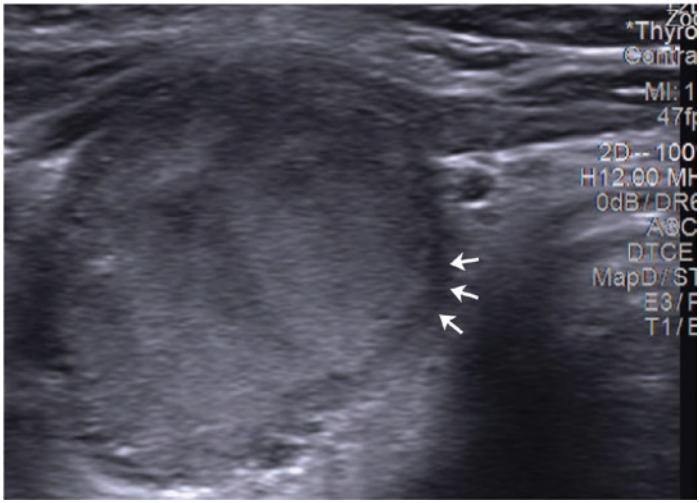

Image 9.4 A solid nodule with smooth margins . A solid, hypoechoic nodule in the superior pole of the right thyroid lobe with smooth margins, transverse view. In addition to smooth margins, this nodule also features a hypoechoic "halo" (arrows), which is often found in benign lesions. The halo is thought to result from the nodule compressing the vasculature within the adjacent thyroid parenchyma.

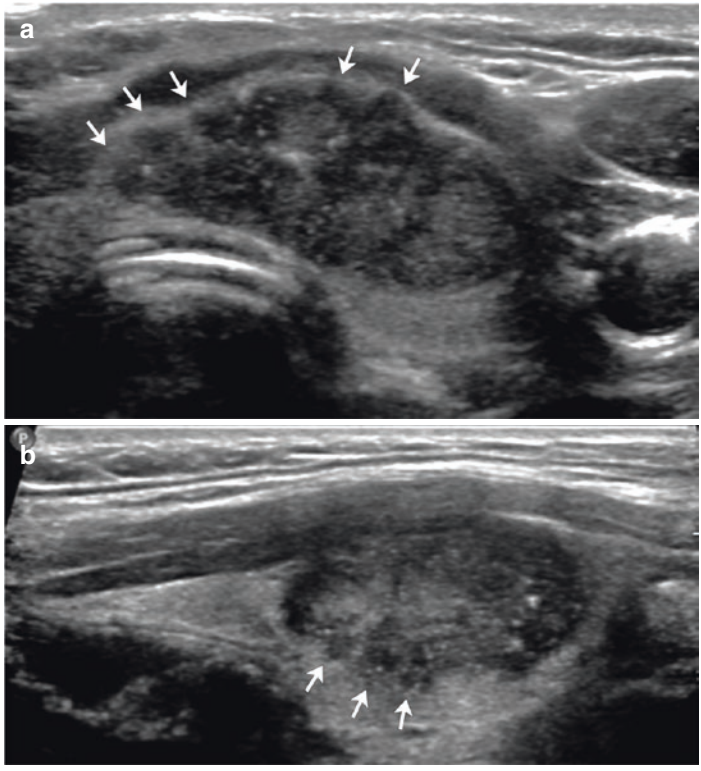

Image 9.5 Irregular/infiltrative margins. A nodule with irregular margins located in the mid pole of the right thyroid lobe on transverse (**a**) and sagittal (**b**) views. Irregular margins (arrows) suggest malignant infiltration of adjacent thyroid parenchyma. This nodule was found to be diffuse sclerosing variant of papillary thyroid carcinoma on surgical pathology

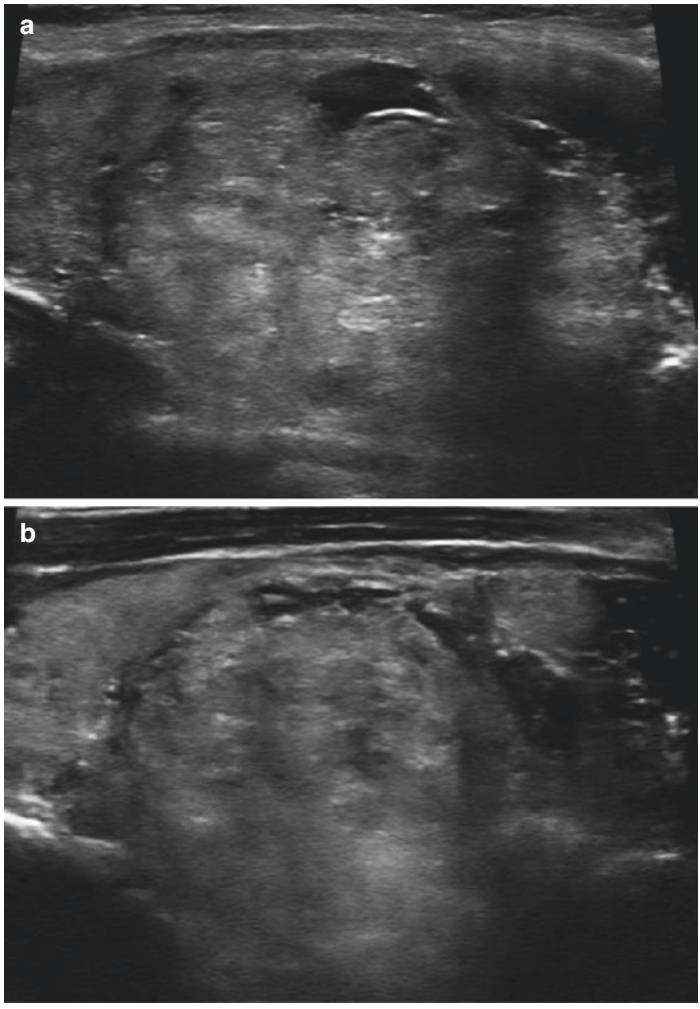

Image 9.6 Poorly defined margins. Transverse (**a**) and sagittal (**b**) views of a large, heterogeneous solid nodule within the left thyroid lobe with a poorly defined border between the nodule and the surrounding thyroid parenchyma. The nodule was confirmed to be benign on surgical pathology

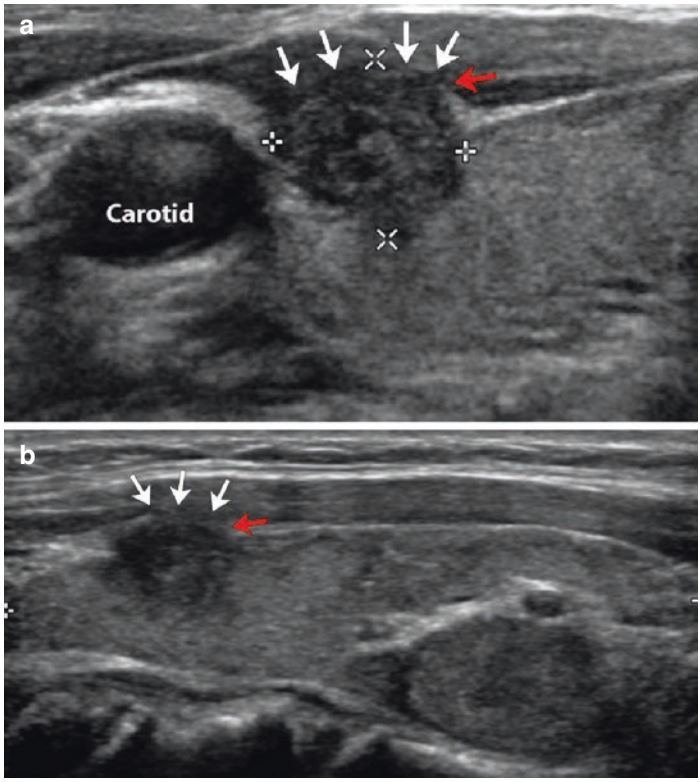

Image 9.7 Extrathyroidal extension. A right superior pole nodule with infiltration into the neighboring strap muscles (white arrows) on transverse (**a**) and sagittal views (**b**). The red arrows show discontinuity of the thyroid capsule. Papillary thyroid carcinoma with extrathyroidal invasion was confirmed on surgical pathology

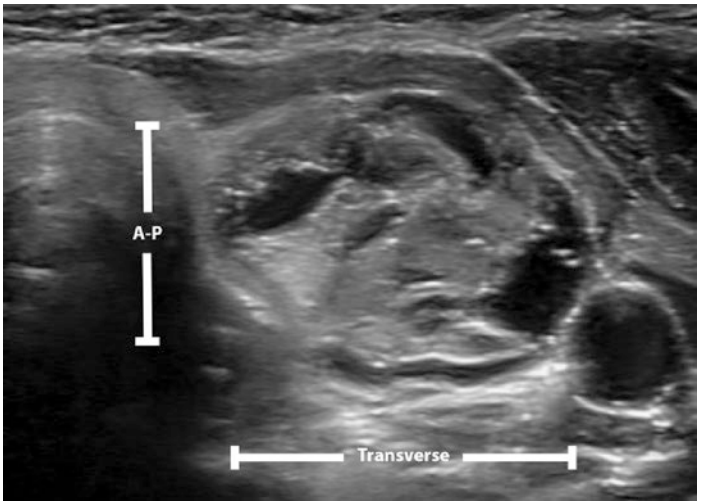

Image 9.8 Wider than tall. A large, complex cystic nodule in the mid pole of the left thyroid lobe with greater transverse diameter than antero-posterior diameter. The nodule contains echogenic foci that most likely represent comet tail artifact. The nodule was benign on surgical pathology

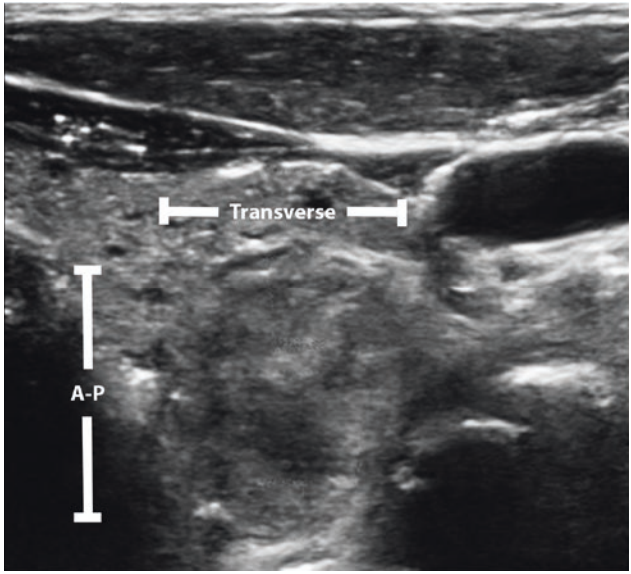

Image 9.9 Taller than wide. A heterogeneous, solid nodule with a greater antero-posterior diameter than transverse diameter within the inferior pole of the left thyroid

Discussion

Sonographic analysis of the shape and margins of a thyroid nodule can help differentiate benign from malignant nodules. Infiltrative, irregular, and lobulated margins have been associated with malignancy. The presence of any of these characteristics should raise the possibility of a malignant lesion for which further evaluation with ultrasound-directed needle biopsy is indicated.

Several challenges in describing a nodule margin on ultrasound should be kept in mind. If the background thyroid tissue is heterogeneous, as in Hashimoto's thyroiditis, margin characteristics may be more difficult to accurately visualize. Also, determining the difference between an infiltrative and indistinct border, particularly for small heterogeneous nodules, can be difficult.

Indistinct or poorly defined margins have not been associated with malignancy, unlike true infiltrative margins. Interobserver variability in the assessment of nodule margins is high and may depend on the skill and experience of the sonographer. All of these factors must be kept in mind when deciding on appropriate management and a nuanced approach to thyroid nodules based on margin and shape is recommended.

Extrathyroidal extension on ultrasound suggests invasion of the nodule beyond the thyroid capsule. The capsule of the thyroid gland usually appears as a bright white line that is uniform. When the border of a nodule interrupts this well-defined plane, malignancy should be suspected. Malignant tumor can also be visualized extending outside of the gland into surrounding structures, such as the strap musculature or carotid sheath. Intratracheal growth is difficult to appreciate on ultrasound. When present, extension beyond the gland suggests more advanced or aggressive disease and additional axial CT imaging with contrast will help to formulate an optimal surgical plan.

The shape of a thyroid nodule can also provide valuable information. It is important to consider the relationship between the antero-posterior diameter and transverse diameter. Several studies associate malignancy with a "taller than wide" shape, in which the antero-posterior to transverse ratio, as measured in the transverse plane, is greater than 1. This finding is not highly sensitive, but can be quite specific, particularly for smaller cancers.

Further Reading

Chan BK, Desser TS, McDougall IR, Weigel RJ, Jeffrey RB Jr. Common and uncommon sonographic features of papillary thyroid carcinoma. Ultrasound Med. 2003;22(10):1083–90.

Hoang JK, Lee WK, Lee M, Johnson D, Farrell S. US features of thyroid malignancy: pearls and pitfalls. Radiographics. 2007;27:847–65.

Kim E-K, Park CS, Chung WY, Oh KK, Kim DI, Lee JT, Yoo HS. New sonographic criteria for recommending fine-needle aspiration biopsy of nonpalpable solid nodules of the thyroid. AJR Am J Roentgenol. 2002;178(3):687–91.

Koike E, Noguchi S, Yamashita H, Murakami T, Ohshima A, Kawamoto H, Yamashita H. Ultrasonographic characteristics of thyroid nodules: prediction of malignancy. Arch Surg. 2001;136(3):334–7.

Leenhardt L, Menegaux F, Franc B, Delbot T, Mansour G, Hoang C, Guillausseau C, Aurengo H, Le Guillouzic D, Turpin G, Aurengo A, Chigot JP, Hejblum G. Selection of patients with solitary thyroid nodules for operation. Eur J Surg. 2002;168(4):236–41.

Calcification and Echogenic Foci of Thyroid Nodules

10

Chelsey Baldwin and Rachel Pessah-Pollack

Key Points

- "Hyperechoic foci" is a nonspecific term referring to focal, bright echogenic structures.
- Sonographic pattern and distribution of calcification in a nodule can aid in estimating the risk of malignancy and determine whether a biopsy is needed.
- Distinguishing ultrasound features is operator dependent. Their negative or positive predictive value is influenced by the presence or absence of other suspicious or reassuring features.
- Correct identification of echogenic foci due to colloid (comet tail and dependency of the focus within a microcyst) will suggest a benign lesion and can prevent unnecessary biopsies.

C. Baldwin
Division of Endocrinology and Metabolism, The George Washington University, Washington, DC, USA

R. Pessah-Pollack (✉)
Division of Endocrinology, Diabetes and Metabolism, NYU School of Medicine, New York, NY, USA

L. S. Eldeiry et al. (eds.), *Handbook of Thyroid and Neck Ultrasonography*, Contemporary Endocrinology,
https://doi.org/10.1007/978-3-031-18448-2_10

- Macrocalcifications are hyperechoic foci larger than 1 mm, with indeterminate significance and need to be evaluated in conjunction with other US findings.
- Microcalcifications are echogenic foci measuring 1 mm or less in size that suggest malignancy (most commonly papillary thyroid carcinoma (PTC), sometimes medullary thyroid cancer).
- FNA is recommended for solid nodules > or equal to 1 cm with microcalcifications or indeterminate echogenic foci.
- History of prior ablative procedures including radiofrequency ablation (RFA) and radioactive iodine therapy can represent benign causes of both micro- and macrocalcifications.

Introduction

The sonographic appearance of a thyroid nodule may be used to estimate the risk of malignancy and to decide whether a biopsy is indicated. While individual features are suggestive, combining features and pattern recognition are key to ultrasound (US) risk stratification of thyroid nodules. The specificity of a single ultrasound feature for identifying malignancy can partially depend on the presence or absence of other ultrasound features. The sensitivity, specificity, and diagnostic accuracy of ultrasound features associated with thyroid malignancy are variable in different series and appear to be partially operator-dependent. Real time interpretation is more reliable, especially with nodules that may have ambiguous features (e.g. irregular borders versus infiltrative margins.) This chapter focuses specifically on the significance of calcifications and echogenic foci in the evaluation of thyroid nodules.

- **Echogenic foci**: The term echogenic foci is a nonspecific descriptor of hyperechoic foci within or surrounding a thyroid nodule. Ultrasound waves are distorted as they traverse tissues of different densities or encounter impenetrable structures or calcifications. The pattern and location of the structures, and whether the

US waves penetrate deeper to delineated echogenic foci, provide information about nodule composition and probability of malignancy. It is important to recognize that interobserver variability represents a limitation of echogenicity assessment.

- **Calcifications**: Deposits of calcium appear as echogenic foci and can be further classified based on size and presence or absence of acoustic shadowing.
  - **Macrocalcifications** are dense, coarse echogenic foci accompanied by acoustic shadowing that are larger than 1 mm at the longest diameter.
  - **Microcalcifications** are punctate (1 mm or less in size) hyperechoic spots without acoustic shadowing that may represent psammoma bodies. These are associated with a higher likelihood of PTC.

Case Presentation 1

A 30-year-old female presented after a bystander at a public event pointed out a visible lump in her neck. She had no significant past medical history; however, her mother had a history of PTC. Physical exam revealed a 3 cm firm nodule to the right of the midline that moved with swallowing. No cervical lymphadenopathy was palpated on exam. TSH was normal at 1.36 mIU/L. Neck ultrasound demonstrated a 2.7 × 1.2 × 2.4 cm nodule in the right lobe (Image 10.1).

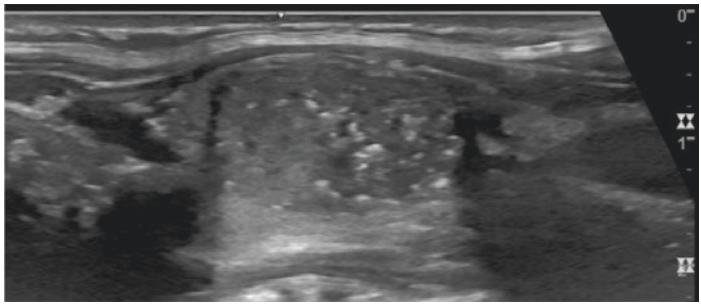

Image 10.1 Sagittal image of a solid, hypoechoic nodule located within the right thyroid lobe that contains scattered non-shadowing hyperechoic foci consistent with microcalcifications (note macrocalcifications present as well)

Table 10.1 Differential diagnosis

1. Hyperplastic thyroid nodule
2. Colloid nodule
3. Papillary thyroid cancer
4. Medullary thyroid carcinoma

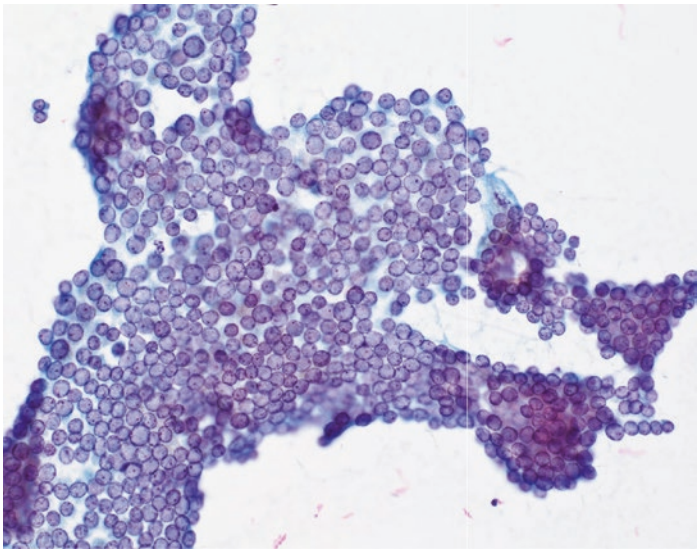

Image 10.2 Cytological examination demonstrated enlarged, overlapping nuclei with powdery chromatin with intranuclear cytoplasmic inclusions (arrow), consistent with papillary thyroid carcinoma (Bethesda VI). (Wright Giemsa stain, ×10)

Biopsy was indicated based on the size and ultrasound appearance of the nodule. Differential diagnosis is listed in Table 10.1. Ultrasound-guided fine needle aspiration (FNA) of the right thyroid nodule was performed. Cytology demonstrated atypical follicular cells arranged in papillary groups with enlarged oval, irregular nuclei with fine chromatin, intranuclear grooves, and intranuclear pseudo-inclusions, consistent with a diagnosis of PTC (Bethesda category VI) (Image 10.2).

The patient subsequently underwent a total thyroidectomy. Histopathology showed a 3.7 cm tall cell variant PTC (Image 10.3a, b). Thirteen examined central lymph nodes were positive for metastatic disease, with the largest metastatic deposit measuring 6 mm. She was treated with radioactive iodine and currently remains disease free.

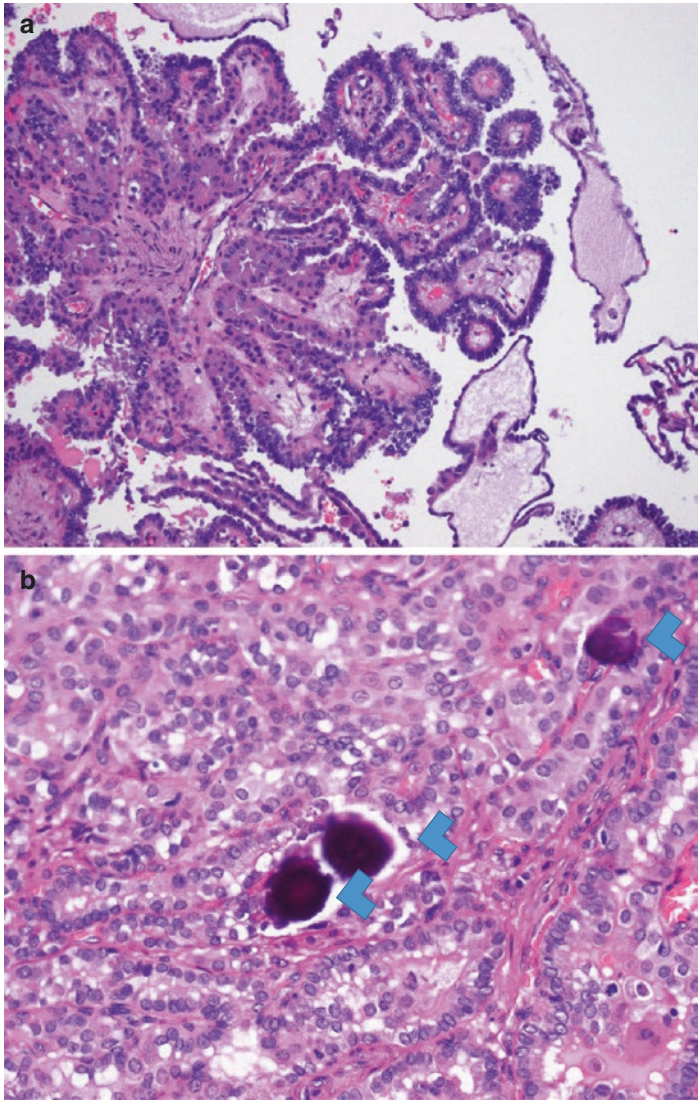

Image 10.3 (**a**) Histopathology demonstrates features of classic PTC: crowded follicular cells with enlarged, overlapping nuclei forming papillae (H&E, ×4). (**b**) At higher magnification, crowded follicular cells with enlarged nuclei and powdery chromatin can be appreciated next to psammoma bodies (arrowheads) (H&E, ×20)

Case Presentation 2

A 63-year-old woman was incidentally noted to have thyroid nodules on carotid Doppler scanning. She had no compressive or obstructive symptoms, personal history of head or neck radiation, or family history of thyroid cancer. On thyroid ultrasound, she had a normal sized thyroid gland with a 0.9 × 0.7 × 0.8 cm right lower pole hypoechoic nodule with numerous macrocalcifications (Images 10.4 and 10.5). No abnormal lymph nodes were noted.

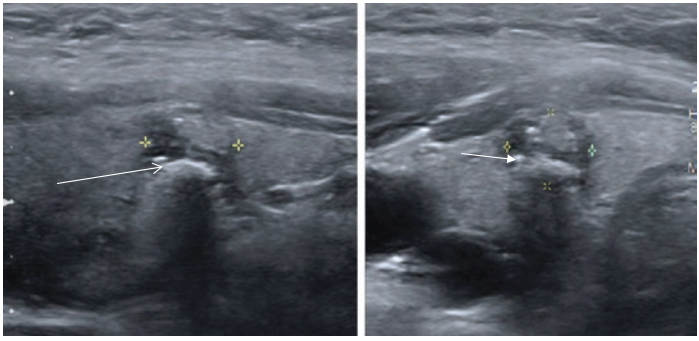

Image 10.4 Macrocalcifications (arrows) are noted in this sub-centimeter thyroid nodule in both the inside of the nodule and the periphery (left: sagittal, right: transverse)

Image 10.5 Sagittal view of another small nodule with macrocalcifications

Based on the size (<1 cm) of this nodule and absence of other concerning features, such as abnormal lymph nodes, fine needle aspiration (FNA) was not recommended. The size and ultrasound appearance of this nodule have remained stable for the past 5 years.

Thyroid Nodule Echogenic Foci and Calcifications: Additional Examples (see Images 10.6, 10.7, 10.8, 10.9, 10.10, 10.11, and 10.12)

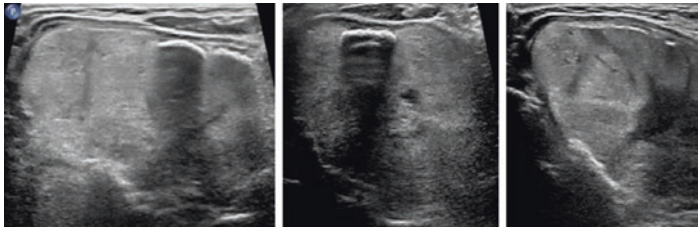

Image 10.6 Three examples of benign calcification: Macrocalcification (left and middle). Large, benign nodule with dense rim calcification (right)

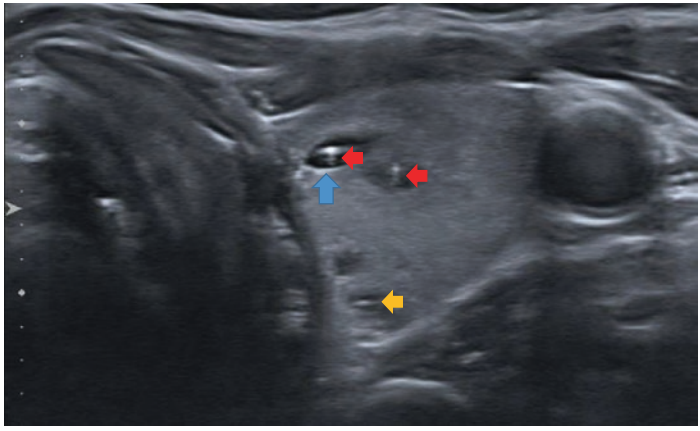

Image 10.7 Echogenic foci within an anechoic nodule may be found within a colloid nodule and may demonstrate classic "comet tail" artifact (red arrows), which represents inspissated colloid. Echogenic foci with comet tail artifact freely distributed in a cystic component predict a benign nodule. Posterior acoustic enhancement is a linear hyperechoic artifact, due to an increase in ultrasound wave reverberation against the normal thyroid parenchyma, that occurs at the posterior edge of a cyst (blue arrow) or even within a mixed solid and cystic nodule, posterior to cystic spaces (yellow arrow)

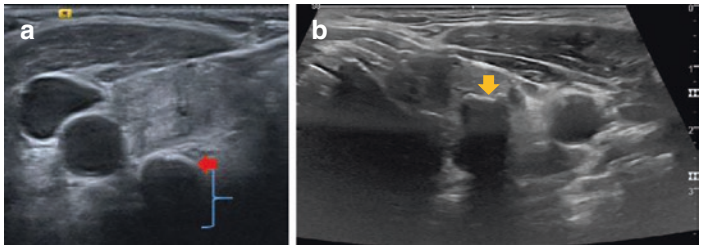

Image 10.8 (**a**) Eggshell Calcification (red arrow). The continuous calcifications are impermeable to ultrasound waves, resulting in posterior acoustic shadowing (blue bracket) and limiting further characterization of the nodule. (**b**) Slightly irregular calcification with shadowing (yellow arrow), limiting evaluation of the deep component of the lesion

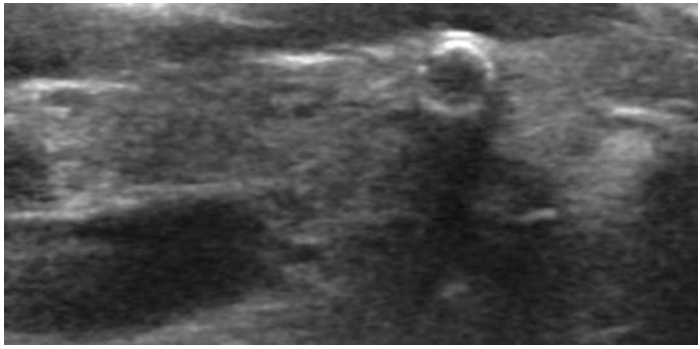

Image 10.9 Benign peripheral calcifications

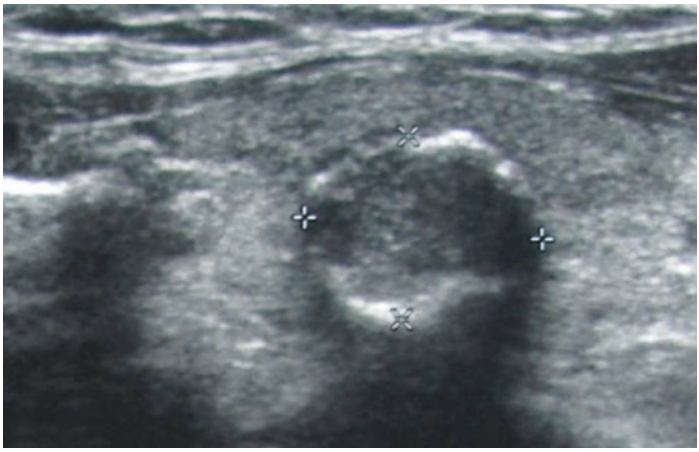

Image 10.10 Discontinuous rim calcifications. Interruptions in eggshell calcifications are indeterminate. As a result, the finding warrants FNA. Biopsy of this nodule was consistent with PTC

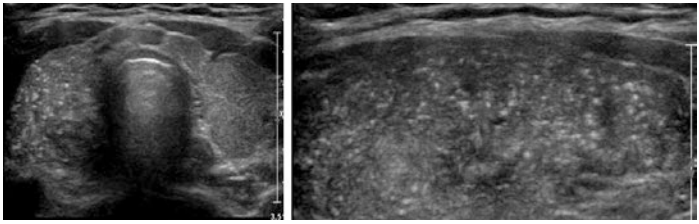

Image 10.11 Microcalcifications are seen diffusely scattered throughout the right lobe (left transverse, right sagittal) of a patient with underlying Hashimoto's disease. Pathology showed the diffuse sclerosing variant of PTC. The appearance indicates diffuse infiltration of the lobe or possibly local lymphatic spread

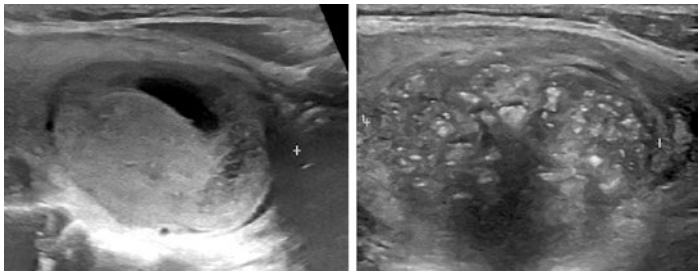

Image 10.12 Thyroid nodule ablation-induced calcifications: thyroid nodule ablative procedures, e.g. ethanol ablation or radiofrequency ablation (RFA), can cause necrosis and subsequent calcification. Familiarity with these typical consequences and imaging appearance of nodule ablation can prevent unnecessary clinical concern and FNAs. Left: Pre-RFA right thyroid nodule (sagittal image). Right: 4 weeks post-RFA, scattered calcifications are noted due to radiofrequency-induced coagulative necrosis with both micro- and macrocalcification deposition

Discussion

Echogenic foci are hyperechoic or bright echoes on B-mode ultrasound. Accurate interpretation of hyperechoic foci in addition to the other characteristics of a nodule is required to determine the risk of malignancy.

Hyperechoic foci are created by focal dense structures that cause a strong reflection of the ultrasound waves, represented as a bright echo on the image. Near-complete reflection of ultrasound waves with acoustic shadowing beyond the structure is caused by larger, macrocalcifications or densely concentrated microcalcifications, leading to posterior acoustic shadowing.

Macrocalcifications are large flecks of calcium (larger than 1 mm at the longest diameter) that can be either within the thyroid nodule or on the periphery. These shadowing, hyperechoic foci are usually seen as large bright echoes on ultrasound. In addition to calcification, they can be caused by dense fibrosis. Macrocalcifications have a nonspecific clinical significance. They are generally dystrophic, secondary to central necrosis or old hemorrhage in the lesion and do not indicate an

increased risk of malignancy. They should be evaluated in combination with other suspicious features, specifically additional microcalcifications, irregular margins, texture, vascularity, and shape.

Peripheral rim or eggshell calcifications can be either discontinuous or completely circumferential rim calcifications (Images 10.8a,b, 10.9 and 10.10). Interrupted peripheral calcifications in association with a soft tissue rim outside of the calcification may potentially indicate malignancy and ultimately on pathology may demonstrate tumor invasion in the area of disrupted calcification (Image 10.10). The 2015 American Thyroid Association Management Guidelines for Adult Patients with Thyroid Nodules and Differentiated Thyroid Cancer cite the presence of nodular extrusion as having a very high association with malignancy and a higher likelihood of tumor invasion in the region of disrupted calcifications.

Microcalcifications are small flecks of calcification measuring 1 mm or less in size, appearing as bright hyperechoic foci on sonographic images. The presence of microcalcifications in a thyroid nodule is associated with a higher likelihood of PTC. On histopathology of thyroid tissue, microcalcifications are felt to correlate with the round, calcified psammoma bodies seen in PTC.

Psammoma bodies are not found within the follicular cell and are therefore uncommon in follicular variant PTC or follicular neoplasms. Microcalcifications can be limited to the nodule itself or scattered throughout the thyroid gland, concerning for lymphatic dissemination within the gland (Image 10.11). Similarly, microcalcifications within cervical lymph nodes are diagnostic of lymphatic locoregional spread of PTC. Benign causes of microcalcifications are possible, including benign involution or trauma due to procedures, such as FNA or nodule ablation (Image 10.12). However those calcifications are usually larger and denser.

It should be recognized that the ultrasonographic presentation of medullary thyroid carcinoma (MTC) includes both microcalcifications and macrocalcifications. The presence of visible microcalcifications in nodules with histopathology consistent with MTC has been noted to be as high as 50%–60% in some studies.

Further Reading

Haugen B, et al. 2015 American Thyroid Association management guidelines for adult patients with thyroid nodules and differentiated thyroid cancer. Thyroid. 2016;26(1, 1):–133. https://doi.org/10.1089/thy.2015.0020.

Kobaly K, Kim CS, Langer JE, Mandel SJ. Macrocalcifications do not alter malignancy risk within the American Thyroid Association sonographic pattern system when present in non-high suspicion thyroid nodules. Thyroid. 2021:1542–8. https://doi.org/10.1089/thy.2021.0140.

Lacout A, Chevenet C, Thariat J, Marcy PY. Thyroid calcifications: a pictorial essay. J Clin Ultrasound. 2016;44(4):245–51. Epub 2016 Feb 18. https://doi.org/10.1002/jcu.22345.

Malhi HS, Velez E, Kazmierski B, Gulati M, et al. Peripheral thyroid nodule calcifications on sonography: evaluation of malignant potential. Am J Roentgenol. 2019;213:672–5.

Taki S, Terahata S, Yamashita R, Kinuya K, Nobata K, Kakuda K, Kodama Y, Yamamoto I. Thyroid calcifications: sonographic patterns and incidence of cancer. Clin Imaging. 2004;28(5):368–71. https://doi.org/10.1016/S0899-7071(03)00190-6.

Vascularity of Thyroid Nodules

11

Navya M. Reddy and Matthew J. Levine

Key Points

- Thyroid nodule vascularity can be described based on location and pattern of flow.
- Due to the poor sensitivity and specificity of vascularity as the sole predictor of malignancy, other ultrasound characteristics (e.g. echogenicity, margins, calcifications, etc.) may play a more important role in nodule risk stratification.
- In light of its questionable utility, vascularity has not been included in the ATA, AACE, ITNUWG, or TIRADS scoring systems for thyroid nodules.
- There have been many examples, including cases presented in this chapter, of hypervascular nodules that proved to be benign.
- Future direction/research is exploring objective rather than subjective categorization of nodule vascularity and risk of malignancy.

N. M. Reddy (✉) · M. J. Levine
Division of Diabetes and Endocrinology, Scripps Clinic, La Jolla, CA, USA
e-mail: levine.matthew@scrippshealth.org

L. S. Eldeiry et al. (eds.), *Handbook of Thyroid and Neck Ultrasonography*, Contemporary Endocrinology,
https://doi.org/10.1007/978-3-031-18448-2_11

Introduction

The primary focus of this chapter is to discuss the utility of vascular studies in the evaluation of thyroid nodules. The color Doppler characteristics of a thyroid nodule cannot be used to confidently predict or exclude malignancy. Increased vascularity does not predict increased risk of malignancy as previously thought, as underscored by case presentations to follow, and the pattern of vascularity also does not conclusively predict benignity vs. malignancy. The discrepancies between studies may be due to the fact that in some studies, thyroid vascularity was assessed subjectively, rather than using a quantifiable, objective approach. We will discuss the need for further investigation of the significance of vascularity of thyroid nodules, particularly for the identification of malignant nodules.

It is also important to note that thyroid vascularity may have additional utility outside of the scope of malignancy risk evaluation. For example, vascularity can be used to define a thyroid nodule's margin, with a vascular halo defining the border of the nodule; this is discussed elsewhere in the text. The vascularity of the gland may be increased in chronic autoimmune thyroiditis, in contrast to acute or subacute thyroiditis, postpartum or silent thyroiditis. Additionally, vascularity may be used to differentiate between the types of amiodarone-induced thyrotoxicosis. More specifically, there is absent vascularity in type 2 AIT, which is secondary to thyroid destruction, in contrast to the variable degree of vascularity encountered in type 1 AIT, where there is a hyperfunctioning gland.

- The arterial supply to the thyroid gland is via two main arteries, which are the superior thyroid artery and the inferior thyroid artery.
- The venous drainage from the thyroid is carried by the superior, middle, and inferior thyroid veins, which form a venous plexus around the thyroid gland.
- The vascularity of the thyroid parenchyma can be determined using a visual scale:

  - pattern 0: blood flow limited to the peripheral thyroid arteries. Parenchymal flow is absent (parenchymal refers to the central area of the thyroid gland),
  - pattern I: mild parenchymal flow,
  - pattern II: clearly increased color flow with a diffuse, homogenous distribution,
  - pattern III: markedly increased color flow with a homogenous distribution.
- With respect to thyroid nodules, vascularity refers to the pattern of blood flow. The description of thyroid nodule vascularity is based on the ratio and distribution of blood flow within a particular nodule. This can be determined by the color Doppler component of the ultrasound exam.
- Central vascularity indicates that greater than 50% of the vascularity is located in the center of the nodule, while peripheral vascularity denotes greater than 50% of vascularity is in the periphery of the nodule.
- Avascular refers to the absence of blood flow within a nodule.
- Thyroid nodule vascularity has been classified as follows:
  - type I vascularity refers to the complete absence of flow within the nodule,
  - type II refers to perinodular flow, and,
  - type III vascularity indicates intranodular flow with multiple vascular poles chaotically arranged, with or without significant perinodular vessels.

Case Presentation 1

Central Vascularity: A 41-year-old woman was seen in consultation regarding a thyroid nodule. She reported symptoms of upper respiratory infection followed by residual dry, nonproductive cough and pressure sensation in the lower throat region. She had no prior history of thyroid disease or risk factors for thyroid carcinoma. She denied dysphagia. A nodule was palpated on physical exam and ultrasound showed a 3.1 cm solid, hypoechoic right thyroid nodule with smooth borders, increased vascularity and microcalcifications (Images 11.1 and 11.2). The nodule was characterized as highly suspicious FNA was recommended and that showed benign (Bethesda II) cytology.

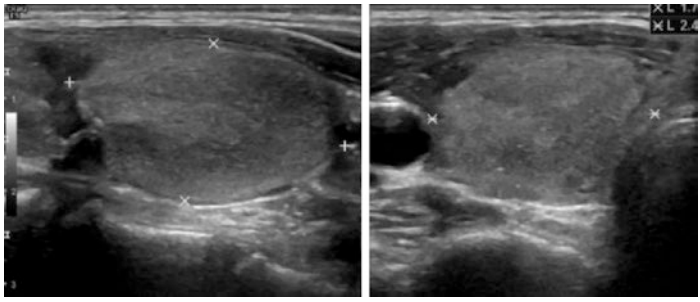

Image 11.1 Longitudinal (left) and transverse (right) images of the right lobe nodule

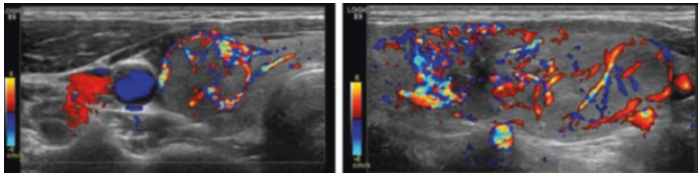

Image 11.2 Color Doppler imaging of the nodule showing central vascularity, transverse (left) and longitudinal (right)

Case Presentation 2

Peripheral Vascularity: A 76-year-old woman with a past medical history of hypothyroidism, hyperparathyroidism with nephrolithiasis, hypertension, and hyperlipidemia was evaluated for a thyroid nodule that was incidentally discovered on CT scan performed for lung nodules. She underwent parathyroidectomy 40 years prior to her presentation, which resulted in left thyroid lobectomy. She was euthyroid on levothyroxine replacement and reported no prior exposure to radiation, history of cancer, or family history of thyroid cancer. Neck ultrasound showed a 3.2 × 2.5 × 2.6 right lobe solid, smooth, hypoechoic nodule with no echogenic foci and with peripheral vascularity (Image 11.3). The nodule was classified as intermediate suspicion due to its size and hypo-echogenicity, and FNA was advised. Cytology was called benign (Bethesda II).

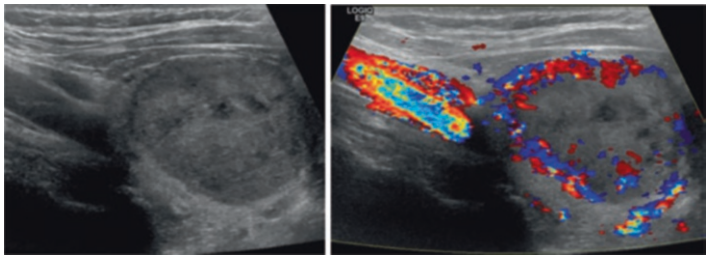

Image 11.3 Longitudinal views of the right lobe nodule (left), which shows peripheral vascularity on color Doppler (right)

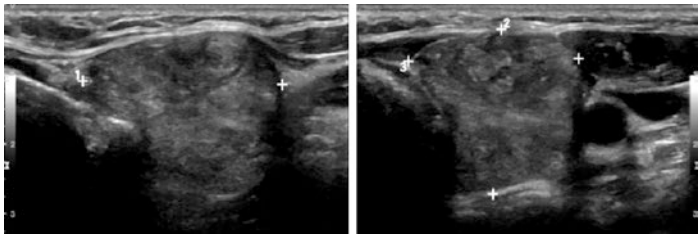

Image 11.4 Longitudinal (left) and transverse (right) views of a solid, 2.8 × 2.3 × 2.4 cm hypoechoic, taller-than-wide left lobe nodule without vascularity and with irregular borders

Case Presentation 3

Avascularity: A 71-year-old woman with a history of hypothyroidism on levothyroxine replacement was seen for a thyroid nodule. While looking in the mirror, she noted a new neck growth that was palpable on physical exam. Ultrasound showed a left-sided nodule measuring 2.8 cm in the largest dimension; the nodule was avascular, without calcification, taller-than-wide, and had irregular borders (Images 11.4 and 11.5). A biopsy was recommended and cytology was called malignant (Bethesda VI). The specimen showed papillary thyroid carcinoma with papillary follicular groups with nuclear overlap, nucleomegaly, nuclear grooves, and rare intra-nuclear inclusions. She subsequently underwent total thyroidectomy with central neck dissection. Surgical pathology revealed multifocal papillary thyroid carcinoma, tall cell variant;

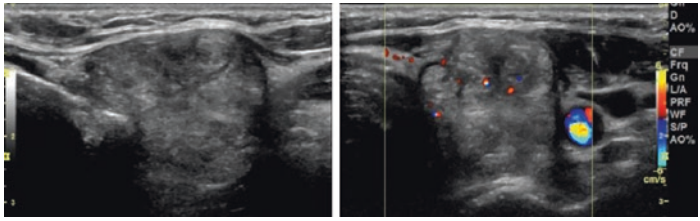

Image 11.5 The left-sided nodule is avascular on color Doppler, longitudinal (left) and transverse (right)

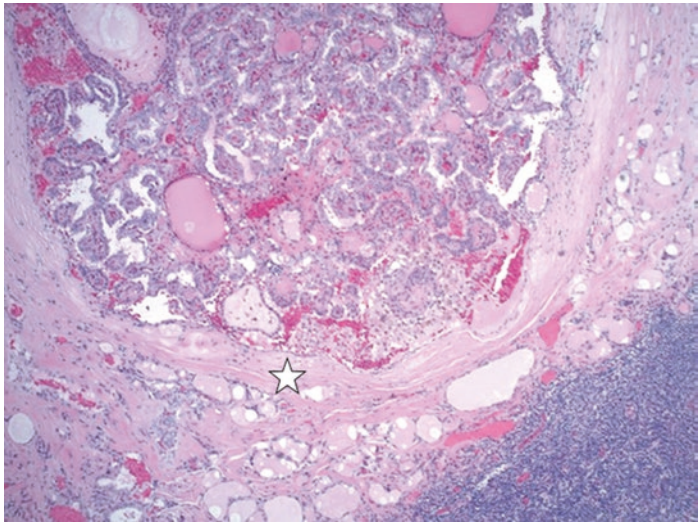

Image 11.6 Lymph node metastasis—papillary neoplasm present within a capsule (star) and associated with lymphocytes, consistent with tumor metastasis in a lymph node (H&E, ×10)

the greatest area measuring 3.3 cm in the left lobe with perineural and extrathyroidal invasion. One of three central neck lymph nodes was involved with tumor, with the largest metastatic deposit measuring 4 mm (Images 11.6 and 11.7). The tumor was classified as pT3bN1a. She was subsequently treated with radioactive iodine. Post-therapy whole body imaging and subsequent surveillance testing indicated no distant metastasis or persistent disease.

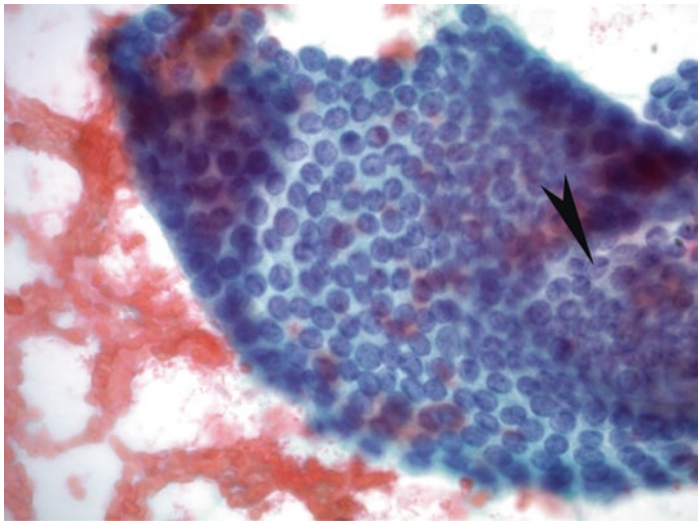

Image 11.7 Nuclear detail of papillary thyroid cancer cells showing crowding, overlapping, and finely granular chromatin with small punctate nucleoli and occasional nuclear grooves (arrow) (PAP stain, ×40)

Discussion

The role of thyroid nodule vascularity and vascular pattern in the prediction of thyroid cancer has been controversial. In addition, vascularity within a thyroid nodule may represent a variety of underlying processes, as listed in Table 11.1.

Several studies have examined the utility of vascularity in the identification of malignancy. In one study of consecutive patients with nonpalpable thyroid nodules measuring from 8 to 15 mm, 31 of 402 thyroid nodules were malignant. With Doppler ultrasound, an intranodular vascular pattern was present in 74% of the malignant nodules. The addition of a second suspicious feature, such as microcalcifications, resulted in a higher specificity for the prediction of malignancy (95%), although with a corresponding decrease in sensitivity (29%). The specificity of irregular margins or intranodular vascularity was 85% and 80.8%, respectively, in this

Table 11.1 Differential diagnosis of vascularity in a thyroid nodule

1. Autoimmune thyroid disease
2. Benign adenoma
3. Malignant thyroid nodule
4. Metastasis from extrathyroidal malignancy

study. The addition of color flow Doppler to ultrasound imaging increased the screening sensitivity and accuracy in identifying malignant thyroid nodules in comparison to conventional sonography.

Hypervascularity, however, has been reported to be a more frequently encountered feature of follicular and medullary thyroid carcinoma than papillary carcinoma. This is underscored in the American Thyroid Association (ATA) guidelines, which indicate that vascularity is less useful for predicting malignancy in papillary thyroid carcinoma in contrast to follicular thyroid carcinoma.

In contrast, however, other studies have not shown a correlation between intranodular vascularity and malignancy. These reports have shown that most thyroid cancers lack intranodular vascularity, with most hypervascular nodules representing benign adenomas. In the case series we have presented, vascularity did not correlate with malignancy.

The proposed explanation for these conflicting results relates to the subjective nature of the visual assessment of vascularity, leading to higher interobserver variability. Quantifiable, more objective approaches to the assessment of vascularity have been proposed to address this issue. In a study of a computer-aided approach that allowed for the quantification of thyroid parenchymal vascularity and lymph node vascularity with color Doppler ultrasound, an algorithm was created to calculate a "vascular index" of the peripheral and central regions of thyroid nodules. The results indicated that central vascularity rather than peripheral vascularity was associated with thyroid malignancy.

Taken together, all of these findings suggest that increased vascularity within a thyroid nodule is not a strong predictor of increased risk of malignancy, and therefore the significance of this

feature in the ultrasound assessment of thyroid nodules remains uncertain. Thus, thyroid nodule guidelines have changed and no longer use this in the risk stratification criteria. This also underscores the need for further investigation of the significance of vascularity in thyroid nodules and the need for continued research to clarify its role in identifying malignant nodules.

Further Reading

Appetecchia M, Solivetti FM. The association of colour flow doppler sonography and conventional ultrasonography improves the diagnosis of thyroid carcinoma. Horm Res. 2006;66(5):249–56. Epub 2006 Oct 2. PMID: 17016052. https://doi.org/10.1159/000096013.

Baig FN, van Lunenburg JT, Liu SYW, et al. Computer-aided assessment of regional vascularity of thyroid nodules for prediction of malignancy. Sci Rep. 2017;7:14350. https://doi.org/10.1038/s41598-017-14432-7.

Bogazzi F, Bartalena L, Brogioni S, Mazzeo S, Vitti P, Burelli A, Bartolozzi C, Martino E. Color flow doppler sonography rapidly differentiates type I and type II amiodarone-induced thyrotoxicosis. Thyroid. 1997;7(4):541–5. https://doi.org/10.1089/thy.1997.7.541.

Bogazzi F, Bartalena L, Brogioni S, Burelli A, Manetti L, Tanda ML, Gasperi M, Martino E. Thyroid vascularity and blood flow are not dependent on serum thyroid hormone levels: studies in vivo by color flow doppler sonography. Eur J Endocrinol. 1999;140(5):452–6. https://doi.org/10.1530/eje.0.1400452.

Chung J, Lee YJ, Choi YJ, et al. Clinical applications of doppler ultrasonography for thyroid disease: consensus statement by the Korean Society of Thyroid Radiology. Ultrasonography. 2020;39(4):315–30. https://doi.org/10.14366/usg.20072.

Haugen BR, et al. 2015 American Thyroid Association management guidelines for adult patients with thyroid nodules and differentiated thyroid cancer: the American Thyroid Association guidelines task force on thyroid nodules and differentiated thyroid cancer. Thyroid. 2016;26(1):1–133. https://doi.org/10.1089/thy.2015.0020.

Lai X, Liu M, Xia Y, et al. Hypervascularity is more frequent in medullary thyroid carcinoma: compared with papillary thyroid carcinoma. Medicine (Baltimore). 2016;95(49):e5502. https://doi.org/10.1097/MD.0000000000005502.

Papini E, Guglielmi R, Bianchini A, Crescenzi A, Taccogna S, Nardi F, Panunzi C, Rinaldi R, Toscano V, Pacella CM. Risk of malignancy in nonpalpable thyroid nodules: predictive value of ultrasound and color-dop-

pler features. J Clin Endocrinol Metabol. 2002;87(5):1941–6. https://doi.org/10.1210/jcem.87.5.8504.

White AM, Lasrado S. Anatomy, head and neck, thyroid arteries. In: StatPearls [Internet]. Treasure Island, FL: StatPearls. https://www.ncbi.nlm.nih.gov/books/NBK560666/. Accessed 29 Jul 2021.

Yang GCH, Fried KO. Most thyroid cancers detected by sonography lack intranodular vascularity on color doppler imaging: review of the literature and sonographic-pathologic correlations for 698 thyroid neoplasms. J Ultrasound Med. 2017;36(1):89–94. Epub 2016 Dec 1. https://doi.org/10.7863/ultra.16.03043.

Parathyroid Imaging

12

Barry Sacks

Key Points

- Imaging should not be used to establish the diagnosis of hyperparathyroidism. It should be reserved for patients with established hyperparathyroidism who are candidates for surgery.
- Ultrasound should be the initial imaging study. It is safe, cost-effective, involves no radiation, and allows evaluation of both the parathyroid and thyroid glands. A strongly positive exam may obviate the need for any additional imaging.
- The disadvantage of ultrasound is operator dependence. Even with expertise, the diagnosis of multi-gland disease is less accurate than for a single adenoma.
- Demonstration of intra-lesional hypervascularity is a very helpful finding, but lack of vascularity does not exclude the lesion being a parathyroid adenoma.

B. Sacks (✉)
Department of Radiology, Beth Israel Deaconess Medical Center, Boston, MA, USA
e-mail: bsacks@bidmc.harvard.edu

L. S. Eldeiry et al. (eds.), *Handbook of Thyroid and Neck Ultrasonography*, Contemporary Endocrinology,
https://doi.org/10.1007/978-3-031-18448-2_12

- The appearance of a parathyroid adenoma on US and 4DCT, although usually classic, can also be atypical on either study.
- FNA for PTH provides extremely valuable information. A positive PTH is usually markedly elevated (in the high hundreds or thousands). A positive test unequivocally confirms the diagnosis of a parathyroid adenoma.
- 4DCT should be considered when the ultrasound is either nondiagnostic or inconclusive.
- Sestamibi should be considered a back-up exam when US and 4DCT are inconclusive, or performed if the patient has a contraindication to contrast injection.

Introduction

This chapter focuses predominantly on ultrasound (US) imaging in the work-up of patients with primary hyperparathyroidism. US examination of these patients is mandatory because it is safe, cost-effective, easily available, accurate, and involves no radiation exposure. However, US also has limitations and most patients usually require a complementary imaging study. For many years, the imaging algorithm in patients with confirmed primary hyperparathyroidism who were considered surgical candidates was nuclear imaging with Technetium Sestamibi scan (usually with SPECT/CT), followed by ultrasound. If those two studies were either inconclusive or discordant, 4DCT was performed. Although many institutions and endocrinologists still adhere to this sequence of exams, the accuracy of 4DCT has significantly impacted the initial imaging algorithm. The combination of US, followed by 4DCT provides the maximum "bang for the buck," identifying both orthotopic (eutopic) and ectopic enlarged glands, in addition to multi-gland disease. Ultrasound as the initial exam provides the ability to both localize abnormal parathyroid glands and simultaneously evaluate the thyroid gland. If thyroid nodules are detected and require FNA preoperatively, this can be recommended or

often even performed at the same visit. Sestamibi scan still plays an important role in the localization of parathyroid disease, but is currently a "back-up" study, when the initial two studies are inconclusive or if the patient has a contraindication to the contrast injection required to perform 4DCT (allergy or renal dysfunction).

Case Presentation

A 61-year-old woman with a history of osteopenia presented with fatigue. She had a known history of Hashimoto's thyroiditis and a stable, benign right thyroid nodule. Hyperparathyroidism was diagnosed, with serum calcium levels ranging from 10.8 to 11.5 mg/dL and elevated parathyroid hormone (PTH) levels of 95–105 pg/mL. 25 hydroxy-vitamin D level was low at 22 ng/mL.

Initial imaging with ultrasound demonstrated thyroid heterogeneity consistent with Hashimoto's thyroiditis (Image 12.1), with the characteristic associated numerous, small reactive lymph nodes bilaterally, and the previously biopsied (benign) right thyroid nodule. A hypervascular extrathyroidal nodule at the left lower pole was also identified, with a slightly hyperechoic center. The differential diagnosis included an atypical parathyroid adenoma or a reactive lymph node (Table 12.1).

The hypervascularity on ultrasound was more suggestive of a parathyroid adenoma. The patient subsequently underwent a 4DCT scan, which showed the left lower pole lesion brightly enhancing, consistent with a parathyroid adenoma. She underwent surgery, where a left lower pole parathyroid adenoma was confirmed and resected. Intraoperative PTH level dropped from 93 pg/mL preoperatively to 15 pg/mL post-excision of the lesion, confirming a cure of her parathyroid disease.

In an attempt to explain the unusual ultrasound findings, the histopathology was reviewed. Was the appearance due to a moderate amount of central fat or fibrosis? As demonstrated in the slides below (Image 12.2), a few patchy areas of fat and fibrosis were present, with a prominent vessel; however, the findings essentially confirmed a classical, hypercellular parathyroid adenoma.

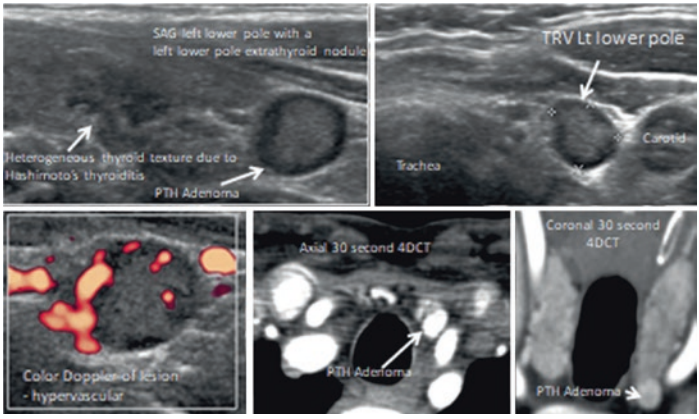

Image 12.1 Upper left: Sagittal view of the left thyroid lobe demonstrating heterogeneous echotexture (left arrow) and an unusual nodule at the lower pole, extrathyroidal, suggestive of either a reactive lymph node with a fatty center (common in Hashimoto's) or parathyroid adenoma (right arrow). Upper right: Transverse view of the left lower pole showing the same lesion. Bottom left: A color flow Doppler image showing vascularity of the lesion with a polar vessel. Bottom center: Four-dimensional CT (4DCT) was performed (often necessary in patients with Hashimoto's because of the difficulty in differentiating lymph nodes from enlarged parathyroid glands on ultrasound). The axial arterial image shows dramatic enhancement of the nodule at the left lower pole (arrow). This prominent early enhancement is not consistent with a lymph node (which usually shows minimal and delayed slight enhancement) and strongly suggests a parathyroid adenoma. Bottom right: A coronal view (different window settings) demonstrating the left lower pole parathyroid adenoma

Table 12.1 Differential diagnosis

1. Reactive lymph node associated with Hashimoto's thyroiditis
2. Atypical parathyroid adenoma

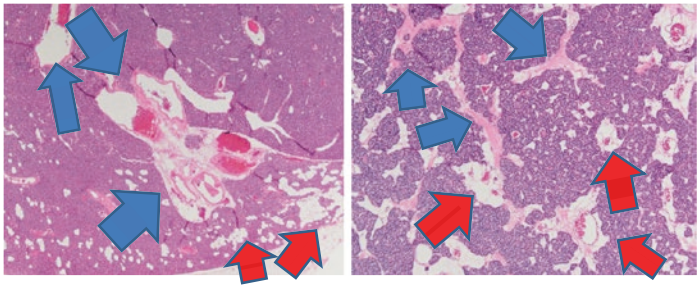

Image 12.2 Pathology: Left: Hypercellular parathyroid with large blood vessels (blue arrows). Scattered pockets of adipose tissue at the periphery (red arrows). Right: Central portion exhibiting microfollicular architecture, with interspersed strips of fibrosis (blue arrows) and adipose tissue (red arrows)

Parathyroid Embryology and Anatomy

Briefly, the inferior parathyroid gland originates from the third pharyngeal pouch (together with the thymus) and travels down to the normal (orthotopic) location behind the lower pole of the thyroid lobe (Image 12.3, left panel). However, the lower pole gland can remain either in its original location (undescended), any place along the path on which it descends, or overshoot, ending up in the mediastinum—all ectopic locations. The upper gland originates from the fourth pharyngeal pouch and travels down, medial and in a posterior course ending behind the upper pole of the thyroid. The upper pole gland can also fail to descend, deposit along the descending path, or overshoot and end up in the posterior mediastinum. These ectopic locations are always posterior to the recurrent laryngeal nerve. All the orthotopic and possible ectopic locations are demonstrated in Image 12.3, right.

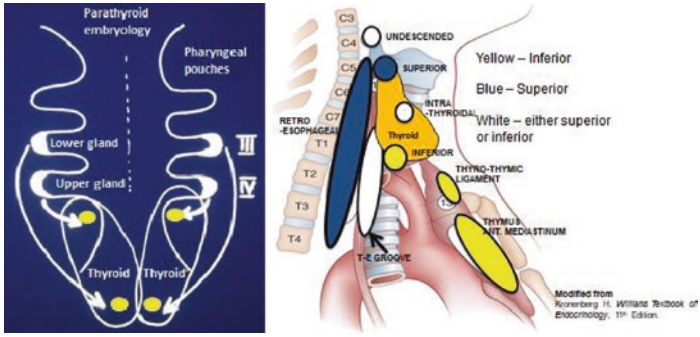

Image 12.3 Anatomy of the expected locations of NORMAL and ECTOPIC parathyroid glands/adenomas (yellow = lower pole gland, blue = upper pole gland, white = either upper or lower pole glands)

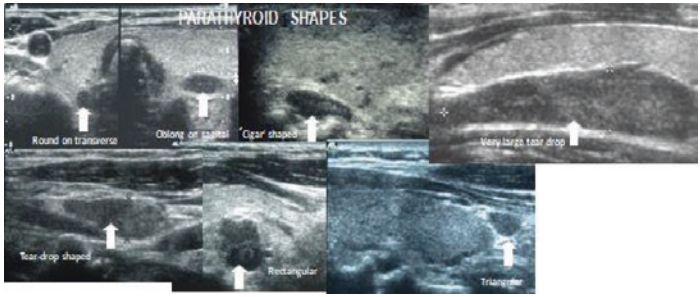

Image 12.4 Multiple examples of parathyroid adenomas (arrows). Hypoechoic compared to the thyroid and variable in size and shape. The shape is determined by the space in which the adenoma develops

Parathyroid Adenomas: Additional Examples

Echotexture While a classic parathyroid adenoma is hypoechoic relative to the thyroid gland, as discussed earlier, the distinction may not be as stark in patients with underlying thyroiditis. The texture may also be atypical as shown in the examples below (Image 12.4). Cystic change is also possible.

Shape Parathyroid adenomas have variable shapes, depending on the anatomic location of the lesions. The enlarged glands are often soft and molded by the immediate surrounding structures, resulting in unusual shapes (Image 12.4).

Size Parathyroid adenomas are very variable in size. Normal parathyroid glands are in the range of 3-4 mm in size and not usually identifiable on ultrasound. Parathyroid adenomas can measure from 4 to 5 mm up to 7 cm in size. There is poor correlation between size and function: small lesions can produce marked hyperfunction and very large lesions may present with minimally elevated calcium and PTH levels.

Vascularity Parathyroid adenomas are typically hypervascular on color Doppler (Image 12.5a, b). Hypervascularity strongly supports the diagnosis, but a lack of hypervascularity on color Doppler does not exclude it (Image 12.5c).

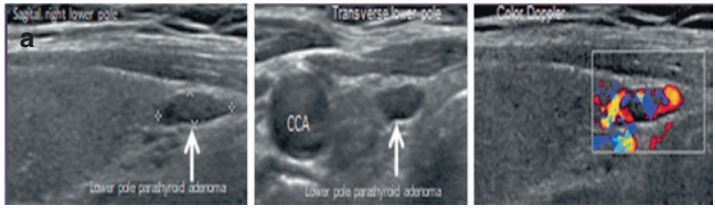

Image 12.5 (**a**) Sagittal and transverse views of a right lower pole adenoma demonstrate a hypoechoic, extrathyroidal lower pole nodule, hypervascular on Color Doppler (image right). (**b**) Transverse view of a hypoechoic parathyroid adenoma in the right thyroid bed (left panel) that is hypervascular on color Doppler (right panel). (**c**) Transverse view through the left lobe demonstrating a small left upper pole parathyroid adenoma (left panel). Color Doppler shows the adenoma is avascular (right panel). Vascularity is a very helpful US finding but the absence of vascularity does not rule out parathyroid adenoma

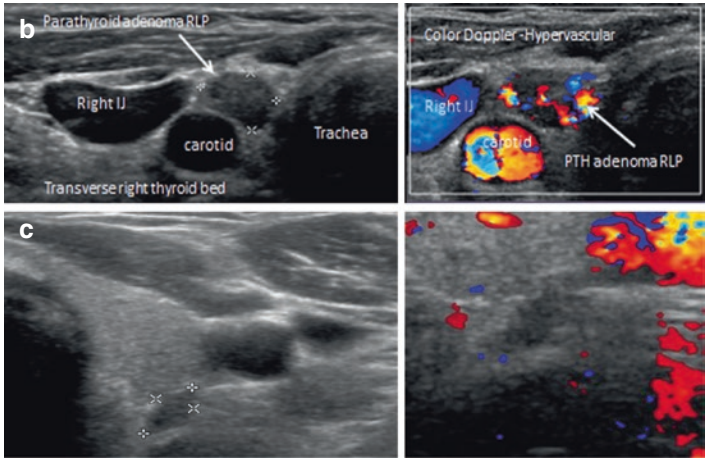

Image 12.5 (continued)

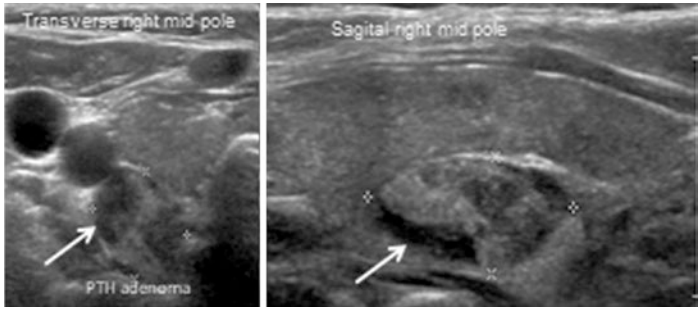

Image 12.6 Unusual mixed echotexture of a parathyroid adenoma with hypoechoic and hyperechoic elements

Atypical Appearance of Parathyroid Adenomas (Images 12.6, 12.7, and 12.8)

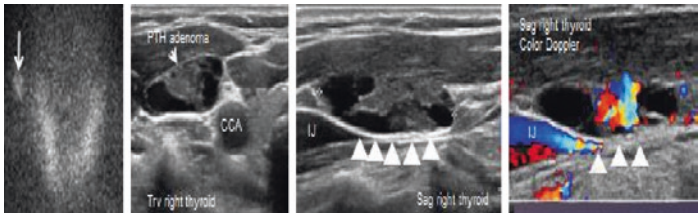

Image 12.7 Ectopic, solid, and cystic parathyroid adenoma. Sestamibi (left panel, arrow) shows activity lateral to the right upper pole of the thyroid gland. Ultrasound image in transverse view demonstrates the mixed composition (second panel), and sagittal view shows the lesion compressing the right IJ, likely located within the carotid sheath (third panel, arrowheads). Color Doppler shows very vascular solid tissue surrounded by cystic elements (right panel)

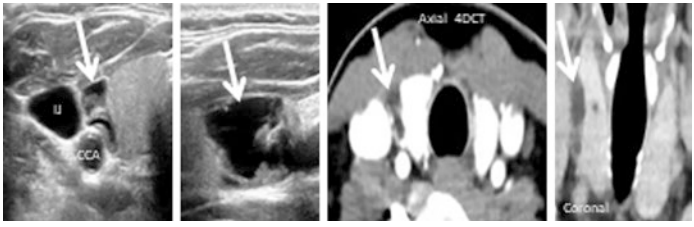

Image 12.8 Predominantly cystic lesion is noted adjacent to the right upper pole of the thyroid with solid, septal elements on US (left 2 panels with arrows). Also seen on the 4DCT images (right 2 panels with arrows: left image, axial view; right image, coronal view). Differential—exophytic, cystic thyroid nodule vs cystic parathyroid. FNA for PTH confirmed a parathyroid adenoma

Ectopic Locations of Parathyroid Adenomas (Images 12.9, 12.10, 12.11, and 12.12)

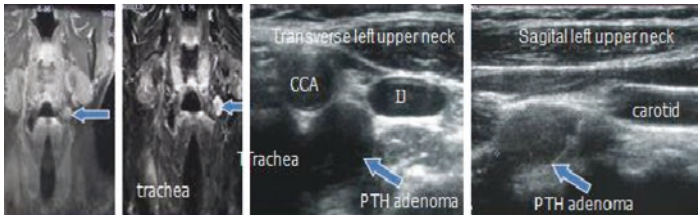

Image 12.9 MRI shows an adenoma high in the neck, just below the salivary glands. This is an undescended left lower pole gland. On the left, 2 MRI sequences demonstrate the adenoma (arrows). This was confirmed by ultrasound (middle and right panels with arrows) and subsequent FNA for PTH

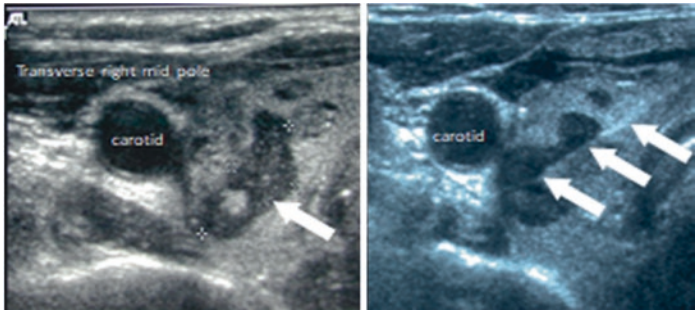

Image 12.10 An unusual right-sided intrathyroidal lesion was noted, atypical for a thyroid nodule (left panel, transverse image). FNA for PTH (right panel with arrows pointing to the needle in the nodule) was markedly elevated, confirming an intrathyroidal parathyroid adenoma

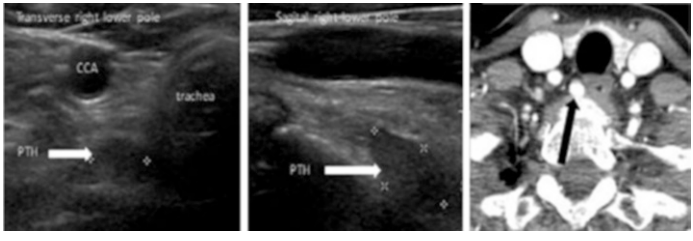

Image 12.11 Ultrasound raises the possibility of a very posterior and medial, hypoechoic nodule below the right lower pole of the thyroid (left panel, transverse view; middle panel, sagittal view). Because it was at the lower limits of visibility by ultrasound, 4DCT was performed and confirmed a classic parathyroid adenoma adjacent to the esophagus (right image, arrow), representing a parathyroid adenoma arising in the ectopic right upper pole gland

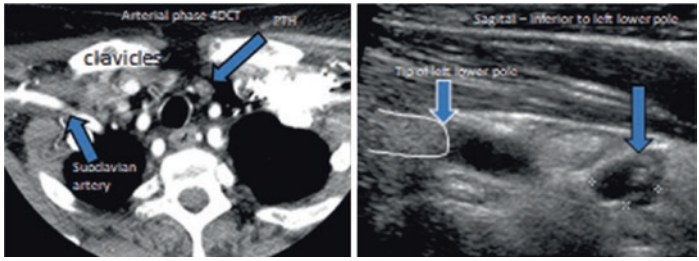

Image 12.12 Initial ultrasound was nondiagnostic. 4DCT showed a poorly enhancing lesion below the left lower pole of the thyroid (left panel, right arrow). Repeat US with angling into the upper mediastinum demonstrated a mostly cystic lesion (right panel, right arrow), which also explained why the lesion demonstrated poor enhancement. Aspiration revealed a dramatic elevation in PTH

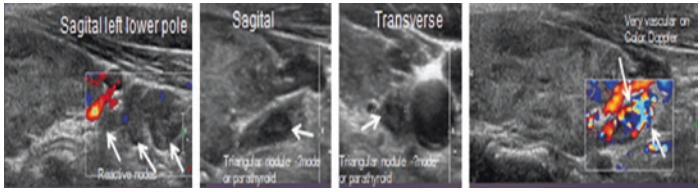

Image 12.13 Patient with Hashimoto's thyroiditis: US demonstrates patchy thyroid texture and reactive lymph nodes at the lower pole (left panel, arrows). One nodule had an unusual triangular shape (middle 2 panels, sagittal and transverse views). Color Doppler showed hypervascularity, suggesting a parathyroid adenoma and differentiating it from the avascular lymph nodes (right panel)

Associated Thyroid Diseases Complicating Parathyroid Adenoma Localization (Images 12.13, 12.14, and 12.15)

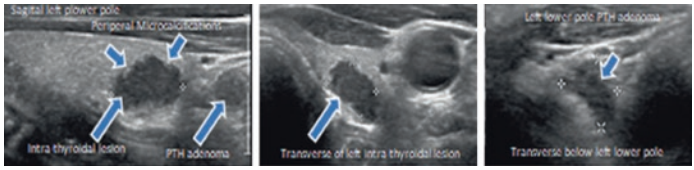

Image 12.14 Ultrasound demonstrates two nodules: An extrathyroidal parathyroid adenoma and a lower pole thyroid nodule (left panel, sagittal view with arrows; middle panel, transverse view with arrow of left lower pole thyroid nodule; right panel, transverse view of parathyroid adenoma inferior to the left lobe). The thyroid nodule is hypoechoic with foci of peripheral micro-calcification. Preoperative FNA was consistent with papillary thyroid carcinoma. Parathyroidectomy and thyroidectomy were performed at surgery

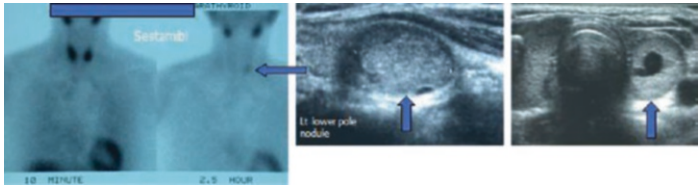

Image 12.15 False positive sestamibi scan: Dense activity is noted at the left lower pole of the thyroid gland, persisting on the delayed views (left panel, arrow). Ultrasound shows the activity correlates with a thyroid nodule in the same location (middle panel, sagittal view; right panel, transverse view). FNA of the thyroid nodule is recommended before proceeding to parathyroid surgery, due to its US characteristics

4DCT

This imaging modality has significantly improved the preoperative localization of parathyroid adenomas. Adenomas in the normal (orthotopic) location are detectable, but the major advantage of 4DCT is its ability to identify ectopic adenomas (Images 12.17

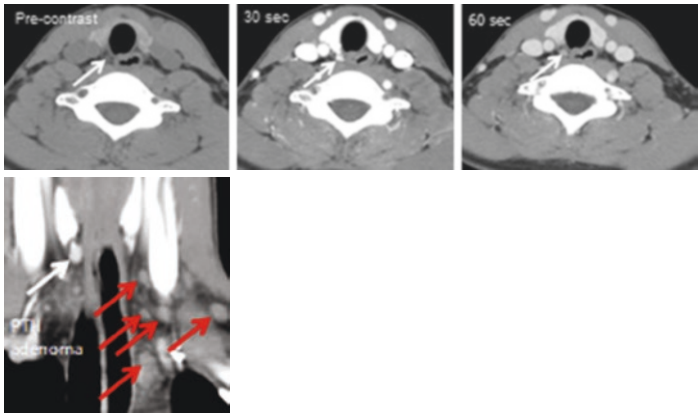

Image 12.16 Classic 4DCT. Top left: Axial images pre-contrast show the parathyroid adenoma to be less dense than the thyroid (thyroid density is due to iodine content). Top middle: Following a bolus of IV contrast, there is dramatic enhancement of the adenoma. Top right: Delayed scans at 60–90 s show rapid washout of the contrast from the adenoma. Bottom left: A coronal view demonstrates the difference between enhancement of the adenoma on the right (white arrow) and the poorly enhancing nodes on the left (red arrows)

and 12.18), both in the neck and chest, in addition to the detection of double adenomas and multi-gland disease. Interpretation can in some cases be extremely difficult when the adenomas are closely applied to or within the thyroid gland or are small. However, in those particular scenarios, they are usually easily identified by ultrasound, making the two studies complementary. 4DCT requires the administration of a bolus of intravenous contrast (which may be contraindicated in patients with renal dysfunction or contrast allergy). Lastly, interpretation of the 4DCT scans requires both skill and experience.

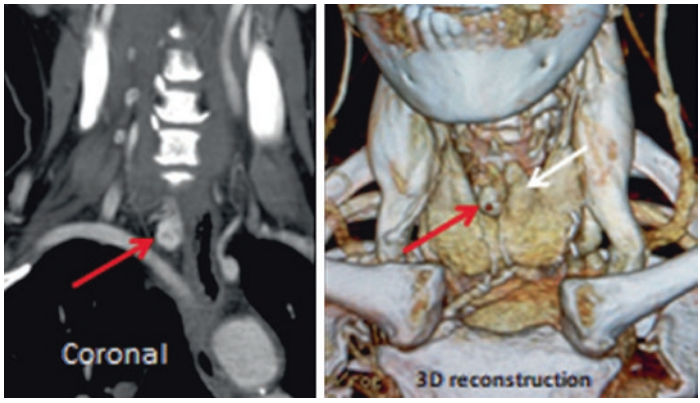

Image 12.17 Left: Coronal view showing a parathyroid adenoma far posterior, consistent with an ectopic right upper pole gland. Right: 3D reconstruction showing the adenoma (red arrow) and an incidental pyramidal lobe of the thyroid (white arrow)

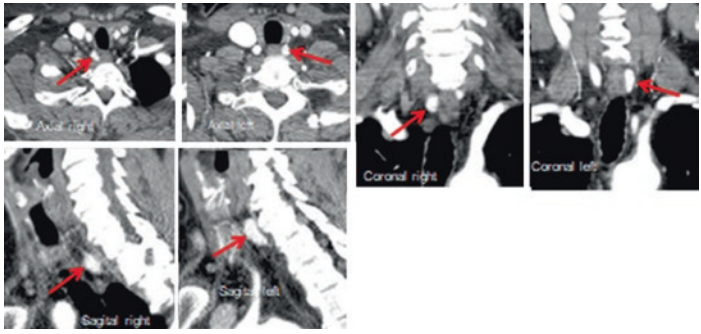

Image 12.18 Bilateral parathyroid adenomas. Top two left panels: Axial views of bilateral ectopic right and left upper pole adenomas (arrows). Top right panels. Coronal views of the adenomas. Lower left panels: Same ectopic upper pole double adenomas in sagittal projection

A minimum of three sequences is obtained, from the skull base to the carina. The first scan is obtained without contrast, the next 30 seconds after the initiation of the contrast bolus (100 cc at 4 cc/second), and finally, a delayed scan at 75 seconds. A classic parathyroid adenoma appears as a soft tissue nodule less dense than the thyroid (the same density as the surrounding muscle) and enhances brightly on the 30 second scan, with the contrast washing out rapidly by the 60-80 second scan (Image 12.16, arrows).

Discussion

Ultrasound identification of enlarged parathyroid glands is most accurate when the enlarged glands are in the expected normal (orthotopic) anatomic location, adjacent to and behind the thyroid. A major advantage of US is the ability to identify intrathyroidal adenomas. Double adenomas and multi-gland disease can be diagnosed, but it is a less accurate modality than for a single adenoma. The major disadvantage of ultrasound is that it is entirely operator-dependent. For parathyroid adenoma localization in particular, US requires specific expertise and dedication, knowing where to search for both normally positioned glands and the potential ectopic glands. Image quality is important, influenced by the ultrasound equipment, the type of transducer, patient anatomy, and the status of the thyroid gland.

Parathyroid adenomas are typically hypoechoic on ultrasound when compared to the adjacent thyroid gland. The textural differences are less obvious when there is underlying thyroid disease, particularly with Hashimoto's thyroiditis. Graves' disease, subacute thyroiditis, and chronic lithium administration will have a similar effect in diminishing the textural difference, rendering the diagnosis of parathyroid adenoma by ultrasound more challenging. An additional diagnostic challenge in the setting of Hashimoto's disease is the common finding of multiple reactive lymph nodes, particularly at the lower poles of the thyroid gland, given the potential large size of the nodes, for which distinction from a parathyroid adenoma can be difficult. Color Doppler is very helpful when classical hypervascularity or a polar artery is

demonstrated. However, the absence of hypervascularity does not exclude a parathyroid adenoma. When in doubt, 4DCT will help localize and establish the diagnosis as occurred in the patient in our Case Presentation.

Some additional pitfalls that may potentially diminish the ability to obtain a satisfactory ultrasound exam include:

1. An ectopic location of the adenoma, which may be less accessible or inaccessible by ultrasound, or more difficult to differentiate from lymph nodes (e.g. undescended lesions in the high neck or those in the deep posterior neck; retro-esophageal lesions, or those within the carotid sheath or mediastinum).
2. Patients with a very large, short neck.
3. A very large multinodular goiter, where the thyroid lobes are large enough to limit visualization. Extension of the thyroid lobes or nodules into the thoracic inlet will also limit the evaluation of the lower pole glands.

Further Reading

Akerström G, Malmaeus J, Bergström R. Surgical anatomy of human parathyroid glands. Surgery. 1984;95:14–21.

Lappas D, Noussios G, Anagnostis P, Adamidou F, Chatzigeorgiou A, Skandalakis P. Location, number and morphology of parathyroid glands: results from a large anatomical series. Anat Sci Int. 2012;87:160–4.

Lubitz CC, Stephen AE, Hodin RA, Pandharipande P. Preoperative localization strategies for primary hyperparathyroidism: an economic analysis. Ann Surg Oncol. 2012;19:4202–9.

Sacks BA, Pallotta JA, Cole A, Hurwitz J. Diagnosis of parathyroid adenomas: efficacy of measuring parathormone levels in needle aspirates of cervical masses. AJR Am J Roentgenol. 1994 Nov;163(5):1223–6.

Solorzano CC, Carneiro-Pla D. Minimizing cost and maximizing success in the preoperative localization strategy for primary hyperparathyroidism. Surg Clin North Am. 2014;94:587–605.

Cervical Lymph Nodes

13

Hien Tierney

Key Points

- Enlarged cervical lymph nodes are a common finding and the differentiation of benign vs malignant lymphadenopathy is done with a combination of imaging and fine needle biopsy.
- A persistently enlarged lymph node in an adult that does not have reassuringly benign characteristics on ultrasound should be considered suspicious until proven otherwise.
- Benign lymph nodes most often appear ovoid, well-circumscribed, and have a preserved echogenic hilum.
- Malignant lymph nodes most often appear rounded, hypoechoic, and have an absent echogenic hilum. Prominent vascularity may also be present.

H. Tierney (✉)
Atrius Health/Harvard Medical School, Boston, MA, USA
e-mail: hientue_tierney@atriushealth.org

L. S. Eldeiry et al. (eds.), *Handbook of Thyroid and Neck Ultrasonography*, Contemporary Endocrinology,
https://doi.org/10.1007/978-3-031-18448-2_13

- Cystic necrosis within a lymph node is suggestive of carcinoma; however, this needs to be distinguished from other benign cystic lesions of the cervical region.
- Ultrasound followed by fine needle biopsy should be considered for any persistently enlarged or suspicious-appearing lymph node or neck mass.
- Fine needle aspiration for thyroglobulin washout (or calcitonin, in the case of suspected MTC) should be considered when there is suspicion of metastatic thyroid cancer.

Introduction

Cervical lymphadenopathy may be broadly classified as benign or malignant in nature, with management being determined by the underlying disorder associated with the lymphadenopathy. A careful physical exam is an important component of the initial evaluation of cervical lymphadenopathy and multiple large, firm nodes should raise the level of suspicion for possible malignancy. However, physical examination alone is an unreliable method for assessing lymphadenopathy and ultrasound is considered the preferred imaging modality for the initial evaluation of metastatic lymph nodes. Ultrasound can significantly inform the diagnostic process by assessing the size, morphology, and position of such lymph nodes.

Lymph nodes are described based on their location in the neck (Fig. 13.1).

- Level I extends from the mandible to the hyoid bone in the submental midline region.
- Level II encompasses the region from the skull base to the hyoid bone along the submandibular gland anteriorly to the posterior border of the sternocleidomastoid muscle posteriorly.
- Level III represents lymph nodes between the hyoid bone superiorly and the cricoid cartilage inferiorly, between the

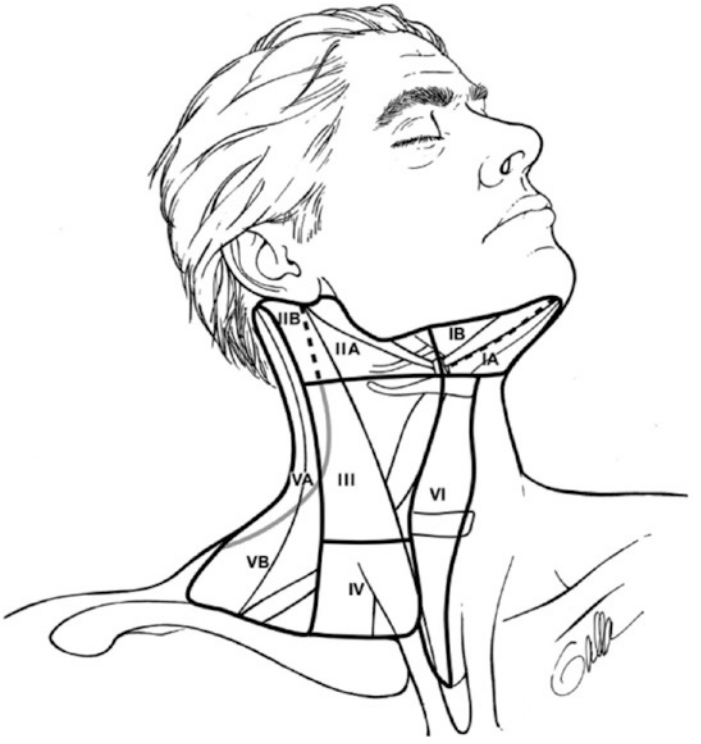

Fig. 13.1 Anatomic boundaries of the levels of the neck used to describe the location of cervical lymphadenopathy

anterior and posterior borders of the sternocleidomastoid muscle.

- Level IV extends from the cricoid cartilage to the clavicle, from the anterior border of the sternocleidomastoid muscle to the lateral edge of the anterior scalene muscle.
- Level V represents the posterior triangle from the posterior border of the sternocleidomastoid muscles to the anterior border of the trapezius muscle.
- Level VI represents the central compartment from the hyoid bone above to the suprasternal notch below, between the medial borders of both common carotid arteries.

Ultrasound characteristics that help to differentiate benign versus malignant lymph nodes include:

Benign
- Normal hypoechoic echotexture
- Elongated shape
- Presence of a central hilar line
- Vascularity limited to the central hila
- Well-defined, smooth border
- High long/short axis ratio

Malignant
- Hyper- or hypo-echogenicity
- Round shape
- Loss of the central hila
- Abnormal or peripheral vascularity on color Doppler
- Irregular borders
- Calcifications (usually micro-calcification)
- Cystic degeneration or focal cysts

Case Presentation

A 64-year-old man presented with a 2-month history of dysphonia. He had no sore throat or dysphagia and no personal or family history of thyroid disease. He was a nonsmoker. On clinical examination, a firm, 3 cm right-sided thyroid mass was noted. Laryngoscopy demonstrated right vocal fold paresis. TSH was normal. Neck ultrasound showed a right thyroid nodule, taller than wide, that was markedly hypoechoic, measuring 2.7 × 2.1 × 3.0 cm with internal vascularity. In the central neck, there was a 0.8 cm round lymph node with indistinct borders and lack of a central hilum (Image 13.1) and in level IV, there was another 2.5 cm enlarged abnormal-appearing lymph node (Image 13.2). A subsequent CT scan confirmed the ultrasound findings.

The patient underwent ultrasound-guided FNA and cytology was consistent with medullary thyroid carcinoma (MTC) (Image 13.3). Preoperative evaluation for MTC was performed including RET oncogene testing and testing for pheochromocytoma, which

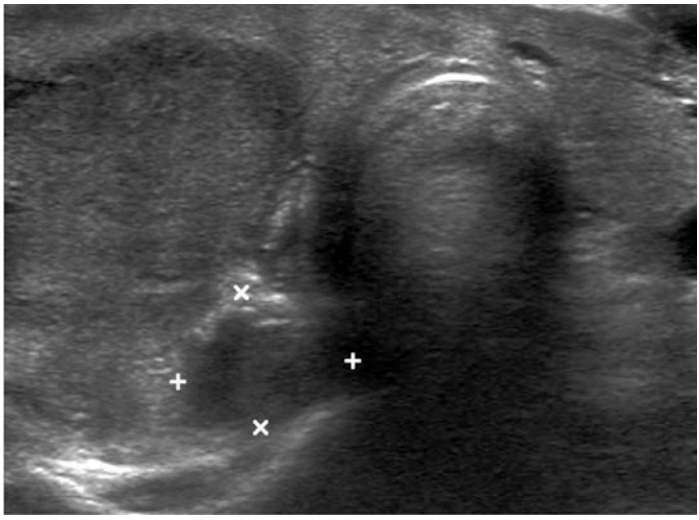

Image 13.1 Level VI abnormal-appearing lymph node. Note the round shape, indistinct borders, and lack of a central hilum

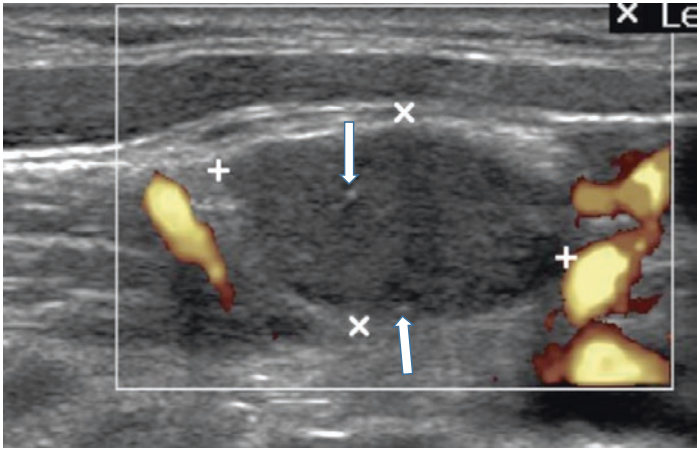

Image 13.2 Level IV abnormal-appearing lymph node. The node appears enlarged, heterogeneous, and demonstrates peripheral vascularity. Again note the lack of a central hilum. There are 2 micro-calcifications (arrows)

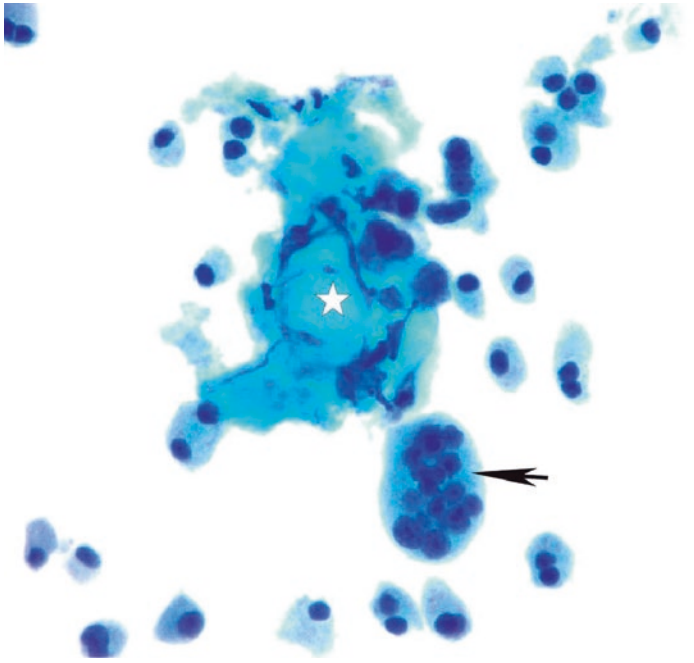

Image 13.3 Round to ovoid, and multinucleated plasmacytoid-shaped cells (arrow) with thick amorphous amyloid deposits (star), consistent with a diagnosis of MTC (Thin-prep cytology, PAP stain, ×60)

was negative. Preoperative calcitonin and CEA values were markedly elevated at 5108 pg/mL (<10 pg/mL) and 163 ng/mL (0–2.5 ng/mL), respectively. The patient underwent total thyroidectomy with bilateral central and lateral neck dissection. Pathology showed a 3.2 cm MTC with extensive bilateral lymph node involvement in 19 of 44 lymph nodes (Image 13.4).

Cervical Lymph Nodes and Lateral Neck Masses: Additional Examples

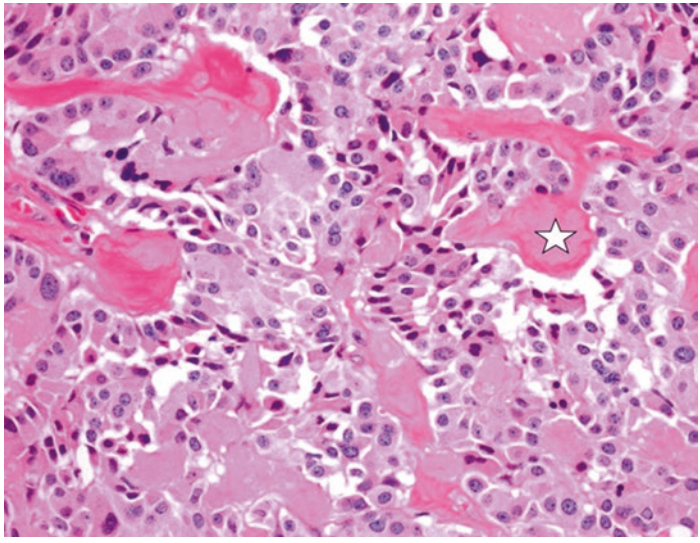

Image 13.4 Nests of irregular spindled and plasmocytoid-shaped cells with amyloid deposits (star) typical of MTC (H&E, ×60)

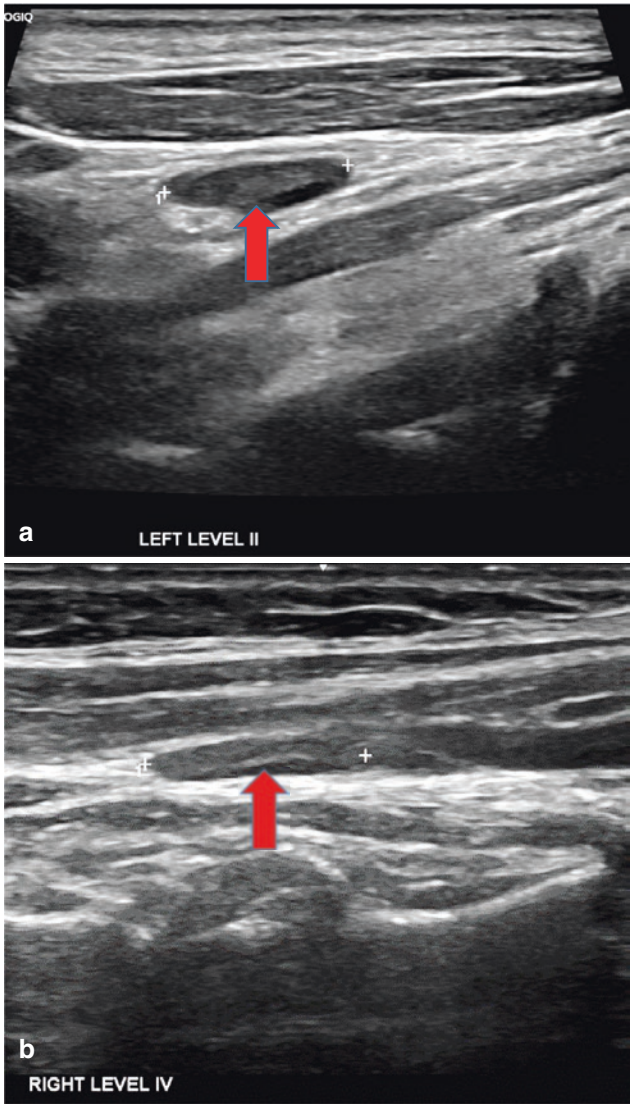

Image 13.5 (**a**–**c**) Benign cervical lymph nodes, each with preservation of the echogenic hilum (red arrows). Benign lymph nodes appear elongated or ovoid and have well-defined borders

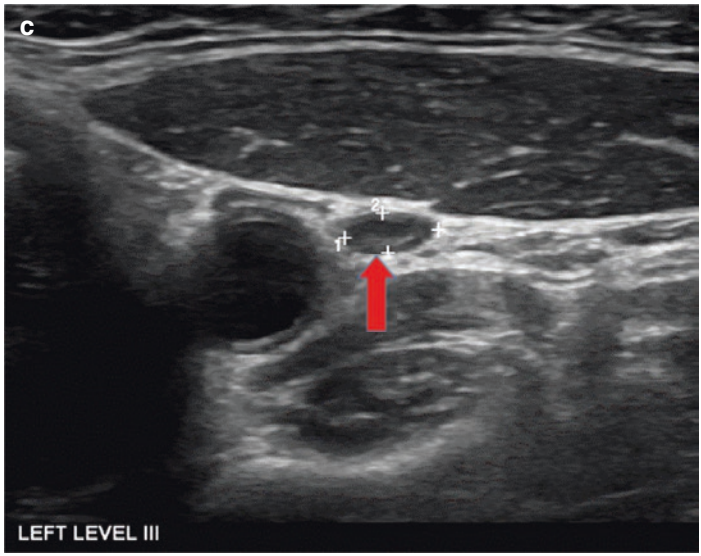

Image 13.5 (continued)

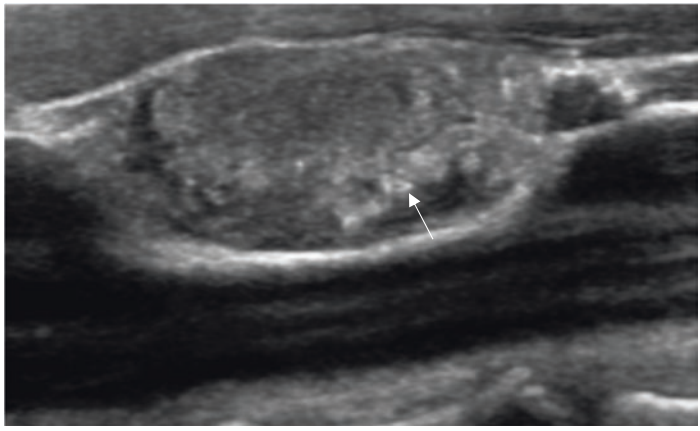

Image 13.6 Solid level IV lymph node metastasis from papillary thyroid carcinoma. Note the rounded nodular contour of the node, irregular border, and scattered micro-calcifications (arrow)

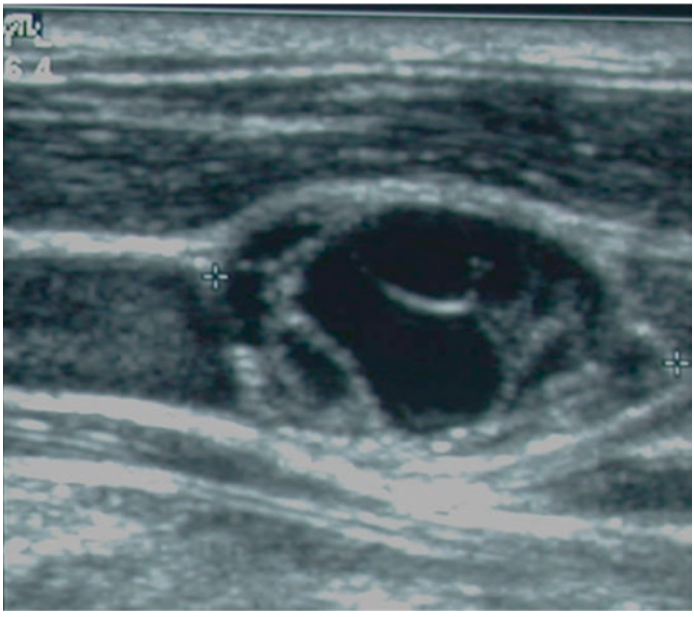

Image 13.7 Cystic lymph node metastasis from papillary thyroid carcinoma

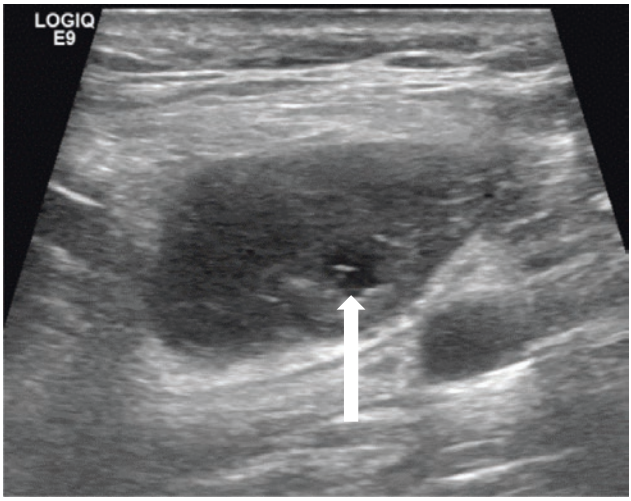

Image 13.8 Metastatic squamous cell carcinoma to a level II lymph node demonstrating irregular shape with an area of cystic necrosis (arrow)

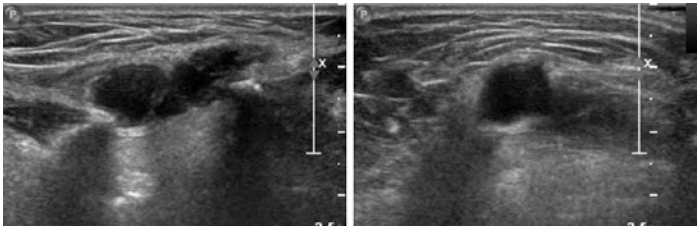

Image 13.9 Ultrasound of a midline thyroglossal duct cyst (left panel sagittal, right panel transverse). These well-circumscribed congenital lesions can be confused with prelaryngeal "Delphian" nodes, which can harbor malignancies from laryngeal and thyroid tumors. Thyroglossal duct cysts usually lie along the thyrohyoid membrane, while prelaryngeal nodes are found along the cricothyroid region

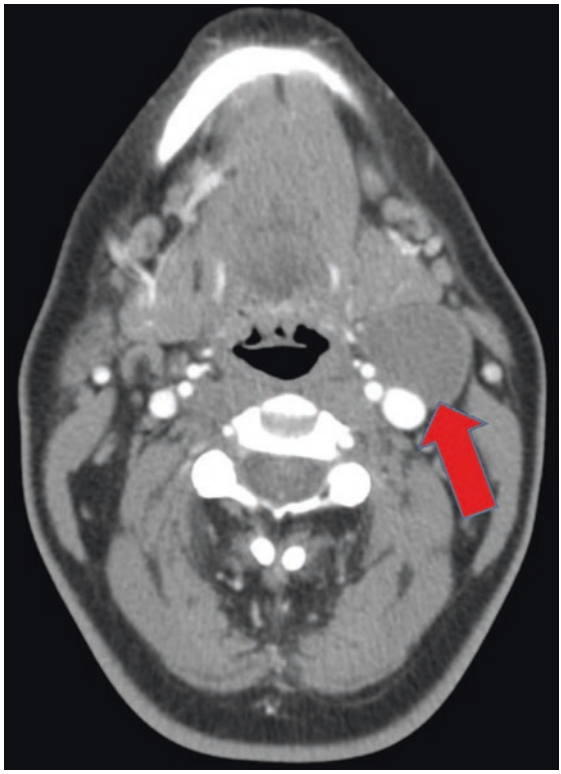

Image 13.10 Axial contrast CT image of a congenital branchial cleft cyst in left level II of the neck. Note the lesion may be confused with a cystic lymph node and has slight mural wall thickening (arrow), likely due to previous infection

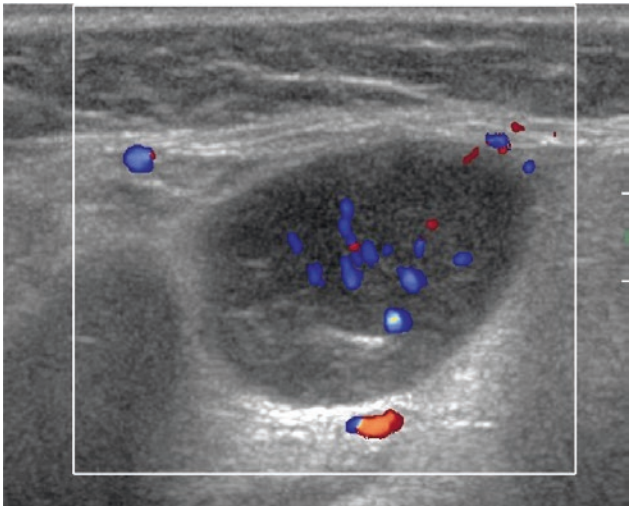

Image 13.11 Lymphoma node that is enlarged, round, and does not have a hilum. These lymph nodes are usually homogeneous, with relatively low level internal echoes. They can be diffusely vascular on color Doppler

Discussion

Cervical lymphadenopathy can be a common finding in the general population and a thorough clinical examination and diagnostic testing are necessary to determine the underlying cause (Table 13.1). Pertinent history includes the patient's age, any symptoms of infection, and other symptoms of localized or generalized malignancy, such as dysphonia, dysphagia, sore throat, and weight loss. A persistently enlarged cervical lymph node in an adult should be carefully evaluated and there should be a high suspicion for malignancy until proven otherwise. Lymph nodes that remain enlarged for more than 4 weeks without any other identifiable cause should have further evaluation.

On physical exam, assessment of nodal distribution is one important factor in the initial evaluation. Lymph nodes up to 3 cm may be followed for a short period of time in level 2, but those that are larger than 2 cm in other regions in the neck are more suspicious for a malignant process. Fixed, firm nodes in multiple regions of the neck are a worrisome finding.

Table 13.1 Differential diagnosis

1. Malignant lymphadenopathy
2. Benign reactive lymphadenopathy (a) Infectious (b) Inflammatory (e.g. Hashimoto's thyroiditis)
3. Benign neck masses (a) Branchial cleft cyst (b) Thyroglossal duct cyst (c) Lipoma (d) Neurogenic tumors (paraganglioma, schwannoma) (e) Vascular lesions (f) Congenital lesions (dermoid cyst, teratoma) (g) Parathyroid adenomas

Ultrasound is the primary initial diagnostic tool in the evaluation of persistent lymphadenopathy. Considering all the characteristics of the lymph node or lesion including size, location, echogenicity, shape, borders, vascularity and taking into consideration patient risk factors for malignancy helps distinguish suspicious from benign lesions.

Benign reactive lymph nodes often appear elongated and ovoid with a well-defined border and with preservation of the echogenic, fat-containing hilum. By comparing the length of the longest and shortest axis of the node, an "L/S ratio" can be calculated, with benign lymph nodes most often having an L/S ratio > 2 (Image 13.5a–c). In contrast, malignant lymph nodes usually display a rounded contour with an L/S ratio < 2, are hypoechoic, and have no visible echogenic hilum. A peripheral halo and prominent vascularity are more commonly seen in malignant processes. Metastatic lymph nodes from papillary thyroid carcinoma may demonstrate punctate calcifications and hyper-echogenicity (Image 13.6). Intra-nodal cystic necrosis is also suggestive of metastases (Images 13.7 and 13.8). However, cystic change can be seen in benign processes, such as in thyroglossal duct cysts, which present high in the midline at the level of the hyoid bone, and in congenital branchial cleft cysts which most often present in the lateral mid-neck (Images 13.9 and 13.10).

Fine needle aspiration is recommended for any suspicious-appearing or persistently enlarged cervical lymph node. In most solid lymph nodes, fine needle aspiration is both highly sensitive and specific for distinguishing benign reactive lymphadenopathy from malignancy. Cystic lymph nodes may be harder to diagnose with needle biopsy because often the biopsy demonstrates only acellular cyst fluid. In some cases, repeat needle biopsy, core biopsy, and even excisional biopsy can be considered if fine needle biopsy is non-diagnostic. Excisional biopsy combined with flow cytometry is especially useful to diagnose lymphoproliferative disorders once fine needle biopsy suggests an abnormal population of lymphocytic cells (Image 13.11). In head and neck squamous cell carcinoma, immunohistochemistry for certain markers such as p16 can help to identify HPV-related cancers and thereby help to guide prognosis and treatment.

To help diagnose differentiated thyroid cancer, thyroglobulin measurement of the fine needle aspiration washout should be employed. Thyroglobulin is only produced by follicular cells, and its presence in non-thyroidal tissue is indicative of metastatic spread of differentiated thyroid cancer. Caution should be taken when sampling thyroglobulin in lymph nodes found in level VI (the central neck), because of a higher risk of inadvertently sampling thyroid tissue in this region, which can lead to false positive results. In contrast, thyroglobulin washout may be less useful in cases of undifferentiated thyroid tumors, such as anaplastic carcinoma, as these thyroid cancers do not reliably produce thyroglobulin. Similarly, MTC will not be detected by thyroglobulin washout and testing will lead to false negative results if this condition is not considered. In some institutions, calcitonin levels can be measured in lymph node aspirates to help diagnose suspected MTC. Ultimately, a high level of suspicion based on patient and ultrasound factors followed by fine needle biopsy are the key components of the evaluation of persistent lymphadenopathy in the cervical region.

Further Reading

Asimakopoulos P, Nixon IJ, Shaha AR. Differentiated and medullary thyroid cancer: surgical management of cervical lymph nodes. Clin Oncol (R Coll Radiol). 2017;29(5):283–9.

Cervical SM. Lymphadenopathy. In: Head and neck and endocrine surgery. Thieme Medical Publishers; 2016. p. 163–90.

Grani G, Fumarola A. Thyroglobulin in lymph node fine-needle aspiration washout: a systematic review and meta-analysis of diagnostic accuracy. J Clin Endocrinol Metab. 2014;99(6):1970–82.

Gupta A, et al. Sonographic assessment of cervical lymphadenopathy: role of high-resolution and color doppler imaging. Head Neck. 2011;33(3):297–302.

Khanna R, Sharma AD, Khanna S, Kumar M, Shukla RC. Usefulness of ultrasonography for the evaluation of cervical lymphadenopathy. World J Surg Oncol. 2011;9:29. https://doi.org/10.1186/1477-7819-9-29.

Anatomy and Selected Non-thyroid Neck Findings

14

Mary Beth Cunnane, Gregory W. Randolph, and Amy Juliano

Key Points

- Incidental masses in the neck, other than thyroid nodules, are uncommon.
- In select cases, a definitive benign diagnosis can be made on US alone. These include simple lipoma, thyroglossal duct cyst without solid tissue or calcification, plunging ranula, and diffuse inflammatory conditions of the sali-

The original version of the chapter has been revised. A correction to this chapter can be found at https://doi.org/10.1007/978-3-031-18448-2_15

M. B. Cunnane (✉)
Department of Radiology, Massachusetts Eye and Ear Institute, Boston, MA, USA
e-mail: MaryBeth_Cunnane@MEEI.HARVARD.EDU

G. W. Randolph
Department of Otorhinolaryngology, Head and Neck Surgery, Massachusetts Eye and Ear Infirmary, Boston, MA, USA

A. Juliano
Department of Radiology, Massachusetts Eye and Ear Infirmary, Boston, MA, USA
e-mail: amy_juliano@meei.harvard.edu

L. S. Eldeiry et al. (eds.), *Handbook of Thyroid and Neck Ultrasonography*, Contemporary Endocrinology,
https://doi.org/10.1007/978-3-031-18448-2_14

vary glands (sialadenitis), without or with an obstructive sialolith (the latter may also be visible on ultrasound).
- Outside of these specific examples, a patient with a newly identified mass in the neck should be referred for ENT evaluation and contrast-enhanced CT or MRI for further characterization prior to biopsy.

Introduction

Whereas the other chapters in this volume have focused on ultrasound findings related to thyroid and parathyroid disease, or cervical lymph node ultrasonography, the goals of this chapter will be to review ultrasound anatomy and to discuss additional cervical lesions that may be incidentally found when evaluating the thyroid gland (Image 14.1).

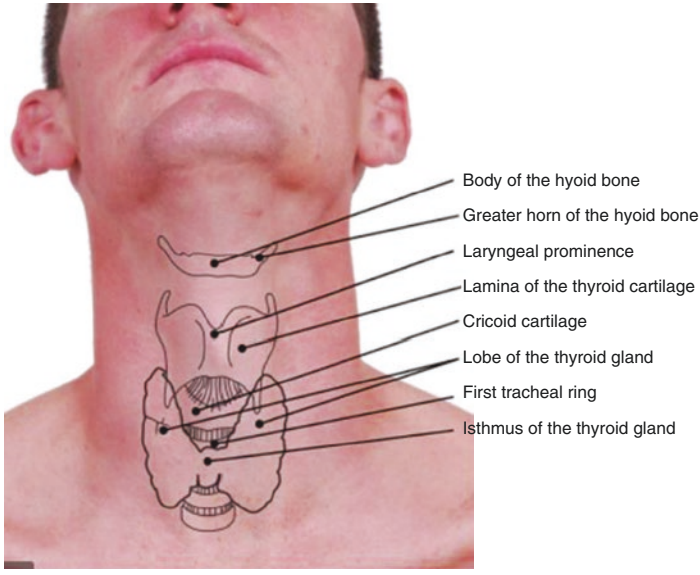

Image 14.1 Surface anatomy of the neck (source: Lumley, J. Surface Anatomy: The Anatomical Basis of Clinical Examination. 2008, 4th ed.)

Normal Ultrasound Anatomy

For review, the index images below demonstrate several landmarks that are important to recognize when scanning the thyroid gland (Images 14.2, 14.3, 14.4, and 14.5).

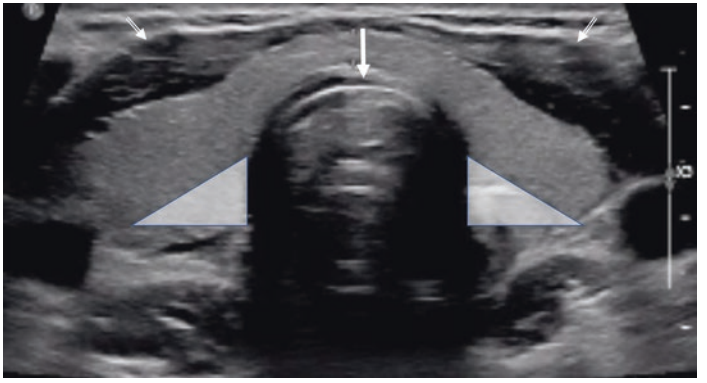

Image 14.2 In this transverse image at the level of the thyroid isthmus, double lined arrows mark the strap muscles bilaterally. A solid arrow indicates the trachea; note the echogenic line along the anterior aspect and the shadowing along the lateral aspects. White triangles denote the location of the "danger triangle" of the tracheoesophageal groove, so named because it represents a potential location of the recurrent laryngeal nerves

Image 14.3 In this image, the multilayered wall of the esophagus is clearly seen in the left tracheoesophageal groove (arrow)

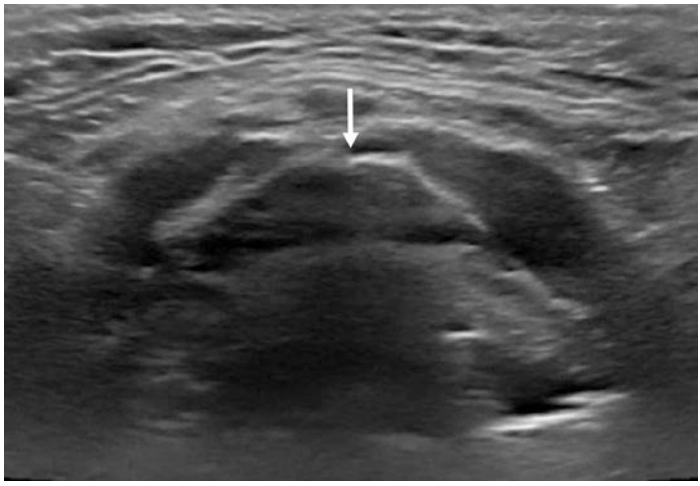

Image 14.4 The hyoid bone (arrow) can be recognized as a curved echogenic focus in the superior midline neck with posterior acoustic shadowing. This is an important landmark for the recognition of thyroglossal duct cysts

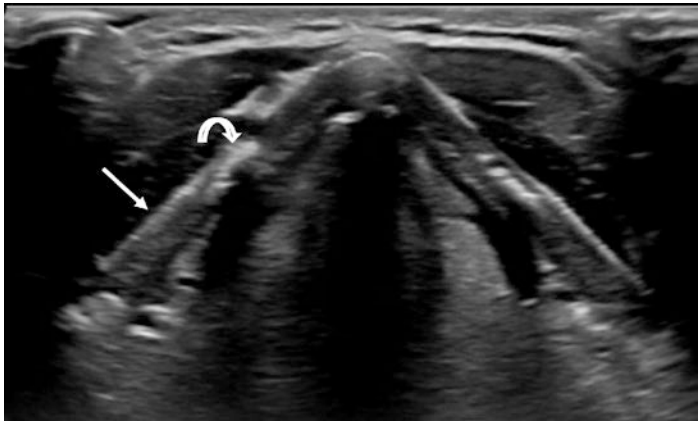

Image 14.5 The thyroid cartilage is easily seen during thyroid ultrasound. As a patient ages, the thyroid cartilage progressively mineralizes, but this can occur in a discontinuous fashion with ossified and non-ossified components coexisting. In this image, the straight arrow indicates non-ossified thyroid cartilage. The curved arrow indicates ossified thyroid cartilage which is echogenic with posterior acoustic shadowing. The larynx is partially visualized through the non-ossified components

Evaluation of Incidental Findings in the Neck

Occasionally during thyroid ultrasound, an unsuspected abnormality is identified in the neck or the patient requests evaluation of a palpable or visible neck mass, keeping in mind that skin folds, sag of submental soft tissue, and asymmetric clavicular heads, which may be identified by the patient as a palpable "lump," are not actual neck lumps. For lesions encountered outside of the thyroid, the initial step for developing a differential diagnosis is to identify the location of the lesion. Inflammatory conditions such as sialadenitis, benign masses, and malignancies (either primary malignancies or metastatic nodes) may all present as neck masses.

There are certain neck lesions with characteristic appearances that can safely be considered benign. These include simple lipomas, plunging ranulas, and thyroglossal duct cysts that do not contain solid components or calcification. Sialadenitis and sialolith with ductal dilation are additional benign inflammatory conditions that can be appreciated on neck US.

Outside of these examples, a mass in the adult neck should be considered malignant until proven otherwise. It is extremely important for the thyroid sonographer to avoid generalizing the approach to characterizing thyroid nodules to the remainder of the neck. For example, while cystic composition is a benign feature of thyroid nodules, cystic change within a lymph node is concerning for malignancy. Table 14.1 outlines typical differential diagnoses for abnormalities at various sites within the neck.

Case Presentation 1

A patient presented with a neck mass located immediately to the left of midline, under the jaw. Ultrasound imaging is shown below (Image 14.6).

Although thyroglossal duct cysts can occur anywhere along the path of descent of the thyroid, the majority are at or just inferior to the hyoid bone, as in this case. They may be entirely cystic or contain echogenic debris. Papillary thyroid carcinoma may occur within thyroglossal duct cysts, arising in fewer than 5% of cases; however, FNA of any solid or vascular component is warranted to exclude this possibility.

Table 14.1 Differential diagnosis of neck masses by location

I. Angle of the mandible, along anterior border of sternocleidomastoid muscle
Abnormal jugulodigastric lymph node Reactive Infectious lymphadenitis Histiocytic conditions (Rosai Dorfman, Kikuchi) Lymphoma Metastasis Parotid tail tumor Second branchial cleft cyst (**only** if metastatic lymph node has been excluded by biopsy) Lipoma
II. Submandibular space
Abnormal submandibular lymph node (metastasis, lymphoma) Abnormal submandibular gland Benign or malignant submandibular tumors Acute sialadenitis IgG4, Sjogren, other chronic inflammatory/autoimmune conditions Stone Plunging ranula Lipoma
III. Parotid gland
Benign and malignant parotid tumors Acute sialadenitis (with or without abscess) IgG4, Sjogren, other chronic inflammatory/autoimmune conditions Stone Benign and malignant intraparotid lymph nodes
IV. Carotid space
Schwannoma Paraganglioma Aneurysm/pseudoaneurysm
V. Supraclavicular space
Reactive lymph node Metastatic lymph nodes from thyroid cancer Metastatic lymph nodes from chest or abdomen primary malignancies Lymphoma Lipoma

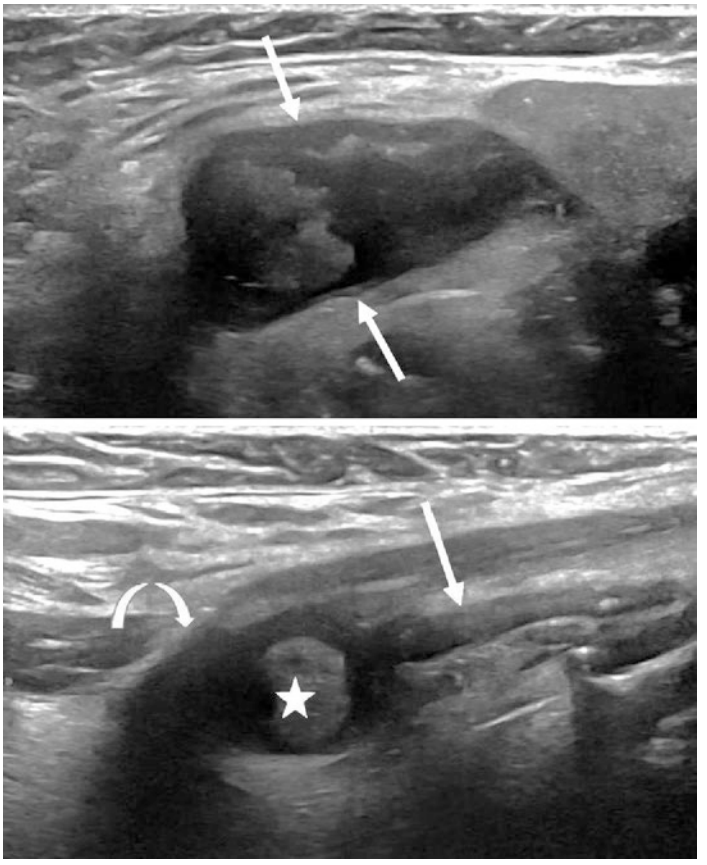

Image 14.6 Transverse image (top) showing a cystic and solid lesion (between white arrows) just to the left of midline that contacts the medial border of the left submandibular gland. Sagittal image (bottom) where the mass is labeled with a star. Note the curved arrow, which indicates shadowing by the hyoid bone superior to the lesion, and the straight arrow indicating the thyroid cartilage inferior to the lesion

Case Presentation 2

A patient who had a prior history of radiation for Hodgkin's lymphoma developed a new palpable neck mass. Ultrasound of the mass is shown below (Image 14.7).

Schwannomas are benign nerve sheath tumors that typically present either with dysfunction of the underlying nerve or as an asymptomatic mass. As they enlarge, they may grow along the length of the nerve (Image 14.7, bottom, white arrows showing

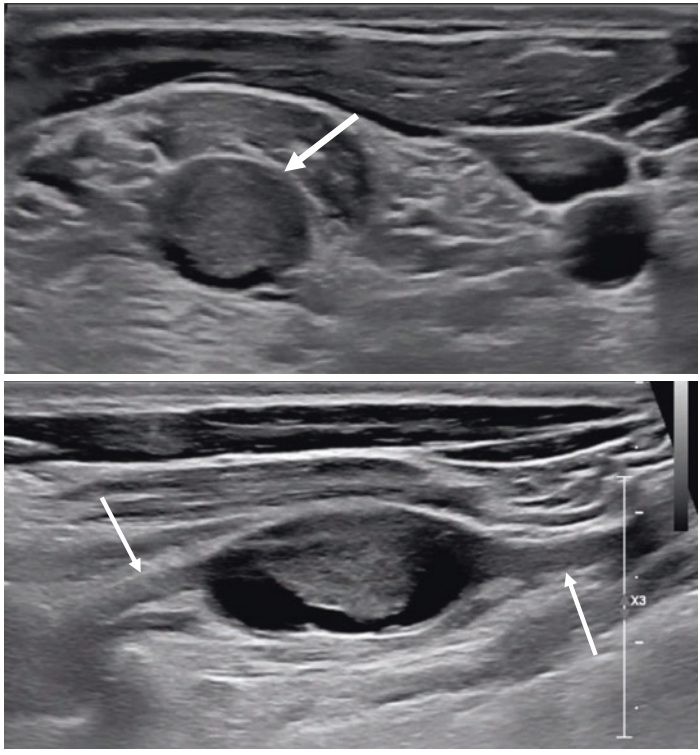

Image 14.7 Transverse image (top) of a rounded, well-circumscribed soft tissue nodule. Sagittal view (bottom) showing the nodule to be cystic and solid and to have linear structures extending from it (arrows). FNA was attempted but was aborted due to severe lancinating pain in the hand which the patient experienced when a needle was placed in the mass

nerve from which Schwannoma arises), attaining a spindle shape on coronal or sagittal imaging. Fine needle aspiration (FNA) may demonstrate Schwann cells; however, if the Schwannoma arises from a sensory nerve, the patient may be unable to tolerate the biopsy, leading to inadequate sampling.

Case Presentation 3

A lymph node survey is performed in a patient with a suspicious thyroid nodule, in order to evaluate for possible metastases. As the upper jugulodigastric chain is scanned, a rounded hypoechoic focus is identified in the parotid tail (Image 14.8).

The tail of the parotid gland lies adjacent to the upper jugulodigastric lymph nodes at the angle of the mandible and can be visualized during evaluation of this region. There are normally occurring lymph nodes in the parotid that have the same appearance as benign lymph nodes in other regions of the neck. Occasionally, nodules in the parotid gland are encountered. Most parotid nodules are benign (e.g. parotid pleomorphic adenomas) and demonstrate well-defined margins. They may be markedly hypoechoic and demonstrate posterior acoustic enhancement

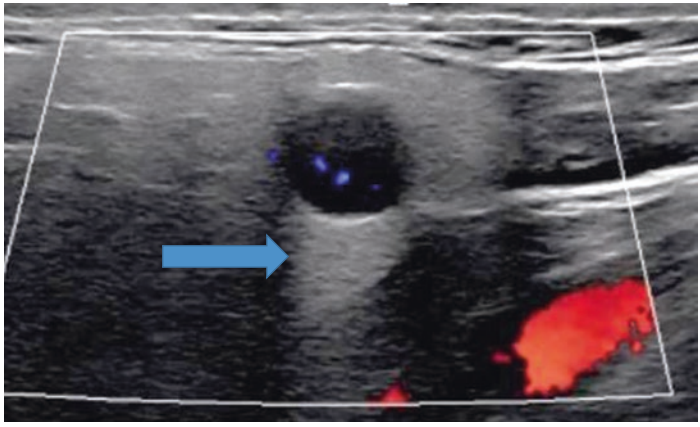

Image 14.8 This well-circumscribed nodule, demonstrates enhanced through transmission/posterior acoustic enhancement (arrow), but there is a small amount of blood flow within the lesion, suggesting the nodule is solid rather than cystic

which can lead to confusion with cysts; however, cysts should be completely anechoic, whereas parotid nodules have some internal echoes and may also demonstrate internal blood flow. A lack of worrisome ultrasound features does not reliably distinguish between a benign parotid neoplasm and a low grade malignancy and, for this reason, these nodules should be evaluated, typically with FNA.

Case Presentation 4

During a follow-up visit with ultrasound for a thyroid nodule, a patient reported a posterior neck mass. Sagittal images demonstrate a mass in the subcutaneous soft tissues that is hyperechoic to the adjacent muscle (Image 14.9).

Lipomas present clinically as palpable, soft masses. They may slowly enlarge over time and are a common finding in an otherwise well patient. On ultrasound, lipomas are usually hyperechoic relative to adjacent muscle and typically contain linear echogenicities. Lipomas should be carefully examined for solid components or vascularized septations as these features may be seen in liposarcomas (Image 14.9).

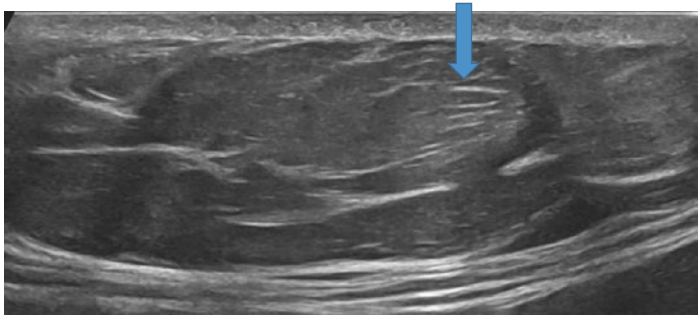

Image 14.9 There are linear echogenic bands within the mass (arrow), which are parallel to the skin surface. Physical examination revealed a soft neck mass that had been present for many years

Case Presentation 5

A 14-year-old boy with a family history of multiple paragangliomas presents to his doctor with a hoarse voice. ENT evaluation demonstrates right vocal cord paresis. Ultrasound of the neck demonstrates a heterogeneous, well-circumscribed mass lesion that closely abuts the spine (Images 14.10 and 14.11).

Because of his family history and the involvement of the carotid space, a paraganglioma was suspected. This was confirmed with octreotide scanning.

Paragangliomas, including glomus vagale and carotid body tumors, are rare neck masses arising from chromaffin cells, which tend to be closely associated with the internal carotid artery or carotid bifurcation. Involvement of the carotid space may also be seen with vagal Schwannoma. As these tumors can be very vascular and may secrete catecholamines, further work-up should be performed prior to FNA, and should include biochemical testing and contrast-enhanced CT or MRI.

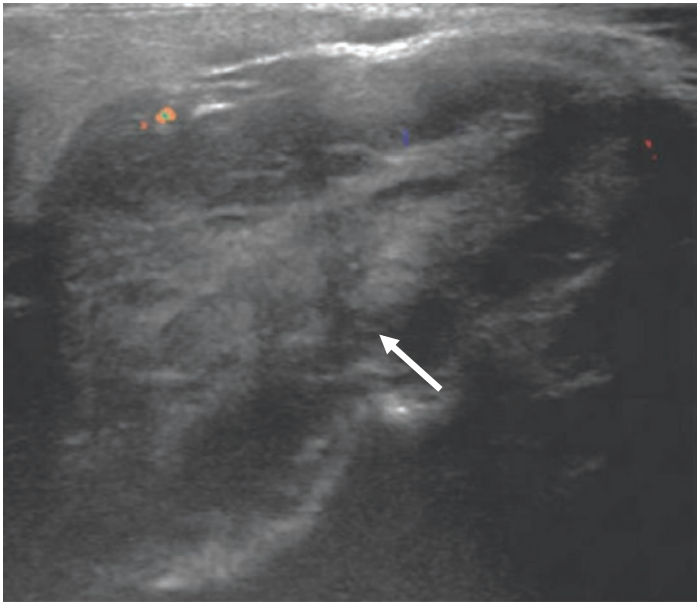

Image 14.10 Sagittal image through the neck demonstrates a large, heterogeneous solid nodule without significant internal vascularity (arrow)

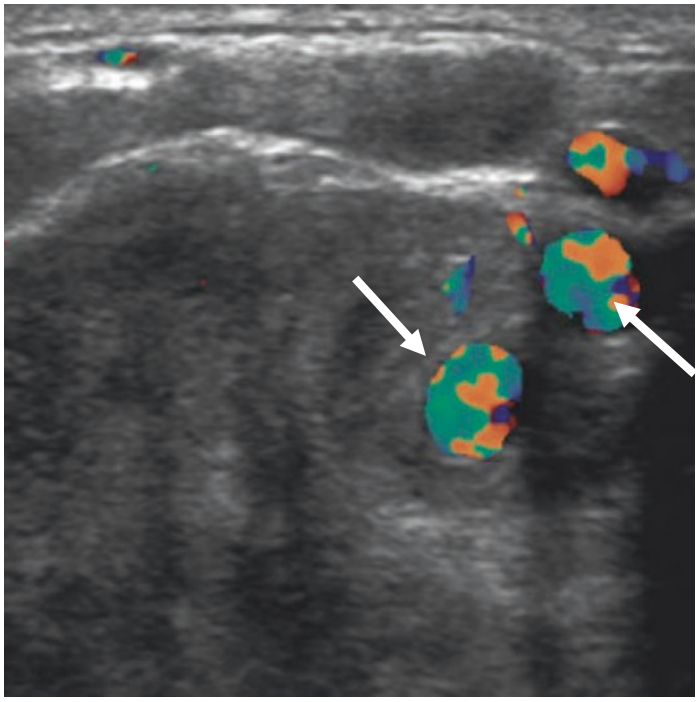

Image 14.11 Transverse images through the lesion demonstrate tumor surrounding the carotid bifurcation (arrows)

Case Presentation 6

A 65 year old woman reported a lump in the submandibular space. Scanning over the site of the palpable abnormality demonstrated an enlarged submandibular gland with heterogeneous echotexture and dilated ducts (Images 14.12 and 14.13).

Sialoliths are concretions within the salivary ducts and are more common in the submandibular gland than in the parotid gland. They result in pain and swelling of the gland, which is particularly noticeable during eating. They can be recognized as a focus of increased echogenicity associated with posterior shadowing. There is often dilation of the duct proximal to the stone and there may be swelling and inflammatory change within the gland as a result of the obstruction.

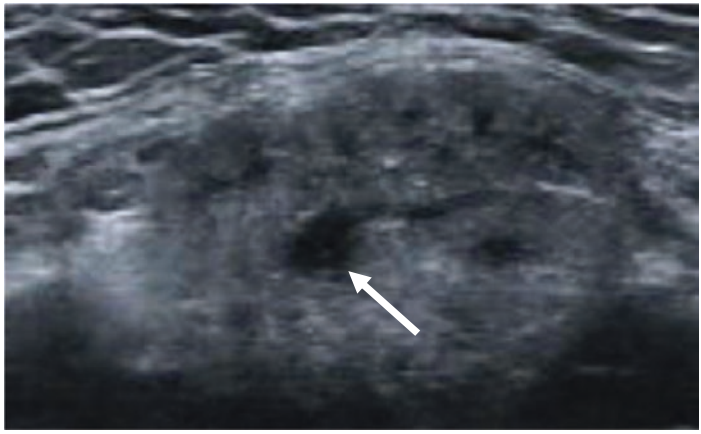

Image 14.12 Sagittal view through the submandibular gland demonstrates heterogeneous echotexture. The submandibular duct (arrow) is dilated

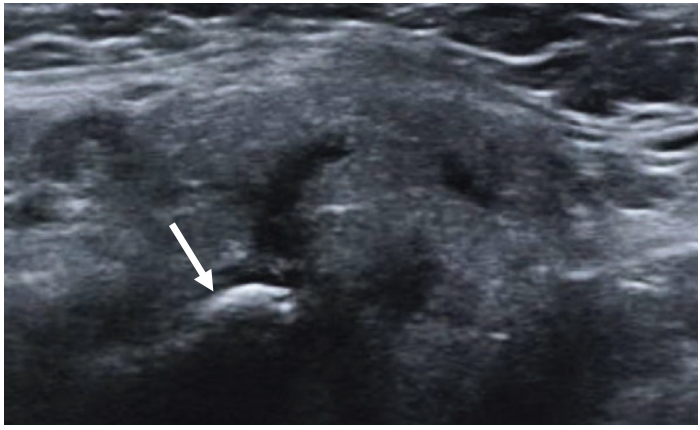

Image 14.13 An image obtained closer to the hilum of the gland shows an echogenic curvilinear focus with posterior shadowing (arrow), representing an obstructing sialolith within the submandibular duct

Case Presentation 7

A 25-year-old man reported swelling in the submandibular region. Ultrasound demonstrated a fluid-filled structure in the submandibular space (Images 14.14 and 14.15).

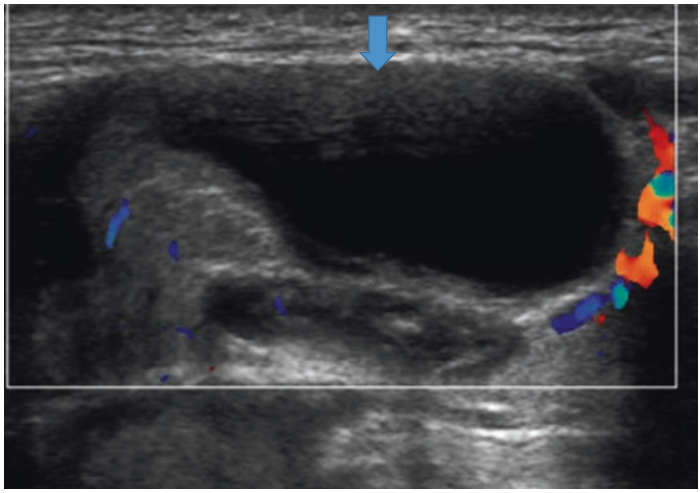

Image 14.14 Transverse image through the submandibular space demonstrates a well-circumscribed hypoechoic structure without internal flow (arrow)

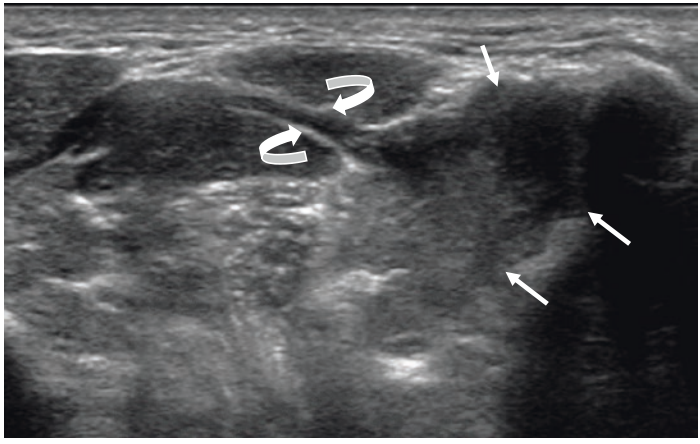

Image 14.15 The cystic structure is shown to be contiguous with the left sublingual gland (straight arrows) which has herniated through a defect in the mylohyoid muscle (curved arrows), consistent with plunging ranula

The sublingual gland contains numerous individual ducts. Obstruction of any of these ducts may result in a sialocele of the sublingual gland, also termed a ranula. As they grow larger, these may herniate into the submandibular space, either posterior to the free edge of the mylohyoid muscle or through defects in the mylohyoid muscle (as in this case).

Case Presentation 8

A 56-year-old man reported a neck mass at the angle of the mandible (Image 14.16).

Direct laryngoscopy with biopsy diagnosed HPV-associated squamous cell carcinoma of the tongue base, and this cystic mass was recognized to be a metastasis.

In thyroid nodules, cystic composition is a reassuring finding. In the lateral neck, most masses encountered in an adult are lymph

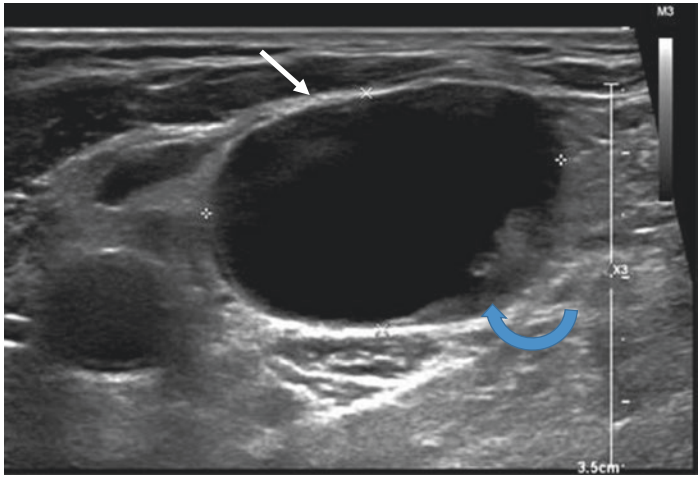

Image 14.16 Transverse image demonstrates a predominantly cystic mass (arrow) just lateral to the carotid artery, with a small focus of solid tissue or debris within it (curved arrow)

nodes and cystic change within a lymph node is a very concerning finding, as it is seen in metastasis from both papillary thyroid cancer and HPV-associated oropharyngeal cancer. In both types of cancer, the primary tumor may be very small. Thus, the index of suspicion for malignancy should remain high, even without identification of a primary.

When performing FNA of cystic masses in the lateral neck, the needle should be preferentially directed into the solid portion of the nodule. If possible, fluid should be sent for thyroglobulin analysis to detect papillary thyroid carcinoma.

Discussion

A wide variety of abnormalities may be seen and evaluated on physical examination of the neck. A history of a new neck mass occurring in the setting of pain or redness suggests infection or inflammation. Thus, incidental neck infections and masses are rare on thyroid US. It is useful to understand some basic principles of differential diagnosis when an abnormality is encountered. In the salivary glands, swelling may represent obstruction, sialadenitis, or tumor. At the angle of the mandible, a mass may represent a malignant lymph node. In the central neck superiorly, thyroglossal duct cysts, abnormal submandibular lymph nodes, and plunging ranulas are possibilities. Table 14.1 outlines additional possibilities organized by location.

Unless a benign diagnosis can be definitively made with imaging (sialolith, lipoma, etc.), newly discovered masses in the adult neck will require FNA or core biopsy to establish a diagnosis. It is critical to remember that cystic change within a lesion does not exclude malignancy, as both papillary thyroid cancer and HPV-associated oropharyngeal cancer may present with cystic lymph nodes. A reasonable strategy for the work-up of a newly diagnosed indeterminate mass lesion in the neck includes ENT evaluation and contrast-enhanced CT or MRI.

Further Reading

Ahuja AT, King AD, Kew J, King W, Metreweli C. Head and neck lipomas: sonographic appearance. AJNR Am J Neuroradiol. 1998;19(3):505–8.

Bansal AG, Oudsema R, Masseaux JA, Rosenberg HK. US of pediatric superficial masses of the head and neck. Radiographics. 2018;38(4):1239–63.

McMahon C, Yablon C. Chapter 23—Overview of musculoskeletal ultrasound techniques and applications. In: Rumack CM, Levine D, editors. Diagnostic ultrasound. 5th ed; 2017. p. 856–76.

Pynnonen MA, Gillespie MB, Roman B, Rosenfeld RM, Tunkel DE, Bontempo L, Brook I, Chick DA, Colandrea M, Finestone SA, Fowler JC, Griffith CC, Henson Z, Levine C, Mehta V, Salama A, Scharpf J, Shatzkes DR, Stern WB, Youngerman JS, Corrigan MD. Clinical practice guideline: evaluation of the neck mass in adults. Otolaryngol Head Neck Surg. 2017;157(2_suppl):S1–S30.

Stoia S, Băciuț G, Lenghel M, Badea R, Băciuț M, Bran S, Cristian D. Ultrasonography techniques in the preoperative diagnosis of parotid gland tumors - an updated review of the literature. Med Ultrason. 2021;23(2):194–202.

Thompson LD, Herrera HB, Lau SK. A clinicopathologic series of 685 thyroglossal duct remnant cysts. Head Neck Pathol. 2016;10(4):465–74. https://doi.org/10.1007/s12105-016-0724-7.

Correction to: Handbook of Thyroid and Neck Ultrasonography

Leslie S. Eldeiry, Nora M. V. Laver, Gregory W. Randolph, Barry Sacks, and Jeffrey R. Garber

Correction to:
L. S. Eldeiry et al. (eds.), *Handbook of Thyroid and Neck Ultrasonography*, https://doi.org/10.1007/978-3-031-18448-2

Owing to an unfortunate oversight, the book was inadvertently published with errors in few author names and affiliations.

The corrections are listed below:

1. The organization name for authors Amy Juliano and Greg Randolph was incorrect and has been changed to "Massachusetts Eye and Ear Infirmary".

2. The name "Gregory Randolph" was duplicated in the contributors list and this has been removed. The name Gregory W. Randolph which was inconsistent between chapters 9 and 14 has been made consistent.

The updated original version for this book can be found at
https://doi.org/10.1007/978-3-031-18448-2_9
https://doi.org/10.1007/978-3-031-18448-2_14

L. S. Eldeiry et al. (eds.), *Handbook of Thyroid and Neck Ultrasonography*, Contemporary Endocrinology,
https://doi.org/10.1007/978-3-031-18448-2_15

Index

L. S. Eldeiry et al. (eds.), *Handbook of Thyroid and Neck Ultrasonography*, Contemporary Endocrinology,
https://doi.org/10.1007/978-3-031-18448-2